Regulation of the inositol phosphatases SHIP and PTEN by the costimulatory receptor CD28 in T lymphocytes

Burgess, Steven James

Award date:
2003

Awarding institution:
University of Bath

REGULATION OF THE INOSITOL PHOSPHATASES SHIP AND PTEN BY THE COSTIMULATORY RECEPTOR CD28 IN T LYMPHOCYTES

SUBMITTED BY

STEVEN JAMES BURGESS

For the degree of PhD
Of the University of Bath
2003

Signed...S.Burgess..... Date...27/2/2003.....

ProQuest LLC
789 East Eisenhower Parkway
P.O. Box 1346
Ann Arbor, MI 48106-1346

Table of contents

List of Figures

Introduction

Page Number

Materials and Methods

Results

List of Tables

Page Number

Abbreviations

Ag	Antigen
APC	Antigen presenting cell
BCR	B cell receptor
BTK	Bruton's tyrosine kinase
CD	Cluster of differentiation
CK2	Casein kinase 2
CTLA-4	Cytotoxic T lymphocyte associated antigen-4
DAG	Di-acyl glycerol
DAP	Dual adapter for phosphotyrosine and 3-phosphoinositides
ERK	Extracellular regulated kinase
GAB2	Grb 2 associated binding protein 2
GEF	Guanine nucleotide exchange factor
Grb2	Growth factor receptor binding protein 2
GSK3	Glycogen synthase kinase 3
ICAM	Intracellular adhesion molecule
ICOS	Inducible costimulator
Ig	Immunoglobulin
IFN	Interferon
IL	Interlukin
ITAM	Immunoglobulin tyrosine based activation motif
ITIM	Immunoglobulin tyrosine based inhibition motif
JNK	C-Jun N-terminal kinase
k Da	Kilodalton
LAT	Linker for activated T cells
LY294002	2-(4-moropholinyl)-8-phenyl-4H-1-benzyopyran-4-one
MAPK	Mitogen activated protein kinase
mAb	Monoclonal antibody
MHC	Major histocompatability complex
NFAT	Nuclear factor of activated T cells
NFκB	Nuclear factor κ B

PD-1	Program death-1
PH	Pleckstrin homology
Px	Phox domain
PDK-1	Phosphoinositide dependent kinase-1
PI 3-K	Phosphatidylinositol 3-kinase
$15dPGJ_2$	15-deoxy-$\Delta^{12,14}$-prostaglandin J_2
PKB	Protein kinase B
PKC	Protein kinase C
PLC	Phospholipase C
PPAR	Peroxisome proliferator agonist receptor
PPRE	Peroxisome proliferator response element
PTB	Phosphotyrosine binding domain
PtdIns	Phosphatidylinositol
PTEN	Phosphatase and tensin homologue deleted on chromosome ten
PTK	Protein tyrosine kinase
SH2	Src homology 2 domain
SH3	Src homology 3 domain
Shc	SH2 containing adapter protein
SHIP	SH2 containing inositol phosphatase
SHP2	SH2 containing protein tyrosine phosphatase 2
SLP-76	SH2 domain containing leukocyte protein of 76 kDa
SOS	Son of sevenless
TAPP	Tandem PH-domain –containing protein
TCR	T cell antigen receptor
Th	T helper cell
TRIM	T cell receptor interacting membrane protein
TZD	Thiazolidinediones
ZAP-70	Zeta associated protein of 70 kDa

Abstract

D-3 phosphoinositides produced by the activated lipid kinase phosphatidylinositol 3-kinase (PI 3-K) regulate a diverse array of cellular biological responses in T cells including proliferation, differentiation, migration and apoptosis. These functional responses can be checked by inositol phosphatases such as SHIP and PTEN which metabolise the lipid PI(3,4,5)P_3 and thus ultimately regulate PI(3,4,5)P_3–dependent signalling cascades. Expression of these important phosphatases was determined in commonly used leukemic T cell lines as well as peripheral human T-lymphoblasts. The cell line Jurkat lacked expression of both SHIP and PTEN whereas the CEM and MOLT-4 T cell lines expressed SHIP but not PTEN. T-lymphoblasts derived from healthy volunteers, as expected, expressed both phosphatases. This difference in phosphatase expression was associated with alterations in D-3 phosphoinositide profiles and in the activation status of PI(3,4,5)P_3-dependent signalling molecules including protein kinase B (PKB).

Evidence is presented that SHIP is a downstream target for CD28-activated protein tyrosine kinases and can itself co-associate with *in vitro* kinase activity. This tyrosine phosphorylation of SHIP following CD28 stimulation was shown to be independent of PI 3-K activation. Following stimulation, SHIP was shown to bind to the adapter protein $p62^{dok}$ and GRID, which may help mediate the biological function(s) of SHIP. The *in vitro* assays revealed phosphatase activity of SHIP to be constitutive *in vitro* with no significant enhancement being observed following CD28 stimulation. PTEN, unlike SHIP, was not tyrosine phosphorylated following CD28 stimulation but did co-precipitate with *in vitro* kinase activity and with several unidentified phosphoproteins, all of which appear to form part of a multimeric protein complex that assembles post CD28 stimulation.

The role of PPARγ, a member of the nuclear hormone superfamily and its various ligands were assessed for their inhibitory effects on T cell proliferation. The prostaglandin 15dPGJ_2, a proposed natural ligand for PPARγ, proved to be a potent inhibitor of primary T cell and SEB-activated T-lymphoblasts proliferation in response to various stimuli. The synthetic PPARγ agonist,

troglitazone inhibited T cell proliferation induced by a 'physiological' stimulus (IL-2 or CD3/CD28) but ineffective at inhibiting T cells induced by the non-physiological stimulus PMA/Ionomycin. On an equimolar basis, troglitazone was found to be a less potent inhibitor as $15dPGJ_2$. In addition the structurally related synthetic compound ciglitazone had no detectable inhibitory effect on T cell proliferation irrespective of the stimulus used. These data adds to the existing evidence that certain PPARγ agonists may have therapeutic potential in T cell-mediated anti-inflammatory disorders.

Acknowledgements

I would like to acknowledge my supervisor Dr. Stephen Ward who has guided me through this study during the past few years. Many thanks to past and present members of various laboratories who have helped and offered assistance. Special mentions must go to my colleagues Marisa and Laura who have been there in times of stress and provided me with great friendship throughout this study.

Many thanks to the 'boys from bas' namely Alex, John/Sarah and Dean who have provided a constant stream of friendship and who have shared the blood, sweat and beers!!

I'd like to thank my brother Robert for his continued support, advice and encouragement as well as Gemma, Carole and Colin who have helped me endlessly during this PhD.

Finally, and most importantly, I acknowledge my father and best friend, the legendary Bob Burgess. A source of great love, friendship, humour as well as emotional and financial support. You are sorely missed.

Introduction

Overview of T-lymphocyte function

Lymphocytes provide both the specificity and memory that are key characteristics of what is termed the adaptive or acquired immune response. B cells and T cells are the two major populations of lymphocytes involved in the adaptive immune response. T cells originate from precursor stem cells in the bone marrow and migrate to the thymus where they mature into antigen specific T cells that are non-responsive to self-antigens. T cells can be grouped into two subpopulations: T helper (Th) cells and T cytotoxic (Tc) cells which can be identified by the expression of the cell surface antigen markers CD4 and CD8 respectively (figure 1). Th cells provide help to B cells via direct cell interactions and by producing cytokines that are critical for B cell proliferation and differentiation. Th cells can be further sub divided into Th1 and Th2, which are characterised by their cytokine expression profile (figure 1). Th cells can only recognise antigen via the T cell receptor (TCR) when it is associated with class II major histocompatability complex (MHC) proteins expressed on antigen presenting cells (APCs). Tc cells recognise antigen in complex with MHC class I proteins and, as their name suggests, mediate the killing of infected cells, primarily those infected with viruses.

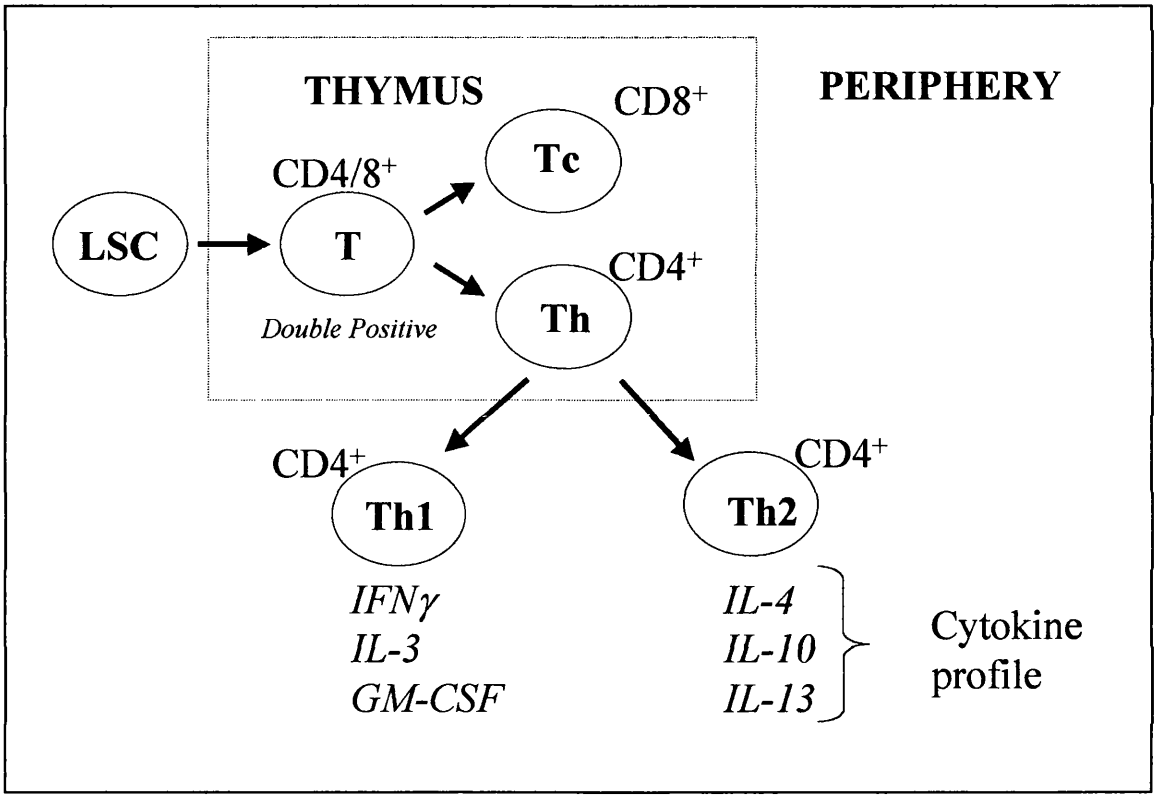

Figure 1: Maturation of T cells. Precursor lymphoid stem cells (LSC) derived from the bone marrow migrate and mature into T cells in the thymus. Expression of T cell surface markers such as CD4 and CD8 determine the biological fate of the T cell. Thus expression of CD8 renders the cell a cytotoxic T cell. In contrast, expression of CD4 defines the cell as a T helper cell that can be further subdivided into Th1 and Th2 subsets characterised by their cytokine expression profiles.

T Cell Development

Progenitor T cells are attracted to the thymus via chemotactic signals and proliferate and differentiate along several different developmental pathways to generate functionally distinct subpopulations of mature T cells. These T cell developmental pathways also correlate with TCR-gene rearrangements giving rise to the enormous range of diversity and specificity exhibited by T cells. Thymic T cells (thymocytes) exhibit changes in various surface receptors during T cell development which can be tracked via flow cytometry. Initially, immature thymocytes lack detectable surface levels of the co-receptors CD4 and CD8 and are thus referred to as double negative thymocytes. These can differentiate into T cells bearing $\alpha\beta$ TCR or $\delta\gamma$ TCR. The majority of these thymocytes develop $\alpha\beta$ TCR and also begin to express both the CD4 and CD8 co-

receptors. However it is estimated that most thymocytes (~90%) do not mature and are eliminated by apoptosis due to the failure to produce functional TCR during TCR gene rearrangement. $CD4^+/CD8^+$ double positive thymocytes further differentiate into either single positive $CD4^+$ or $CD8^+$ thymocytes and enter rounds of positive and negative selection to produce mature T lymphocytes. The mechanisms underlying the transition of double positives to single positive thymocytes is currently being unravelled and there is growing evidence for a role of the mitogen activated protein kinase 1 (MAPK) signalling in this process (Germain 2002). In general, high levels of MAPK-1 signalling promotes the generation of $CD4^+$ single positive thymocytes whilst interference of MAPK1 activity results in the production of $CD8^+$ thymocytes (Sharp *et al* 1997). Positive selection ensures that thymocytes expressing TCRs can recognise and interact with cells bearing MHC molecules whilst those that do not are eliminated by apoptosis. MHC-restricted thymocytes that survive positive selection undergo negative selection, during which those that bind too strongly to MHC proteins or self-antigens are, again, eliminated by apoptosis. Thereby tolerance to self-antigens is achieved by removing potentially auto-reactive T cells. Thymocytes that bind self-MHC proteins weakly are able to survive and develop into mature T lymphocytes and enter into the periphery.

The Immunological Synapse

T-lymphocyte activation requires multiple receptor interactions between the TCR bearing T cell and the APC containing a recognisable antigenic peptide in complex with the MHC proteins for a sustained period of time. The point of contact between the T cell and APC has been termed the immunological synapse, and been shown to be a highly ordered platform that favours signal transduction (Monks *et al* 1998 and van der Merwe *et al* 2000). The use of fluorescently labelled receptors, incorporated into T cells and APCs has allowed 'real-time' visualisation of the formation of the immunological synapse by confocal microscopy (Grakouwi *et al* 1999). At the initial point of contact, T cells stop migrating and a central adhesion junction is formed between LFA-1 and ICAM-1 (figure 2). MHC-peptide and TCR molecules are presumed to interact and 'sample' each other outside the central adhesion junction. During the next 5

minutes MHC-peptide and the TCR relocate into the centre of the contact area with ICAM-1/LFA-1 receptors shifting outside of the centre to form a peripheral stabilisation ring (figure 2). The mature immunological synapse has also been defined as a supramolecular activation cluster (SMAC) characterised with increased densities of receptors and signalling molecules. The centre of the mature SMAC contains co-receptors such as CD4/CD8 and co-stimulatory receptor pairs such as CD28/B7, CD2 and its ligand CD48 (Wülfing and Davis 1998). These receptors may serve to act as 'molecular rulers' in the synapse by excluding larger inhibitory receptors as well as providing biochemical signals to the T cell (figure 2). This occurs with the transmembrane protein tyrosine phosphatase CD45, a negative regulator of T cell activation, is excluded from the mature synapse (Rogers *et al* 1996). The synapse is reported to be stable for upto 1 hour after its initial formation (Monks *et al* 1998), within a time frame correlated with full T cell activation.

The immunological synapse and SMAC formation occurs within membrane rafts, sphingolipid/cholesterol-enriched membrane microdomains found in all mammalian cell types. These dynamic membrane microdomains were initially characterised by their lack of solubility in Triton-X100. Essential signalling components in T cell activation are enriched in membrane rafts, for example the src protein tyrosine kinase (PTK) $p56^{lck}$ (Montixi *et al* 1998), tyrosine phosphorylated TCR ζ chain (Kosugi *et al* 1999), CD28 (Viola *et al* 1999) and the adapter LAT (Lin *et al* 1999). In contrast CD45 a tyrosine phosphatase, has a low affinity for membrane rafts (Rogers *et al* 1996) and therefore excluded from the synapse. Membrane rafts therefore provide an effective platform to concentrate positive signalling molecules whilst excluding inhibitory proteins/receptors from the SMAC and thus orchestrate multiple signalling cascades.

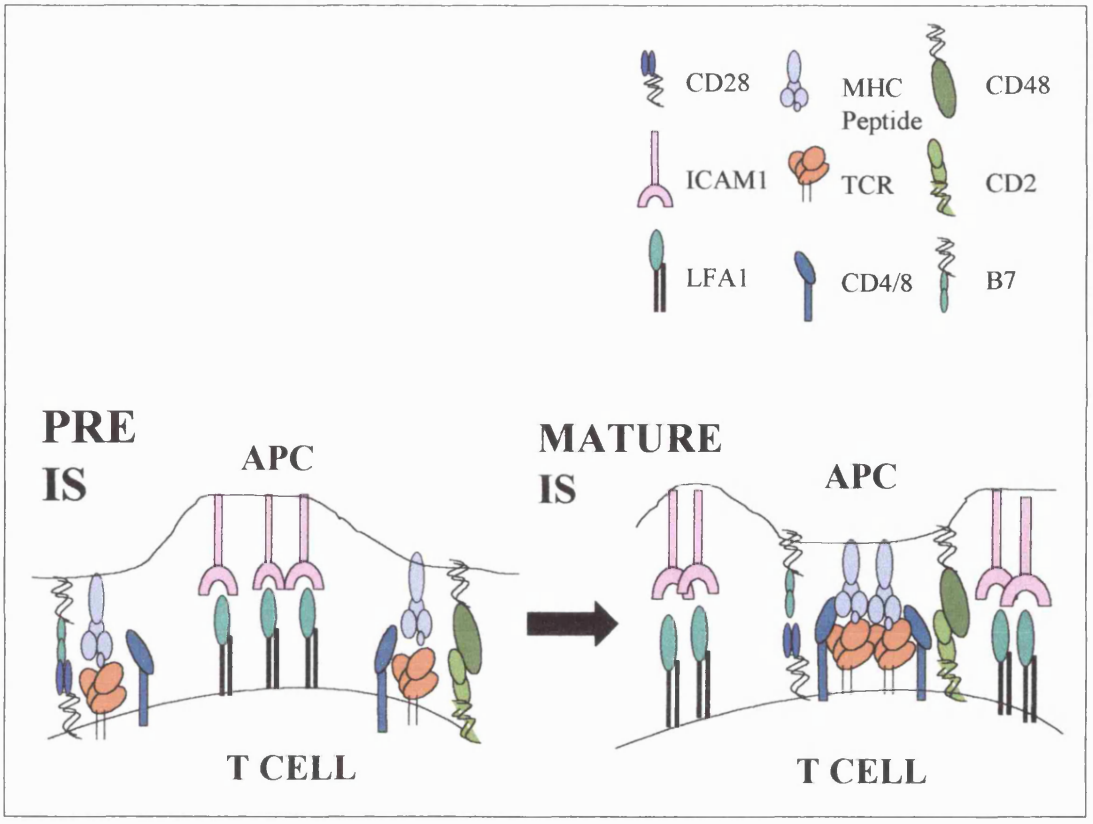

Figure 2. Model for immunological synapse (IS) formation between a T cell and an APC. An initial inner adhesion ring platform is formed between ICAM 1 and LFA-1 receptors with TCR and accessory receptors around the periphery (left panel). Within the time frame of approximately 5 minutes the TCR, CD28, CD2 and their corresponding ligands migrate into the centre and can begin to signal. The adhesion molecules forming a stable outer ring resembling a 'bullseye' structure (right panel).

Models of T lymphocyte activation.

The multiple receptor interactions of the immunological synapse between T cells and APCs culminate in a series of ordered events. An early activation marker is the production and secretion of IL-2, a growth factor for T cells as well as a whole host of cytokines. This coincides with the upregulation of the IL-2 receptor (IL-2R), CD69 and CD40L. T cells then enter a proliferative phase from quiescent cells to blast transformed T cells before entering a differentiation phase, which may require several rounds of cell division. T cells receive their primary signal via antigen/MHC presented by APC. However, this is insufficient for optimal activation, with accessory or co-stimulatory receptors providing the

additional input to exceed the thresholds set by the T cell. This has led to the concept of the 2 signal model with regards to T cell activation, with the TCR/CD3 complex supplying signal 1 and co-stimulatory receptors e.g. CD28 engaged with the B7 receptors, providing signal 2 (figure 3). Failure of the T cell to receive this co-stimulatory signal can push the cell in to a state of annergy or unresponsive to further antigenic encounter or even apoptosis. The 2-signal model for T cell activation has been updated and modified with the discovery of additional co-stimulatory receptors such as the CD28 homologue ICOS (Hutloff *et al* 1999). CD28-primed T cells upregulate ICOS that can interact with B7 related proteins, which are thought to drive Th2 differentiation into effector cells. T lymphocyte activation can be controlled via inhibitory receptors such as CTLA-4 (Lee *et al* 1998), structurally related to CD28, which can outcompete CD28 for B7 binding thus denying the T cell co-stimulatory input. The biochemical response to some of the key receptor engagements in T cell signalling will be further considered.

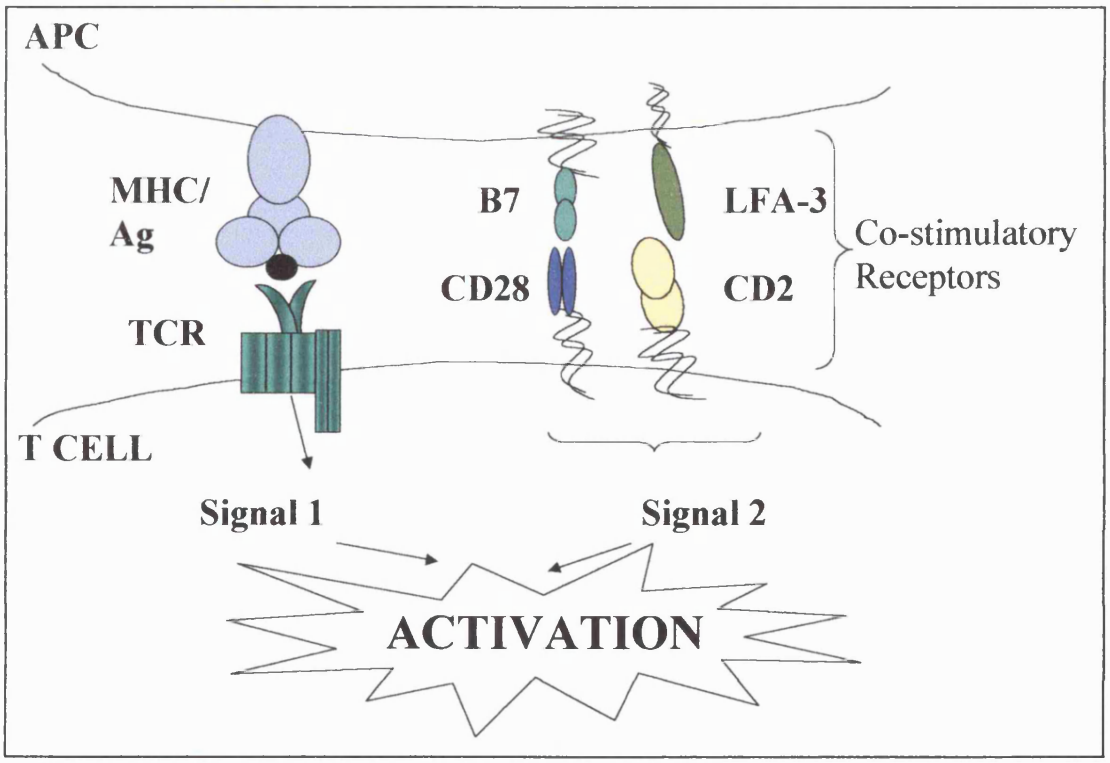

Figure 3. The 2 signal model for T cell activation. Engagement of TCR with MHC/antigen induces the specificity and primary signal (signal 1) of the T cell which alone is insufficient for full activation. Ligation of co-stimulatory receptors (signal 2) such as CD28 and CD2 exceed inhibitory thresholds and in conjunction with signal 1 drive cell-proliferation, T-lymphoblast formation and IL-2 secretion.

TCR signalling.

TCR-mediated tyrosine phosphorylation and regulation of adapter proteins.

The primary biochemical response to TCR stimulation via MHC-antigen complex or anti-CD3 mAb is the activation of src family PTK such as Lck and Fyn. This correlates with a rapid increase in phospho-tyrosine content of a number of src PTK substrates, within 5 seconds of TCR triggering (June *et al* 1990). Binding of Lck to the CD4/CD8 co-receptors places it into juxtaposition with the TCR and enables the kinase to phosphorylate motifs termed immunoreceptor tyrosine-based activation motifs (ITAM) present on ε, γ and δ subunits of the CD3 complex and on the TCRζ chain (figure 4). Phosphorylated ITAMs serve as docking sites for Src Homology 2 (SH2) domain containing signalling molecules in which to propagate cell signalling. The syk family PTK member ZAP-70 is able to bind a tyrosine phosphorylated ITAM on the TCRζ chain (Chan *et al* 1991) and then become activated by CD4/CD8-assocaited Lck-mediated phosphorylation (figure 4).

A major substrate for ZAP-70 is the adapter protein LAT (Zhang *et al* 1998). Tyrosine phosphorylated LAT is able to recruit phospholipase C γ (PLCγ) to the membrane via its SH2 domain and become tyrosine phosphorylated itself. LAT has proved to be a central player in directing signal transduction in T cells. Tyrosine phosphorylated LAT is able to recruit and associate with signalling proteins such as Grb-2 and SLP-76, the lipid kinase Phosphatidyl inositol 3-kinase (PI 3-K) and the protooncogene c-Cbl, thereby integrating diverse biochemical signals. The importance of LAT is highlighted in the LAT-deficient Jurkat T cell line, in which the TCR-mediated tyrosine phosphorylation of key signalling proteins such as PLC-γ is attenuated, abolishing Ca^{2+} flux (Zhang *et al* 1999).

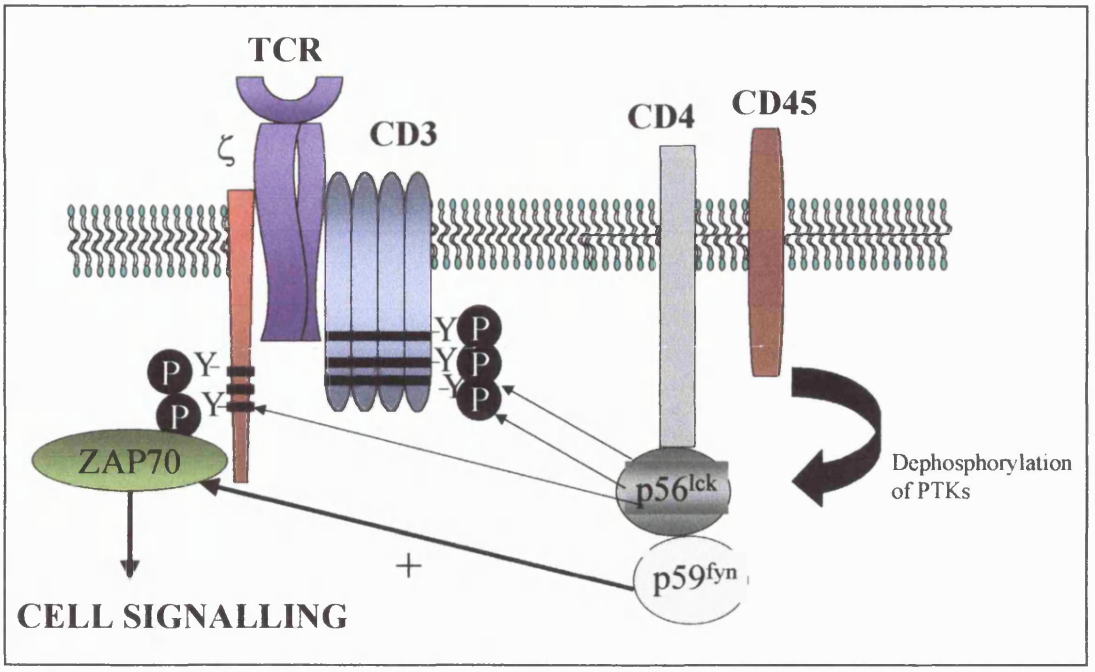

Figure 4: Activation of TCR. Following stimulation via antigen, ITAM motifs become tyrosine phosphorylated via the CD4-coreceptor-bound PTKs $p56^{lck}$ and $p59^{fyn}$, which were primed via dephosphorylated and acivated by the transmembrane phosphatase CD45. Phosphorylated ITAMs can bind to SH2 domain containing proteins including ZAP-70 that can be further positively regulated by $p56^{lck}$ and subsequently allow initiation of cell signalling.

Effector pathways downstream from the TCR – Calcium dependent signal.

Active, tyrosine phosphorylated PLCγ cleaves phosphatidlyinositol 4,5-bisphosphate and generates the well-characterised second messengers inositol-1,4,5-trisphosphate (IP3) and diacylglycerol (DAG). IP3 production initiates the depletion of intracellular Ca^{2+} stores. The resultant Ca^{2+} flux coupled with the presence of DAG, results in the activation of PKC (Weiss *et al* 1987). The rise in intracellular Ca^{2+} levels leads to the activation of the serine/threonine phosphatase calcineurin, which can dephosphorylate the transcription factor Nuclear Factor of Activated T cells (NFAT). This dephosphorylation event promotes translocation of NFAT from the cytosol to the nucleus where it can participate along with the AP-1 family of transcription factors in the regulation of IL-2 gene transcription (Jain *et al* 1995). PKC signalling pathways are also believed to impinge on the AP-1 and NFAT transcription factors (figure 5).

TCR-mediated regulation of the Mitogen Activated Protein Kinases (MAPK)

LAT along with its 9 conserved phosphorylatable tyrosine residues is central to linking the TCR to downstream mitogenic signals. This is primarily achieved via the recruitment of the adapter Grb-2 in complex with the guanine nucleotide exchange factor Sos to phosphorylated LAT. Membrane targeted Sos, now in juxtaposition with inactive GDP-bound Ras, is able to GTP-load and hence activate Ras. GTP-Ras is able to recruit the mitogen Raf-1 to the membrane where it can activate by serine/threonine phosphorylation Mek kinase which in turn can activate the MAPKs, Erk 1 and Erk 2 (figure 5). This well characterised pathway has been shown to be essential in thymocyte differentiation (Alberola-Ilia *et al* 1995). Targets for Erk 1 and Erk 2 in T cells include the transcription factors Elk-1 and serum response factor (Turner *et al* 1997) which impinge on response elements regulating cytokine transcription.

TCR-mediated activation of PI 3-K

PI-3K can couple to stimulated TCR via the transmembrane adapter proteins LAT (Zhang *et al* 1998) and TRIM (Bruyns *et al* 1998). These associations occur through interaction of the regulatory p85 domain with YxxM motifs on the adapter protein. Recruitment of PI 3-K elevates levels of D-3 phosphoinositides (Ward *et al* 1992) which can interact with proteins bearing Pleckstrin Homology (PH) domains (figure 5). Membrane targeted proteins can drive anti-apoptotic signals and cytoskeletal rearrangements (PI 3-K signalling cascades are discussed in more detail later).

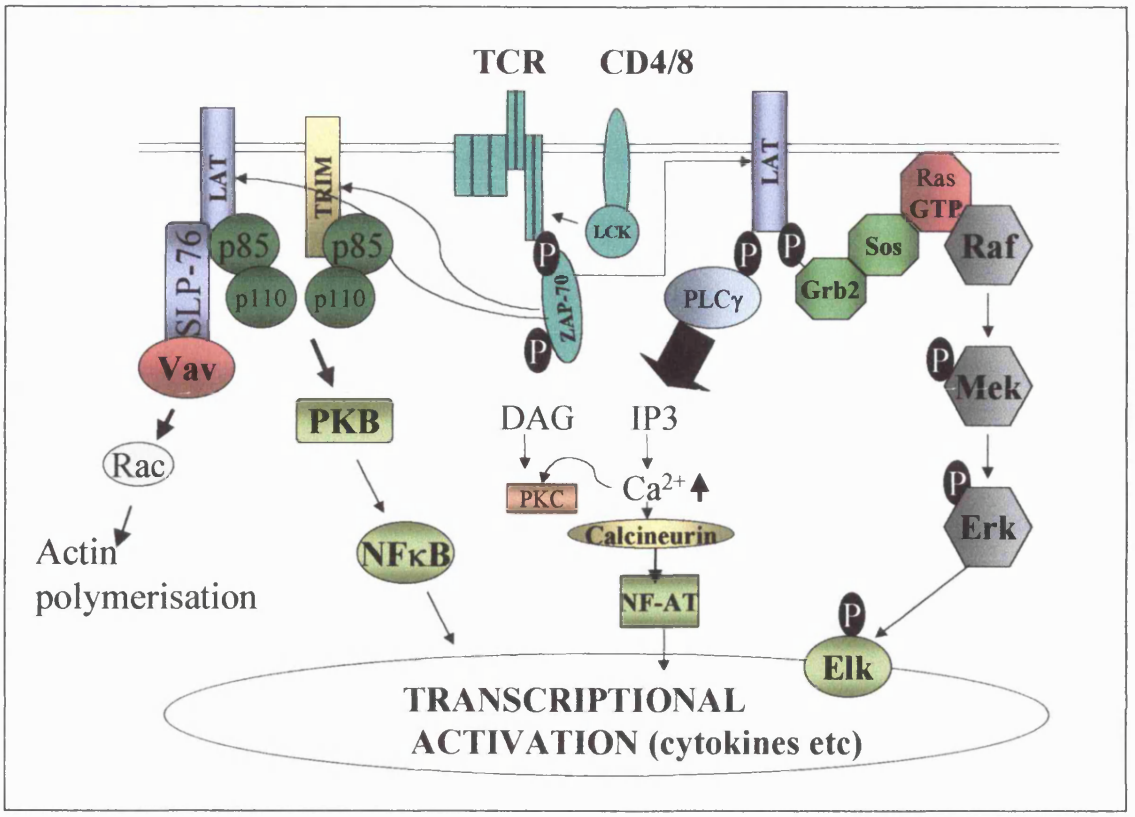

Figure 5. TCR coupling to intracellular signalling cascades following stimulation via MHC/antigen. Binding of the TCR to antigen leads to rapid tyrosine phosphorylation via co-receptor bound $p56^{Lck}$. Subsequent phosphorylation of ZAP-70 results in the tyrosine phosphorylation of transmembrane adapter proteins including LAT and TRIM that acts as a molecular scaffold. The Grb-2-Sos protein complex interacts with LAT thus allowing the activation of the Ras/MAPK pathway. LAT also recruits PLCγ where it can be activated leading to hydrolysis of PI (4,5)P_2 forming IP3 and DAG, hence initiating the calcium-signalling pathway. Both TRIM and LAT can bind to the p85 adapter subunit of PI 3-K thus initiating activation of PI 3-K driven cascades. LAT can also bind the guanine nucleotide exchange factor Vav via the adapter protein SLP-76. Vav can positively regulate Rac, another GTPase implicated in actin reorganisation. The culmination of these signalling cascades is necessary for transcription of cytokines important in initiating T cell activation.

Costimulatory receptors: CD28/B7 families

Secondary signals termed co-stimulation are needed alongside stimulation of the TCR by antigen to achieve full activation of the T cell. These co-stimulatory signals are provided by the CD28 family members upon engagement of their B7 ligands. The CD28/B7 family members are listed in table 1. These receptors share several common structural and functional features but interestingly can orchestrate varied biological outcomes of the T cell upon appropriate ligand

engagement (table 1). The biological function of each of the CD28 receptor family members will be discussed in more detail with particular emphasis on CD28.

RECEPTOR	LIGAND(S)	BIOLOGICAL CONSEQUENCE
CD28	**B7.1 and B7.2**	**ACTIVATION**
CTLA-4	**B7.1 and B7.2**	**INHIBITION**
ICOS	**B7h/ LICOS/ B7H2**	**ACTIVATION**
PD-1	**B7H1/ PD-L-1**	**INHIBITION**

Table 1: CD28 family of receptors, their ligands and biological outcomes upon receptor engagement.

CD28-Structure and expression

CD28 is a non-tyrosine kinase, type 1 transmembrane receptor expressed on 95% of $CD4^+$ and 50% on $CD8^+$ T cells. CD28 is composed of two glycosylated 44 kDa chains containing a single disulphide-linked immunoglobulin domain. The mature protein contains 202 amino acid residues, 41 of which comprise a short, species conserved, cytoplasmic domain that initiates CD28-derived signals. The ligands for CD28 and its structural homologue CTLA-4 are the B7 family of receptors namely, B7.1 (CD80) and B7.2 (CD86) that are expressed on professional APCs such as dendritic cells, monocytes and activated B cells (June *et al* 1994). The B7 ligands are also members of the immunoglobulin superfamily. Interestingly, both B7.1 and B7.2 ligands bind to CTLA-4 more avidly than CD28 (Linsey *et al* 1994). Lacking catalytic activity, CD28 generates cell signals by recruiting cellular proteins. There are 4 potential tyrosine residues on CD28, which once phosphorylated could bind to SH2 domain containing proteins. $Tyrosine^{173}$ in the CD28 cytoplasmic tail falls within the YxxM sequence motif that predicts binding of PI 3-K when phosphorylated. There are also two proline rich regions that conform to SH3 domain consensus binding sites and that are known to be important in the binding of Lck (Holdarf *et al* 1999 and figure 6).

CD28 signal transduction-Activation of PTK

Characterisation of CD28 signal transduction has revealed some controversial differences due to the particular T cell model being used and mode of activation. Like TCR signalling, stimulation of CD28 leads to rapid activation of PTK and tyrosine phosphorylation within the cytoplasmic tail that can be abrogated by treatment with herbimycin A (Lu *et al* 1992). Analysis of tyrosine phosphorylated proteins in T cell lysates following CD3 or CD28 stimulation reveal similar patterns but there are unique CD28-mediated tyrosine phosphorylated proteins of 62 kDa, 75 kDa and 100 kDa implying CD28 utilises distinct as well as similar signalling pathways to CD3 (Vandenberghe *et al* 1992). Both B7 ligands have been shown to be equivalent in terms of their ability in regulating PTK (Nunès *et al* 1996). Under *in vitro* conditions Lck has been shown only to phosphorylate Y^{173} within the CD28 cytoplasmic tail whilst the Tec family kinase ITK is able to phosphorylate all four tyrosine residues (King *et al* 1997 and figure 6). ITK is activated and recruited to CD28 via a Lck and PI 3-K dependent mechanisms, thus placing Lck and PI-3K upstream of ITK in CD28 signalling events (Lu *et al* 1998).

CD28 association with PI 3-K

CD28 can couple to PI 3-K via a rapid and sustained physical association of the regulatory p85 subunit of PI 3-K interacting with the (p)Y^{173} YxxM motif as predicted (Pages *et al* 1994 and figure 7). This is accompanied by a sustained elevation in D-3 phosphoinositides in particular PI (3,4,5) *P*3, a potent second messenger system (Ward *et al* 1992). CD28 was subsequently shown to activate the PI 3-K effector PKB in a wortmannin dependent fashion (Parry *et al* 1997). The role of PI 3-K in CD28-mediated costimulation is discussed in more detail later.

CD28 coupling to MAPK signalling pathways

CD28 binding to Grb2 at (p) Y^{173} and subsequent activation of Ras/Erk pathway has been reported (Nunès *et al* 1994). These experiments were performed by cross-linking CD28 with agonistic mAbs. Subsequent ligation of CD28 with B7.1

did not induce similar effects suggesting differential regulation of CD28 signalling cascades with different stimuli.

Both TCR and CD28 can mediate the tyrosine phosphorylation of the guanine nucleotide exchange factor Vav, thus displaying a point of integration between TCR and CD28 signalling pathways (Salojin *et al* 1999). Vav is able to regulate the activity of rac by GTP loading, which leads to the activation of the JNK MAPK pathway via PAK. Formation of these JNK cascades can regulate NF-κB and AP-1 transcription factor complexes and regulate IL-2 production via binding to the appropriate response element (figure 7).

Additional downstream targets for CD28

The adapter protein $p62^{dok}$ is a target for CD28 but not CD3 –activated PTK. The role of this multifunctional adapter protein has still yet to be validated, but has been reported to be involved in the conversion of GTP-Ras to inactive GDP-Ras in B cells and thus the regulation of mitogenic signalling through associating with Ras-GAP proteins. The proto-oncogene adapter protein Cbl is also a target for tyrosine phosphorylation following CD28/CD3 ligation (Nunès *et al* 1996). Cbl has been proposed to negatively regulate cell signalling through targeting proteins for degradation. A newly identified adapter Grid has recently been described as also binding to the (p) Y^{173}xxM motif via its own SH2 domain with binding kinetics similar to PI3-K (Ellis *et al* 2000). Grid, which is structurally related to Grb-2 and principally expressed in T cells, possesses an SH3-SH2-SH3 domain structure and co-immunoprecipitates with the adapters SLP-76 and $p62^{dok}$. The interaction of Grid with $p62^{dok}$ may serve as a mechanism for its tyrosine phosphorylation.

Cbl has been postulated as a negative regulator of T cell activation by targeting Syk PTK for degradation. There is also evidence that Cbl can influence CD28 activation by suppressing TCR-mediated Vav activation (Chiang *et al* 2000). Tyrosine phosphorylation of PLCγ and resultant Ca^{2+} flux has also been described at least in the Jurkat cell line. Again there seems to be some degree of controversy over the particular T cell model used and mode of activation as

the co-stimulatory signal appears to be insensitive to inhibition of cyclosporin A and thus independent of Ca^{2+} and calcineurin.

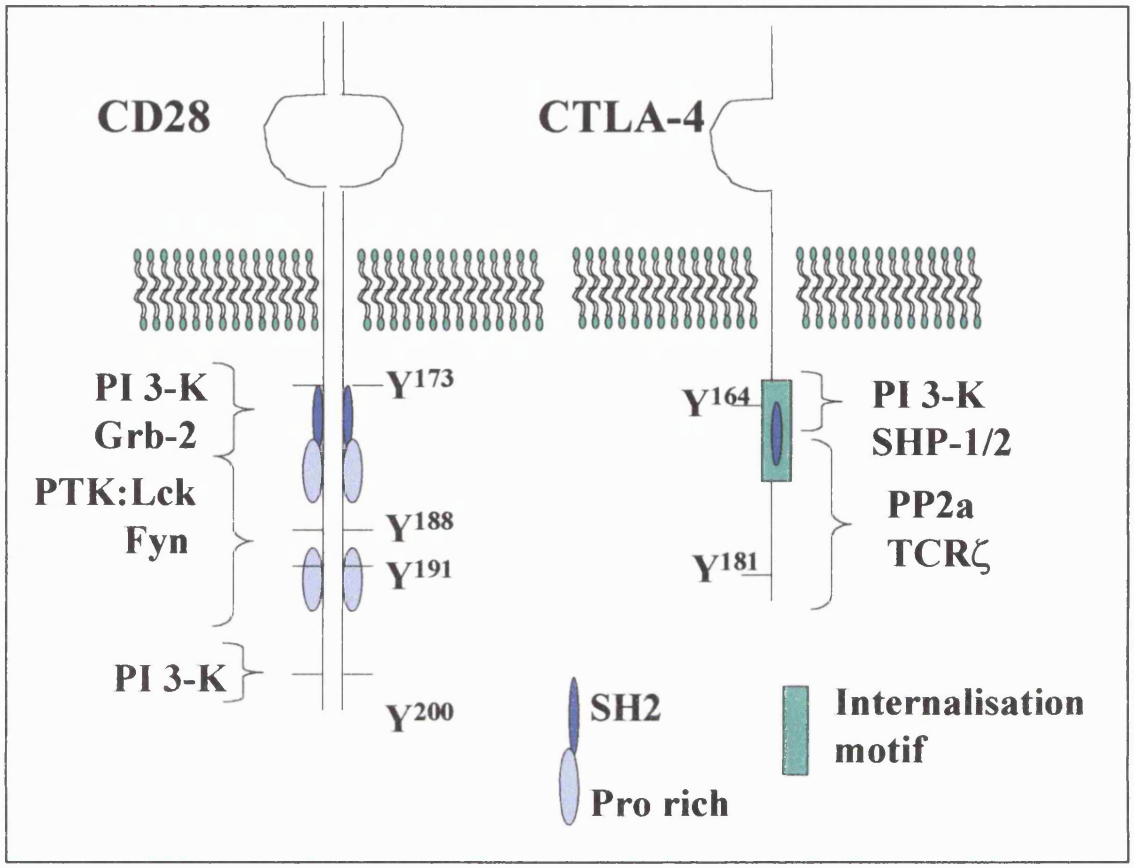

Figure 6: Structure of CD28 and CTLA-4 showing relevant residues and domains in forming protein-protein interactions. Both CD28 and CTLA-4 contain tyrosine residues which once phosphorylated can form docking sites with SH2 containing proteins; for example the p85 adapter subunit of PI 3K.

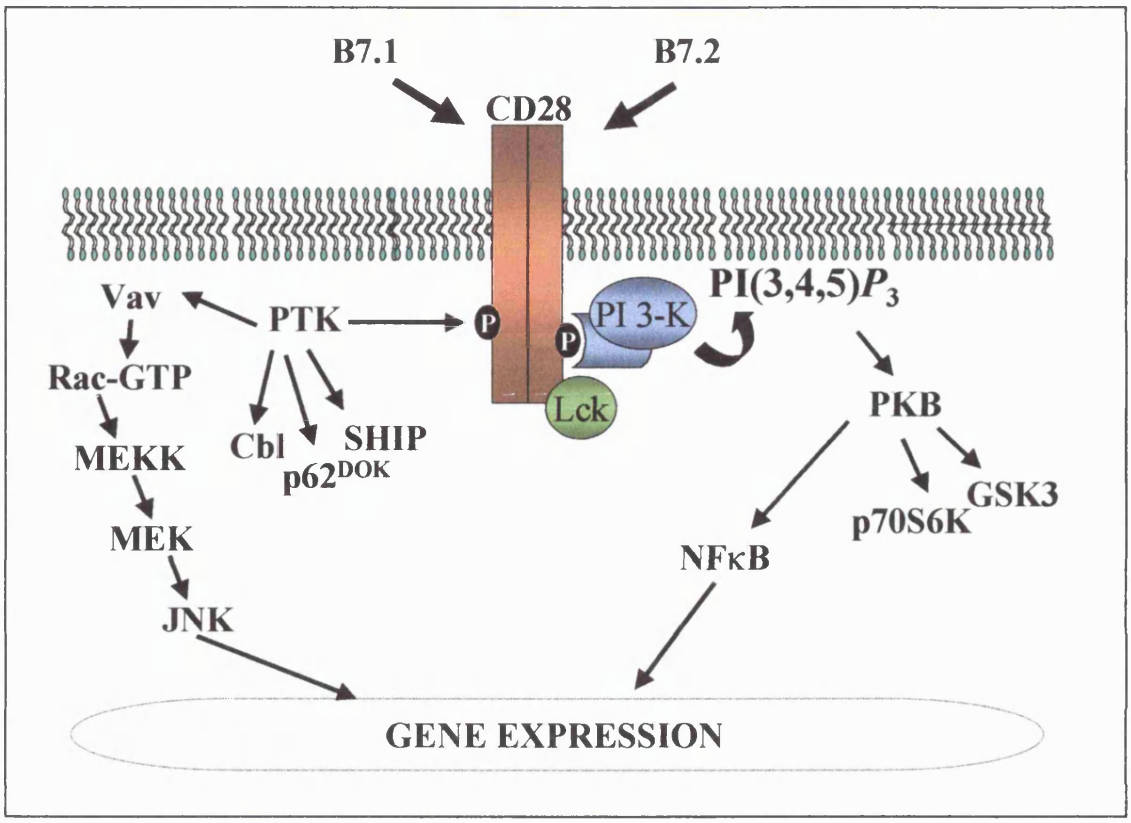

Figure 7: Signal transduction by the T cell co-stimulatory molecule CD28. Ligation of CD28 by the B7 ligands mediates the tyrosine phosphorylation of the cytoplasmic tail of CD28. This allows docking of signalling molecules such as PI 3-K via SH2 domains. Lipid products of PI 3-K are able to mediate the activation of PKB, which has multiple downstream effectors and can ultimately regulate gene expression via NFκB. Multiple substrates can be phosphorylated by CD28-activated-PTK including the exchange factor Vav. GTP-loaded Vav can regulate the Jnk/MAPK cascades that can also regulate gene expression.

Inducible costimulator (ICOS).

ICOS is a novel T cell immune receptor whose surface expression is induced on activated T cells (Hutloff *et al* 1999). ICOS shares 30-40% sequence homology to CD28/CTLA-4 and the *ICOS* gene maps to the CD28 locus (2q 33-34), which suggests ICOS may function as a costimulator and that the gene products of CD28/CTLA-4/ICOS arose by gene duplication (Coyle *et al* 2000). ICOS, like CD28, contains an extracellular Ig domain and a YxxM motif in the cytoplasmic tail (Hutloff *et al* 1999). Its expression is reported to be enhanced by CD28 ligation. A novel B7-like ligand has recently been identified for ICOS and termed B7-H2. This molecule shares 20% sequence homology with B7.1 (Wang *et al* 2000). Much progress has been made with regards to the function of ICOS and

appears that it is vital for effective T helper sell responses (Tafyri *et al* 2001 and Hutloff *et al* 1999). This is supported by the observation that T cells from $ICOS^{-/-}$ deficient mice fail to produce IL-4 when stimulated (Dong *et al* 2001). Therefore it appears therefore that ICOS may be a critical component in the induction of humoral immune responses, moreover its blockade may provide a novel therapeutic approach for the treatment of inflammatory disease such as asthma (table 2).

Cytotoxic T lymphocyte associated antigen-4 (CTLA-4)

Lymphocyte responses are determined by the interplay of both stimulatory and inhibitory signals with the strength and timing of the appropriate signal deciding the outcome. CTLA-4 (CD152) is a member of the CD28 class of receptors, sharing the same B7 ligands and exhibiting 30% sequence homology. Unlike CD28, however, CTLA-4 mediates an inhibitory signal and acts to attenuate immune responses (Thompson *et al* 1997). CTLA-4 surface expression is low or absent in resting T cells and resides mainly in intracellular vesicles through its encoded intracellular localisation motif. Upon stimulation, CTLA-4 containing vesicles traffic to the cell surface, although overall surface expression is still modest even at its peak 72 hours post stimulation (Algere *et al* 1996). Low expression of CTLA-4 is somehow compensated by the 20-100-fold increased affinity for the B7 ligands when compared to CD28. CTLA-4 has a shorter cytoplasmic tail than CD28 and lacks intrinsic enzymatic activity, but does contain tyrosine residues capable of being phosphorylated, including a YxxM motif (figure 5). The essential, regulatory role of CTLA-4 in controlling the immune respons is drastically demonstrated in CTLA-4 $^{-/-}$ knockout mice. Their phenotype is embryonic lethal due to massive lymphoproliferation and multiple organ destruction (Tivol *et al* 1997).

The signalling mechanisms by which CTLA-4 delivers its inhibitory actions are poorly defined. Recent evidence suggests that CTLA-4 regulate cell cycle progression but not apoptosis. Primarily, this can be shown due to a by down-regulation of IL-2 production (Brunner *et al* 1999). Stimulation of CTLA-4 leads to its tyrosine phosphorylation by Lck allowing its subsequent interaction with SH2 domain containing proteins. As expected PI 3-K can bind to (p)YxxM motif

(Schenider *et al* 1995). SHP-1 and SHP-2, protein tyrosine phosphatases, have both reported to bind CTLA-4 (Lee *et al* 1998), as has the serine/threonine phosphatase PP2A (Chaung *et al* 2000). However these protein interactions with CTLA-4 remain controversial, as the experiments were performed using phospho-CTLA-4 peptide fragments to 'fish out' potential interacting molecules and may not therefore, representative of what actually occurs *in vivo* following receptor stimulation. Recruitment of stimulated, phosphatase-bound, CTLA-4 complexes to the immunological synapse can be visualised as regulating a number of key mitogenic proteins as well a means to sequestering B7 signals. The blockade of these surface antigens has potentially wide reaching therapeutic implications.

Program Death-1 (PD-1)

PD-1 is a 50-55 kDa type I transmembrane protein of the Ig superfamily expressed on mature T and B cells following activation (Ishida *et al* 1992). PD-1 shares about 30% homology with CD28 and CTLA-4 and as its name suggests, plays an important role in down regulating T cell activity. The ligands for PD-1, designated PD-L, are also members of the Ig superfamily and are expressed on a wide range of cell types. PD-1 contains a consensus an immunoreceptor tyrosine-based inhibition motif (ITIM) in the cytoplasmic tail. ITIMs are thought to mediate negative signalling events via the recruitment of phosphatases (discussed in more detail later). The cytoplasmic tyrosine phosphatase SHP-2 has been reported to bind to the ITIM on PD-1 (Freeman *et al* 2000) and may be a part of the mechanism of PD-1inhibitory regulation.

Therapeutic implications of costimulatory molecule blockade

As the importance of costimulatory molecules in T cell function emerged it became apparent that blockade of such signals could be of potential therapeutic value in T cell-mediated immunological disorders. Utilising the high affinity of CTLA-4 for its respective B7 ligands, a CTLA-4-Ig fusion protein has shown promise in inhibiting islet xenograft rejection and has been also shown to induce immune tolerance (Lenschow *et al* 1992). CTLA-4-Ig are able to block T cell proliferation by binding to B7 ligands with high affinity on APC thus denying T

cells co-stimulatory signals through CD28. In addition, the severity of experimental autoimmune encephalitis in rodents, an experimental model of rodent multiple sclerosis can also be reduced with CTLA-4-Ig (Croxford *et al* 1998). Promising phase I trials of CTLA-4-Ig have already been completed in the treatment of patients with autoimmune psoriasis vulgaris (Abrams *et al* 1999). The diverse range of human diseases in which CD28/B7 blockade may hold promise is highlighted in table 2. The recent identification of other costimulatory molecules such as ICOS, which is expressed primarily on Th2 cells, could provide another target for therapeutic blockade and may hold promise in the treatment of Th2-mediated pathologies including asthma.

Autoimmune diseases	Transplant rejection	Inflammatory diseases
Psoriasis	**Solid organs**	**Asthma**
Rheumatoid Arthritis	**Cell transplants**	**Inflammatory bowl diseases**
Multiple sclerosis	**Bone marrow**	
Systemic lupus		

Table 2: Human diseases where blockage of CD28/B7 co-stimulation could have therapeutic potential.

Phosphoinositide 3-kinase

Phosphoinositide 3-kinases (PI 3-K) are a family of lipid kinases that are able to phosphorylate the D-3 position of the inositol head group of phosphoinositide lipids, and thereby generating bioactive second messengers, in particular phosphatidylinositol 3,4,5-trisphosphate (PI(3,4,5)P_3) (figure 8). The lipid products of PI 3-K, collectively termed D-3 phosphoinositides, regulate cell signalling by interacting with and recruiting proteins containing the pleckstrin homology (PH) domain to the membrane where its activity can be regulated. The last decade has witnessed extraordinary interest into PI3-K signalling due to the fact of the increasingly diverse array of cellular processes that PI 3-K is involved in. PI 3-K family members can be grouped into three main classes on

the basis of their *in vitro* lipid specificity, structure and mode of regulation (figure 9).

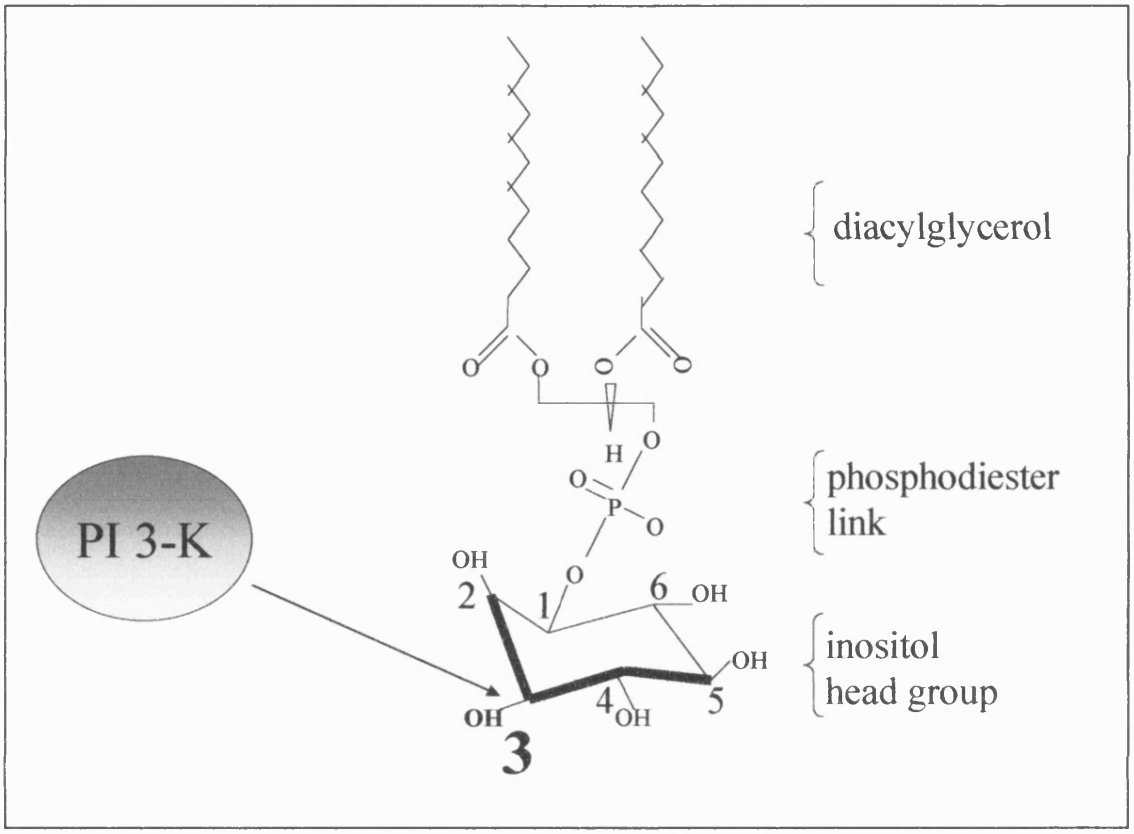

Figure 8. Schematic structure of PI (3,4,5)P_3. Phosphorylation of D-3 position hydroxyl group on PI (4,5)P_2 by PI 3-K forming the bioactive second messenger PI (3,4,5)P_3.

Class 1 PI 3-K

It is generally believed that the class 1a isoform of PI 3-K is the most important with regards to lymphocyte activation. This class of enzymes is comprised of a 110 kDa catalytic subunit that can associate with specific adapter units termed p85 (figure 9). Class 1a PI 3-Ks are also have a distinguished by their ability to interact with ras through a unique ras-binding domain. Within the 1a class of PI 3-K there are multiple isoforms of each subunit. α, β and γ forms of the p85 subunit and α, β and δ forms of the p110 catalytic subunit (Vanhaesebroeck *et al* 1997). Interestingly, the expression of 110δ is restricted to leukocytes (Chantry *et al* 1997) whereas the other catalytic subunits are more widely distributed perhaps indicating a central role for this subunit in leukocyte signalling. Recent evidence has also shown that p110δ can autophosphorylate

on Ser^{1039}, with a resultant negative effect on its lipid kinase activity (Vanhaesebroeck *et al* 1999). A recent mechanism in negatively regulating PI 3-K signalling has been proposed with the discovery of a novel kinase termed SH2-doamin containing kinase-1 (SHK-1). This novel dual specificity kinase abrogates PI 3-K-dependent-chemotaxis and impairs the activation of PKB, a downstream marker of PI 3-K activation (Moniakis *et al* 2001).

The p85 adapter subunit is able to recognise and associate via its SH2 domains with the (p)YXXM motif (where x is any amino acid) present on the intracytoplasmic tail of many cell surface receptors including CD28 and CD2 (figure 6). Thus, following stimulation and tyrosine phosphorylation of the YXXM motif, p85 is able to recruit p110 from the cytoplasm to the inner leaflet of the membrane where its substrates are localised. p85 is able to mediate signals via SH3 domain interaction of PTK such as $p59^{fyn}$, enhancing IL-2 transcription in T cells independently of the p110 catalytic subunit (Kang *et al* 2002).

Class 1B PI 3-K is identified by the p110γ catalytic subunit associated with a unique 101 kDa regulatory adapter subunit (figure 9). The crystal structure of p110γ has been elucidated (Walker *et al* 1999). The p100γ/p101 heterodimers are regulated by the Gβγ subunits of G proteins, and therefore signal through seven transmembrane G protein coupled receptors including those for chemokines. This has lead to the theory of class 1b PI 3-K being involved in migration along chemotactic gradients. This is consistent with the observed CD28 for B7 binding thus denying the T cell co-stimulatory input. The biochemical response to some of the *key*

Class II PI 3-K

Class II PI 3-Ks contain a defining C-terminal C2 domain allowing it to bind phospholipids in a Ca^{2+} dependent manner and are thus predominately membrane located (figure 9). Three isoforms of class II PI 3-K exist in humans, PI 3-K C2α, β and γ encoded by separate genes. The preferred substrates for class II PI 3-K is PI(4)*P* distinguishing it from class I PI 3-Ks which have a preference for PI(4,5)P_2. There have been no firm indications that this class of PI 3-K bind to adapter subunits or are capable of interacting with ras. The

regulation of this class of PI 3-K and their coupling to signalling pathways in response to extracellular stimuli are not well understood. Chemokines such as monocyte chemoattractant protein-1 (MCP-1) can induce an increase in lipid kinase activity in class II PI3-K immunoprecipitates (Turner *et al* 1998).

Class III PI3-K

Class III PI 3-Ks only utilises PtdIns as a substrate and is likely to be responsible for the generation of phosphatidylinositol 3-phosphate (PI3*P*) in cell membranes (figure 9). A single class of this PI 3-K has been identified in mammalian cells and this is a homologue of the yeast vesicular sorting protein Vps34p; suggesting a role for it in the membrane trafficking of proteins.

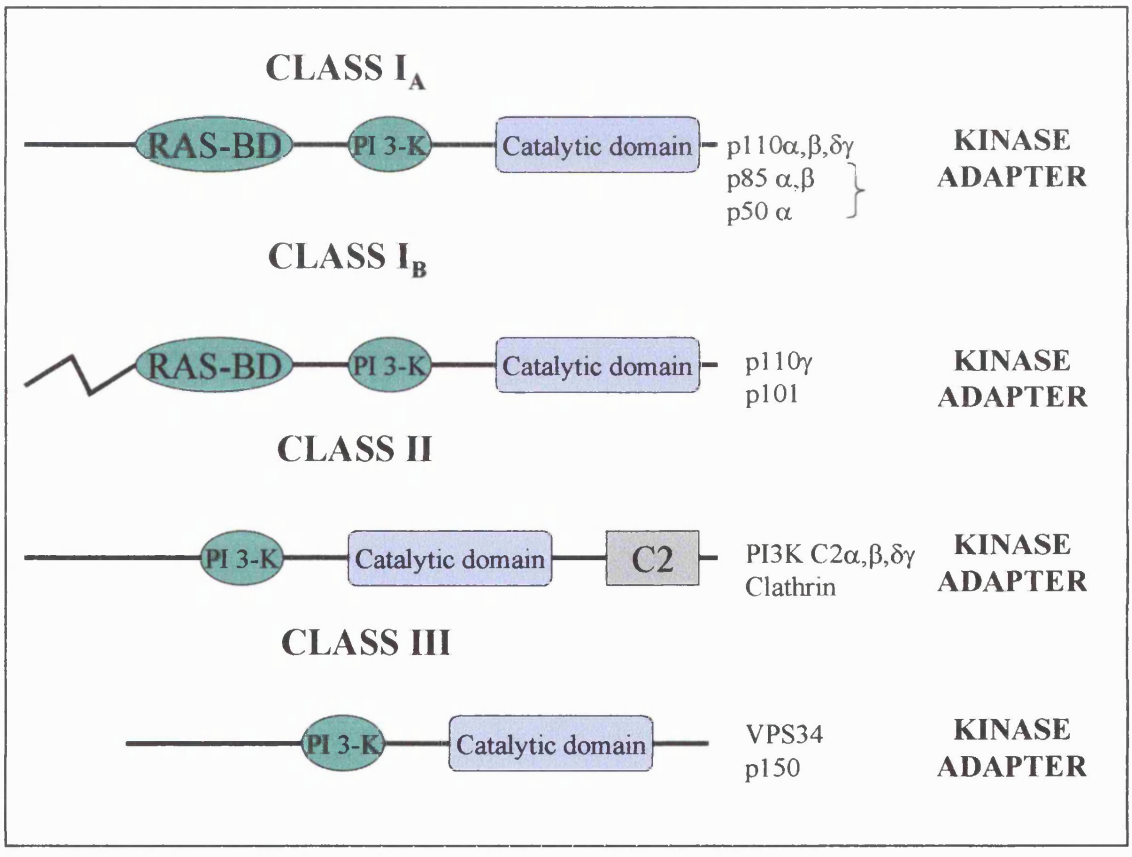

Figure 9. Schematic structures of the different class catalytic subunits of PI 3-K. Each contain a conserved catalytic domain with varied *in vitro* substrate specificity but contain different regulatory motifs including ras binding domain in class I and a C2 domain exhibited by class II PI 3-K. Specific adapter subunits are capable of binding to particular catalytic subunits as indicated.

Approaches to study PI 3K function

There are two widely used inhibitors of PI 3-K, wortmannin and LY 294002, both of which have proved invaluable in dissecting PI 3-K signalling pathways. Both inhibitors function by blocking the ATP-binding site of the catalytic subunit of PI 3-K thereby preventing phosphate transfer. Wortmannin is a non-competitive, cell-permeable fungal metabolite with an IC_{50} of 5nM. LY294002 has a higher IC_{50} of approximately 1 μM and is more widely used than wortmannin because of its greater half-life and stability, even though it does not inhibit class II PI 3K-C2α. The role of PI 3-K in CD28-mediated co-stimulation has been assessed using such pharmacological inhibitors. Both wortmannin and the structurally unrelated LY294002 can abrogate co-stimulation and IL-2 production in primary T cells (Ward *et al* 1995). Accordingly, site directed mutagenesis of the Y^{173} residue within CD28 has also been linked to impaired co-stimulation. However the role of PI 3K in CD28-mediated costimualtion is still controversial, some laboratories having shown that PI 3-K is somewhat dispensable for co-stimulation in Jurkat and murine T cells (Truitt *et al* 1996).

Genetic approaches have also been used to functionally assess PI 3K. For example, $p85\alpha^{-/-}$ deficient mice exhibit impaired B cell development and premature death (Fruman *et al* 1999). Deletion of p110α however has been shown to be embryonic lethal, suggesting an essential role for this subunit in development (Bi *et al* 1999). In contrast p110γ knockout mice are still viable but have impaired immune cell function. For example, neutrophils and macrophages display impaired chemotaxis to chemotatic stimuli (Condliffe *et al* 1999).

D-3 Phosphoinositides and phosphoinositide binding domains

PI(3)*P* is constitutively present in mammalian cells and lipid levels remain largely unaltered upon cellular stimulation. In contrast, levels of PI(3,4)P_2 and PI(3,4,5)P_3 are very low making up less than 1% of the PtdIns pool although

concentrations increase markedly upon cell stimulation. Proteins are able to interact with these D-3 phosphoinositides through specific binding domains.

The FYVE domain is named after the first four proteins shown to contain it –Fab 1p, YOTB, Vac 1p and early endosome antigen 1. FYVE domains are approximately 80 amino acids in length, are characterised by the presence of cysteine rich zinc-finger-like motifs and are able to interact with PI(3)*P*. Such domains are frequently found in proteins involved in vesicular trafficking events. The molecular basis of PI(3)P binding by FYVE domains is attributed to a positively charged patch of amino acids ((R/K)(R/K)HHCR) on an antiparallel beta sheet. Phox domains (PX), named for their presence in p40/7phox subunits in NADPH oxidase, are another recently characterised protein component capable of selective binding to PI(3)*P* (Kanai *et al* 2001).

The best-characterised D-3 phosphoinositide-binding domain however is the PH domain, named through its homology to domains in the protein pleckstrin (Lemmon *et al* 1996). The six conserved residues lie in the N-terminal region of the PH domain in a Lys-X-Sma-X_{6-11}-Arg/Lys-X-Arg-Hyd-Hyd motif (where 'X' is any amino acid, 'Sma' is a small amino acid and 'Hyd' is a hydrophobic acid) and this has been shown to mediate or be responsible for PI(3,4,5)P_3 binding (Isakoff *et al* 1998). Approximately 250 proteins expressed in humans contain such domains, with many having a varying affinity for particular D-3 phosphoinositides (Dowler *et al* 2001). Some of the proteins with varying 3-phosphoinositides binding affinities are summarised in table 3.

D-3 phosphoinositide	**PI(3,4,5)P_3 only**	**PI(3,4,5)P_3 and PI(3,4,)P_2**	**PI(3,4,)P_2 only**	**PI(3)*P***	
Binding domains	PH	PH	PH	FYVE	PX
Binding Proteins	PDK-1 BTK	PKB DAPP	TAPP	EEA1/ Fab1	p40/7phox

Table 3: D-3 phosphoinositide binding domains and some examples of preferred lipid-interacting proteins. Note that PKB and DAPP are able to interact with both PI(3,4,)P_2 and

PI(3,4,)P_2 (Dowler *et al* 2001). Abbreviations: **TAPP-1** tandem PH-domain–containing protein, **DAPP-1** dual adapter for phosphotyrosine and 3-phosphoinositides.

Downstream effectors of PI 3K dependent signalling cascades

PKB

PKB, a member of the AGC kinase family, is a serine/threonine protein kinase whose activity is wholly dependent on the generation of D-3 phosphoinositides via PI 3-K. PKB can positively and negatively regulate a plethora of target proteins and is therefore viewed as a critical upstream mediator of multiple biological processes (figure 10). In resting, unstimulated cells PKB resides in the cytoplasm, upon addition of stimulus to the cells and formation of PI(3,4,5)P_3, the PH domain of PKB mediates the cellular relocation to the inner surface of the membrane and also inducing a conformational change exposing regulatory phosphorylation sites (Meier *et al* 1997). The kinase activity of PKB is regulated by phosphorylation on residues Thr^{308} and Ser^{473} (figure 9). The PH domain containing protein, phosphoinositide dependent kinases-1 (PDK-1) is able to phosphorylate Thr^{308}, whereas an uncharacterised PDK-2 is thought to be responsible for the phosphorylation at Ser^{473} (Alessi *et al* 1997 and figure 9). Recent evidence indicates that PDK-2 may in fact be PDK-1, as it has been demonstrated that PDK-1 can associate with a PDK-1 interacting fragment-1 (PIF-1) which subsequently allows phosphorylation of both residues of PKB (Balendran *et al* 1999). The phosphorylation status of PKB *in vivo* can be monitored upon cellular stimulation via Western blotting of whole cell lysates with specific anti-phospho-PKB antibodies. The translocation and activation of PKB can be inhibited by pre-treatment with the PI 3-K kinase inhibitor wortmannin, further indicating the essential role of PI 3-K in this signalling pathway.

Another downstream target for PDK-1 is p70S6 kinase, which is also a member of the AGC kinase family (Alessi *et al* 1997). PDK-1 phosphorylates p70S6 kinase on residue thr^{252} within the carboxyl tail leading to its activation. This family of rapamycin sensitive kinases catalyse the phosphorylation of the 40S ribosomal subunits leading to increased translation of mRNA and hence protein

synthesis. Accordingly inhibition of PDK-1 activation blocks downstream activation of p70S6 kinase and blocks G1-S phase transition of the cell cycle (Flynn *et al* 2000). Embryonic stem cells that lack PDK-1 have greatly reduced PKB and p70S6 kinase activity in response to cellular stimulation (Williams *et al* 2000). PKC members namely PKCζ and PKCδ can be phosphorylated in the activation loop sites by PDK-1 in a 3'-phosphoinositide-dependent manner (Legood *et al* 1998). PKCζ can mediate the activation of mitogen/Erk-1 kinase (MEK), thus PI 3-K can impinge on Erk signalling cascade via a ras-independent mechanism.

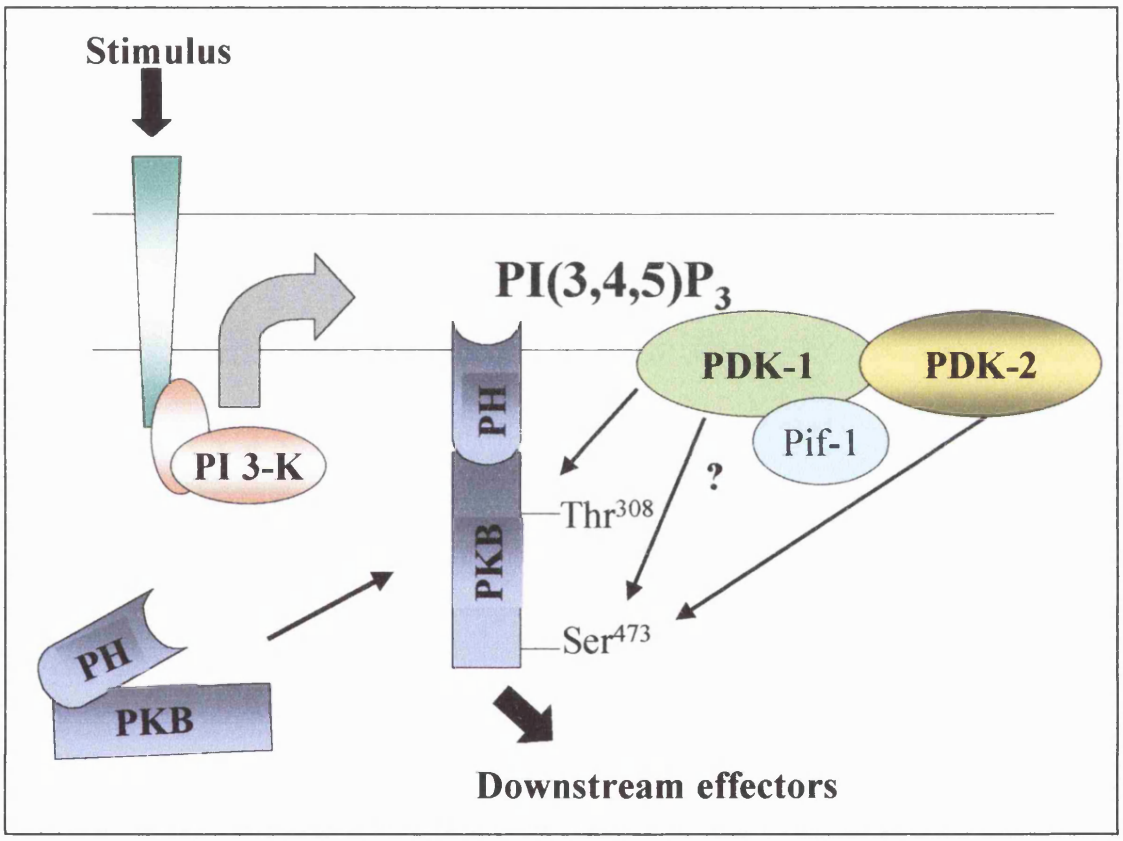

Figure 10: Diagram of PKB activation. PKB is recruited to the cell membrane via its PH domain interaction with PI(3,4,5)P_3 undergoing a conformational change and exposing regulatory phosphorylation sites. Subsequent phosphorylations on residues Thr^{308} and Ser^{473} by PDK-1/PDK-2 lead to activation of PKB that initiates PKB driven signalling pathways. *In vitro* studies suggest that Pif-1 may substitute for PDK-2 in certain cellular contexts.

The activity of PKB has been intimately linked to cellular survival. It can phosphorylate the apoptotic protein BAD on residue Ser^{136} causing it to disassociate from, and relieve the inhibition of, the pro-survival protein Bcl-x_L

(Datta *et al* 1997). PKB recognises consensus sequences in caspase 9 and PKB-mediated phosphorylation can inactivate its protease activity. PKB is also able to phosphorylate and negatively regulate members of the Forkhead transcription factors, which are responsible for the regulation of apoptotic genes including Bcl-x_L (Brunet *et al* 1999). Forkhead transcription factors are thought to promote the expression of Fas ligand, a key cell surface molecule that initiates apoptotic-signalling pathways. PKB is also able to positively regulate the activity of transcription factors. It can phosphorylate IκB, an inhibitory component of NFκB transcription factor, and mediate its degradation. Removal of this inhibitory constraint allows NFκB to move into the nucleus and bind to appropriate response elements (Kane *et al* 1999).

CD28 has been reported to activate PKB in a wortmannin dependent fashion (Parry *et al* 1997). CD28-mediated PKB activation can activate pro-survival pathways and increase expression of Bcl-x_L, a cell survival factor (figure 8). Consistent with PKBs pro-survival effects, CD28 has also been shown to be resistant to the apoptotic effect of fas (CD95) ligation (Mcleod *et al* 1998). The role of PKB in co-stimulation is still a matter for debate. Recent evidence has shown that CD28-mediated activation of PKB is central in upregulation of IL-2 and IFNγ but not Th2 cytokines (Kane *et al* 2001).

Glycogen Synthase kinase 3 (GSK3) is a multi-functional serine threonine kinase which lies downstream from PKB. As its name suggests GSK-3 is able to positively regulate the activity of glycogen synthase. GSK3 is able to phosphorylate cyclins especially cyclin-D1, and promotes their degradation (Ref-Diehl *et al* 1998). Phosphorylation of GSK3 by PKB inhibits its catalytic activity. Targets of PKB are summarised in figure 11.

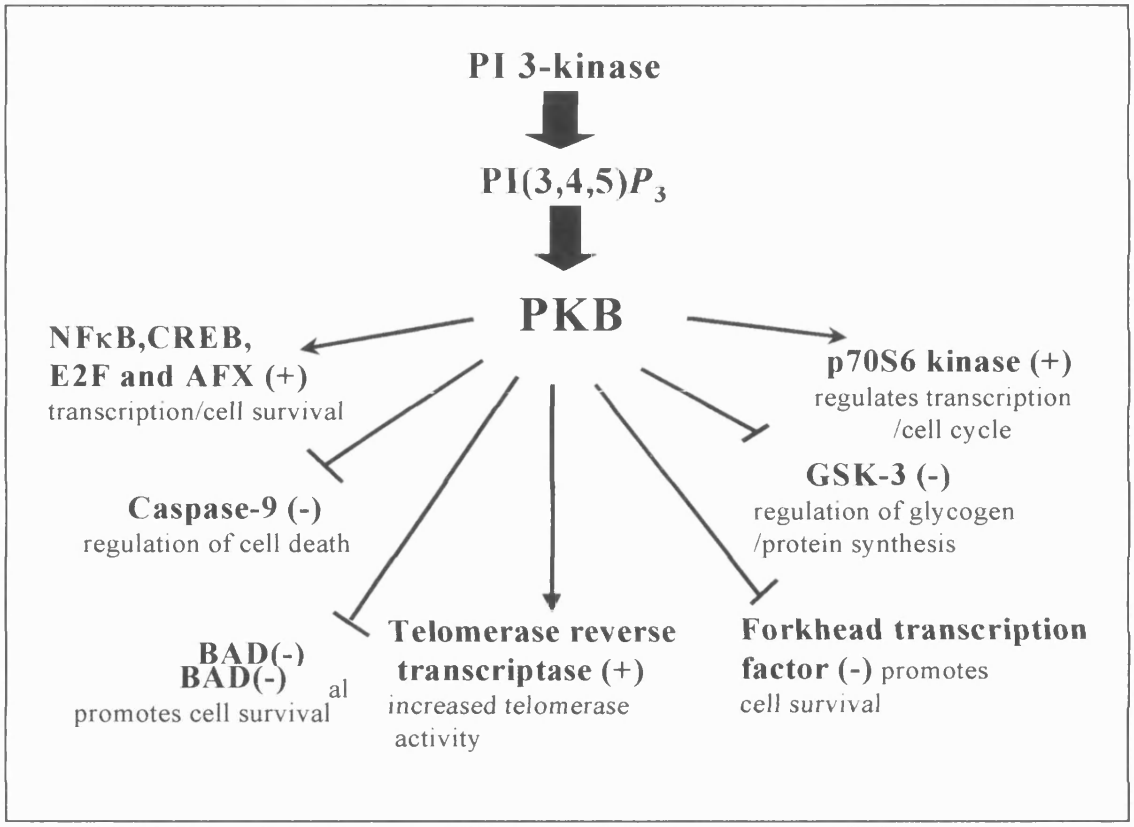

Figure 11: Multiple cellular targets for PKB. The serine threonine kinase PKB can positively and negatively regulate a host of substrates and therefore impinge upon multiple cellular processes including transcription, translation, apoptosis, glucose transport and cell division.

PI 3-K regulation of Tec family protein kinases

TEC family kinases, which include Tec and bruton's tyrosine kinase (BTK), are not membrane anchored like src kinases. The amino terminal PH domain can bind to PI 3-K products, which allows membrane localisation and subsequent phosphorylation by src kinases to achieve activation (Debnath *et al* 1999). Accordingly, PH domain mutation in Tec kinase as seen in X-linked agammaglobulinema (XLA) leads to defective Tec activation (Vihnen *et al* 2000). Activated Tec can phosphorylate PLCγ which results in IP3 and DAG generation from PI(4,5)P_2 and results in Ca^{2+} mobilisation.

PI 3-K regulation of small GTPases

There is accumulating evidence that PI 3-K plays an essential role in regulating the actin cytoskeleton by coupling to small GTPases. Small GTPases cycle between an inactive GDP-bound and an active GTP-bound form. PI 3-K is able

to indirectly regulate the activity of such GTPases by modulating the activity of exchange factors that control GTP-loading. For example, CD28-activated-PI 3-K is able to regulate the activity of Rac, a regulator of actin remodelling, via activating the guanine nucleotide exchange factor Vav which can bind D-3 phosphoinositides via PH domains (Klasen *et al* 1998). Vav-mediated activation of Rac can be inhibited by pre-treatment with PI 3-K inhibitors. Other GTPases such as the Arf family of proteins, which regulate membrane traffic, are also implicated in PI 3-K–driven signalling cascades although the mechanism by which they achieve this remain unclear.

PH-domain containing adapter proteins

A variety of adapter proteins that associate with PI 3-K lipid products have been identified and their function are starting to be analysed. The adapter protein $p62^{dok}$ contains an array of motifs involved in cell signalling including SH2/SH3 and PH domains. However no evidence has been found to suggest that the PH domain of $p62^{dok}$ interacts with D-3 phosphoinositides to date. The adapter $p62^{dok}$ may play a specific role in CD28-mediated co-stimulation as it a unique substrate for CD28 but not CD3-activated PTK (Nunes *et al* 1996). GTPase activating proteins (GAPs), which convert active GTP-bound Ras into the inactive GDP-bound state, have been reported to associate with $p62^{dok}$, implying a role for this adapter in controlling mitogenic signals. $p62^{dok}$ has also been found to associate with the SH2 domain containing inositol 5'poly-phosphatase (SHIP) which will be discussed in more detail later.

The family of Grb-2 related adapter-binding proteins (GAB) also contain PH domains. These adapters can orchestrate protein-protein interactions with Grb-2, Shc and p85 in response to IL-3 stimulation (Craddock *et al* 1997). Like p62dok, Gab-2 is also a target for PTK following cell stimulation by IL-3. This enables it to interact with SH2 domain containing proteins including the protein tyrosine phosphatase SHP-2.

The adapter proteins termed TAPP and DAPP also contain PH domains but are novel due to the fact that they can bind PI(3,4)P_2 with high affinity (Dowler *et al* 1999). This class of lipid is thought to be a product the action of 5'

phosphatases such as SHIP (discussed later). Such adapter proteins may recruit uncharacterised effectors and initiate PI(3,4)P_2 driven signal transduction thus increasing the scope and diversity of PI 3-K signalling.

Metabolism of PI(3,4,5)P_3 by inositol phosphatases

Small increases in D-3 phosphoinositides in cells can result in the initiation of diverse functional responses. It is therefore of major importance that the levels of these bioactive lipid second messengers are tightly regulated. The cell has adapted a variety of mechanisms to achieve this through expressing distinct phosphatases that remove particular phosphate residues from the inositol ring, thus antagonising the action of PI 3-K. The following sections will introduce the 3' and 5' families of phosphatidylinositol phosphatases and their role in modulating PI 3-K-mediated signalling cascades.

PTEN

The tumour suppressor, phosphatase and tensin homologue deleted on chromosome 10 (PTEN), is a 3' phosphatase capable of dephosphorylating PI(3,4,5)P_3 to PI(4,5)P_2 and thus acts in opposition to PI 3-K. The chromosomal location of PTEN (10q23) has been linked with cancers including those of the brain, bladder and prostate, where partial or entire loss of chromosome 10 is exhibited (Lundgren *et al* 1988). Linkage analysis of Cowden's disease, a cancer predisposition syndrome, has also implicated the PTEN locus (Nelen *et al* 1996). These and other findings suggested that PTEN was a novel tumour-suppressor that plays a vital role in controlling cell growth, and that its loss leads to formation of several types of cancer.

The PTEN gene encodes a 55 kDa protein, which contains the cysteine/arginine-based structure motif present in a variety of dual-specificity phosphatases (Myers *et al* 1997). *In vitro* analysis revealed that PTEN could de-phosphorylate a limited array of acidic phosphotyrosine and phosphothreonine protein substrates (Myers *et al* 1997). Further analysis of PTEN function revealed that PTEN exhibits 3' phosphatase activity towards PI(3,4,5)P_3 (Maehama *et al* 1998). The lipid phosphatase activity of PTEN was subsequently shown to be critical for its tumour suppressor function (Myers *et al*

1998). PTEN consists of 403 amino acids with the phosphatase domain lying within the N-terminal region (figure 12). PTEN is expressed in all tissue and cell types in humans. The crystal structure of PTEN has been determined and revealed an enlarged active site capable of accommodating its phosphoinositide substrate (Lee *et al* 1999). Recently PTEN2 a membrane–associated, testis specific isoform was described (Wu *et al* 2001). This novel enzyme is able to dephosphorylate PI(3,4,5)P_3 *in vitro* but seems to have a preference for the related D-3 phosphoinositide lipid PI(3,5)P_2. The carboxyl-terminal region contains two PEST sequences and a PDZ motif (postsynaptic density protein), which is dispensable for tumour suppressor function (Goergescu *et al* 1999). PEST sequences function in targeting proteins with short intracellular half-lives for protein degradation whereas PDZ domains have been implicated in mediating protein-protein interactions. The c-terminus of PTEN is believed to be important for maintaining protein stability as C-terminal deletion mutants are rapidly degraded (Vazquez *et al* 2000).

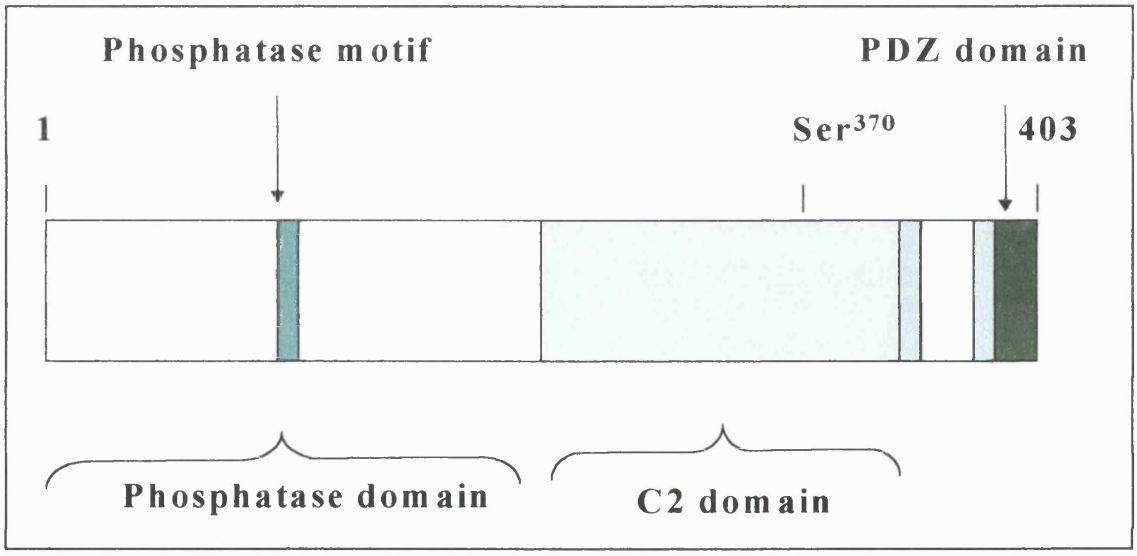

Figure 12: Schematic structure of PTEN protein showing relevant functional domains. PTEN is composed of an N-terminal 3'-phosphatase region and a C-terminal region containing two PEST sequences involved in targeting proteins for degradation, and a PDZ domain which can mediate protein-protein/membrane interactions. Within the C-terminus of PTEN lay serine/threonine residues, which can be phosphorylated and may confer protein stability.

Approaches used to study PTEN function: PTEN deficient cell lines and PTEN knockouts

PTEN has been overwhelmingly linked to the suppression of the PI 3-K pathway (Simpson *et al* 2001). The role of PTEN in controlling cellular processes and development is dramatically seen in mice *PTEN*$^{-/-}$ knockouts that die early in embryogenesis (Di Cristofano *et al* 1998). *PTEN*$^{+/-}$ heterozygotes are susceptible to a broad range of tumours and also develop an autoimmune disorder through the Fas-induced death of activated T cells (Di Cristofano *et al* 1999). Interestingly, T cell-specific deletion of the *PTEN* gene results in defects in central and peripheral tolerance, implying a central role for this phosphatase in T cell homeostasis and self-tolerance (Suzuki *et al* 2001). Introduction of PTEN into PTEN null cells leads to rapid downregulation of PKB activity as exhibited by the decreased levels of phospho-PKB. Overexpression of PTEN reduces G_1 cell cycle progression and inhibition of the PKB signalling pathways (Ramaswamy *et al* 1999) and can inhibit the activation of Rac (Kim *et al* 2002).

Regulation of PTEN activity

How expression, catalytic activity and localisation of PTEN is regulated is still unclear. It can be phosphorylated *in vivo* by casein kinase 2 (CK2) at its carboxyl tail especially, on Ser^{370} (Vazquez *et al* 2000). Phosphorylation of PTEN has been linked to increased protein stability and may mediate PTEN function. Additionally, phosphorylation of PTEN has been reported to induce its participation in an undefined protein complex (Vazquez *et al* 2001). *In vitro*, PTEN has been reported to interact with focal adhesion kinase (FAK) and cause its dephosphorylation (Tamura *et al* 1999). The exact nature of these protein interactions is unclear, but is probably mediated via PTENs PDZ domain. PTEN expression is also a target for regulation in mammalian cells. The early growth response-1 (egr-1) transcription factor has been reported to directly activate the *PTEN* gene and increase its expression during irradiation induced signalling (Virolle *et al* 2001). Accordingly, egr-1$^{-/-}$ mice are not capable of upregulating *PTEN* expression after exposure to ultra-violet light. The

Peroxisome Proliferator Receptors γ (PPARγ) and the anti-inflammatory nature of PPARγ agonists have also been reported to upregulate PTEN protein expression (Patel *et al* 2001). The PPAR family of nuclear hormone receptors will be discussed in more detail.

Other D-3 Phosphatases: Myotublarin

Myotublarin is another class of 3-phosphoinositide phosphatase. Studies have implicated myotublarin in the regulation of PI(3)*P* lipid levels, which have shown to be crucial in intracellular trafficking events (Corvera 2001). Inactivating mutations in the genes encoding myotublarin leads to the onset of X-linked myotublar myopathy indicating the important regulatory role of this phosphatase. Another myotublarin related protein MTMR3 has been identified and shown to have novel PI(3,5)P_2 substrate specificity *in vitro* and *in vivo,* thus defining the first route for the cellular production of PI(5)*P* (Walker *et al* 2001).

Inositol 5-Phosphatases

There are numerous inositol 5-phosphatases, all of which are magnesium-dependent phosphomonoesterases, that can be grouped into 4 broad classes depending on their substrate specificity (table 4). There are 4 known substrates for 5-phosphatases namely the water-soluble Ins(1,4,5)P_3 and Ins(1,3,4,5)P_4 and the lipids PI(4,5)P_2 and PI(3,4,5)P_3. As their name suggests, 5-phosphatases selectively catalyse the dephosphorylation from position 5 on the inositol ring and members of this family are defined by two signature motifs (FI)W*X*GD*X*N(F/Y)R and (R/N)*X*P(S/A)(WT)(C/T)DR(I/V)(L/I) which define the proteins as inositol polyphosphate 5'phosphatases (Jefferson *et al* 1996). The following sections will focus on the group III 5'phosphatases that comprise the SH2 domain containing Inositol 5' (poly)-Phosphatase (SHIP) and related proteins.

Group	Substrate(s)	5-Phosphatase	Function	Reference
I	Ins(1,4,5)P_3 Ins(1,3,4,5)P_4	Platelet - 5'phosphatse	Terminates $Ca2^+$ signalling	(Matzaris *et al* 1994)
II	Ins(1,4,5)P_3 Ins(1,3,4,5)P_4 PI(4,5)P_2 PI(3,4,5)P_3	OCRL Synaptojanin Synaptojanin II	Synaptic vesicular trafficking, Lysosome trafficking	Majerus *et al* 1999)
III	Ins(1,3,4,5)P_4 PI(3,4,5)P_3	SHIP-1 SHIP-2	Inhibitory signalling of PI 3-K	(Damen *et al* 1996)
IV	PI(3,4,5)P_3	Group IV phosphatase	Unknown	(Jackson *et al* 1995)

Table 4: Table to summarise the grouping of inositol 5-(poly)-phosphatases, their substrate specificity and function. Type III phosphatases comprise the SHIP proteins that will be discussed in more detail in this section.

SHIP proteins: Structure and expression

The diverse role of SHIP in modulating inositol signalling has been the focus of much research. SHIP exhibits selective specificity to inositol substrates that are phosphorylated on the 3' position on the inositol ring i.e. PI-3K products (Damen *et al* 1996) and therefore generate the products PI(3,4)P_2 and Ins(3,4)P_2 respectively (figure 13). SHIP was initially observed as a 145 kDa protein that becomes tyrosine phosphorylated in response to cytokine receptor stimulation

(Damen *et al* 1993). SHIPs enzymatic activity does not appear to be dependent on tyrosine phosphorylation. Rather, it is believed that SHIP is a constitutively active cytosolic protein, and therefore its cellular localisation is critical to its mechanism of action towards its substrates (Phee *et al* 2000). Edmunds *et al*, however, have demonstrated a correlation with tyrosine phosphorylation of SHIP following CD28 stimulation and an increase in phosphatase activity towards an Ins(1,3,4,5)P_4 substrate *in vitro*.

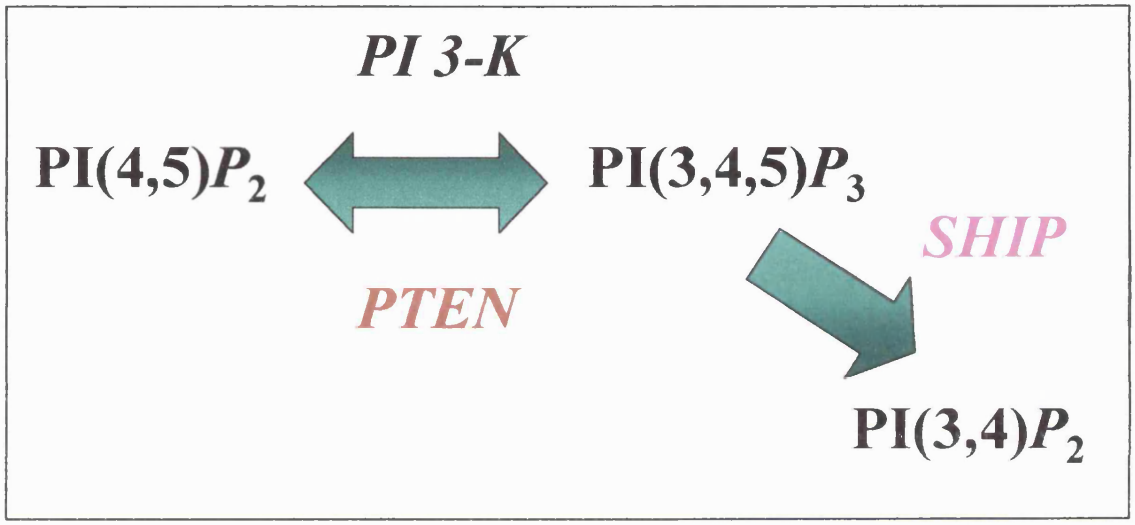

Figure 13: Metabolism of PI(3,4,5)P_3 by the phosphatases PTEN and SHIP. PTEN directly antagonises the catalytic activity of PI 3-K whereas the 5-phosphatase SHIP is able to generate another D-3 phosphoinositide PI(3,4)P_2 potentially initiating PI(3,4)P_2 driven signalling cascades.

The human SHIP gene has been mapped to chromosome 2 between 2q36 and 2q37 (Ware *et al* 1996). SHIP contains 1190 amino acid residues and a plethora of motifs that can mediate multiple protein-protein interactions (figure 14). It contains a conserved N-terminal SH2 domain that is vital for its ability to associate with signalling proteins. The central region of SHIP encodes the 5-phosphatase domain, whilst the C-terminal contains phosphotyrosine binding sites (PTB) and several putative PxxP motifs that may mediate interactions with proteins containing SH3 domains. C-terminal truncations of SHIP result in the generation of 135 and 125 kDa isoforms of SHIP (Damen *et al* 1998). Interestingly, it has been reported that p135 SHIP can substitute for p145 SHIP in inhibitory signalling in B cells (March *et al* 2000). The C-terminus of SHIP,

although lacking catalytic activity, is essential for hydrolysis of PI(3,4,5)P_3 and the resultant inhibition of PI(3,4,5)P_3 (Damen *et al* 2001) and FcγRIIB1 inhibitory signalling events in B cells (Aman *et al* 2000). Membrane targeting of these SHIP mutants was able to restore the activity suggesting that the C-terminus is important in localisation and/or stabilisation of SHIP at **the plasma membrane.**

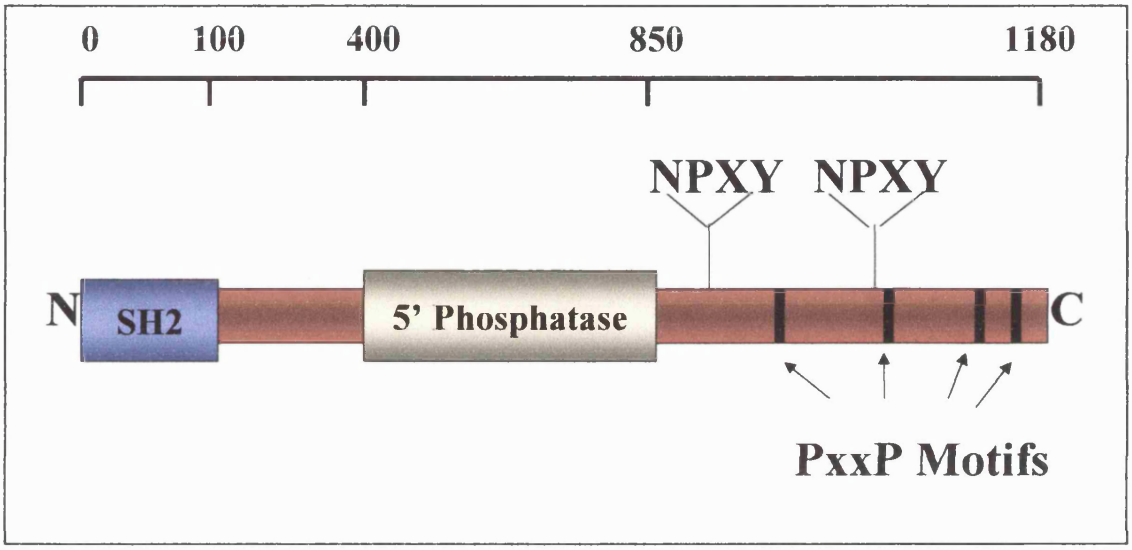

Figure 14: Schematic structure of p145 SHIP showing relevant functional domains and approximate scale in amino acids of the mature protein. SHIP contains an N-terminal SH2 domain which can interact with specific phosphotyrosine residues and a central, conserved 5'phosphatase catalytic domain. The c-terminal contains several motifs involved with protein-protein interactions including proline rich (PxxP) motifs and motif that are involved with PTB interactions.

Expression of SHIP is restricted to haemopoietic cells and in cells of the testis (Liu *et al* 1998), although the role of this membrane-localised phosphatase in spermatogenesis is unclear. In 1997, a second 5'phosphatase was cloned containing homology to the type-III phosphatase SHIP and was therefore termed SHIP 2 (Pesesse *et al* 1997). In contrast to SHIP, SHIP2 is ubiquitously expressed in all tissue types and is co-expressed with SHIP in T and B lymphocytes, however the degree of functional overlap between the two phosphatases, if any, are poorly defined (Bruyns *et al* 1999). Its mRNA levels being particularly high in heart, skeletal muscle. SHIP 2 has the same substrate specificity as SHIP i.e. it only hydrolyses the 5'-phosphate residue on D-3-phosphorylated inositides or phosphatidylinositides. SHIP 2 possesses the

same overall structure as SHIP, with an N-terminal SH2 domain, a central 5' phosphatase domain and proline-rich/PTB motifs at the C-terminus.

SHIP2 exhibits 40% overall sequence homology to SHIP and migrates at 155 kDa on SDS-PAGE gels. SHIP and SHIP2 however display little homology to the 3'-phosphatase PTEN. A novel form of SHIP termed s-SHIP (stem cell SHIP) has recently been identified and is expressed in embryonic and haemopoietic cells, but not in lineage-committed or mature haemopoietic cells (Tu *et al* 2001). This novel 104 kDa splice variant of mature SHIP lacks an N-terminal SH2 domain and does not become tyrosine phosphorylated following cellular stimulation (unlike other SHIP isoforms).

SHIP knockout mice

Mice which are $SHIP^{-/-}$ are viable and almost indistinguishable from their wildtype littermates. $SHIP^{-/-}$ mice do not appear to have an increased susceptibility to cancer, although they do exhibit haemopoietic perturbations and a decreased life span (Helgason *et al* 1998). Macrophages from $SHIP^{-/-}$ mice have decreased Fcγ receptor-mediated phagocytic capability, implying a role of SHIP in phagocytosis (Cox *et al* 2001). The *SHIP* gene therefore has not been designated as a tumour suppressor like PTEN as $PTEN^{-/-}$ mice exhibit a far more severe phenotype being embryonic lethal. The presence of other SHIP homologues such as SHIP2 may be able to compensate somewhat for loss of SHIP, in deficient mice, as SHIP2 is also expressed in haematopoietic cells. Lack of SHIP in $SHIP^{-/-}$ mice has been reported to play critical roles in B cell development and responsiveness (Helgason *et al* 2000). B cells derived from such mice display enhanced proliferation and therefore suggesting that SHIP may play a role as a negative regulator of immune cell signalling. In addition neutrophils and mast cells from $SHIP^{-/-}$ mice have been shown to be less susceptible to programmed cell death induced by various apoptotic stimuli or by growth factor withdrawal (Liu *et al* 1999). Interestingly, SHIP 2 has been proposed to control insulin sensitivity as mice *SHIP 2* $^{-/-}$ mice lead to increased sensitivity to insulin that results in perinatal death (Clement *et al* 2001). Adult mice heterozygous for SHIP 2 have increase glucose tolerance, characterised

by increased recruitment of glucose transporters (GLUT 4) and glycogen synthesis.

Biological roles of SHIP in cell signalling

The diverse mechanisms of SHIPs biological function in haemopoietic cells are beginning to be unravelled. SHIP has been proposed to be a negative regulator of the PI 3-K signalling pathway through hydrolysis of PI(3,4,5)P_3 (Liu *et al* 1999). This reduction in PI(3,4,5)P_3 correlates with reduced PKB activity and cellular survival despite the *in vitro* data suggesting that PKB can associate with the lipid product of SHIP hydrolysis, PI(3,4,)P_2. The mechanism of SHIPs negative regulation of PKB activity probably occurs via regulating its membrane localisation from the plasma membrane to the cytoplasm (Carver *et al* 2000 and figure 15). Presumably cytosolic PKB is unable to mediate its anti-apoptotic signals thus rendering the cell more susceptible to apoptosis.

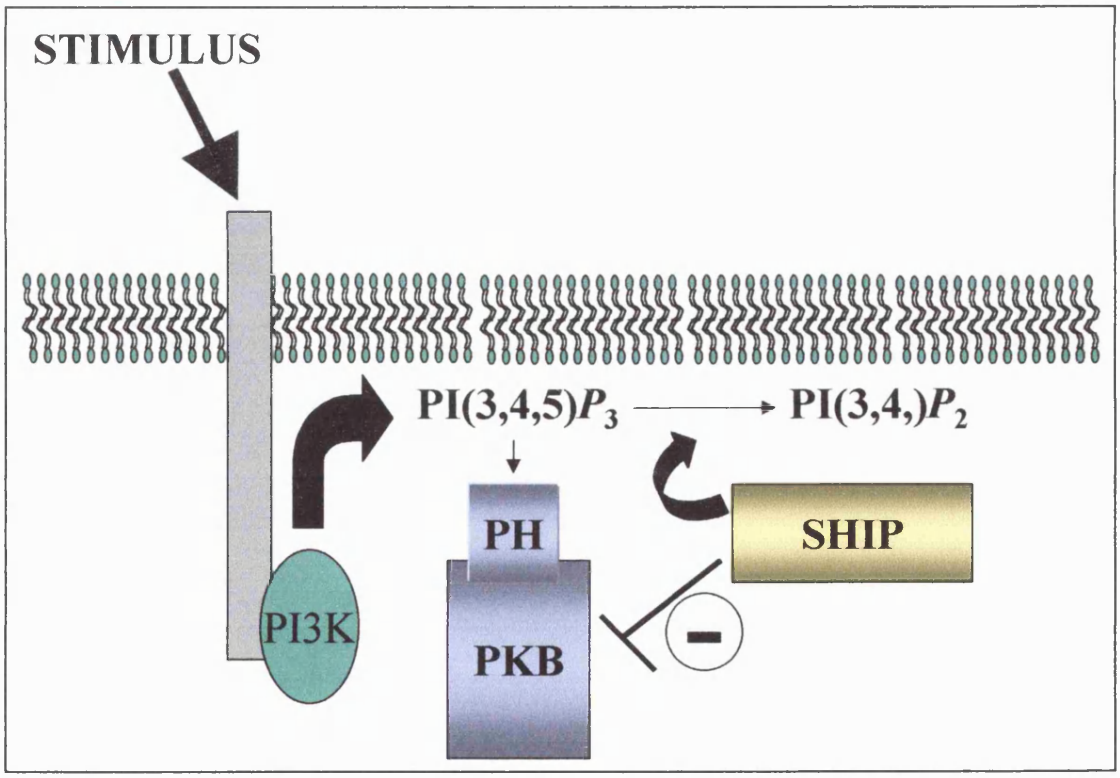

Figure 15: Model for regulation of PKB activity by SHIP. Cell stimulation can induce PI 3-K to elevate PI(3,4,5)P_3 levels and mediate the activation of PKB and its downstream effectors. Membrane localisation of SHIP can result in the hydrolysis of PI(3,4,5)P_3 to PI(3,4)P_2 which abrogates PKB membrane association and thus negatively regulate PKB-driven signalling cascades.

It is interesting to note that SHIP is a downstream target for a large number of cytokine receptor/antigen receptor-activated PTK (Liu *et al* 1997 and Edmunds *et al* 1999). The kinase(s) responsible for the tyrosine phosphorylation of SHIP remain undefined. In T cells, recombinant $p56^{lck}$ has been demonstrated to phosphorylate SHIP (Lamkin *et al* 1997). The tyrosine phosphorylation of SHIP has been linked to its cellular redistribution form the cytosol to the plasma membrane (Edmunds *et al* 1999). The adapter proteins Shc and Grb-2, important positive mediators of the Ras/MAPK mitogenic pathways are able to bind to SHIP following cellular stimulation (Damen *et al* 1996 and Harmer *et al* 1999). Shc is able to bind to tyrosine phosphorylated SHIP via PTB domain interaction with NPXY motifs and also via the SH2 domain of SHIP as determined by co-immunoprecipitation studies of wildtype and mutant SHIP (Lamkin *et al* 1997 and Liu *et al* 1997). The functional consequences of these protein interactions are presently unclear. SHIP may employ these adapters to serve its membrane localisation and subsequent positioning to its PI(3,4,5)P_3 substrate. Alternatively, SHIP may sequester these adapters and disrupt the Sos/Shc/Grb2 protein scaffold, thereby potentially negatively regulating the Ras/MAPK pathway (Tridandapani *et al* 1997 and figure 16). The consequences of these protein-protein interactions clearly deserve further investigation.

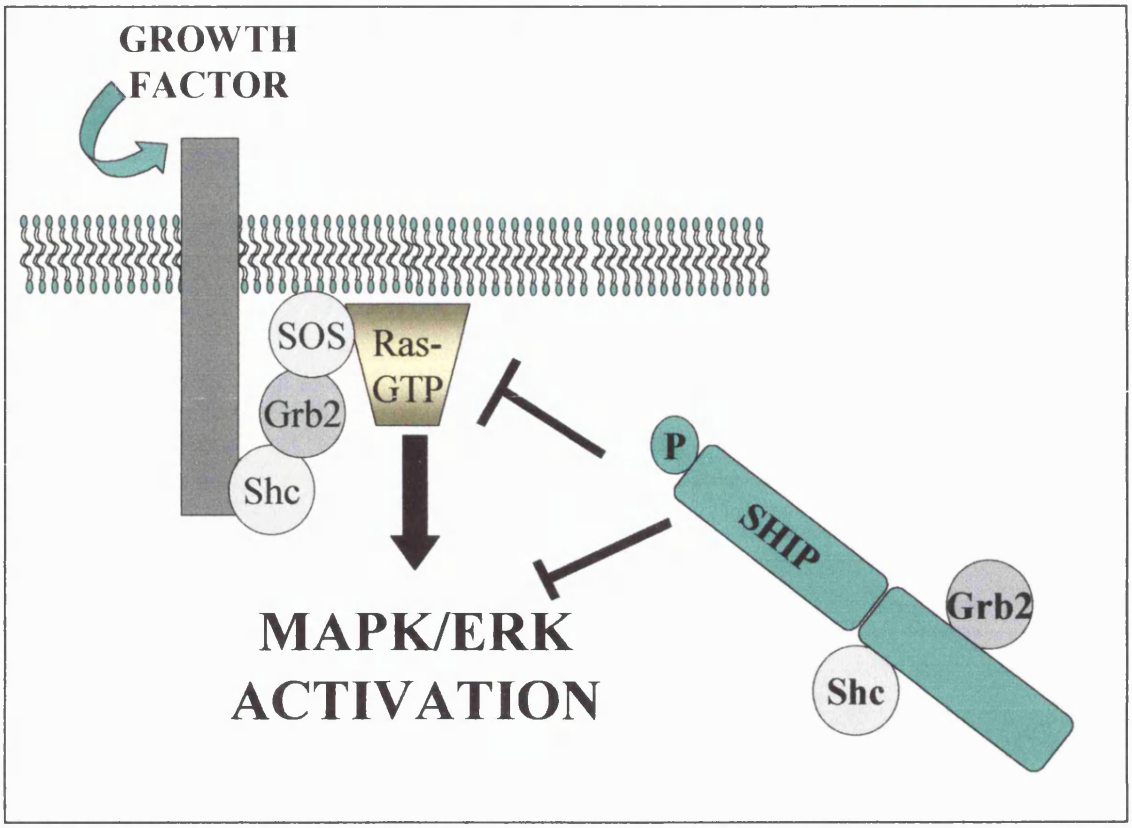

Figure 16: Potential mechanism for the regulation of MAPK/ERK mitogenic pathways by SHIP following cellular stimulation. SHIP can become tyrosine phosphorylated by unidentified tyrosine kinases, which interact with proteins with SH2/PTB domains. SHIP is thus able to sequester proteins/co-factors (i.e. Shc/Grb-2) involved in activating ras thus leading to down-modulation of ras effector pathways.

Another prominent protein that can bind to SHIP following cellular stimulation is the protein tyrosine phosphatase SHP-2 (Sattler *et al* 1997). This interaction occurs within the SH-2 domain of SHIP, as assessed by immunoprecipitation studies, although these interactions may be mediated indirectly via other proteins (Liu *et al* 1997). Following cellular stimulation and tyrosine phosphorylation, SHIP is subject to dephosphorylation possibly by SHP-2. The effect of dephosphorylation is to alter SHIPs cellular distribution and down-regulate functional activity.

The amino terminal SH2 domain of SHIP binds selectively for immunoreceptor tyrosine-based inhibition motifs (ITIM). These motifs are found on various inhibitory receptors that following tyrosine phosphorylation recruit proteins, including SHIP and the protein tyrosine phosphatase SHP-1, to the receptor,

thus initiating inhibitory signalling events. Many of the negative signalling capabilities of SHIP proteins have been elucidated by the study of the Fcγ receptors in B cells.

Positive signals in B cells are generated when antigen encounters and crosslinks B cell receptors (BCR), with resultant activation of PI 3-K and generation of PI(3,4,5)P_3. The non-receptor Tec-family kinase, Bruton tyrosine kinase (Btk), can then interact with PI(3,4,5)P_3 via its PH domain, thereby tethering it to the membrane and allowing it to activate PLCγ2. This lipase can then hydrolyse the abundant lipid PI(4,5)P_2 to form DAG and IP3 which activate PKC and respectively stimulate the release of Ca^{2+} (figure 17). All these positive signals culminate in B cell proliferation and the generation of high affinity antibodies beneficial to the host. In contrast, negative signalling in B cells occurs when saturated levels of antibody co-ligate the BCR with the FcγRIIB. This receptor crosslinking ultimately generates inhibitory signals, which abrogates B cell proliferation and differentiation. A key step in this inhibition is the recruitment of SHIP, via its SH2 domain, to the ITIM motif in the FcγRIIB, placing it in juxtaposition with PI(3,4,5)P_3 and converting it to PI(3,4,)P_2. This eliminates the high affinity binding site for Btk and mediates its return to the cytoplasm (Bolland *et al* 1998 and Scharenberg *et al* 1998). SHIP is therefore able to attenuate Ca^{2+} signals in B cells leading to reduced B cell proliferation and susceptibility to apoptosis (figure 17).

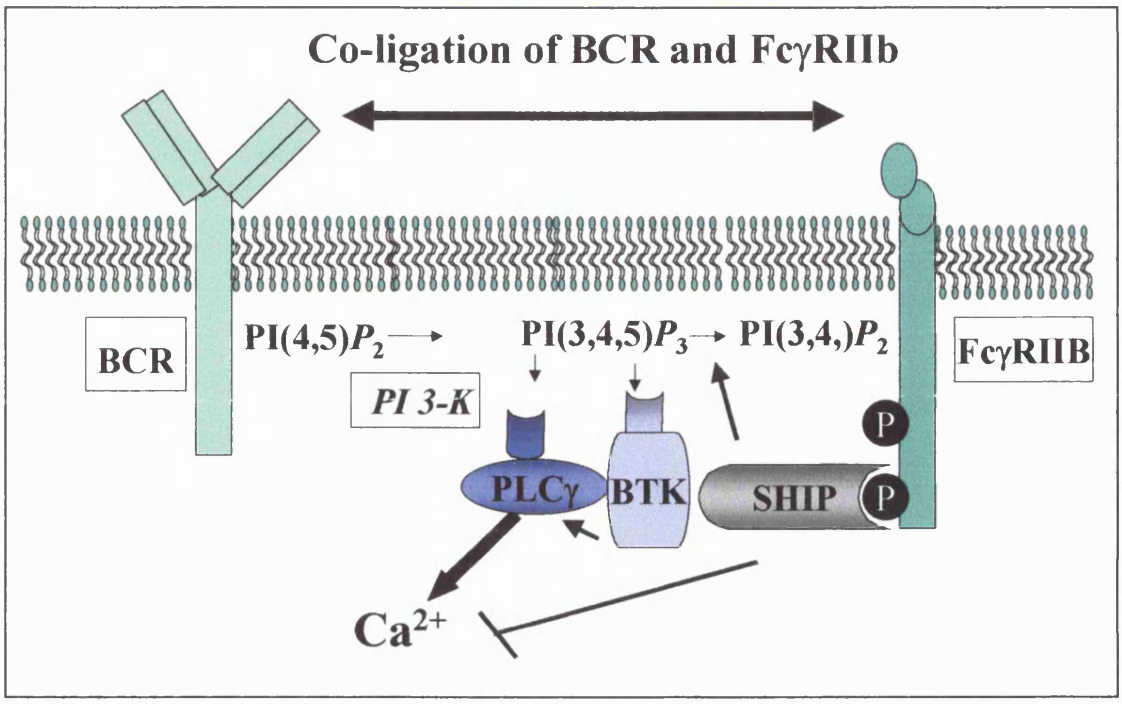

Figure 17: SHIP attenuation of calcium signalling following BCR/FcγRIIB inhibitory signalling. Stimulation of BCR results in recruitment of PI 3-K and formation of PI(3,4,5)P_3 which forms high affinity binding sites for Btk and PLCγ. Subsequent activation of PLCγ results in activation of the calcium-signalling pathway. Antibody co-ligation with FcγRIIb results in the tyrosine phosphorylation of ITIMs within its cytoplasmic tail that can recruit SHIP. The subsequent 5'-phosphatase action on PI(3,4,5)P_3 disrupts membrane association of BTK thus blocking PLCγ-mediated Ca^{2+} flux.

SHIP binding to the phosphorylated ITIM in the FcγRIIB receptor has been correlated with a decrease in activation of MAPK. A possible mechanism for this observation may be explained by the ability of SHIP to interact with the PH domain containing adapter protein $p62^{dok}$. SHIP has been shown to associate with tyrosine phosphorylated p62dok via is SH2 domain leading to a decrease in Erk activity following FcγRIIB stimulation (Tamir *et al* 2000). This adapter protein has been previously characterised as binding to p120-rasGAP protein, which can accelerates the conversion of ras-GTP into inactive ras-GDP and thus negatively regulates the MAPK pathway (figure 18). Such a protein assembly has been observed in CD150 signalling a co-receptor expressed in T and B cells also known as SLAM and has been linked to the inhibition of expression of IFNγ (Mikhalap *et al* 1999).

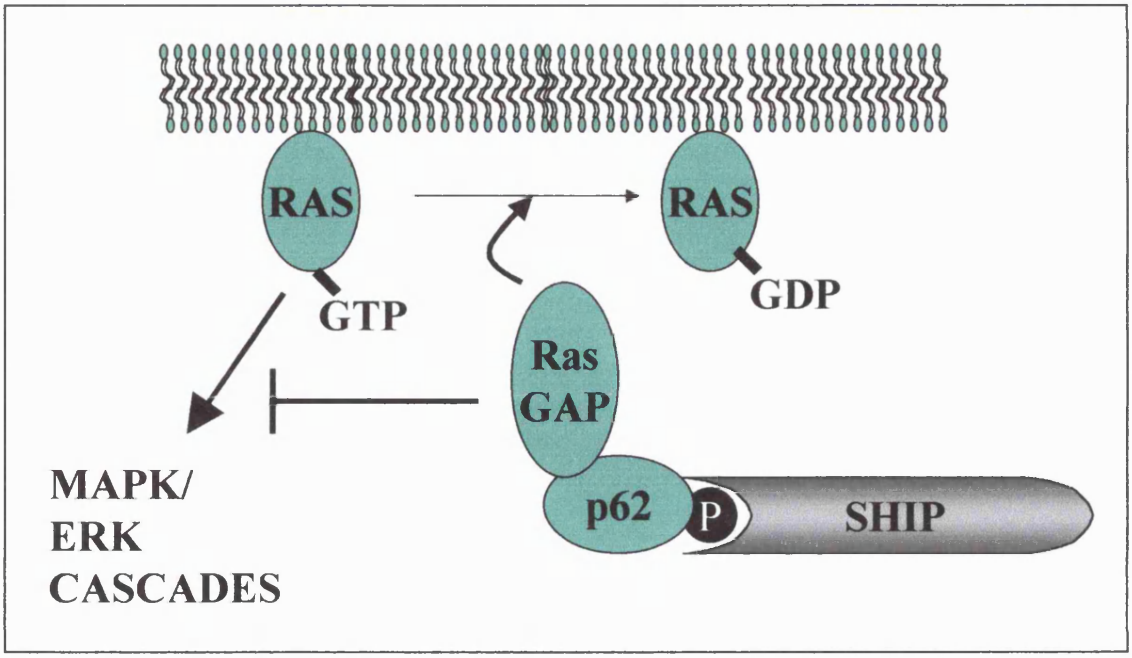

Figure 18: SHIP regulation of MAPK/Erk signalling via regulation of Ras. SHIP is able to associate via its SH2 domain to the adapter protein p62 that complexes with the p120-rasGAP, which is able to mediate the conversion of active-GTP-bound ras to inactive-GDP-bound ras thus negatively regulating MAPK signalling cascades.

SHIP has been mainly thought of as exerting negative or inhibitory signals. However, there are situations where SHIP actually enhances a functional response. In a myeloid cell line overexpression of wildtype SHIP significantly enhanced cell adhesion to intracellular adhesion molecules 1 (ICAM1), whereas expression of a phosphatase 'dead' SHIP had no positive effect (Rey-Ladino *et al* 1999). This implies that the increase in PI(3,4)P_2 levels following SHIP-mediated hydrolysis of PI(3,4,5)P_3 may be of importance in cell adhesion. SHIP has been shown to set thresholds for the degranulation of mast cells. Degranulation, with subsequent release of inflammatory mediators, can be achieved via an IgE-mediated mechanism involving PI 3-K. Interestingly, IgE addition to SHIP$^{-/-}$ mast cells, but not in wildtype counterparts, resulted in massive degranulation (Huber *et al* 1998). The c-terminus of SHIP was shown to be essential for this effect as assessed by the use of mutant SHIP constructs (Damen *et al* 2001).

Peroxisome Proliferator-Activated Receptors (PPAR)

The PPARs were identified as nuclear receptors that upon appropriate agonistic treatment could increase the size and number of peroxisomes in rodents (Issemann *et al* 1990). The peroxisome is a subcellular organelle with wide ranging functions including removal of molecular oxygen and the synthesis of glycerolipids. Initial characterisation of PPARs revealed that the receptor functioned in lipid metabolism by regulating genes involved in β-oxidation and fatty acid metabolism within the peroxisome organelle thus regulating lipid metabolism (Dryer *et al* 1993). These ligand-dependent nuclear transcription factors comprise a family of three subtypes termed PPARα, PPARβ/δ and PPARγ, each encoded by three separate genes and displaying a distinct pattern of tissue expression and ligand specificity (table 5). The function of the PPARs is generally far removed from the biochemistry and proliferation of the peroxisome organelle itself.

Upon ligand binding, PPARs undergo a conformational change and form heterodimers with 9*cis*-retonoic acid receptors (RXR) and bind to specific peroxisome proliferator response elements (PPRE) in their target genes (figure 19). PPREs consist of a direct repeat of the nuclear receptor hexameric AGGTCA recognition sequence separated by one or two nucleotides (Ijenberg *et al* 1997). Structurally PPARs contain a variable N-terminal domain containing a DNA binding motif that includes two zinc fingers. The c-terminus contains a dimerisation domain and a large hydrophobic pocket that allows ligand binding (Nolte *et al* 1998). Ligand-dependent transcription of the PPARs requires a highly conserved motif, termed activating function-2 (AF-2) located at the C-terminus of the protein. AF-2 domains are common in ligand-dependent nuclear receptors and are required for effective interaction with co-activating proteins and therefore regulation of target genes. Although PPAR-β/δ is widely expressed it's ligands and function are ill-defined (table 5). The lack of any characterised ligand for the PPARβ/δ isoforms place them in the category of an orphan receptors. PPAR α/γ isoforms have a more restricted tissue expression

and a more defined function (table 5). The following sections will focus on the role of PPARγ isoform in inflammatory responses in haemopoietic cells.

Isoform	Size	Expression	Function	Ligand
PPARα	**468aa**	**Liver, Kidney** **Heart** **Muscle**	**Anti-inflammatory** **Lipid metabolism**	**Leukotriene B4**
PPARβ/δ	**441aa**	**Ubiquitous**	**Largely unknown**	**Long chain fatty acids**
PPARγ	**479aa**	**Adipose** **Blood-lineage**	**Anti-inflammatory** **Gene expression** **Apoptosis** **Cell differentiation**	**Prostaglandin (15-deoxy-$\Delta^{12,14}$-prostaglandin J_2)** **Thiazolidinedio-nes (TZDs)**

Table 5: Distinguishing characteristics of the isoforms of the PPARs. The ligands and function for the PPAR β/δ isoform are poorly characterised. PPARα is expressed predominately in muscle, liver and kidney tissues and its natural ligands are Leukotriene B4. PPARγ is found abundantly expressed in adipose tissue and immune cells and has many potential natural agonists, the best characterised being prostaglandin J_2.

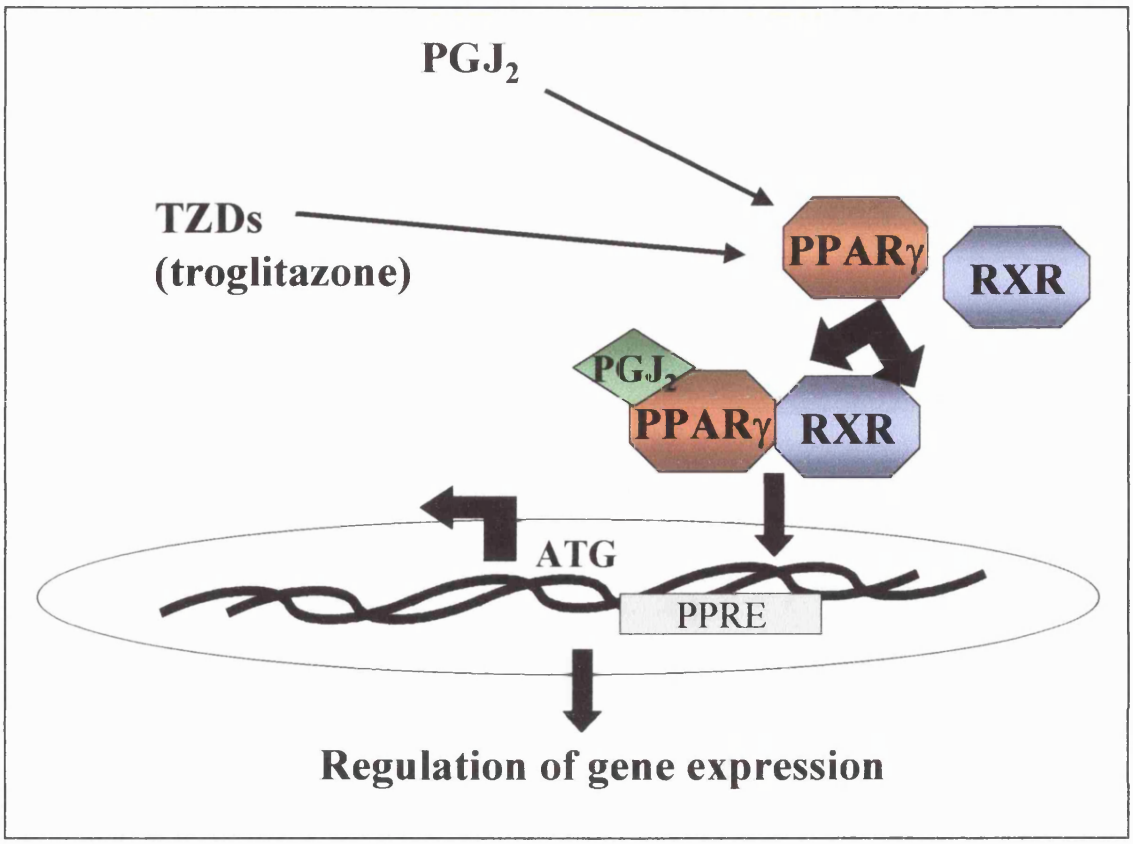

Figure 19: Mechanism of action for gene regulation by PPARγ. Ligand-activated PPARγ is able to form a heterodimer with the retonoic acid receptor and bind to specific PPARγ response elements (PPRE) upstream of target genes and modulate their expression. PPREs consist of a direct repeat of the nuclear receptor hexameric AGGTCA recognition sequence separated by one or two nucleotides.

Function of PPARγ

PPARγ is the most intensively studied PPAR isoform and is known to participate in an increasingly diverse array of biological responses. PPARγ receptors are abundantly expressed in adipocytes and expressed at lower levels in hepatocytes and haemopoietic cells including T cells (Harris *et al* 2001). There are two distinct isoforms of PPARγ termed PPARγ-1 and PPARγ-2 differing by a 30 amino acid extension within the N-terminal domain, which differ in their tissue distribution (Mukherjee *et al* 1997). The natural ligand for PPARγ is the prostaglandin 15-deoxy-$\Delta^{12,14}$-prostaglandinJ_2 (15d-PGJ_2), a product of arachidonic acid breakdown via a cyclooxgenase (COX) dependent mechanism (figure 20). Synthetic tyrosine-based thiazolidinediones (TZDs) compounds are selective agonists for PPARγ and include troglitazone, pioglitazone and

ciglitazone, which have made clinical headway's in the treatment of type II diabetes by sensitising tissues to the effects of insulin (Grossman *et al* 1997). However troglitazone has recently been withdrawn for clinical treatment due to adverse effects on the liver. Interestingly, these drugs were initially developed without knowledge of their molecular target and their mechanism of the action remains poorly defined.

PPARγ activation promotes cell differentiation in a variety of cell types and has been proposed as a master regulator of adipocyte differentiation. PPARγ is able to upregulate genes essential for adipocyte fatty-acid uptake, glucose transport and lipogenesis (Kliewer *et al* 1995). Indeed retroviral expression of PPARγ in cultured fibroblasts induced differentiation of these cells into adipocytes upon addition of PPARγ agonists (Tontonoz *et al* 1994). More recently activation of PPARγ has been shown to induce the differentiation of monocytes into macrophages and to regulate expression of the scavenger receptor CD36 (Moore *et al* 2001). It has been reported that regulation of PPARγ in adipocytes can be depressed by phosphorylation via MAPK (Shoa *et al* 1998).

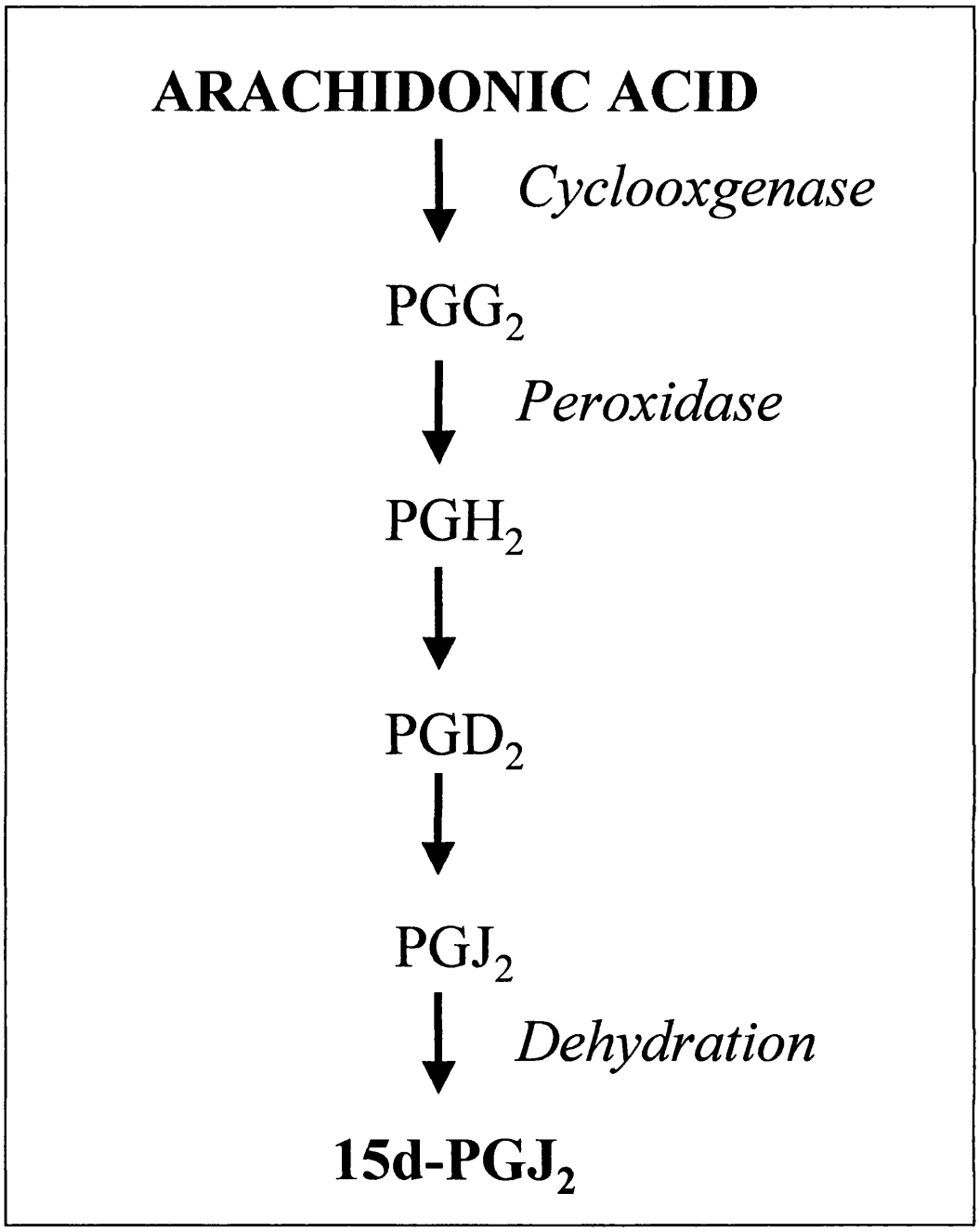

Figure 20: Generation of 15d-PGJ_2 from arachidonic acid. Cyclooxgenase and molecular oxygen forms the cyclic prostaglandin PGG_2. Successive peroxidase and dehydration events leads to the generation of the PPARγ ligand 15d-PGJ_2.

Like PPARα, PPARγ has many reported anti-inflammatory effects. In macrophages, PPARγ has been demonstrated to reduce cytokine production (TNFα, IL-1 IL-8) via treatment with 15d-PGJ_2, used at micromolar levels, at the level of gene transcription (Zhang *et al* 2001). Macrophages treated with various PPARγ agonists cannot be activated by various stimuli including IFNγ as assessed a reduction in markers of macrophage activation. T-lymphocytes also

express the PPARγ receptor and treatment with 15d-PGJ_2 has been proposed to induce apoptosis in transformed murine T cells but interestingly not in normal human T cells (Harris *et al* 2002). T-lymphocytes activation can be inhibited by pre-treatment with PPARγ agonists via reduction in IL-2 expression (Yang *et al* 2000). The activated PPARγ receptor was proposed to physically associate with NFAT, thus blocking NFAT binding to the IL-2 promoter with a concomitant reduction in gene expression. Other mechanisms have been proposed to decipher the role of PPARγ in controlling gene expression. PPARγ has been demonstrated to abrogate binding of the AP-1 complex and NFκB to their response elements in target genes (Chung *et al* 2000). PPARγ agonists may possess an clinical potential in the treatment of T cell-mediated diseases including T cell leukaemia. In addition, PPARγ ligands have also shown promise in inhibiting inflammation in epithelial cells (Su *et al* 1999), and may hold promise as a therapy in various inflammatory bowel diseases, including Crohn's disease. Some of the anti-inflammatory effects of PPARγ can be summarised in figure 20.

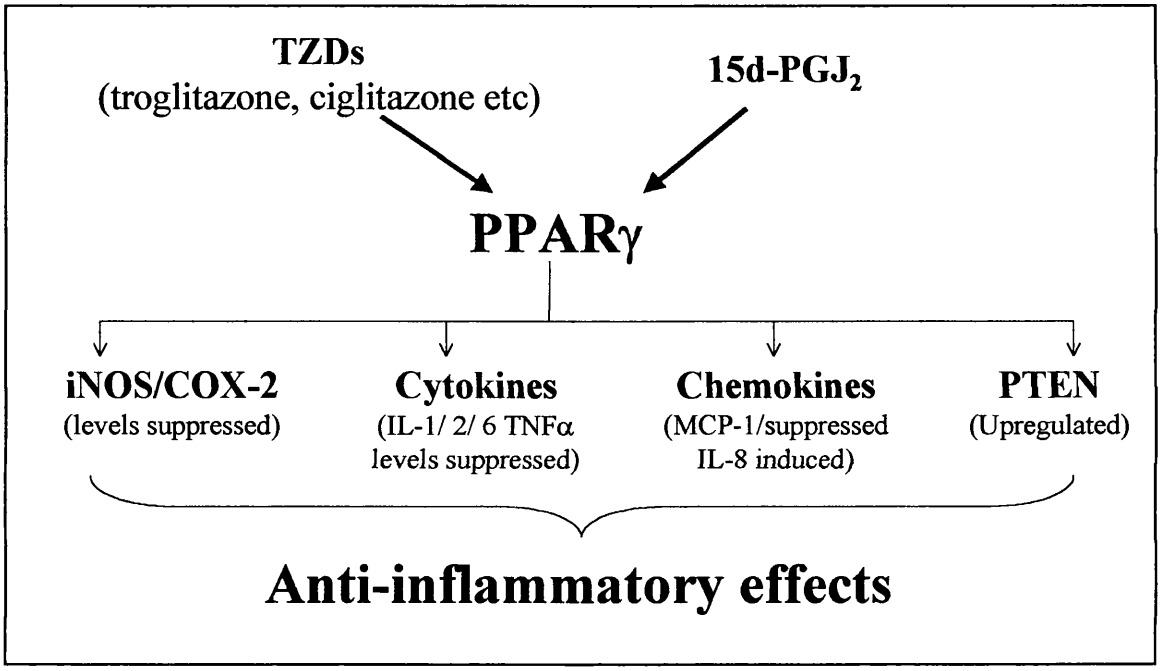

Figure 20: Anti-inflammatory effects of PPARγ. Upon ligand binding by 15d-PGJ_2 or by TZDs, PPARγ can regulate expression of chemokines, cytokines and the tumour suppressor PTEN thus exerting it's anti-inflammatory effect. PPARγ can also downregulate inducible nitric oxide synthase (iNOS) and cyclo-oxygenase-2 (COX-2) both involved in inflammation. PPARγ therefore is an attractive drug-target in inflammatory disorders.

PPARγ receptors and agonists have also been demonstrated in various studies to regulate cell growth and tumour-growth in certain cell types of rodents and to lesser extent, in humans. The anti-proliferative effects of PPARγ ligands in adipocytes had been established for some time before testing on malignant cell lines and tumours. Conflicting evidence from mice and humans has confused the role of PPARγ ligands in controlling cell growth. Initial studies suggested that PPARγ agonists promote tumorigenesis in mice (Leferbvre *et al* 1998) whereas a study in humans supports a protective role for these drugs in colon cancer (Saraff *et al* 1998). Clearly these discrepancies deserve further investigation. An exciting discovery has been the demonstration that PPARγ ligands can mediate their tumour suppressor and anti-inflammatory actions via the upregulation of PTEN (Patel *et al* 2001). Rosiglitazone-activated-PPARγ has been shown to bind too PPAR response elements upstream from the *PTEN* gene and upregulate PTEN protein expression to a level sufficient to antagonise the PI 3-K pathway, thereby reducing levels of active phosphorylated PKB and inhibiting cell growth in macrophages (figure 21). In the same study, SHIP2 phosphatase upregulation was found not to occur. The effect on SHIP expression was unfortunately not determined. This study also demonstrates that PPARγ can upregulate as well as downregulate gene expression upon DNA binding.

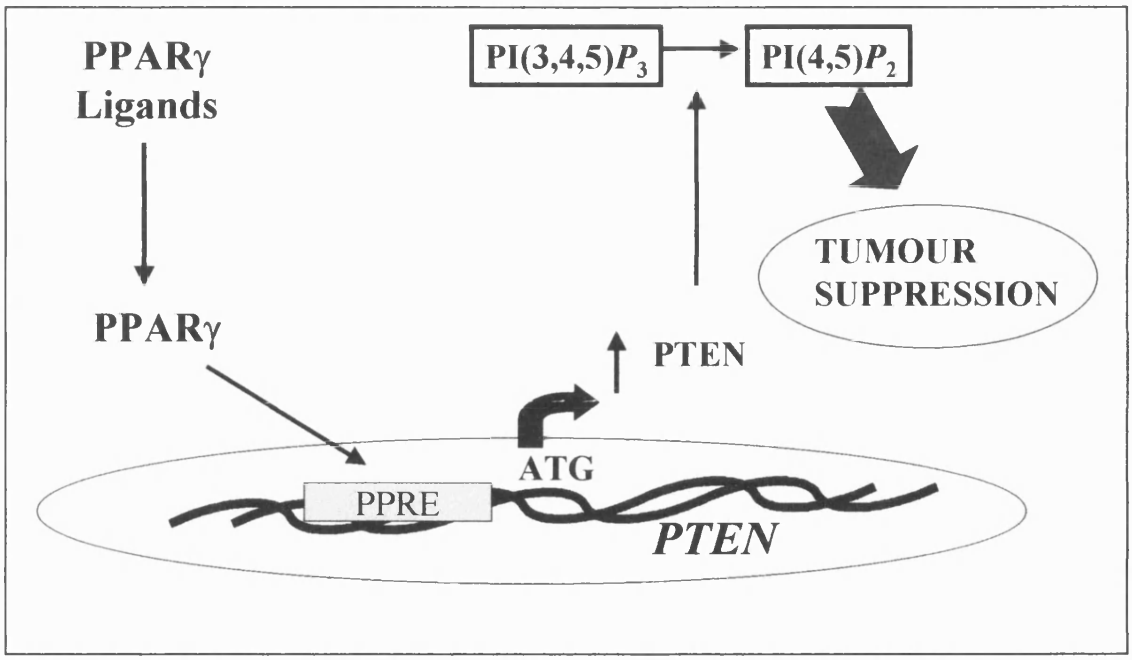

Figure 21: Mediation of tumour suppression by upregulation of *PTEN* via a PPARγ dependent mechanism. PPARγ is able to bind to two PPRE within the *PTEN* gene leading to its upregulation and suppression of PI 3-K driven pathways.

Aims

PI 3-K has been proposed as a pivotal link in T cell activation and it follows, therefore, that D-3 phosphoinositides levels must be tightly regulated to ensure appropriate physiological responses (Ward *et al* 1996). The regulation of PI 3-K signalling and its major lipid product PI(3,4,5)P_3 by the phosphatases SHIP and PTEN in response to different stimuli and in different cell types is currently an area of great interest. Research in human T cells has utilised a variety of T cell lines including the common leukemic cell lines Jurkat, CEM, MOLT-4, HUT 78 as well as 'normal' primary T cells or T-lymphoblasts derived from human volunteers. The primary aims of this study were as follows:

1) To investigate expression of the inositol phosphatases SHIP and PTEN in the leukemic T cell lines and in T-lymphoblasts. The functional consequences of such phosphatase expression were assessed by determining the resting/stimulated ratios for cellular D-3 phosphoinositide lipid levels and attempt to relate this to activation status of downstream PI 3-K effector proteins e.g. PKB.

2) To investigate the regulation of SHIP and PTEN by the receptors CD3 and CD28 in T lymphoblasts and surrogate T cell lines. Additionally, to identify any potential protein complexes involving SHIP and PTEN that forms following CD28 stimulation.

3) To investigate expression of the PPARγ receptor in a variety of T cell models and determine the ability of its ligands to inhibit proliferation under basal conditions and following stimulation with a variety of physiological (CD3/CD28, IL-2) and non-physiological (PMA/Ionomycin) stimuli.

MATERIALS and METHODS

Materials

Materials and reagents including antibodies and radiochemicals used in this study are listed in appendix 1.

Methods

Cell Culture

All cells were cultured at 37°C in an humidified incubator in an atmosphere of 5% $CO_2$and 95% air. All cell lines and T-lymphoblasts were passaged every 2-3 days or when cells reached 1-2$\times10^6$ cells/ml. Cells were placed in liquid nitrogen for long term storage. Cells were pelted for 5 minutes at 400g and resuspended at 10^7 cells/ml in 20% FCS and 10% dimehtyl sulfoxide (DMSO). Cells were placed in cryovials and placed in an appropriate cooler overnight in an -80°C freezer before being placed in liquid nitrogen cylinders. Cells were recovered from liquid nitrogen by thawing rapidly in a 37°C water bath and washing three times in pre-warmed RPMI-1640 and cultured as appropriate.

Murine Hybridoma DC.27 T-cells

Murine hybridomas stably transfected with human CD28 (WT) or human CD28 mutant containing point mutations at tyrosine amino acid residues 173 and 200 in human CD28 (173/200) were a kind gift from Dr. D. Olive (INSERM, Marseilles, France). Murine hybridoma cells were grown in DMEM with 10% v/v FCS, 50 U/ml Penicillin, 50 μg/ml Streptomycin and 50 μM of β-Mercaptoethanol in 175cm^3 tissue culture flasks. The cells grew in a semi-adherent manner, and were passaged by mild agitation of the flask to dislodge adherent cells. Cells were spilt 1:4 and fed with fresh media every 3 days.

Leukemic cell lines

Jurkat, CEM, MOLT-4 and HUT 78 leukemic cells (D. Cantrell, ICRF, UK) were grown in suspension in RPMI-1640 supplemented with 10% v/v FCS, 50 U/ml Penicillin and 50 μg/ml Streptomycin in 175cm^3 tissue culture flasks. Cells were passaged every 2-3 days or when cells reached sufficient density they were split 1:4 into the original volume of pre-warmed media. Jurkat, CEM and MOLT-4 are all examples of established human leukemic T cell lines derived from the peripheral blood from Caucasian patients with an lymphoblast morphology. The T lymphoblast-like cell line Jurkat, has been invaluable tool to monitor T cell signal transduction (Weiss *et al* 1984). Studies using the Jurkat cell line led to the identification of the T cell growth factor IL-2 and its receptor (IL-2R). These discoveries through Jurkat cells provided the catalyst for T cell biology and the characterisation of signalling pathways through antigen receptors. The leukemic cell line CEM is a T lymphoblastoid cell line originally obtained from a 4-year-old Caucasian female with acute lymphoblastic leukaemia (Foley *et al* 1965). The MOLT-4 cell line was established from cells taken from a patient in relapse and also displays T-lymphoblast morphology (Minowada *et al* 1975). HUT 78 cells, derived from the peripheral blood from a patient with serazy syndrome, display properties like a mature helper T cell (Gootenberg *et al* 1981).

Chinese Hamster Ovary (CHO) Cells

CHO cells transfected with CD80 (CHO-B7.1$^+$) and CD86 (CHO-B7.2$^+$) and untransfected parental CHO cells (D. Sansom, Birmingham, UK) were grown in DMEM (without L-glutamine) with 10% v/v FCS, 50 U/ml Penicillin, 50 μg/ml Streptomycin and 20 μM of the nucleosides adenosine, cytidine, uridine, thymidine and guanosine. CHO cells grew in an adherent fashion and were passaged by trypsinisation. When the culture flask was confluent, media was removed and the cells were washed twice in calcium-free PBS (PBS-A) and overlayed with trypsin (0.5%)/EDTA was added to the flask. Cells were incubated briefly at 37°C and cells were dislodged from the flask by mild agitation. Trypsinisation was terminated by the addition 20 ml of fresh culture

medium. Cells were pelleted at 400g for 5 minutes and passaged 1:5 into the original volume of pre-warmed media.

Peripheral Mononuclear Cell (PBMC) Preparation

Peripheral venous blood from healthy donors, free from medication was collected aseptically in 50 ml sterile syringes pre-loaded with heparin at 10 U/ml to prevent blood clotting using an 19-gauge needle. The blood was diluted 1:1 with pre-warmed serum-free RPMI-1640 culture medium, mixed and carefully layered in 35 ml aliquots onto 15ml of Lymphoprep^{TM} in 50 ml disposable polypropylene conical centrifuge tubes. Following centrifugation at 400g for 30 minutes at room temperature the peripheral cell mononuclear layer was removed and washed three times in 50 ml volumes of RPMI at 400g for 10 minutes and a cell count was performed using a haemacytometer.

T Lymphoblast Preparation

The PBMC isolate previously described was resuspended at 1×10^6/ml in RPMI-1640 containing 10% v/v FCS, 50 U/ml Penicillin and 50 μg/ml streptomycin. T lymphoblasts were prepared from the PBMC isolate by incubating PBMC with 1 μg/ml of the super-antigen Staphylococcal Entertoxin B (SEB) for 72 hours (figure 22). After 72 hours, non-adherent cells were washed three times in RPMI-1640 to remove residual SEB and resuspended at 1×10^6 cells /ml in complete RPMI media and supplemented with human recombinant IL-2 at 20 ng/ml every 48 hours for up to 10 days. T lymphoblasts were used for experimentation from day 8-14. Two days prior to experimentation the cells were washed 3 times in RPMI-1640 and resuspended in supplemented medium without IL-2 thus allowing the T lymphoblasts to accumulate in the G_0-G_1 phase of the cell cycle (Sotsios and Ward 2001).

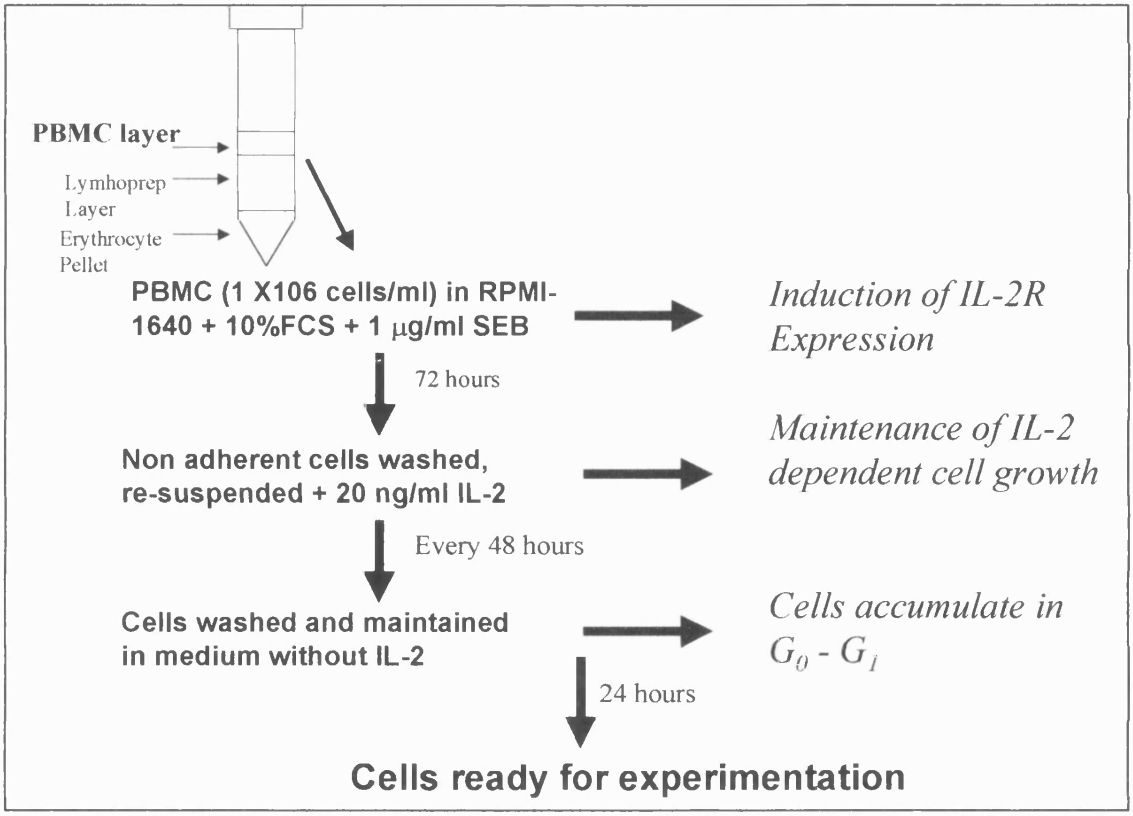

Figure 22: Isolation of PBMC and preparation of T-lymphoblasts. SEB-activated T-blasts were typically cultured for 10-12 days with IL-2 (20ng/ml). Twenty four hours prior to experimentation, cells were washed with serum-free media to accumulate cells in G_0-G_1 phase of cell cycle. Relevant receptor expression (e.g.CD28/CD3) was determined by flow cytometry.

Purification of T Lymphocytes by Negative Selection

Resting T lymphocytes were purified by the immuno-magnetic depletion of B cells, monocytes, dendritic cells, basophills, NK cells and platelets. The PBMC isolate was washed three times to remove residual lymphoprep™ at 350g for 10 minutes and resuspended in 80 μl of PBS-A with 2mM EDTA and 1% w/v BSA for every 1×10^7 cells. 20 μl of a hapten-antibody cocktail containing anti-CD11b, CD16, CD19, CD36 and CD56 antibodies, were added per 10^7 cells, mixed and incubated on ice for 15 minutes with occasional agitation. Cells were washed twice to remove excess antibody in PBS-A. Cells were then resuspended in 80 μl of PBS-A/2mM EDTA/1% w/v BSA per 10^7 cells and 20 μl of anti-hapten microbeads was added per 10^7 cells, mixed and incubated on ice for 15 minutes with occasional agitation. Cells were washed to remove excess beads and

resuspended in 500 μl of PBS-A/2mM EDTA/1% w/v BSA ready for loading onto a MACS CS column previously placed into a magnetic field of a MACS magnet separator. The PBMCs were added to the top of the PBS-A equilibrated column and unstained pure T cells were collected at the bottom into a sterilin tube. The column was washed several times with PBS-A and collected as described to achieve a greater yield of T cells. The collected T cell fraction was counted and viability was assessed by trypan blue exclusion. Purity of the T cell fraction was assessed by flow cytometry (figure 23).

FACS Analysis of cell surface antigens

5×10^4 cells were aliquoted into polypropylene FACS tubes and pelleted 400g for 5 minutes. Cells were washed twice in PBS-A and resuspended in 50 μl of the appropriate primary staining (e.g. anti-CD28/CD3-Appendix 1) used at 10 μg/ml with 25 μl of FCS used to block non-specific binding of antibodies. Cells were shaken and incubated for 30 min at 4°C with occasional agitation by hand. Following incubation, cells were washed twice in ice cold PBS-A via centrifugation (400g for 5 minutes) and resuspended in 50 μl of diluted goat anti-mouse-FITC or anti-rabbit-FITC where appropriate, along with 25 μl of FCS as before. Cells were once again mixed by hand and incubated for 30 minutes at 4°C as previously described. Samples were washed as previously described in PBS-A and analysed immediately or stored in 250 μl of 2% paraformaldehyde overnight at 4°C. FACS analysis done using Becton Dickinson FACS Vantage with a 200nW 488nm argon laser with light being channelled by an FL-1 filter (520nm). Expression of cell surface receptors was confirmed by comparison with relevant isotype control (figure 23).

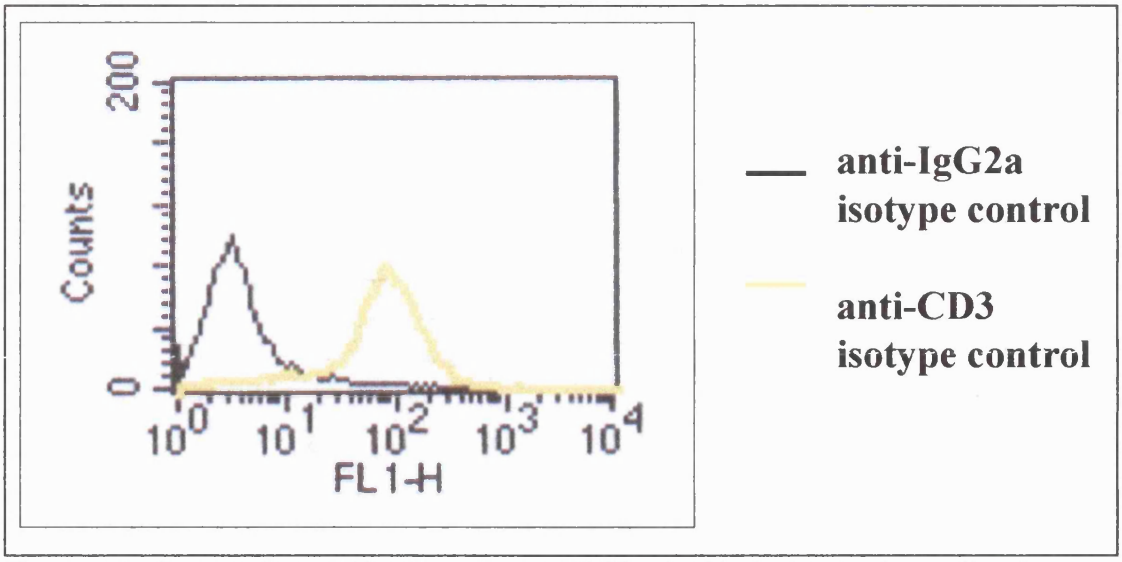

Figure 23: Confirmation of T cell purity by FACS. Freshly isolated primary T cells were incubated with anti-IgG2a isotype control and anti-CD3 mAb (UCHT-1) for desired times before staining with anti-mouse-FITC-conjugated secondary Ab. FACS analysis was achieved by Becton Dickinson FACS vantage using a 200nW 488nm argon laser with light being channelled by an FL-1 filter (520nm). T cell purification yields from peripheral blood were typically ≥95%.

Preparation of Cells for Cell Signalling Experiments

Prior to signalling experiments, cells were harvested from tissue culture flasks and were pelleted by centrifugation (400g, 5min 20°C) and washed three times in serum-free RPMI-1640 to remove serum and growth factors. Where CHO/CHO-B7.1 cells were being used to stimulate T cells lines, cells were removed by trypsinisation as previously described. Cell viability was assessed by trypan blue exclusion and cell counts were performed using a haemacytometer. Cells were resuspended at 10^6-10^7 cells/ml in HEPES buffered serum-free RPMI-1640 in 0.5 ml volumes into eppendorf tubes. Cells were equilibrated in a 37°C waterbath for 30 minutes before experimentation.

Cell Stimulations

If inhibitors were being, these were diluted as appropriate and added to the desired cell aliquot for a minimum of 30 minutes prior to cell stimulation or according to manufacturer guidelines. T cell antibody stimulations e.g. anti-CD28/CD2/CD3 etc (Appendix 1) were achieved by using the appropriate antibody at a concentration of 5 μg/ml, which was placed into the lid of the eppendorf. This concentration of stimulating antibody was shown in previous studies to saturate all surface receptors i.e. antibody is in excess (Ward *et al* 1992). Cells and antibodies were mixed by rapid inversion of the tube and incubated at 37°C for desired times. T-lymphoblasts were stimulated by the cytokine IL-2 at a concentration of 20 ng/ml. Again the cytokine (10 μl) was added to the lid of the tube and mixing was achieved by rapid inversion. T cells which were stimulated with CHO cells and cell CHO transfectants expressing B7.1/B7.2 were resuspended in HEPES buffered RPMI and added to the T cells to achieve a T cell: CHO cell ratio of 3:1 as performed in previous studies (Ward *et al* 1992). T cells were stimulated via co-sedimenting with CHO cells, achieved by mixing by microfuge and then pulsed in a microcentrifuge and incubated for desired times in a 37°C waterbath as previously described. Co-sedimentation would result in cell-cell contact between CD28-bearing T cells and B7-bearing CHO cells.

Cell Lysis and Preparation of Whole Cell Extracts

Cell stimulations were terminated in the following manner: rapid pulsing of cells in a microcentrifuge, removal of supernatant by aspiration and lysing In 500 μl of ice-cold lysis buffer (appendix 2). Samples were incubated on ice for 15 minutes to ensure full lysis and nuclear debris was sedimented by centrifugation at 13000g for 15 minutes at 4°C. Supernatants containing cellular proteins were transferred to a fresh eppendorf tube and used immediately or stored at -20°C. Samples were kept on ice as often as possible to avoid protein degradation.

Acetone Precipitation of Proteins

Total protein was precipitated by the addition of 0.7 ml of ice cold acetone to the whole cell lysate (500 μl). Samples were rotated for 15 minutes at 4°C and subjected to centrifugation at 13000g, 4°C for 15 minutes. The supernatant was removed by aspiration and protein pellets were dried *in vacuo*. The protein pellet was boiled in SDS-Lammeli (reducing) sample buffer and were subjected to SDS-PAGE or stored at -20°C.

Immunoprecipitation of cell extracts

Whole cell extracts were first pre-cleared to eliminate the possibility of non-specific binding to the sepharose beads. Samples were pre-cleared by the addition of 20 μl of 50% slurry of Protein- A or-G and rotated for 30 minutes at 4°C. Protein-A/G was removed by centrifugation and the supernatant was added to a fresh tube along with the appropriate immunoprecipitating antibody at a concentration recommended by manufacturers guidelines (typically betwwen 1-5 μg/ml). Samples were rotated for 2 hours at 4°C. Immune complexes were tagged by the addition of 20 μl of Protein-A or-G and were rotated for another hour at 4°C. Sepharose beads containing the immune complex were sedimented by centrifugation with supernatant being removed by

aspiration. Beads were washed 5 times in lysis buffer as previously described. At the final wash, excess lysis buffer was removed via flat-end Hamilton syringe and the immunoprecipitate/beads were boiled in 30 μl of SDS- Lammeli (reducing) sample buffer.

SDS-PAGE

Whole cell extracts, acetone precipitates and immunoprecipitates were separated using the BioRad Mini protean II equipment. Acrylamide gels (7.5-12%) were prepared as described in the table below. Polymerisation of the gels was achieved via the addition of appropriate volumes of APS and TEMED. After sample loading gels were electerophoresed at 60 V in running buffer (appendix 2) for 20 minutes until the samples were through the stacking gel whereupon voltage was increased to 160V for 1 hour. Alternatively proteins could be separated using 7-17% large gradient gels using vertical slab units SE400 (Hoefer Scientific Instruments, San Francisco) which were run overnight at a constant voltage of 60V. Gel constituents are described in table 6:

	Mini Gels		Gradient gels		
% GEL	7%	17.5%	7%	10%	STACK
Acrylamide (ml)	3.5	8.5	3.75	5	1.6
H_2O (ml)	5.8	-	5.6	4.35	7.3
1M Tris pH 8.8 (ml)	5.6	5.6	5.6	5.6	-
10% SDS (ml)	0.25	0.25	0.25	0.25	-
Upper Buffer (ml)	-	-	-	-	3.5
Sucrose (g)	-	1.5	-	-	-
10% APS (μl)	50	50	50	50	65
Temed (μl)	20	20	20	20	12
Final Volume (ml)	30	30	15	15	10

Table 6: Recipes for different percentage acrylamide gels commonly used for SDS-PAGE.

Gel transfer

Proteins were transferred onto nitrocelluose using a semi-dry transfer graphite electrode (Pharmacia, Biotech, Uppsal, Sweden). 3 mm paper and nitrocelluose was cut to the size of the gel and a gel transfer sandwich was prepared. This consisted of four pieces of 3 mm paper, pre wetted in semi-dry transfer buffer (appendix 2) which was then added to the anode electrode followed by the nitrocellulose acrylamide gel and finally another four pieces of 3mm paper. Air bubbles were removed by frequent rolling of the sandwich. The cathode electrode was applied and proteins were transferred for 1 hour at 1mA per cm^2.

Immunoblotting

Following gel transfer the efficiency of transfer was visualised by the addition of ponceau-S stain which was subsequently removed by washing in dH_2O. Nitrocelluose membranes were then blocked in either 5% Marvel in TBS or by 5% BSA 1% Ovalbumin in TBS, depending on the preference of the primary antibody (see Appendix 1 for blocking conditions for appropriate antibody), for at least 1 hour. Blocked membranes were then washed three times in TBS and 0.05% (v/v) Tween-20 (TBS-T). Primary antibodies were diluted to the appropriate concentration (Appendix 1) in TBS and the appropriate blocking solution was added to a final concentration of 1% in accordance with manufacturer's guidelines. Primary antibodies were applied for a minimum of three hours at room temperature or overnight at 4°C with shaking. The primary antibody was removed and the membrane washed three times for 10 minutes with TBS-T. A secondary antibody, consisting of horseradish-peroxidase conjugated immunoglobulins specific to the species the primary antibody was raised in was added to the membranes. Secondary antibodies were diluted to 1:1000- 1:10000 in TBS-T and were incubated with the membrane for 1 hour at room temperature with shaking. Excess, unbound secondary antibody was removed as previously described. Antibody-bound proteins were detected using chemi-illuminescence reagent (ECL) and subjected to autoradiography. Where appropriate protein bands from western blots were quantified by densitometry using 'gene snap' software.

Stripping and reprobing of Gels

Determination of equal loading and transfer of blots were achieved by the following method: blots were washed with dH_2O and submerged in stripping buffer (appendix 2) and then incubated in a waterbath for one hour at 60°C with occasional agitation by hand. Following stripping the blots were washed with copious amounts of TBS-T before blocking and reprobing with a different primary antibody as previously described.

In Vitro Protein Kinase Assays

Immunoprecipitates were prepared as described previously. Sepharose- bound immune complexes were washed, as described, three times in ice-cold lysis buffer and twice in protein kinase assay buffer (appendix 2). At the final wash the immunoprecipitates were transferred to 1.5 ml screwlid Starstedt tubes. *In vitro* kinase activity was assayed utilising a method described by Ward *et al* 1992. Briefly, *in vitro* kinase activity of the immunoprecipitates was initiated by addition of 20 μl of kinase assay buffer containing 10 μM (cold) ATP and 10 μCi of [γ-^{32}P]-ATP. Samples were mixed and incubated at room temperature (25°C) for 20 minutes. Reactions were terminated by the addition of 1 ml of lysis buffer containing 30 mM EDTA. The immunoprecipitates were then washed a minimum of 8 times to remove excess isotope and drained and boiled in SDS-sample buffer (reducing) for 10 minutes. Proteins were electerophoresed overnight at 60 mA on a large gradient gel (7%-17%). Gels were then fixed in propan-2-ol: H2O: acetic acid (50:130:20) for 1 hour, rinsed in dH_20 and dried for 2 hours at 60°C. Fixed gels containing the radiolabelled proteins were exposed to Xomat film overnight at -70°C, with screen and visualised by autoradiography.

In Vivo ^{32}-P Lipid Labelling

In vivo analysis of intact cellular D-3 phosphoinositide levels were assayed using a protocol developed by Morgan *et al.* Cells to be ^{32}P metabolically labelled were harvested from culture flasks and depleted of endogenous phosphate by washing in 50 ml volumes of phosphate-free DMEM. Cells were washed three times (350g, 5 min, 25°C) and in between washes cells were incubated in a 37°C for 10 minutes to ensure efficient phosphate depletion. Cells were counted and resuspended at 20×10^6 cells/ml in 10 ml of phosphate free DMEM supplemented with saline-dialysed FCS (phosphate-free FCS) and 20 mM HEPES in a small tissue culture flask. 1mCi of ^{32}P orthophosphoric acid

was added to the cells, gently mixed and incubated in a 37°C water bath for 4 hours.

Following incubation with radioactive label, unincorporated label was removed by washing three times in phosphate free DMEM as described. Cells were resuspended in RPMI-1640 at 20 $x10^6$ cells/120 μl. Inhibitors to be studied were added to the required aliquot and incubated at 37°C in accordance with the manufacturers guidelines. Cells were then stimulated as previously described and incubated for desired times at 37°C typically between 1-10minutes. Reactions were terminated by the addition of 0.7 ml of ice-cold chloroform: methanol: H_20 (32.6%: 65.3%: 2.1% v/v/v), mixed and added to ice, producing a homogenous primary extraction phase. To separate phases 200 μl of Folsh lipids (1 mg of Folsh Lipid in 100 ml of chloroform) and 200 μl of 5 mM Tetrabutyl ammoniumsulphate in 2.4 M HCl was added. Samples were mixed by vortexing and centrifuged at 1000g for 5 minutes to separate phases. The lower organic chloroform layer was removed to a fresh 1.5 ml screwlid starstedt tube containing 5 mM EDTA / 1 M HCl. Samples were vortexed and centrifuged as before. The lower organic phase was removed to a fresh tube and dried *in vacuo*. Once dried, the extracted lipids were deacylated by the addition of 1 ml of 25% methylamine/methanol/N-butanol (4:4:1 v/v/v) per tube. Samples were vortexed vigorously and placed in a 53°C water bath for 40 minutes. Deacylation was terminated by rapid cooling on ice for 5 minutes before being *dried in vacuo* overnight.

Dried lipids were washed by resuspending in 0.5 ml of dH_2O and 0.6 ml of Butan-1-ol/petroleum ether (bp 40-60 °C)/ ethyl formate (20:4:1, v/v). Samples were mixed by vortexing and centrifuged as before to separate phases. The upper phase was discarded and the lower water- soluble phase dried *in vacuo.* Dried, labelled inositides were resuspended in 100 μl of dH_20 and analysed by HPLC using a 12.5 cm Whatman Patrisphere column.

Labelled lipids were applied to the column at a flow rate of 1 ml/min and were eluted from the column using a gradient based on the buffers A (dH_20) and Buffer B (1.25 M Ammonium phosphate $(NH_4)_2HPO_4$ pH 3.8) over a sample run of 90 minutes. The mixing of buffer B (which elutes deacylated P^{32}-labelled lipids) during sample runs were as follows: 0min, 0% B; 5min, 0% B; 45 min, 12%B; 60 min, 30% B; 61 min, 100% B; 65 min, 100% B; 66min 0% B; 90 min, o% A and B. Eluates were mixed with three volumes of Flo-Scint IV scintillant before being quantified by beta radio detector (Canberra Packard). Relevant peaks were measured and recorded via Flo-One software. Identities of peaks were compared with elution times for characterised D-3 phosphoinositides as described by Ward et al (1993 and figure 24). Retention times varied due to slight changes in room temperature and the age of the column.

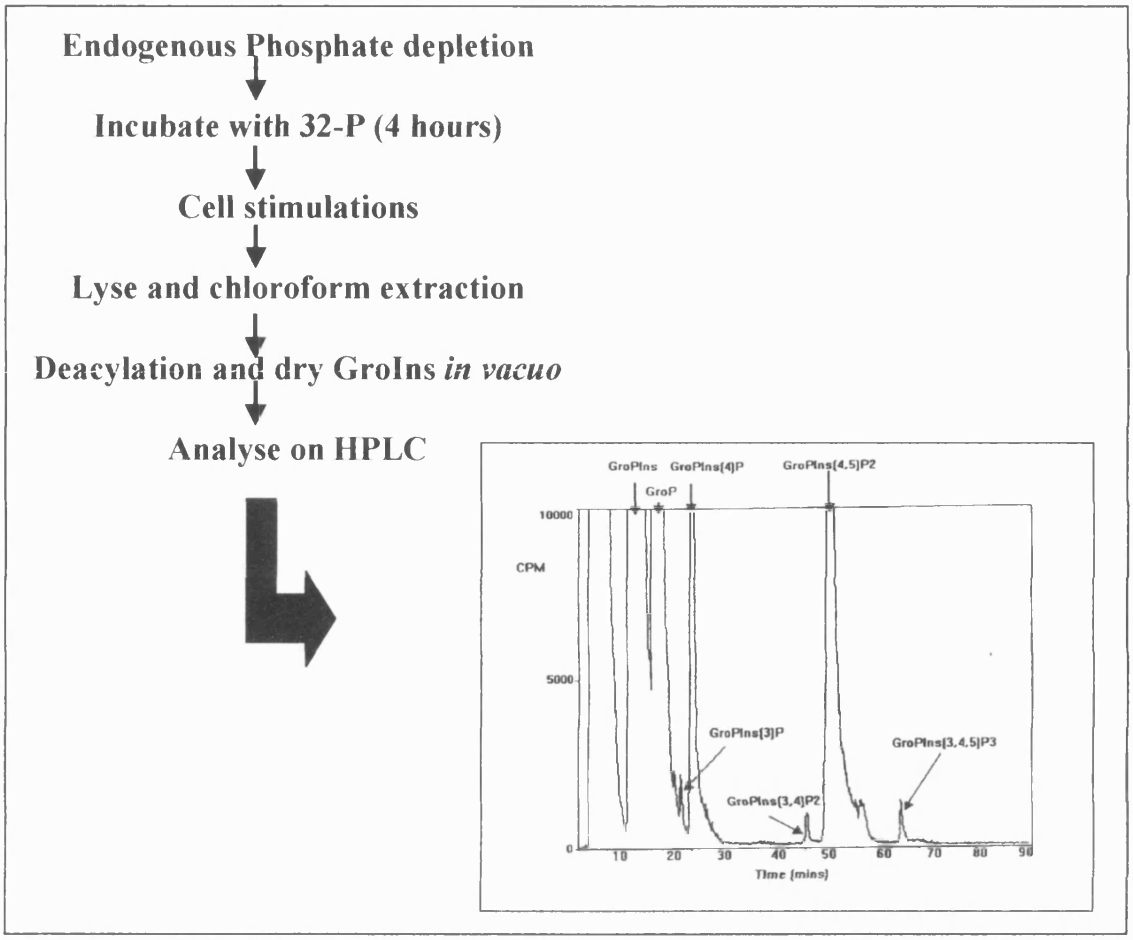

Figure 24: Flow chart to summarise the *in vivo* ^{32}P lipid labelling protocol. Inset,typical HPLC trace of a sample is showing comparative elution times of PI(3,4)P_2, PI(4,5)P_2 and PI(3,4,5)P_3.

In Vitro Phosphatase Assay

This phosphatase assay is based on the assay described by Damen (Damen *et al* 1996). Briefly, cells were prepared, stimulated, lysed and pre-cleared as previously described. Where appropriate, anti-SHIP and anti-PTEN immunoprecipitates were prepared from whole cell lysates. The phosphatase activity from these immunoprecipitates were determined by the *in vitro* hydrolysis of the substrate [^{3}H]-Ins (1,3,4,5) P_4 (IP4). Immunoprecipitates were washed three times in lysis buffer and twice in phosphatase buffer (appendix 2). Drained immunoprecipitates were re-suspended in 25 μl of assay buffer and 16 μM of [^{3}H] IP4 (3μl) was added mixed and incubated at 25°C for 20 minutes. The assay was terminated by the addition of an acidified: chloroform: methanol solution (ratios), mixed by vortex and centrifuged at 1000g for 5 minutes. The

lower aqueous phase was removed into a fresh tube and dried *in vacuo*. Dried inositides were re-suspended in 100 µl of dH_20 and analysed by anion-exchange HPLC using a Patrisphere SAX column (Whatman) using the method described earlier. 1 ml fractions were collected into scintillation tubes and 3 ml of Flo Scint IV was added to each collected fraction. The levels of tritiated fractions were quantified using a 1209 Rack-Beta liquid scintillation counter. Elution times were compared against an untreated IP4 control where 3 µl of IP4 was added to 97 µl of dH_20 and run though the HPLC column.

Proliferation Assays

T cells (Resting T cells, T-Blasts or T leukemic cell lines) were re-suspended in RPMI-1640 supplemented with 10% FCS at a concentration of 1 $x10^6$ cells/ml. Cells were plated at 1 $x10^5$ cells/well in a sterile 96-well tissue culture plate. Treatments were performed in quintuplicate with inhibitors being incubated with the cells for the required length of time as appropriate. Cells were co-stimulated with antibody covalently coupled M-450 Dynabeads (Appendix 1) were done so at 3 bead: 1 cell ratio as described (Sotsios and Ward 2001). All wells were made up to a final volume of 200 µl with complete RPMI. Plates were incubated in a humidified cell incubator at 37°C for 48 hours and then pulsed with 1 µCi [3H]-thymidine (diluted in complete RPMI) per well for a further 14 hours. After the 72-hour incubation plates were harvested using an automated cell harvester into 96-well filter plates (Unifilter™) and washed three times to remove unincorporated [3H]-thymidine. 20 µl of Flo Scint IV was added to each well on the dried plate, sealed and [3H]-thymidine incorporation was subsequently measured with a β-scintillation counter (TopCount™). Mean data was plotted for each point and subjected to students' T test to test for statistical significance.

mRNA extraction and RT-PCR

RT-PCR was used to determine the expression of SHIP and PTEN mRNA. Total RNA was prepared by cells harvesting from tissue culture flasks and washing them once in serum-free RPMI and re-suspending at 5 $x10^6$ cells/ml in PBS. 1 ml of RNAzol™ was added to samples as well as 100 µl of chloroform. The sample was shaken vigorously and left on ice for 15 minutes and centrifuged at 13000g for 15 minutes at 4°C. The upper layer was transferred to a fresh tube containing 500 µl of isopropanol, which was mixed by vortexing and left on ice for a further 15 minutes. Samples were centrifuged as before and the supernatant removed. The RNA pellet was washed with ice-cold 75% ethanol and spun at 7500g for 8 minutes at 4°C. The supernatant was removed and air-dried before being re-dissolved in sterile distilled H_20 and total RNA was quantified using a Gene Quant II RNA/DNA calculator (Pharmacia Biotech, Uppsal, Sweden).

Reverse Transcription

Reverse transcription took place in thin-walled PCR tubes. 1 µg of sample mRNA was added to PCR tube and diluted with 7.5 µl of dH_20 along with 0.5 µg of oligo d'T. Secondary mRNA structures was denatured by heating to 65°C for 5 minutes and storing at 4°C. Following denaturation, a reverse transcription mix was added to the appropriate mRNA consisting of 5x RT-Buffer (Promega), 0.5 mM deoxynucleoside triphosphates, 1 U/µl RNasin and 10U/µl of Moloney-Murine Leukaemia Virus Reverse Transcriptase (MMLV-RT) to a final volume of 25 µl. Samples were place in a PTC-100™ thermocycler and run at 42°C or 60 minutes followed by 95°C for 5 minutes and then stored at 4°C.

Polymerase Chain Reaction

Forward and reverse primers corresponding to coding sequences in the SHIP and PTEN genes were designed (appendix 3). PCR reactions were carried out in thin walled PCR tubes as in the RT reaction. 2 μl of cDNA was added to the tube and a PCR mix was added which included 25 pmol of forward (5') and reverse (3') primers, 10 X PCR buffer (Promega), 200 μM of dNTPs, 1U of Taq (Bioline) and diluted in dH_20 to a volume of 25 μl. The expected size of the PCR products utilising SHIP and PTEN primers was 1 kb. Sample controls with no cDNA were included in the assays and run against all samples and also against the housekeeping gene β-actin as a negative control. Samples were placed in the thermocycler and run at the following program: 1) 94°C, 90 seconds; 2) 94°C, 30 seconds; 3) 58°C 30 seconds; 72 °C 40 seconds with steps 2 and 3 repeated for 35 cycles; 72°C for 5 minutes and cooling to 4°C to finish. 5 μl of 'blue juice' (Sigma) was added to each sample to aid loading prior to agarose gel electrophoresis.

Detection of PCR Products

A 1% agarose gel was made in 1X TBE (appendix 2) mixed with 1 μg/ml ethidium bromide, boiled and cast. 5 μl of samples (positive and negative) were loaded onto the gels and run against a 100 base pair ladder (Promega). Samples were electerophoresed at 100V/0.1 mA and resultant products were visualised with a U.V transilluminator.

Results

Expression of SHIP and PTEN mRNA in T Cell Leukemic Lines and T Lymphoblasts

SHIP was originally identified as a 145 kDa tyrosine phosphorylated protein associated with the adapter shc after stimulation of blood cells by a variety of cytokines and growth factors. SHIP was subsequently cloned and found to be an inositol 5-phosphatase (Damen *et al* 1996). Further work has shown that expression of SHIP is restricted to cells of the haematopoietic system (Liu *et al* 1997). In contrast the inositol phosphatase PTEN, has been shown to have a much wider expression, but is known to be mutated or deleted in a number of human cancers (Cantley and Neel 1999) and has therefore been designated as a tumour suppressor. Little is known about the expression of the phosphatases SHIP and PTEN in the leukemic cell lines CEM, MOLT-4 and HUT 78. These cell lines are often used as models to investigate T cell signal transduction so it was important to characterise the expression of SHIP and PTEN at the level of mRNA. Expression studies were achieved via RT-PCR of all leukemic cell lines and T-lymphoblasts (figure 25).

Analysis of RT-PCR reactions shows that SHIP mRNA is expressed in T-lymphoblasts and the leukemic lines Jurkat, CEM, MOLT-4 and HUT 78. A similar pattern was observed in that regards to expression of PTEN, all leukemic cell lines and T-lymphoblasts were positive for the expression of PTEN mRNA (figure 25).

Expression of SHIP and PTEN Proteins in Leukemic T Cell Lines and T-Lymphoblasts

Whole cell lysates (10^7 cells) were prepared from all leukemic cell lines and T-lymphoblasts and immuno-blotted with anti-SHIP and anti-PTEN monoclonal Abs (figure 26). It was noted that Jurkat cells contained no detectable protein for both SHIP and PTEN although mRNA for both proteins can readily be detected (figures 25). The other leukemic cell lines had a different expression pattern.

MOLT-4 and CEM cells contained protein for SHIP but contained no detectable levels of PTEN. Like Jurkat cells, both MOLT-4 and CEM cells contained mRNA for both SHIP and PTEN. T-lymphoblasts and the HUT-78 leukemic cell line were both positive for the expression of SHIP and PTEN at the level of protein and mRNA.

Figure 25: Expression of SHIP and PTEN mRNA in leukemic cell lines and T-lymphoblasts.

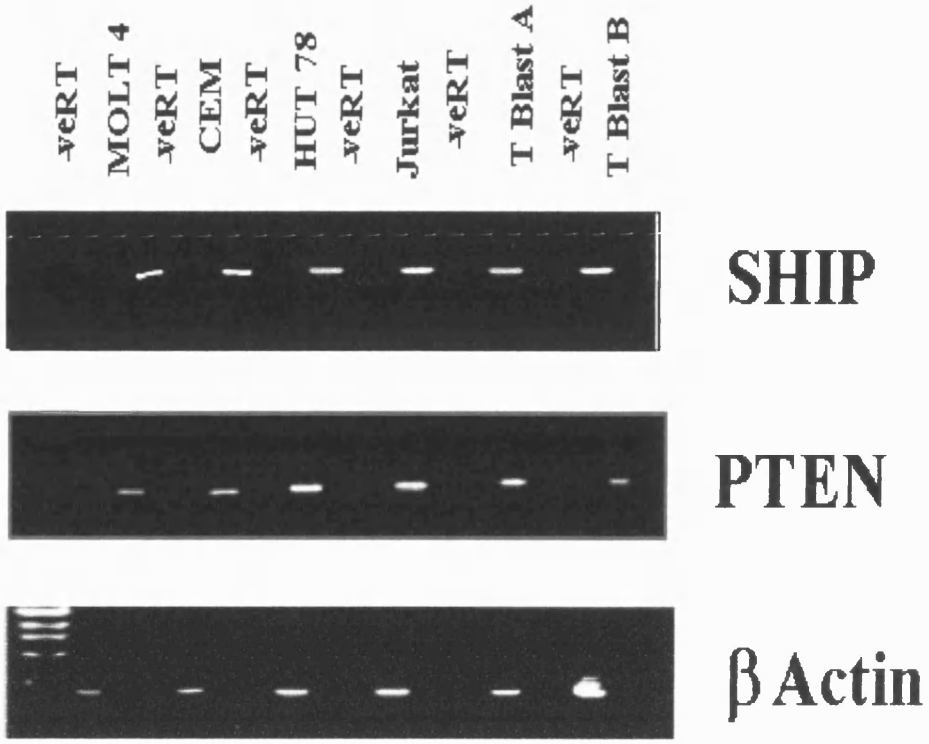

Figure 25: Expression of PTEN mRNA in leukemic cell lines and T-lymphoblasts (A and B denoting different blood donors). mRNA from $5x10^6$ cells was extracted and cDNA was prepared via a reverse transcriptsase reaction. Primers designed to SHIP and PTEN mRNA (appendix 3) was annealed with cDNA from T cell lines and analysed for expression of SHIP and PTEN via PCR as described in *Materials and Methods*. PCR products were resolved on a 1% agarose gel and visualised by UV transillumination. Data is from a single experiment representative of three others.

Figure 26: Expression of SHIP and PTEN protein in T cell and T lymphoblasts.

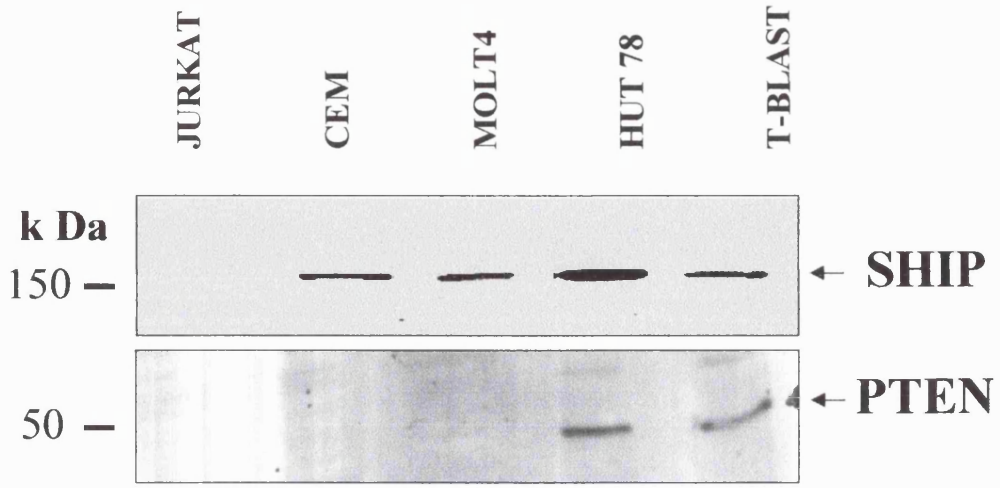

Figure 26: Expression of SHIP and PTEN in T cell lymphoblasts and leukemic cells. 10^7 cells were lysed, proteins were concentrated by acetone precipitation and samples boiled in lamelli sample buffer. Samples were subjected to SDS-PAGE, transferred onto nitrocellulose and immuno-blotted with anti-SHIP mAb and anti-PTEN mAb as described in *Materials and Methods*. Results are from a single experiment representative of 3 independent experiments.

Characterisation of cell surface markers on leukemic cell lines and T-lymphoblasts and CHO/CHO-B7.1$^+$ cells.

The surface expression of relevant receptors was routinely monitored by flow cytometry. Expression of these cell markers verified their use in particular cell assays. CHO cells stably transfected with B7.1 (CHO-B7.1$^+$), the natural ligand for CD28, were a useful functional tool to monitor CD28-mediated signalling events. CHO-B7.1$^+$ offer a more physiological stimulus than anti-CD28 Abs and have been shown to be able to stimulate 3H-thymidine incorporation and PI(3,4,5)P_3 accumulation in T cells (Ward *et al* 1995). CHO-B7.1+ were shown to constantly express B7.1 to a high level (~90%). Parental CHO cells were found to not express the B7.1 and were thus suitable for uses as negative controls (figure 27).

The T leukemic cell lines Jurkat, CEM, MOLT-4 and HUT 78 were also routinely monitored for expression of the cell surface receptors CD28 and CD3 binding compared to that of isotype-matched control antibodies. Jurkat cells expressed high levels of both CD28 (90%) and CD3 (55%) on the cell surface (figure 28). Other T cell leukemic cell lines exhibited lower levels of these T cell surface antigens. In particular MOLT-4 cells expressed reasonable levels of CD28 (35%) but low levels of CD3 (≤10%). CEM cells were also positive for CD28 (50%) with lower levels of CD3 (18%). In contrast HUT-78 were routinely shown to have very low levels of both CD28 (≤5%) and CD3 (≤10%) expression. T-lymphoblasts from healthy human volunteers represent an alternative, more physiological cell model to study CD28 signal transduction. Each batch of SEB-activated T-lymphoblasts was monitored for the expression of CD3, CD28 and the IL-2 receptors before experimental use. Expression levels of CD28, CD3 and IL-2R varied between individuals but were generally over 50% compared to isotype-matched control and thus suitable for signalling-based experiments. Typical expression levels of all cell surface markers in Leukemic cells and T-lymphoblasts are summarised (table 7 and figure 28/29).

	Jurkat	CEM	HUT 78	MOLT-4	T-Blast
CD28	90%	50%	<5%	35%	50%
CD3	55%	<20%	10%	<10%	60%
IL-2	ND	ND	ND	ND	65%

Table 7: Typical percentage expression of T cell surface markers against isotype controls. Nd = not determined.

Figure 27: Expression of cell surface markers on CHO/CHO-B7.1$^+$ cells.

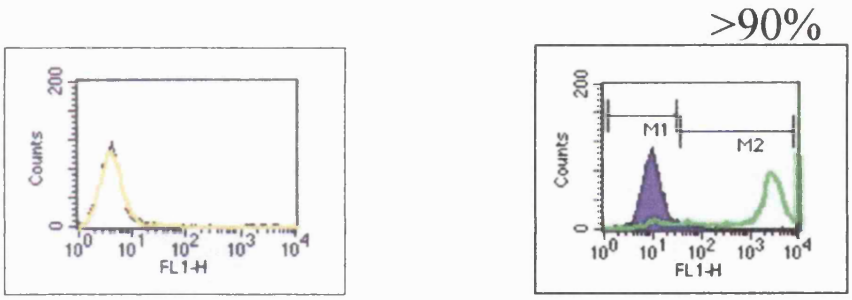

PARENTAL CHO **CHO-B7.1$^+$**

Figure 27: Expression of B7.1 on Parental CHO and CHO-B7.1$^+$ cells. 1x10^5 cells were analysed for B7.1 using a directly conjugated mAb towards B7.1, BB-1 (yellow bar on parental CHO/Green bar on CHO-B7.1$^+$) and an isotype matched control (black line). Cells were analysed for expression using a Becton Dickinson FACS vantage as described in *Materials and Methods*. Results are from a single experiment representative of at least 3 others.

Figure 28: Expression of cell surface markers on leukemic T cell lines

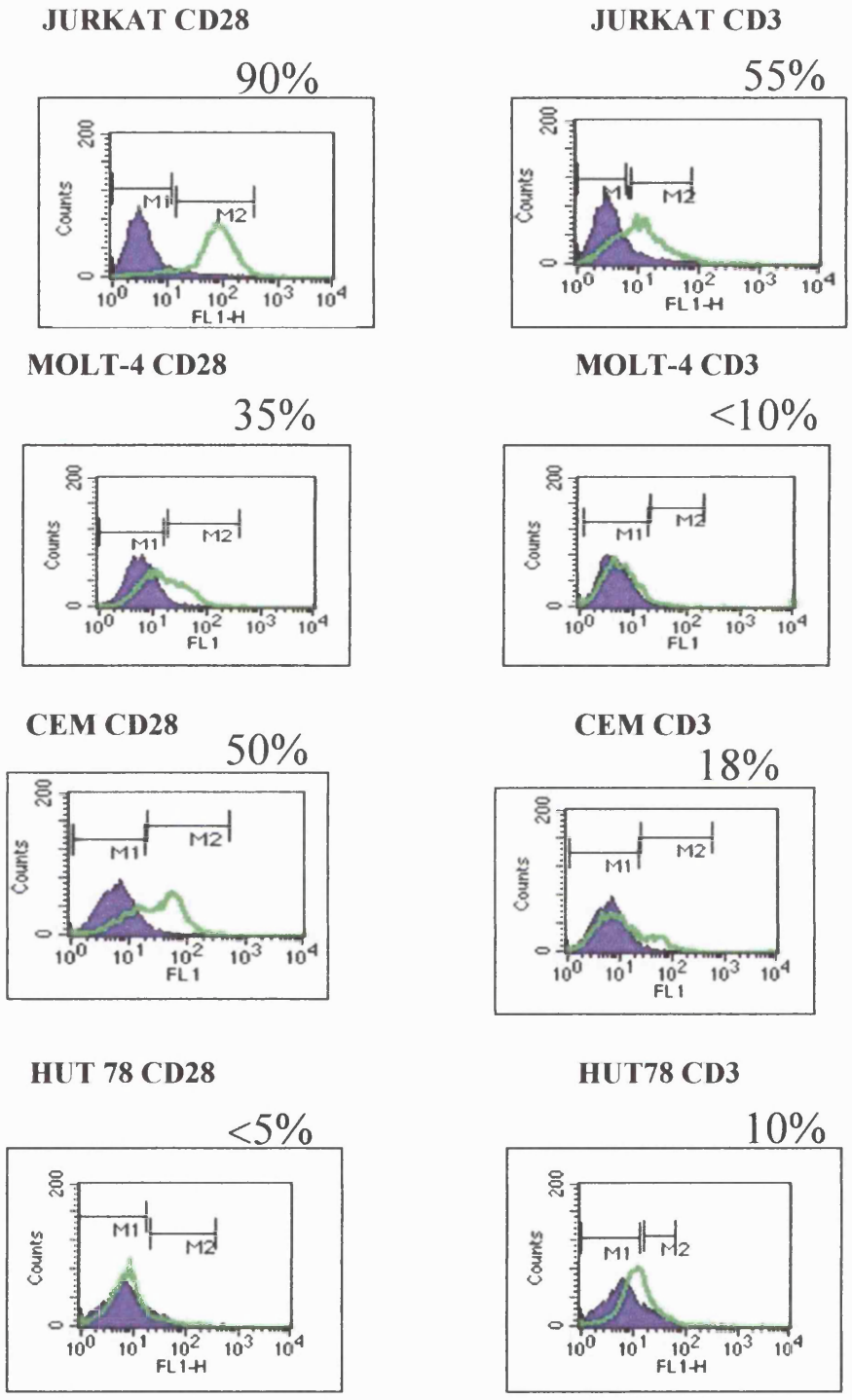

Figure 28: Expression of CD28/CD3 receptors in leukemic T cell lines. $1x10^5$ T cells were analysed for antigens using anti-CD28 and anti-CD3 mAbs against an isotype- matched control (black). Cells were stained with an FITC-conjugated goat anti-mouse secondary Ab and analysed on a Becton Dickinson FACS vantage as described in *Materials and Methods*. Results are from a single experiment representative of at least 3 others.

Figure 29: Cell surface expression of CD28, CD3 and IL-2 receptor in SEB activated T-lymphoblasts.

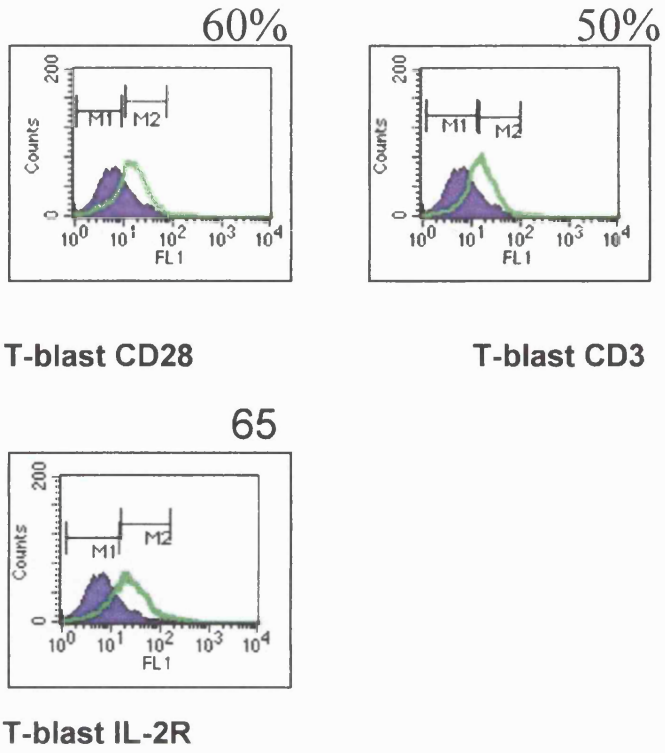

Figure 29: Cell surface expression of CD28, CD3 and IL-2 receptor in SEB activated T-lymphoblasts. $1x10^5$ T-lymphoblasts were analysed for antigens using anti-CD28, anti-CD3 and IL-2R (all green) mAbs against isotype matched controls (black). Cells were stained with an FITC-conjugated goat anti-mouse secondary Ab and analysed on a Becton Dickinson FACS vantage as described in *Materials and Methods*. Results are from a single experiment representative of at least 3 others.

Investigation into D-3 phosphoinositide Levels in Jurkat Leukemic Cells

The leukemic cell line Jurkat has been central to many important discoveries in T cell biology and have been an invaluable tool in characterising cell signalling events (including PI 3-K signalling events) downstream from the TCR, IL-2R and costimulatory molecules such as CD28. The lipid products of PI 3-K regulate an extraordinary number of cellular processes confirming its role as a second messenger in signal transduction (Vanhaesebroeck *et al* 2001). Levels of D-3 Phosphoinositides are regulated by inositol phosphatases such as PTEN and SHIP which therefore regulate downstream effectors of PI 3-K signalling. Considering that T leukemic cell lines and lymphoblasts have differing expression of phosphatases (figure 26), it would be of interest to monitor basal and CD28/CD3 stimulated levels of D-3 phosphoinositides. Levels of D-3 phosphoinositides can be measured *in vivo* by the metabolic labelling of intact cellular pools of ATP with ^{32}P followed by lipid extraction, deacylation and separation and identification of phosphorylated lipids by HPLC analysis. Elution times of phosphoinositides are compared to known retention times of ^{3}H labelled standards characterised by Ward *et al* (1995).

Upon labelling of Jurkat cells it was noted that there was considerable basal level of PI(3,4,5)P_3. Basal levels of PI(3,4,5)P_3 were shown to be around 4600 cpm (figure 30 and table8). Following treatment with the PI3-K inhibitor LY 294002 these levels were reduced to 1600 cpm after 60 minutes and further reducing to 264 cpm after 2-hours treatment (figure 30). Stimulation with CHO-B7.1$^+$ cells resulted in a rapid accumulation of PI(3,4,5)P_3. After 1 minute of CHO-B7.1$^+$ stimulation PI(3,4,5)P_3 increased 4 times above basal levels. This increase was sustained unto 10 minutes where PI(3,4,5)P_3 levels have risen 15 times (73000 cpm) above basal levels. These results are consistent with those previously reported by Ward *et al* (1995). It should also be noted that the rise in PI(3,4,5)P_3 after CHO-B7.1$^+$ ligation was abrogated by pre-treatment with LY 294002 confirming the role of PI 3-K in D-3 lipid accumulation. In contrast to the high basal levels of PI(3,4,5)P_3 in Jurkat cells, PI(3,4)P_2, a lipid thought to be a metabolic product of SHIP hydrolysis of PI(3,4,5)P_3, was found to be comparatively low at 170 cpm in unstimulated Jurkat cells (figure 30 and table 8). Upon stimulation with CHO-B7.1$^+$ cells, PI(3,4)P_2 levels rose moderately to

478 cpm (3-fold increase) after 10 minutes stimulation (figure 30). The increase was not as rapid when compared to the increase in PI(3,4,5)P_3 accumulation following stimulation after 1 minute. It is clear Jurkat cells exhibit much higher levels of PI(3,4,5)P_3 compared to PI(3,4)P_2. Under basal conditions the ratio of PI(3,4,5)P_3 to PI(3,4)P_2 is 27.4 (table 8) whereas upon CD28 stimulation for 10 minutes this ratio increase to 152.7. This marked increase in D-3 phosphoinositide levels and PI(3,4,5)P_3: PI(3,4)P_2 ratios at basal and CD28 stimulated conditions may be partly explained by the lack of SHIP and PTEN which may check D-3 phosphoinositide levels in Jurkat cells.

Figure 30: Measurement of PI(3,4,5)P_3 (top panel) and PI(3,4,5)P_2 (bottom panel) levels in Jurkat cells.

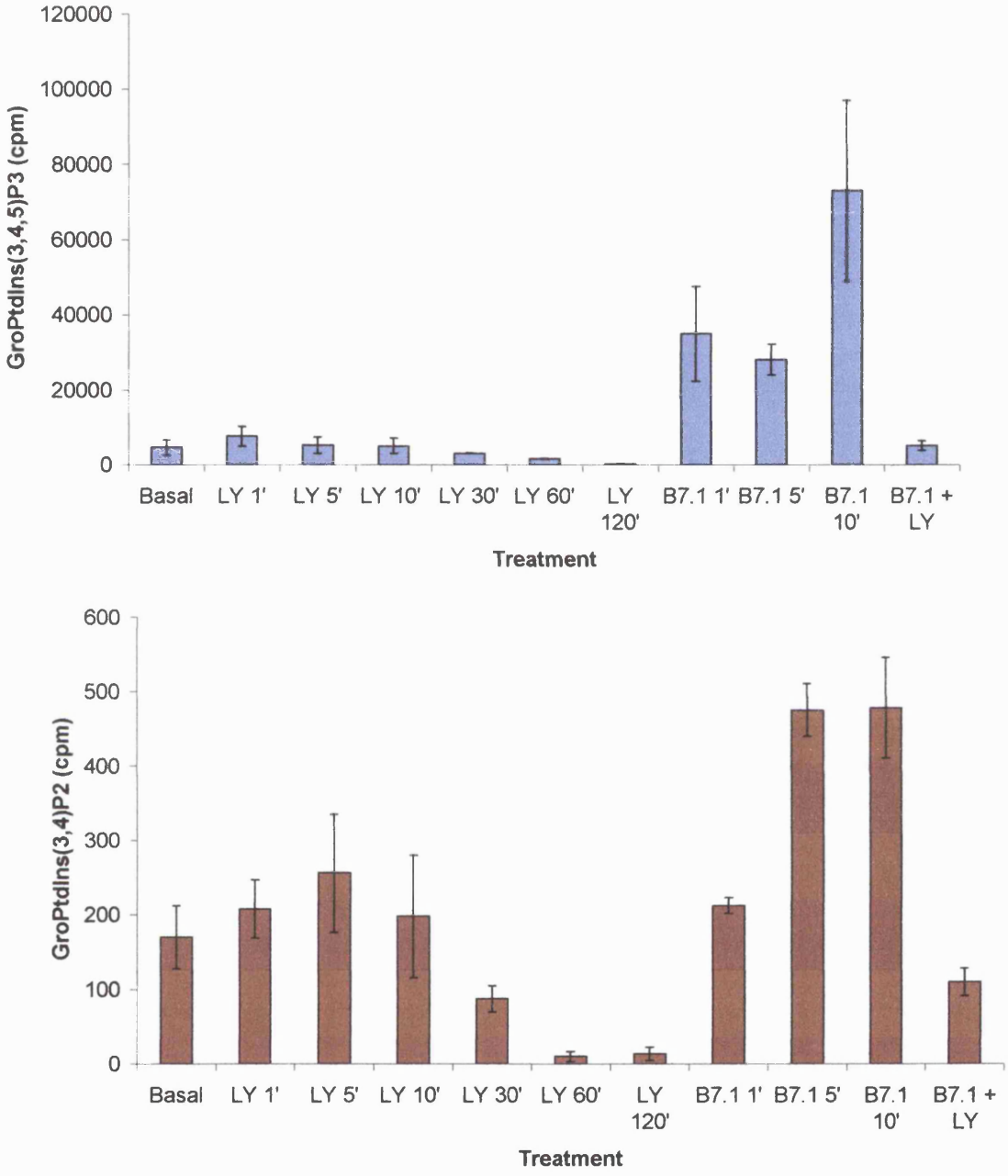

Figure 30: Measurement of PI(3,4,5)P_3 and PI (3,4)P_2 levels in Jurkat cells. Effect of LY294002 and CHO-B7.1$^+$. 2x10^7 cells /point of Jurkats were labelled with ^{32}P, stimulated and lipids extracted. Following deacylation lipids were analysed by anion-exchange HPLC as described in *Materials and Methods*. PI(3,4,5)P_3 is represented by the blue bars and PI (3,4)P_2 is represented by the red bars (note difference in scale). Data is expressed as pooled data ± SEM from 2 experiments.

	PI(3,4,5)P_3 (cpm)	PI(3,4)P_2 (cpm)	Ratio PI(3,4,5)P_3: PI(3,4)P_2
Basal	4670	170	27
CD28 10min	73000	478	152

Table 8: D-3 phosphoinositide levels in basal and CD28 stimulated Jurkat T cells. Data is the mean cpm derived from 2 independent experiments.

Relevance of D-3 Phosphoinositide Levels to PI 3-K-Dependent Signalling Pathways in Jurkat Cells

D-3 phosphoinositides such as PI(3,4,5)P_3 and PI(3,4)P_2 can recruit PH-domain containing proteins from the cytoplasm to the plasma membrane thus leading to its activation. PKB is an example of this in that it is able to interact with D3-phosphoinositides and become activated as a result of phosphorylation on Ser^{473} and Thr^{308} residues by the phosphoinositide-dependent kinases PDK1 and PDK2. Immunoblotting using phospho-specific antibodies to PKB provides an indirect measure to cellular phospho-PKB levels, which relates to PKB activity. This approach was employed to compare basal and stimulated levels of phospho-PKB in the leukemic T cell line Jurkat and to attempt to equate these findings to both SHIP/PTEN protein expression and cellular D-3 phosphoinositide levels measured by ^{32}P *in vivo* lipid labelling.

Consistent with reported literature (Astoul *et al* 2001), it can be clearly seen that Jurkat cells have very high levels of basal phospho-PKB perhaps reflecting the high basal levels of PI(3,4,5)P_3 measured *in vivo* (figure 31). Stimulation of Jurkat cells with B7.1 or with anti-CD3 mAb did not show a significant increase, if at all, in phospho-PKB levels perhaps indicating that PI 3-K signalling is at, or near, to saturation levels under basal conditions. Treatment of Jurkat cells with the PI 3-K inhibitor LY249002 did abolish basal levels of phospho-PKB over a 2-hour period (figure 31). The fact that Jurkat cells do not have the inositol phosphatases SHIP and PTEN to metabolise D-3 phosphoinositides may also

reflect on the apparent slow conversion of phospho-PKB to dephosphorylated PKB. Antibodies to non-phosphorylated PKB verified approximate equal loading.

Figure 31: Basal and stimulated levels of phospho-PKB in Jurkat Cells

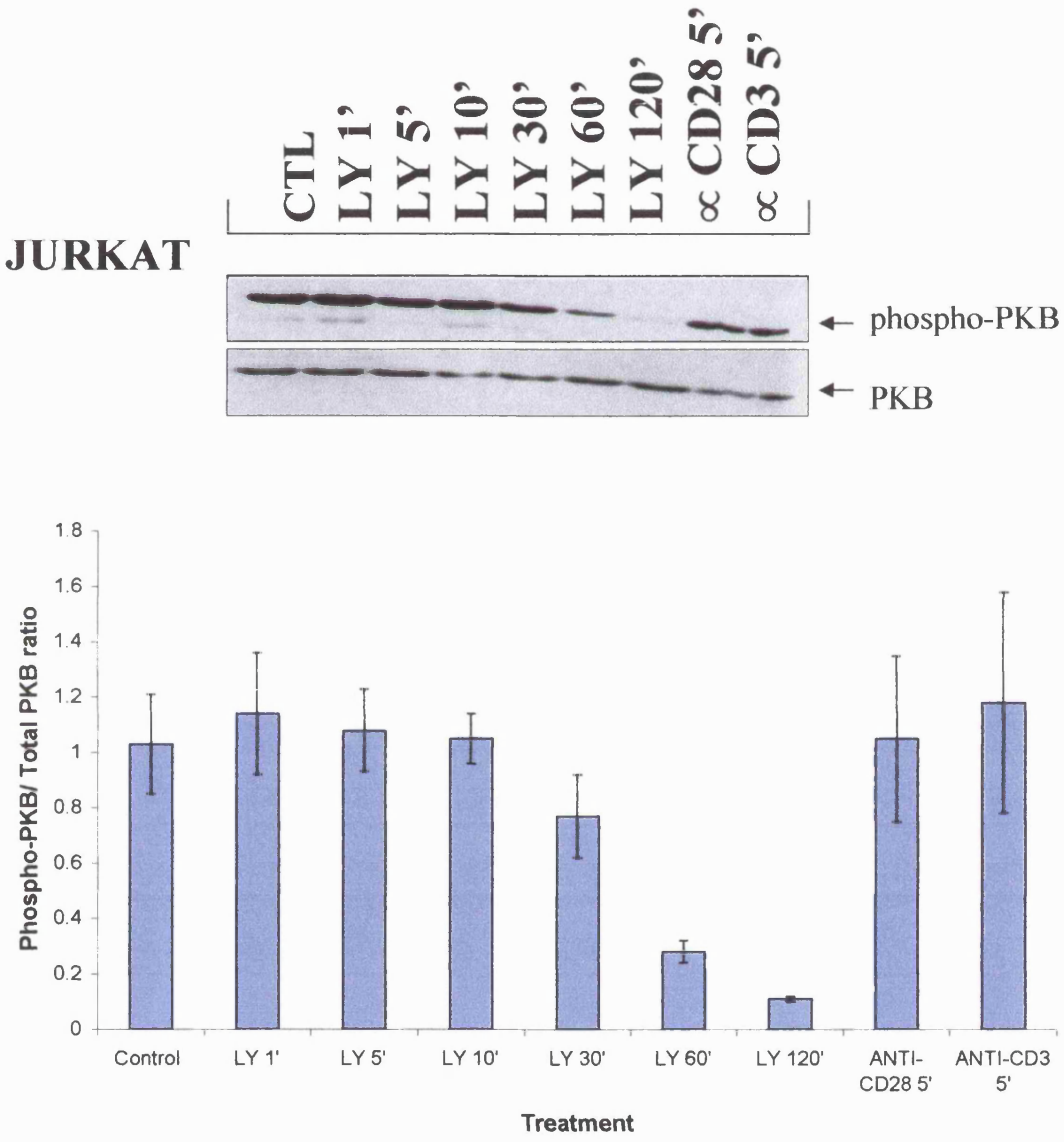

Figure 31: Basal and stimulated levels of phospho-PKB in the Jurkat leukemic T cell line. 10^7 cells per point were treated with LY294002 (10μM) for 1 minute upto 2 hours as shown or stimulated with anti-CD28/CD3 mAbs (9.3/UCHT-1) used at 10μg/ml for 5 minutes. Cell lysates were resolved by SDS-PAGE, transferred onto nitrocellulose and immuno-blotted with an anti-Ser-^{473} phospho-PKB antibody. Equal loading was verified by stripping and re-probing with anti-PKB antibody. Pooled western blot data from two representative experiments were quantified by densitometric analysis and expressed as phospho-PKB: total PKB ratio.

Basal and CD28/CD3 stimulated D-3 phosphoinositide levels in CEM leukemic T cell line

In view of the differing expression of lipid phosphatases between the T cell leukemic lines and T-lymphoblasts, it was hypothesised that accumulation of basal and stimulated levels of D-3 phosphoinositides may vary between cell lines. Thus, CEM cells ($SHIP^+/PTEN^-$) showed reduced basal levels of PI (3,4,5)P_3 when compared to Jurkats cells at the cell equivalent level (figure 32 and table 9). However basal levels of PI (3,4)P_2 were over ten times higher than Jurkat cells (1895 cpm). Ligation of CD28 or CD3 with CHO-B7.1^+ or an anti-CD3 mAb (UCHT-1) resulted in a marked elevation of both PI(3,4,5)P_3 and PI(3,4)P_2. Pre-treatment of cells with LY294002 prior to CD28 stimulation abrogated the increase in D-3 phosphoinositides again suggesting a crucial role for PI 3-K in D-3 phosphoinositide generation. The lower PI(3,4,5)P_3: PI(3,4)P_2 ratio in basal and stimulated CEM cells compared to Jurkat cells suggests that SHIP expression in CEM cells may partially influence the accumulation of PI (3,4,5)P_3, converting it to PI (3,4)P_2 which is found in considerable levels in this cell line.

Figure 32: Measurement of PI(3,4,5)P_3 and PI(3,4,5)P_2 basal and stimulated levels in CEM cells

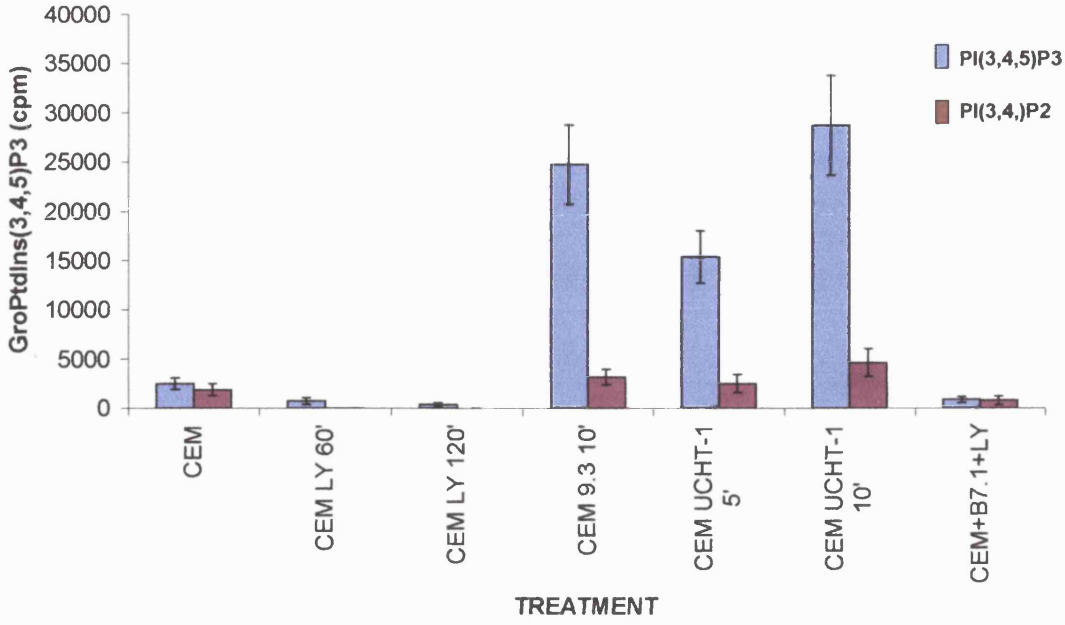

Figure 32: Measurement of PI(3,4,5)P_3 and PI (3,4)P_2 levels in CEM cells. Effect of LY294002 and CHO-B7.1$^+$. 2x10^7 cells /point of CEM were labelled with ^{32}P, stimulated and lipids extracted. Following deacylation lipids were analysed by anion-exchange HPLC as described in *Materials and Methods*. PI(3,4,5)P_3 is represented by the blue bars and PI (3,4)P_2 is represented by the red bars. Data is expressed as mean pooled data ± SEM from 2 independent experiments.

	PI(3,4,5)P_3 (cpm)	PI(3,4)P_2 (cpm)	Ratio PI(3,4,5)P_3: PI(3,4)P_2
Basal	2500	1895	1.3
CD28 10min	28726	4670	6.5

Table 9: D-3 phosphoinositide levels in basal and CD28 stimulated CEM T cells. Data is the mean cpm derived from 2 independent experiments.

Activation of PKB in CEM cells

With the observation that Jurkat cells ($PTEN^-/SHIP^-$) exhibit considerable basal levels of cellular PI(3,4,5)P_3 that could be linked to high basal levels of phosphorylated PKB at ser^{473}, it was decided to investigate if similar observations were seen in CEM leukemic T cells ($PTEN^-/SHIP^+$). Indeed moderate basal levels of phospho-PKB could be seen in CEM cells (figure 33). Upon receptor stimulation of CD28 and CD3, modest increases in phospho-PKB above basal level can be observed that is further highlighted by densitometric analysis from pooled western blot data (figure 33 lower panel). This may suggest that basal levels of phospho-PKB in CEM cells are not quite at saturation levels. Again, treatment of CEM cells with the PI 3-K inhibitor LY294002, used at 10 μM, abolished phospho-PKB levels but an apparent faster rate compared to Jurkat cells perhaps due to the expression of SHIP in CEM cells which can dephosphorylate PI(3,4,5)P_3 and potentially reduce PKB phosphorylation, perhaps by mediating its removal from the plasma membrane to the cytoplasm.

Figure 33: Basal and stimulated levels of phospho-PKB in CEM Cells

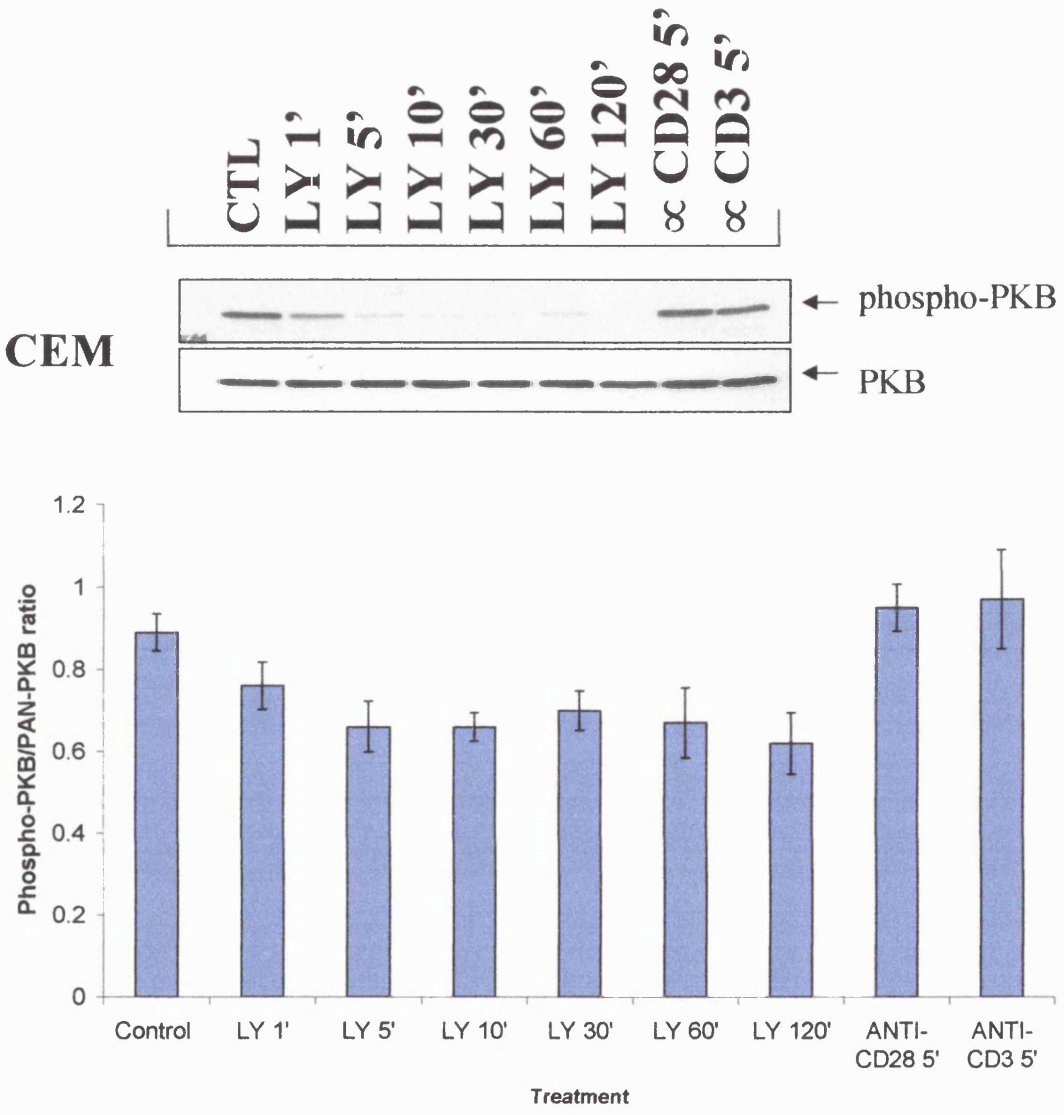

Figure 33: Basal and stimulated levels of phospho-PKB in the CEM leukemic T cell line. 10^7 cells per point were treated with LY294002 (10μM) for 1 minute upto 2 hours as shown or stimulated with anti-CD28/CD3 mAbs (9.3/UCHT-1) used at 10μg/ml for 5 minutes. Cell lysates were resolved by SDS-PAGE, transferred onto nitrocellulose and immuno-blotted with an anti-Ser-^{473} phospho-PKB antibody. Equal loading was verified by stripping and re-probing with anti-PKB antibody. Pooled western blot data from two representative experiments were quantified by densitometric analysis and expressed as phospho-PKB: total PKB ratio.

Basal and CD28/CD3 stimulated D-3 phosphoinositide levels in MOLT-4 leukemic T cell line

The leukemic T cell line MOLT-4 has a similar inositol phosphatase expression as CEM cells in that it expresses SHIP but not PTEN ($PTEN^-/SHIP^+$). P^{32} metabolic lipid labelling of CEM cells highlighted considerable levels of PI(3,4)P_2, the metabolic product of SHIP, which further increased upon cellular CD28/CD3 stimulation. In view of this finding it was investigated if MOLT-4 cells had similar basal and stimulated D-3 phosphoinositide profile.

Levels of PI(3,4,5)P_3 were detectable in unstimulated MOLT cells and were comparable to that observed in CEM cells but were not as high as unstimulated Jurkats. Upon stimulation of CD28 and CD3 on MOLT cells D-3 phosphoinositide levels increased (figure 34 and table 10) with PI(3,4)P_2 levels increasing 3.5-fold after 10 minutes CD28 ligation. Interestingly, basal levels of PI(3,4)P_2 were far lower than that observed in CEM cells. The ratio of PI(3,4,5)P_3 to PI(3,4)P_2 of basal MOLT-4 cells was 3.5, close to the ratio observed in CEM cells but far lower than that observed in Jurkat cells which had a ratio of 27. PI(3,4,5)P_3 levels only elevated 2-fold above basal following CD28 ligation compared to a 15-fold increase observed in Jurkats although surface CD28/CD3 receptor levels were far lower than that observed in Jurkat cells (figure 28) and therefore the capacity to generate D-3 phosphoinositides upon cellular stimulation would be predicted to be reduced. Interestingly the PI(3,4,5)P_3: PI(3,4)P_2 ratio was similar to CEM (table 9/10) and the lower ratio indicates that PI(3,4)P_2 levels are much greater relative to Jurkats.

Figure 34: Measurement of PI(3,4,5)P_3 and PI(3,4,5)P_2 basal and stimulated levels in MOLT-4 cells

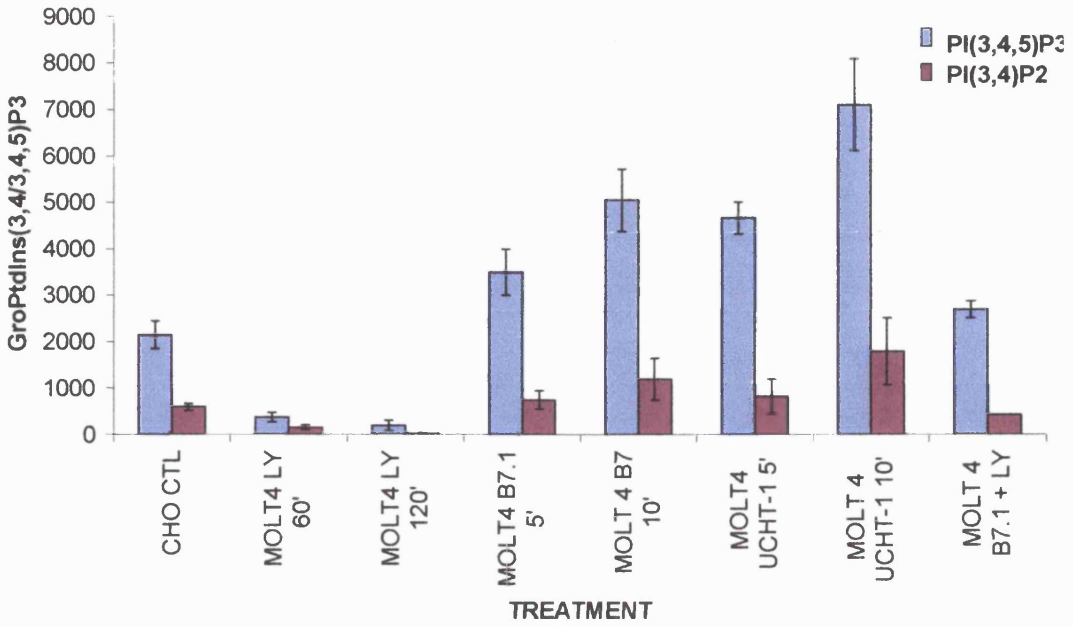

Figure 34: Measurement of PI(3,4,5)P_3 and PI (3,4)P_2 levels in MOLT-4 cells. Effect of LY294002 and CHO-B7.1$^+$. 2x10^7 cells /point of MOLT-4 were labelled with ^{32}P, stimulated and lipids extracted. Following deacylation lipids were analysed by anion-exchange HPLC as described in *Materials and Methods*. PI(3,4,5)P_3 is represented by the blue bars and PI(3,4)P_2 is represented by the red bars. Data is expressed as mean pooled data ± SEM from 2 independent experiments.

	PI(3,4,5)P_3 (cpm)	PI(3,4)P_2 (cpm)	Ratio PI(3,4,5)P_3: PI(3,4)P_2
Basal	2150	614	3.5
CD28 10min	5055	1200	4.2

Table 10: D-3 phosphoinositide levels in basal and CD28 stimulated MOLT-4 T cells. Data is the mean cpm derived from 2 independent experiments

Basal and stimulated levels of phospho-PKB in MOLT-4 leukemic T cells

As with Jurkat and CEM cells it was investigated if MOLT-4 cells ($SHIP^+/PTEN^-$) exhibited detectable basal levels of phospho-PKB. The MOLT-4 cell line had basal levels of phospho-PKB that could be reduced by treatment with the PI 3-K inhibitor LY294002 (figure 35). Interestingly the clearance rate of phospho-PKB levels upon addition of LY294002 was faster than that observed in Jurkat cells (figure 31). Levels of phospho-PKB were barely detectable by 60 minutes of addition of inhibitor whereas detectable levels were clearly visible at 60 minutes after inhibitor addition in Jurkat cells. A similar pattern was also observed in CEM cells. The expression of SHIP may contribute to this increased rate of phospho-PKB clearance in MOLT-4 cells.

Stimulation of MOLT-4 cells with anti-CD28/CD3 mAbs resulted in an marginal increase in cellular phospho-PKB above unstimulated levels (figure 35). This may suggest, like CEM cells, that PI 3-K/PKB signalling is not fully saturated compared to the apparent near saturated levels observed in Jurkat cells. It is of interest to note that despite the low CD3 (< 10%) surface expression as measured by FACS (figure 28) measurable increases in D-3 phosphoinositides and phospho-PKB levels were still observed upon CD3 stimulation.

Figure 35: Basal and stimulated levels of phospho-PKB in MOLT-4 cells

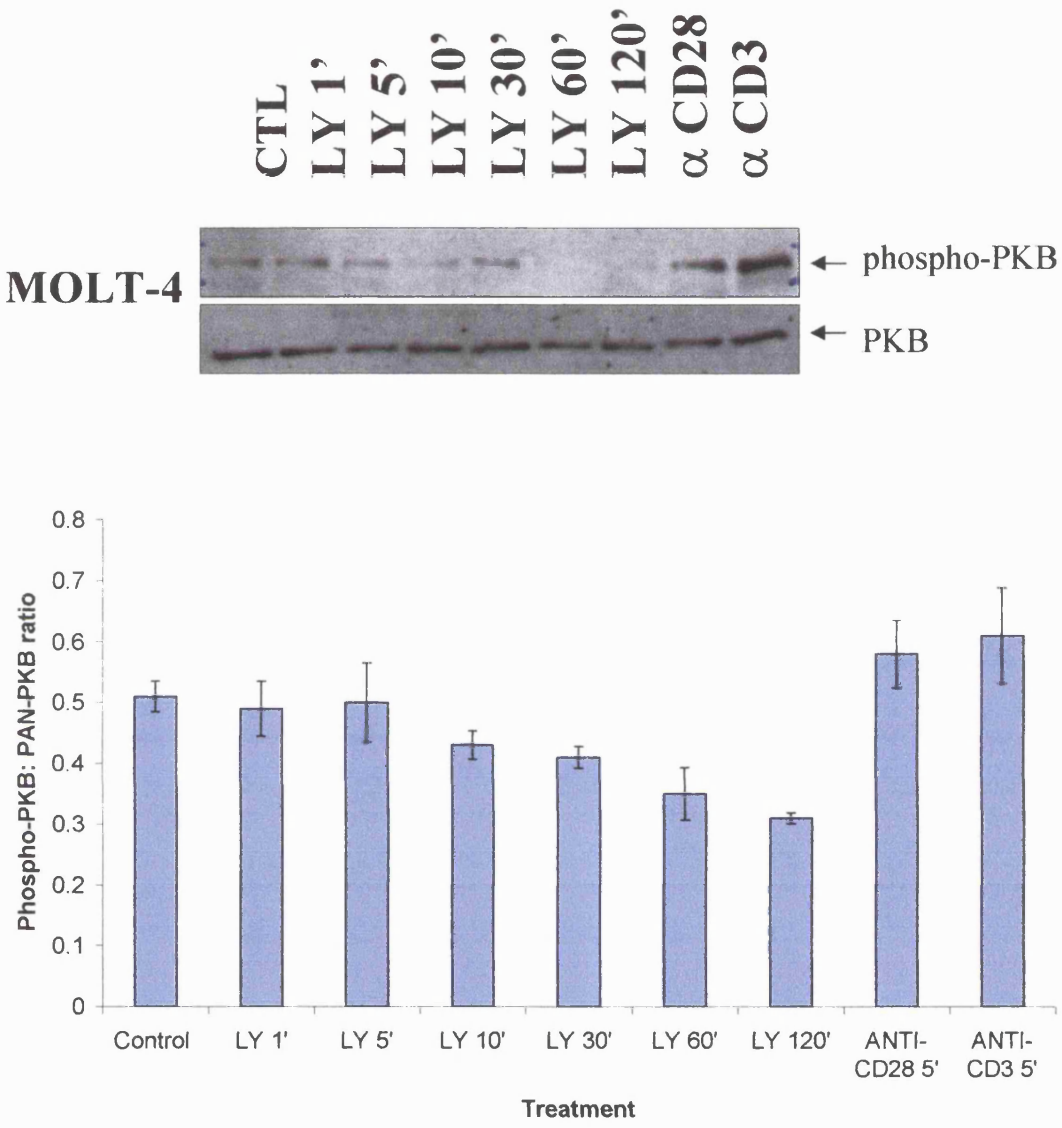

Figure 35: Basal and stimulated levels of phospho-PKB in the MOLT-4 leukemic T cell line. 10^7 cells per point were treated with LY294002 (10μM) for 1 minute upto 2 hours as shown or stimulated with anti-CD28/CD3 mAbs (9.3/UCHT-1) used at 10μg/ml for 5 minutes. Cell lysates were resolved by SDS-PAGE, transferred onto nitrocellulose and immuno-blotted with an anti-Ser-^{473} phospho-PKB antibody. Equal loading was verified by stripping and re-probing with anti-PKB antibody. Pooled western blot data from two representative experiments were quantified by densitometric analysis and expressed as phospho-PKB: total PKB ratio.

Basal and CD28/CD3 stimulated D-3 phosphoinositide levels in HUT 78 leukemic T cell line

Results from this study have confirmed that the leukemic T cell line HUT 78 expresses both SHIP and PTEN ($SHIP^+/PTEN^+$) whereas Jurkat cells express neither phosphatase and CEM and MOLT-4 express SHIP only. Observations so far suggest a role for these phosphatases in PI(3,4,5)P_3 metabolism in T cells and the possible regulation of PKB signalling as determined by phospho-PKB levels in cell lysates. Lipid labelling of HUT 78 cells did reveal reduced basal and stimulated levels of D-3 phosphoinositides compared to all the other T cell lines tested thus far (figure 36). Very little PI(3,4,5)P_3 (289cpm) could be detected in HUT 78 cells under basal conditions whereas PI(3,4)P_2 could not be detected. Upon CD28 and CD3 stimulation approximate PI(3,4,5)P_3 5-fold increased levels above basal were observed although far lower than those observed in other cell lines tested in this study. These increases in PI(3,4,5)P_3 were abrogated by the addition of LY 294002 prior to cellular stimulation. HUT 78 cells did elicit modest detectable increases in PI(3,4)P_2 following stimulation although these levels were still very low (table 11 and figure 36).

It was not the aim of this study to directly compare phosphoinositide levels, with and without external stimulus to the different leukemic T cell lines. It should be stressed that different cell types may incorporate ^{32}P differently, which may result in the apparent varying levels of D-3 phosphoinositides seen between cell lines. The different cell lines, which may differ in size, may also have different basal phosphoinositide lipid pool concentrations. CD28/CD3 receptor expression between the cell lines also significantly varied (figure 28) therefore a direct comparison between stimulated samples is not possible. However the data generated in this study does describe some interesting patterns in relating the relative expression of the phosphatases SHIP and PTEN with particular D-3 phosphoinositide profiles and the suggestion that this may be linked to phospho-PKB levels in these cell lines.

Basal and stimulated levels of phospho-PKB in HUT 78 cells

In contrast to the other T cell lines examined, basal phospho-PKB levels in HUT 78 cells ($PTEN^+/SHIP^+$) were very low and can just be seen visually upon analysis of the western blot (figure 37). As expected, addition of LY294002 rapidly abolished detectable levels of phospho-PKB. Ligation of CD3 receptors by mAbs tended to increase levels of phospho-PKB, but not to extent observed in other stimulated cell lines (figure 37). This may be due in part to low CD28/CD3 receptor expression (<10% CD28/CD3 surface expression) that was observed on these cells during FACS staining (figure 28). Re-probing the blot with PKB verified equal loading and also showed that there were significant amounts of PKB expression. The fact that these cells express both PTEN and SHIP phosphatases could suggest that PI 3-K dependent phosphorylation of PKB is under more stringent control than the other cell lines tested which lack PTEN/SHIP. Thus the low levels of basal phospho-PKB observed in HUT 78 cells may be a result of the efficient metabolism of PI(3,4,5)P_3 by the combined action of PTEN and/or SHIP.

Figure 36: Measurement of basal and stimulated PI(3,4,5)P_3 and PI(3,4,5)P_2 levels in HUT 78 cells

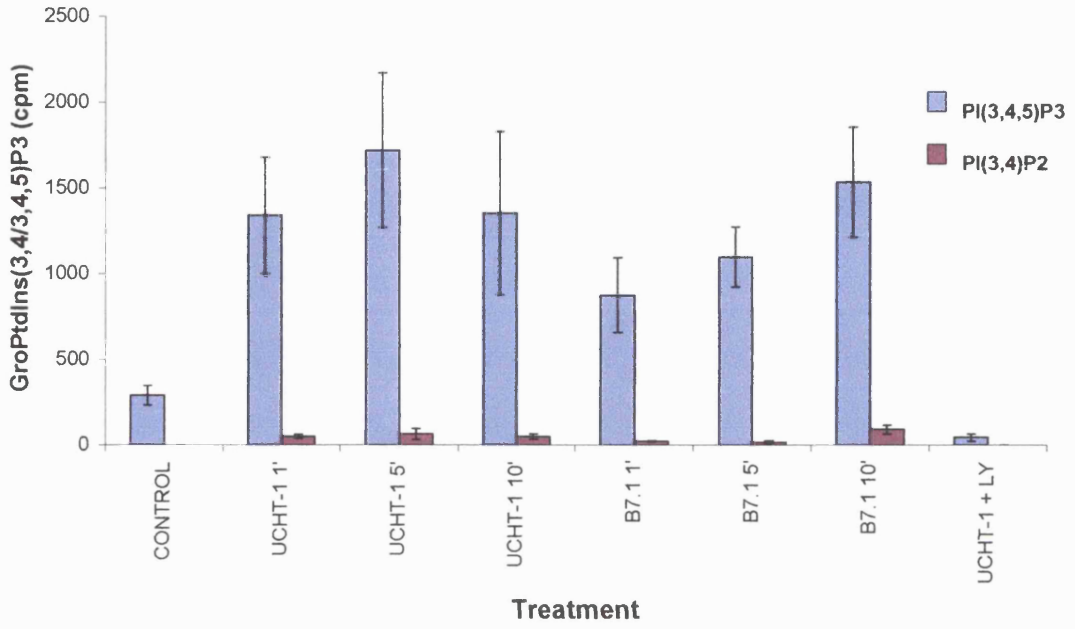

Figure 36: Measurement of PI(3,4,5)P_3 and PI (3,4)P_2 levels in HUT 78 cells. $2x10^7$ cells /point of HUT 78 cells were labelled with ^{32}P, stimulated and lipids extracted. Following deacylation lipids were analysed by anion-exchange HPLC as described in *Materials and Methods*. PI(3,4,5)P_3 is represented by the blue bars and PI(3,4)P_2 is represented by the red bars. Data is expressed as mean pooled data ± SEM from 2 independent experiments.

	PI(3,4,5)P_3 (cpm)	PI(3,4)P_2 (cpm)	Ratio PI(3,4,5)P_3: PI(3,4)P_2
Basal	289	<10	>30
CD28 10min	1535	48	32

Table 11: D-3 phosphoinositide levels in basal and CD28 stimulated HUT 78 T cells. Data is the mean cpm derived from 2 independent experiments.

Figure 37: Basal and stimulated levels of phospho-PKB in HUT 78 cells

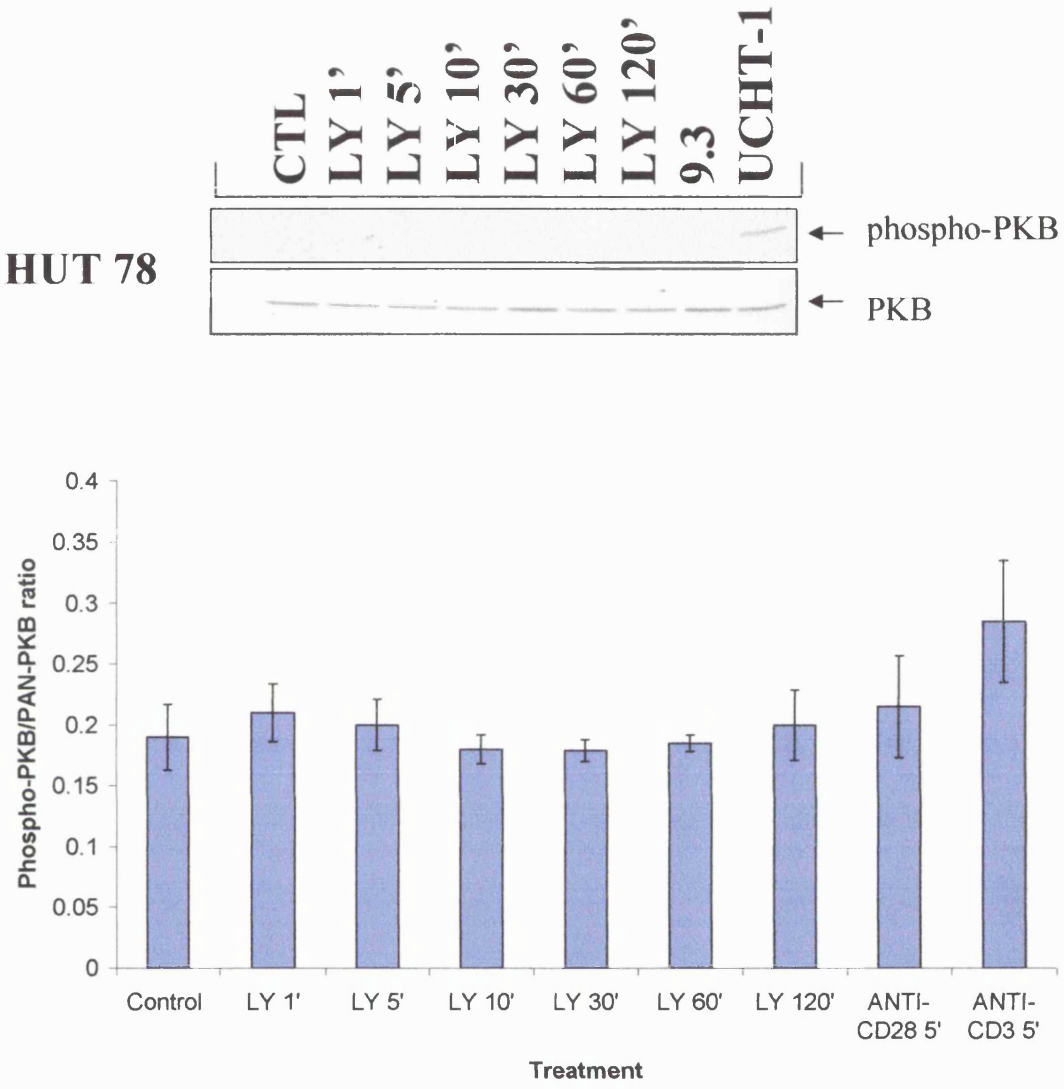

Figure 37: Basal and stimulated levels of phospho-PKB in the HUT 78 cells. 10^7 cells per point were treated with LY294002 (10μM) for 1 minute upto 2 hours as shown or stimulated with anti-CD28/CD3 mAbs (9.3/UCHT-1) used at 10μg/ml for 5 minutes. Cell lysates were resolved by SDS-PAGE, transferred onto nitrocellulose and immuno-blotted with an anti-Ser-^{473} phospho-PKB antibody. Equal loading was verified by stripping and re-probing with anti-PKB antibody. Pooled western blot data from two representative experiments were quantified by densitometric analysis and expressed as phospho-PKB: total PKB ratio.

Basal and Stimulated Levels of D-3 Phosphoinositides in T-Lymphoblasts

Metabolic lipid labelling of the T cell lines tested so far in this study has revealed interesting differences in D-3 phosphoinositide pools which may relate to the differential expression of the lipid phosphatases SHIP and PTEN. Many cell lines by their leukemic nature are defective in key enzymes (such as phosphatases SHIP and PTEN) involved in cellular metabolism. Thus it was deemed important for this study to assess the D-3 phosphoinositide lipid profile of 'real' T lymphoblasts, which are known to express both SHIP and PTEN (figure 26), derived from peripheral blood of healthy human volunteers.

SEB activated T-lymphoblasts ($SHIP^+/PTEN^+$) revealed detectable levels of PI(3,4,5)P_3 (1100 cpm) at the basal level but with relatively low basal levels (101 cpm) of PI(3,4)P_2 (Figure 38 and table 12). Levels of PI(3,4,5)P_3 could be increased by approximately 4-fold by stimulating CD28 and IL-2 receptors present on T-blasts. A more modest increase was also observed upon CD3 receptor stimulation. Stimulation of the IL-2 receptor has been previously reported to activate PI 3-K and induce formation of D-3 phosphoinositides (Ward *et al* 1992). The levels of PI(3,4)P_2 also increased 3-fold upon CD28/IL-2 receptor stimulation. The basal and stimulated PI(3,4,5)P_3: PI(3,4)P_2 ratios in T-blasts was 11 and 10 respectively. Interestingly these ratios fall in between those observed in Jurkat/HUT 78 and CEM/MOLT-4 cell lines. Elevation of PI(3,4,5)P_3 by receptor stimulation in T-blasts could be abrogated by the PI 3-K inhibitor LY294002, indicating the crucial role for PI 3-K in the generation of D-3 phosphoinositides (figure 38).

Basal and stimulated levels of phospho-PKB in T-blasts

T-Lymphoblasts also contained detectable basal levels of phospho-PKB (figure 39) which is expected as they had detectablelevels of PI(3,4,5)P_3 defined by HPLC analysis. Basal levels of phospho-PKB were, once again, rapidly diminished (≤ 5 minutes) by pre-treatment with the PI 3-K inhibitor LY294002. Clearance of phospho-PKB levels upon addition of inhibitor was more rapid than that observed in Jurkat, CEM and MOLT-4 cell lines. Ligation of CD28 and CD3 clearly elevated phospho-PKB levels above those seen at basal levels with a clear increase of phospho-PKB: pan-PKB ratio compared to unstimulated samples (figure 39 lower panel). Approximate equal loading was verified by stripping the membranes and re-probing with PKB antibody.

The data generated may suggest that PI 3-K/PKB signalling is not saturated in basal, unstimulated T-blasts when compared with Jurkat cells. This may be due to in part the expression of SHIP and PTEN in T-blasts which may facilitate efficient metabolism of PI(3,4,5)P_3 and the rapid dephosphorylation of PKB upon treatment of LY294002. In addition, the clear increase in phospho-PKB upon receptor ligation also correlates favourably with strong surface expression of CD3/28 as observed by FACS analysis (figure 28).

Figure 38: Measurement of basal and stimulated PI(3,4,5)P_3 and PI(3,4,5)P_2 levels in SEB-activated T-lymphoblasts

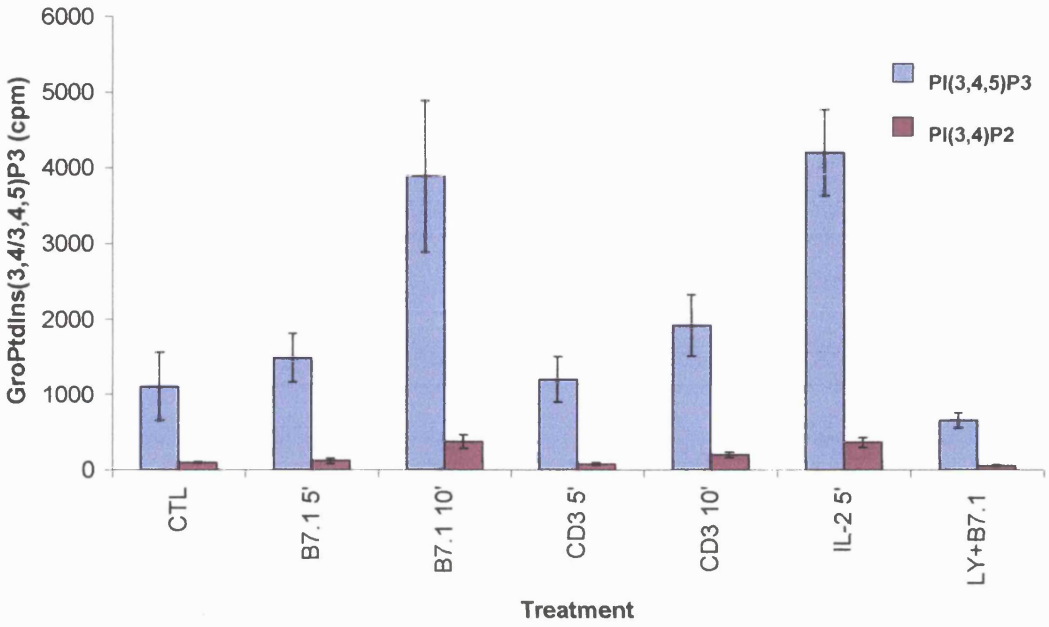

Figure 38: Measurement of PI(3,4,5)P_3 and PI (3,4)P_2 levels in T-lymphoblasts. $2x10^7$ cells /point of T-blasts cells were labelled with ^{32}P, stimulated and lipids extracted. Following deacylation lipids were analysed by anion-exchange HPLC as described in *Materials and Methods*. PI(3,4,5)P_3 is represented by the blue bars and PI(3,4)P_2 is represented by the red bars. Data is expressed as mean pooled data ± SEM from 2 independent experiments. Pooled western blot data from two representative experiments were quantified by densitometric analysis and expressed as phospho-PKB: total PKB ratio.

	PI(3,4,5)P_3 (cpm)	PI(3,4)P_2 (cpm)	Ratio PI(3,4,5)P_3: PI(3,4)P_2
Basal	1110	101	11
CD28 10min	3890	378	10.3

Table 12: D-3 phosphoinositide levels in basal and CD28 stimulated T-lymphoblasts Data is the mean cpm from 2 independent experiments.

Figure 39: Basal and stimulated levels of phospho-PKB in SEB-activated T-lymphoblasts

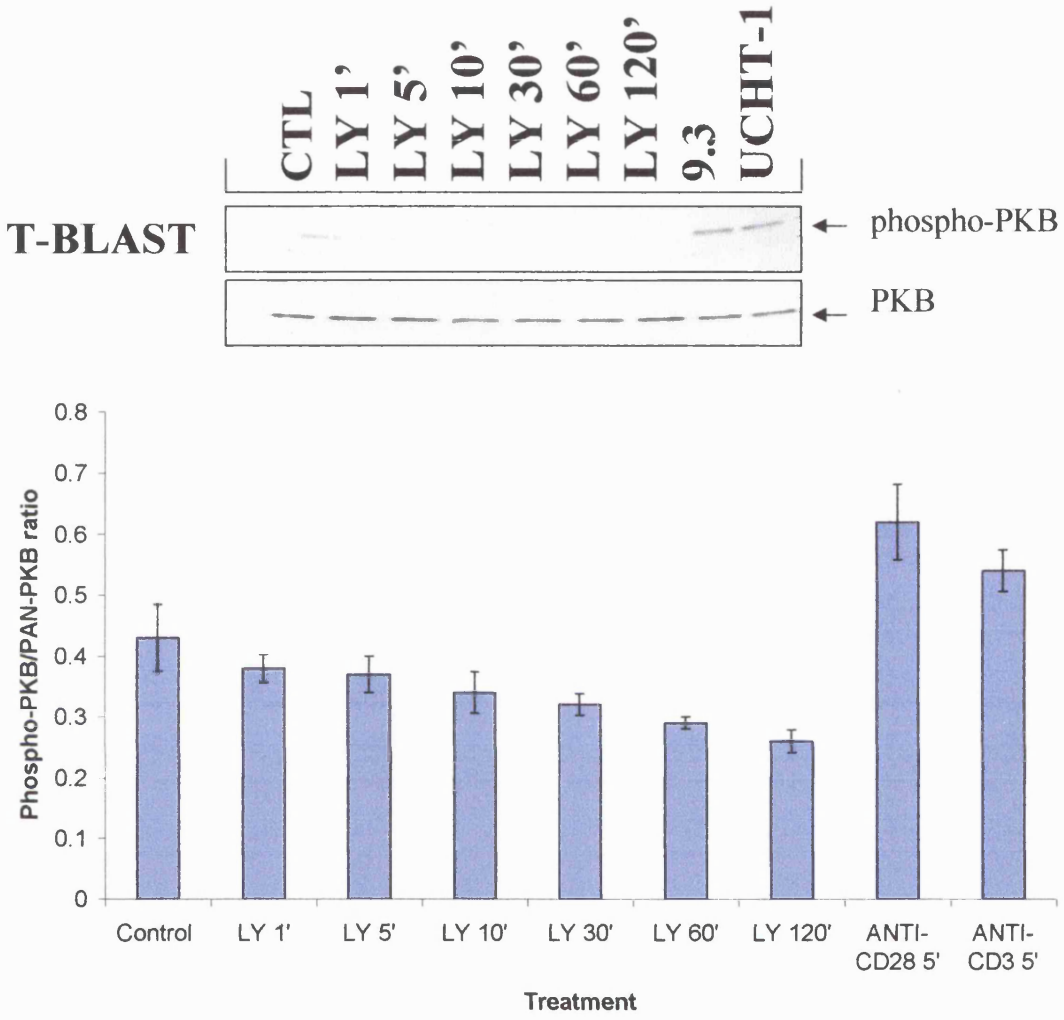

Figure 39: Basal and stimulated levels of phospho-PKB in the T-lymphoblasts. 10^7 cells per point were treated with LY294002 (10μM) for 1 minute upto 2 hours as shown or stimulated with anti-CD28/CD3 mAbs (9.3/UCHT-1) used at 10μg/ml for 5 minutes. Cell lysates were resolved by SDS-PAGE, transferred onto nitrocellulose and immuno-blotted with an anti-Ser-^{473} phospho-PKB antibody. Equal loading was verified by stripping and re-probing with anti-PKB antibody.

Spearman's rank correlation coefficient (r_s) between basal PI(3,4,5)P_3 and phospho-PKB/ total-PKB in T lymphocytes

Data presented so far in this study with leukemic T cell lines and T lymphoblasts suggests a positive correlation between basal PI(3,4,5)P_3 levels and the basal levels of phospho-PKB measured via Western blotting. Basal levels of PI(3,4,5)P_3 and phospho-PKB may be dependent on the expression of the inositol phosphatases SHIP and PTEN. It was decided to investigate if there was a positive relationship between levels of basal PI(3,4,5)P_3 (variable X) and phospho-PKB/ total-PKB (variable y) in the various T cell lines studied using the Spearman's rank correlation coefficient (r_s) statistical test. This coefficient, like other statistical methods based on ranks, does not depend on assumptions about normal distributions. A resultant r_s value between the variables x and y of +1 corresponds to a perfect correlation, a value of 0 represents to no correlation and a value of –1 corresponds to perfect negative correlation.

The test involves scoring a rank for the variables x and y for each T cell line (the number of cell lines represent n). Thus the highest PI(3,4,5)P_3 and phospho-PKB/ total PKB levels between cell lines scores 1, second highest scores 2 and so on forth (table 13). The difference between ranks x and y are then determined giving the value d_i. Each individual d_i value is then squared and used to calculate r_s via the following equation:

$$r_s = 1 - \frac{6 \times \sum (d_i)^2}{n \times (n^2 - 1)}$$

The resultant r_s value can then be compared with published critical p values (appendix 4) and thus determine if there is a significant correlation between the variables.

3 Cell type	SCORE: Basal PI(3,4,5)P_3	SCORE: Phospho-PKB/ total-PKB	RANK: Basal PI(3,4,5)P_3	RANK: Phospho-PKB/ total-PKB	d_i	d_i^2
Jurkat	4670	1.02	1	1	0	0
CEM	2500	0.88	2	2	0	0
MOLT-4	2150	0.51	3	3	0	0
HUT 78	289	0.17	5	5	0	0
T-lymphoblast	1110	0.43	4	4	0	0

$$\sum (d_i)^2 = 0$$

Table 13: Spearman's rank correlation coefficient between basal levels of PI(3,4,5)P_3 and phospho-PKB/ total-PKB in T lymphocytes. Scored data for the variables is ranked as appropriate and the difference between the ranked variables is squared (d_i^2) the sum of which is used to equate the Spearman's coefficient (r_s).

The r_s value, calculated from the equation shown previously, derived from data in table 13 is exactly 1, p value = 0.05, suggesting a significant positive correlation between basal PI(3,4,5)P_3 levels and basal phospho-PKB levels. Thus high basal PI(3,4,5)P_3 generates higher levels of phospho-PKB. This correlation also supports the crucial role for PTEN and SHIP expression in the metabolism of basal levels of PI(3,4,5)P_3 and its vital role for regulating PKB phosphorylation and activation in T lymphocytes. However this correlation does depend on the cell lines having equivalent phosphoinositide pools and PKB protein expression. It is unlikely that is indeed the case, so the result of the Spearman's analysis, although of considerable interest, should be viewed with a degree of caution.

Comparison of basal phospho-PKB in leukemic T cell lines

Figure 40 compares basal phospho-PKB levels of different leukemic cell lines (10^7 cells per point). Again Jurkat cells revealed higher basal levels of phospho-PKB, at the cell equivalent level, compared to the other cell lines tested with HUT 78 again having undetectable basal levels of phospho-PKB. The doublet bands detected, which cannot be readily explained, may be as a result of the detection of various PKB isoforms. This doublet is sometimes seen on some other western blots using phospho/pan-PKB antibodies (see figure 31-Jurkat phospho-PKB western).

However it is accepted that we cannot directly compare phospho-PKB levels between the different cells types studied. For example cells may have varying levels of PKB protein expression that may contribute to the data observed. Another way to overcome this problem would be to load equal amounts of protein (rather than using whole cell equivalents) onto the gel from lysates of each of the cell lines tested. Unfortunately due to time constraints this was not achieved. However it becomes increasingly apparent that there is an intimate pattern between inositol phosphatase expression, D-3 phosphoinositide profiles and the relative activation status of PI(3,4,5)P_3–driven effector proteins including PKB.

Figure 40: Comparison of basal levels of phospho-PKB in leukemic T cell lines.

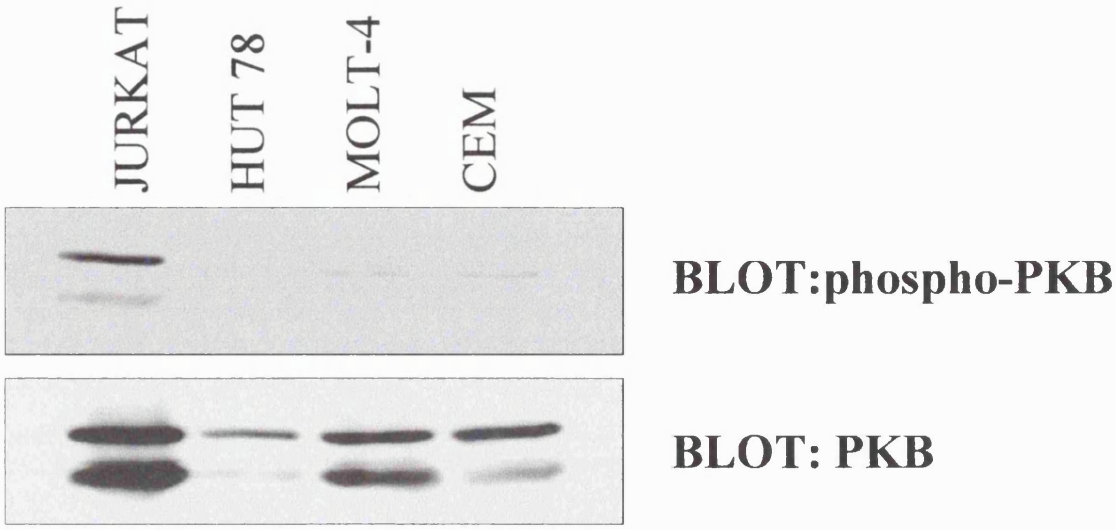

Figure 40: Comparison of basal levels of phospho-PKB in leukemic cell lines. Cell extracts (10^7 cells per point) were lysed, resolved by SDS-PAGE and transferred onto nitrocellulose and immuno-blotted with a phospho-PKB polyclonal antibody as described in *Materials and Methods*. Equal loading was verified by stripping and reprobing with an anti-PKB mAb. Results are from a single experiment representative of 2 others.

Phosphorylation Status of PKB and PKB Effectors in Leukemic Cell Lines and T-Lymphoblasts.

It has been shown that T cell lines studied have different levels of basal and stimulated D-3 phosphoinositides. This appears to determine basal levels of phospho-PKB in these cells. Another way to measure the activation status of PKB is to measure the phosphorylation state of its downstream effectors. A well-characterised downstream target of PKB is the multifunctional serine threonine kinase, glycogen synthase kinase 3 (GSK3). PKB is known to phosphorylate and inactivate GSK3 in a PI 3-K dependent manner (Cross *et al* 1995). Using phospho-specific antibodies to GSK3 we therefore are able to monitor the basal *in vivo* activity of PKB in the T cell lines studied.

It can be seen from figure 41 that Jurkat cells show high constitutive levels of phospho-GSK3 in accordance with its high phospho-PKB levels. Likewise, phospho-GSK3 levels are also high in MOLT-4 and CEM cells but not to the extent as those seen in Jurkat cells. In contrast, HUT 78 cells have lower levels of phospho-GSK-3 perhaps reflecting the low levels of phospho-PKB seen in these cells. T-lymphoblasts also have detectable levels of phospho-GSK3 but again not to the extent of Jurkat cells but interestingly more than MOLT4 and CEM cells. The elevated levels of phospho-GSK3 seen in T-lymphoblasts are not easily explained and may generated as a by-product of the SEB/IL-2 stimulation/maintenance cell culture protocol. Alternatively other poorly characterised signalling pathways may couple to GSK3. The doublet bands seen in the blot most certainly represent GSK3 isoforms (GSK3α and GSKβ) with GSKα being the slightly larger isoform. Equal loading was verified by stripping and reprobing with anti-GSK3 mAb. The conclusions drawn from phospho-PKB data shown in figure 40 suggests that basal levels of active phospho-PKB may regulate the amount of phospho-GSK3 in the cell.

Figure 41: Comparison of basal levels of phospho-GSK3 in leukemic cell lines.

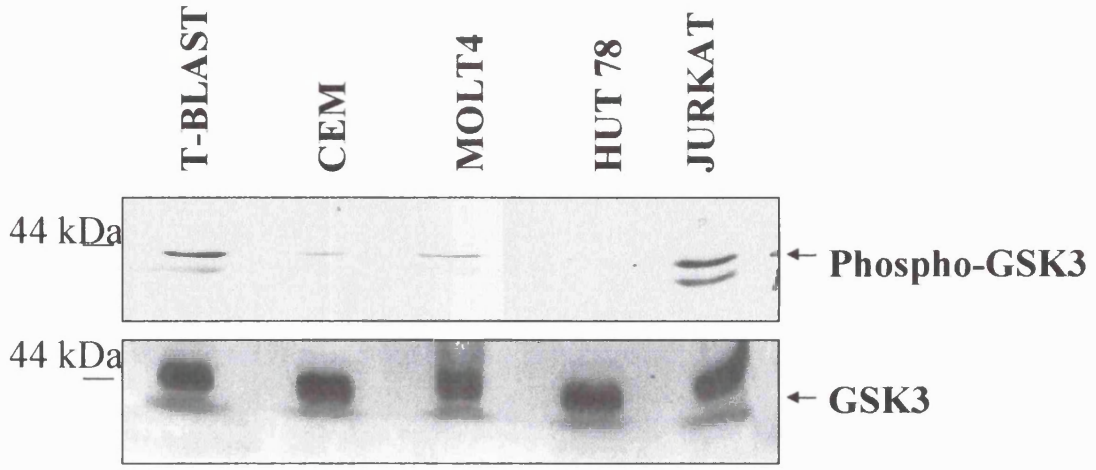

Figure 41: Comparison of basal levels of phospho-GSK3 in leukemic cell lines. Cell extracts (10^7 cells per point) were lysed, resolved by SDS-PAGE and transferred onto nitrocellulose and immuno-blotted with a phospho-GSK3 antibody as described in *Materials and Methods*. Equal loading was verified by stripping and reprobing with an anti-GSK3 mAb. Results are from a single experiment representative of 2 others.

Summary

- All T cell lines and T-lymphoblasts contained mRNA for SHIP and PTEN (figure 25)

- Jurkat cells lack both SHIP and PTEN at the protein level. Interestingly MOLT-4 and CEM cells express SHIP but not PTEN whilst the cell line HUT 78 and T-lymphoblasts expressed both SHIP and PTEN phosphatases at the protein level (figure 26).

- Jurkat cells contained considerable basal levels of PI(3,4,5)P_3 with relatively low basal levels of PI(3,4)P_2. This is reflected in a high basal PI(3,4,5)P_3: PI(3,4)P_2 ratio of 27. Upon CD28 stimulation this ratio increased to 152. These marked increases upon stimulation may be in part due to the lack of SHIP/PTEN expression (figure 30).

- CEM and MOLT-4 ($SHIP^+/PTEN^-$) cell lines had basal PI(3,4,5)P_3: PI(3,4)P_2 ratios of 1.3 and 3.5 respectively. This reflects the increased levels of the SHIP metabolite PI(3,4)P_2 present in the phosphoinositide pool and differs markedly from the situation observed in Jurkats. Upon CD28 stimulation a modest increase in the PI(3,4,5)P_3: PI(3,4)P_2 ratio was observed (CEM = 6.5, MOLT-4 = 4.2) again much lower than Jurkat and perhaps reflecting a functional role for SHIP in PI(3,4,5)P_3 dephosphorylation to PI(3,4)P_2 in CEM and MOLT-4 cells (figure 32 and 34).

- HUT 78 cells had lower, but still detectable, measurable basal levels of PI(3,4,5)P_3 and undetectable basal levels of PI(3,4)P_2 (figure 36). Upon CD28 stimulation D-3 phosphoinositides did increase exhibiting a PI(3,4,5)P_3: PI(3,4)P_2 ratio of 30 perhaps reflecting the relative low levels of PI(3,4)P_2 in HUT 78 cells compared to CEM and MOLT-4.

- T-blasts which express both SHIP and PTEN had measurable basal levels of both PI(3,4,5)P_3 and PI(3,4)P_2 (ratio 11). D-3 phosphoinositides did

increase upon CD28 stimulation but the PI(3,4,5)P_3: PI(3,4)P_2 ratio stayed relatively constant at 10 (figure 38).

- Phospho-PKB levels in Jurkat cells were high in cell lysates and did not detectably increase upon cell stimulation, perhaps suggesting saturation of PI 3-K signalling in this cell line. A slow clearance (over 60 minutes) of phospho-PKB levels was also observed upon treatment with LY 294002 which may reflect slow metabolism of PI(3,4,5)P_3 due to lack of SHIP and PTEN (figure 31).

- CEM and MOLT-4 cells also exhibited basal levels of phospho-PKB and which were only modestly increased upon cellular stimulation. Treatment of LY294002 cleared phospho-PKB levels but at a more rapid rate than that observed in Jurkat cells (figures 33 and 35).

- HUT 78 cells, which express both SHIP and PTEN contained no detectable phospho-PKB under basal conditions (figure 37). Small increases in phospho-PKB levels could be observed upon stimulation although this may be due, at least in part, to low CD3/CD28 receptor expression.

- T-blasts were shown to contain basal phospho-PKB levels, rapidly cleared upon addition of LY294002. Cell stimulation elicited clear increases in cellular levels of phospho-PKB (figure 39).

- Spearman's rank correlation revealed a significant correlation (p value = 0.05) between basal PI(3,4,5)P3 levels and basal phospho-PKB levels in the T cell lines studied.

- Comparison of phospho-PKB and phospho-GSK3 (a downstream target for PKB), between the T cell lines tested revealed high phospho basal levels in Jurkat cells. CEM and MOLT-4 cells exhibited slightly lower levels of phospho-PKB/GSK3 with HUT 78 showing almost undetectable levels of phospho-PKB/GSK3.

Regulation of SHIP and PTEN by CD28 in T cells

Background

Analysis of the structure of SHIP (figure 12) reveals several identifiable motifs that can participate in multiple protein-protein interactions. This suggests that SHIP has diverse signalling capabilities and may not function purely as an inositol phosphatase. A major biochemical event following CD28 ligation is the recruitment and activation of PI 3-K resulting in the accumulation of D-3 phosphoinositides (Ward *et al* 1995). This section will investigate the regulation of the inositol phosphatases SHIP and PTEN by various receptors expressed on different T cell lines with particular emphasis on the co-stimulatory receptor CD28.

Expression of Surface Antigens and SHIP and PTEN Proteins in Murine Hybridoma T Cells

Murine hybridoma T cells (clone DC.27 a kind gift from D. Olive, Marseilles INSERM France), stably transfected with high surface levels of the human CD28 receptor were suitable cells to study CD28 signal transduction. Flow cytometry revealed that CD28 was expressed on the cell surface at high levels (figure 41). Murine cells, stably transfected with a site-mutated human CD28 (ΔYF 173/200) which is unable to recruit PI 3-K (Pages *et al* 1996) were also used to study CD28 regulation of SHIP. These cell lines enables the role of the YXXM motif of human CD28 in the regulation of SHIP to be determined. FACS analysis also revealed high levels of this CD28-mutant receptor on the cell surface (figure 41). Cell lysates from DC.27 cells were shown to express high levels of SHIP as detected from Western blotting using an anti-SHIP Ab (figure 42). Jurkat lysates on the same gel revealed no detectable levels of SHIP as previously confirmed from earlier experiments during this study (figure26).

SHIP is Tyrosine Phosphorylated in Response to CD28 Stimulation in Murine Hybridoma Cells

Ligation of hCD28 with the mAb 9.3 resulted in rapid tyrosine phosphorylation of SHIP by 1 minute (figure 43). Phosphorylation of SHIP was sustained for up to 10 minutes following stimulation. The observed tyrosine phosphorylation was specific to the receptor CD28 as an isotype IgG2a control had no effect on tyrosine phosphorylation of SHIP. This observation also suggests, albeit indirectly, that any possible FcγRIIb receptors present on DC.27 cells are not responsible for the observed tyrosine phosphorylation of SHIP. Multiple bands of SHIP are seen in the reprobe which is most likely to be indicative of the presence of C-terminal-truncated versions of SHIP i.e. p135/p155 SHIP which can be observed when using a SHIP polyclonal Ab recognising an N-terminal epitope of SHIP (Appendix 1).

Figure 41: Expression of transfected (wild type and ΔYF 173/200) human CD28 on DC.27 murine hybridoma cells.

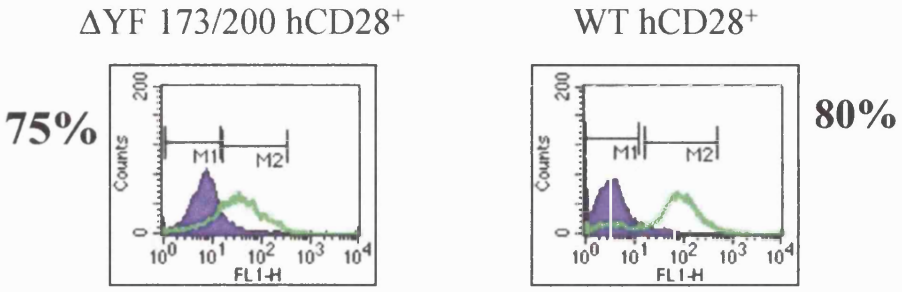

Figure 41: Expression of transfected (wild type and ΔYF 173/200) human CD28 on DC.27 murine hybridoma cells. $1X10^5$ DC.27 cells were analysed for CD28 expression using anti-CD28 9.3 mAb (green bar) against an isotype control IgG_{2a} (blue bar). Cells were stained with an FITC-conjugated goat anti-mouse secondary Ab and analysed on a Becton Dickinson FACS vantage as described in *Materials and Methods*. Results are from a single experiment representative of at least 3 others.

Figure 42: Expression of SHIP in DC.27 murine hybridoma cells

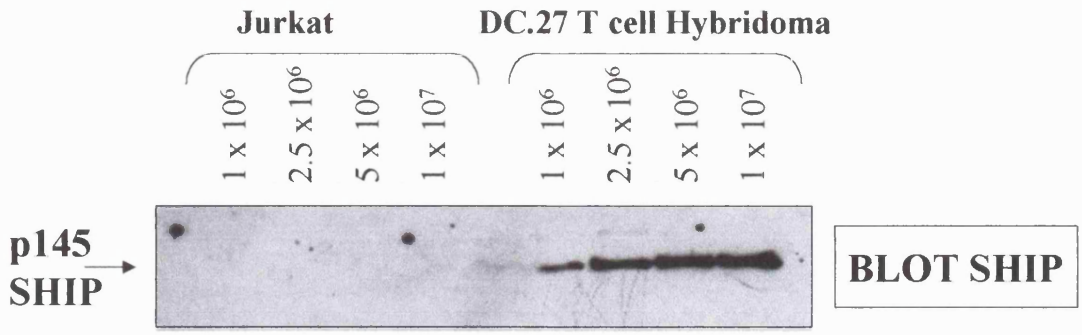

Figure 42: Expression of SHIP DC.27 murine hybridoma cells. Jurkat and DC.27 cells were prepared at the above stated cell equivalents, lysed and proteins precipitated by acetone precipitation as stated in Materials and Methods. Proteins were resolved by SDS-PAGE and transferred to nitrocellulose and immunoblotted with a SHIP mAb. Results are from a single experiment representative of 3 others.

Figure 43: SHIP is tyrosine phosphorylated in response to CD28 ligation in murine DC.27 T cells.

Figure 43: SHIP is tyrosine phosphorylated in response to CD28 ligation in DC.27 cells. 10^7 DC.27 cells were aliquoted and stimulated with the anti-CD28 mAb, 9.3 or isotype matched control IgG_{2a} at 1 μg/ml for the indicated time. Cells were lysed and SHIP was immunoprecipitated using an anti-SHIP mAb. Immunoprecipitates were resolved by SDS-PAGE and transferred to nitrocellulose and immunoblotted with an anti-phosphotyrosine antibody 4G10. Blots were stripped and immunoblotted with anti-SHIP mAb to verify equal loading. Results are from a single experiment representative of 3 independent experiments.

SHIP is Tyrosine Phoshorylated by the CD28 Ligands B7.1 and B7.2 in DC.27 Murine Hybridoma T cells.

Co-sedimentation of wild type expressing hCD28 DC.27 with CHO-B7.1$^+$ cells also resulted in a rapid tyrosine phosphorylation of SHIP (figure 44). It has been demonstrated previously that CHO cells do not express SHIP, hence the source of phosphorylated SHIP in these experiments emanates from DC.27 murine hybridoma T cells and not from CHO cells (Edmunds *et al* 1999). Ligation of CD28 with it's natural ligand B7.1 showed similarities to that observed with the anti-CD28 mAb (9.3) in that it induced rapid tyrosine phosphorylation of SHIP by 1 minute which could be sustained for up to 10 minutes. Ligation of CD28 with CHO-B7.2$^+$ (kind gift from D. Sansom, Birmingham, UK) cells also induced rapid and sustained tyrosine phosphorylation of SHIP (figure 44) with similar kinetics to that observed for CHO-B7.1$^+$ cells. However, it should be noted that murine CD28 might also ligate with CHO-B7.1/2+ and contribute to the effects observed. Previous work however has suggested that mCD28 surface levels are approximately 50 fold-less than transfected hCD28 levels (C. Edmunds personal communication). Unfortunately lack of a suitable staining antibody meant that mCD28 levels couldn't be determined during the course of this study. Nonetheless, these results strongly suggest that SHIP is a biochemical target of CD28-activated PTKs.

SHIP is Tyrosine Phosphorylated in Response to CD3 Ligation in DC.27 Murine Hybridoma T cells.

Stimulation of the TCR is known to induce the tyrosine phosphorylation of SHIP (Lamkin *et al* 1997). Therefore the tyrosine phosphorylation of SHIP in response to stimulation of CD28 and CD3 receptors alone, or in combination, was investigated. Ligation of murine TCR with the anti-CD3 mAb, 2C11 induced the rapid and sustained tyrosine phosphorylation of SHIP to a similar extent as CD28 ligation (figure 45). The multiple tyrosine-phosphorylated bands seen on the blots are most likely the truncated isoforms of SHIP. Ligation of both the CD28 and CD3 receptors together, stimulated further increased levels of tyrosine phosphorylated SHIP, suggesting the existence of positive interaction between the signalling pathways (figure 45).

Figure 44: SHIP is Tyrosine Phoshorylated by the natural CD28 Ligands B7.1 and B7.2 in DC.27 Murine Hybridoma T cells.

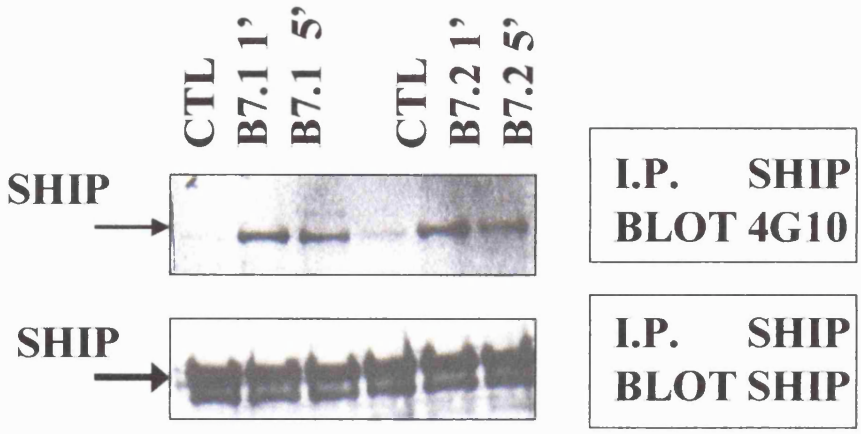

Figure 44: SHIP is tyrosine phosphorylated by the CD28 Ligands B7.1 and B7.2 in DC.27 Murine Hybridoma T cells. 10^7 DC.27 cells were aliquoted left unstimulated as a control (CTL) or stimulated with CHO-B7.1$^+$ or CHO-B7.2$^+$ (at a ratio of 3 DC.27 cells: 1 CHO-B7.1/2$^+$ cell) for the times indicated. Cells were lysed and lysates immunoprecipitated with anti-SHIP polyclonal Ab. Immunoprecipitates were resolved by SDS-PAGE and transferred to nitrocellulose and immunoblotted with an anti-phosphotyrosine antibody 4G10. Blots were stripped and immunoblotted with anti-SHIP mAb to verify equal loading. Results are from a single experiment representative of 2 others.

Figure 45: SHIP is Tyrosine Phosphorylated in Response to CD3 Ligation in DC.27 Murine Hybridoma T cells.

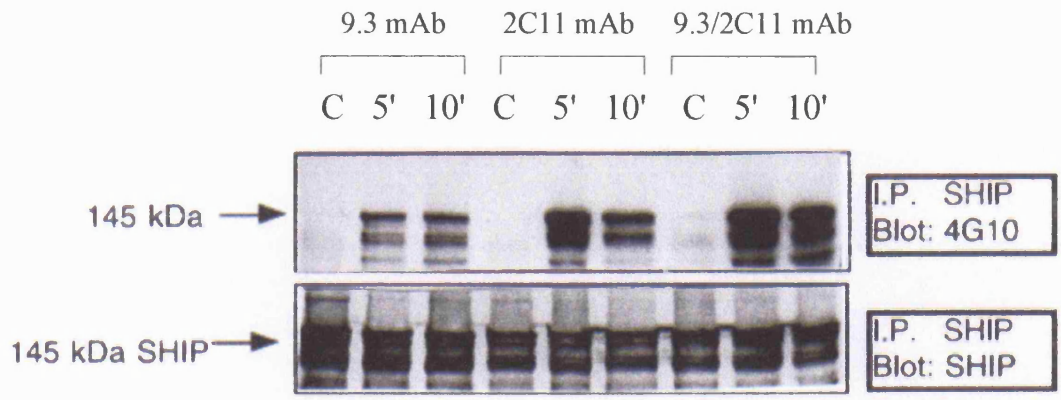

Figure 45: SHIP is Tyrosine Phosphorylated in Response to CD3 Ligation in DC.27 Murine Hybridoma T cells. 10^7 DC.27 cells were aliquoted left unstimulated as a control (CTL) or stimulated with 5 μg/ml anti-CD28 mAb (9.3) or 5 μg/ml anti-CD3 mAb (2C11) alone or in combination. Cells were lysed and SHIP was immunoprecipitated using an anti-SHIP polyclonal Ab. Immunoprecipitates were resolved by SDS-PAGE and transferred to nitrocellulose and immunoblotted with an anti-phosphotyrosine antibody 4G10. Blots were stripped and immunoblotted with anti-SHIP mAb to verify equal loading. Multiple bands seen on the blot are likely to represent the truncated isoforms of SHIP i.e. p135/p145/p155 isoforms of SHIP. Results are from a single experiment representative of 3 independent experiments.

CD28 coupling to PI 3-K is not required for SHIP tyrosine phosphorylation in DC.27 murine hybridoma T cells.

Experiments performed by Edmunds *et al* shows that in unstimulated cells SHIP lies within the cytoplasm, but that it rapidly migrates to the plasma membrane following CD28 stimulation (Edmunds *et al* 1999). It was also shown that no detectable amounts of SHIP could couple to CD28 following receptor stimulation via co-immunoprecipitation studies. One possible mechanism of targeting SHIP to the plasma membrane following CD28 ligation is via the interaction of SHIP or a PH-domain containing co-associating protein with D-3 phosphoinositides formed in response to CD28 activation, thereby allowing its tyrosine phosphorylation by CD28-activated PTK.

DC.27 murine hybridoma T cells expressing stably transfected wild type human CD28 and ΔYF 173/200 mutant (figure 41), previously shown to abrogate PI 3-K recruitment (Pages *et al* 1996), were used to assess the ability of CD28 to tyrosine phosphorylate SHIP following receptor ligation. Mutation of the YXXM PI 3-K binding motif in CD28 did not effect its ability to tyrosine phosphorylate SHIP following stimulation with anti-CD28 mAb when compared with wild type CD28 (figure 46): in both cases up to 50% increases in phospho-SHIP levels being observed after 10 minutes CD28 stimulation. Equal loading was verified by stripping and reprobing with SHIP polyclonal Ab. This suggests therefore, that SHIP or a SHIP-associated protein is not dependent on the generation of PI(3,4,5)P_3 by PI 3-K for its tyrosine phosphorylation SHIP. It also suggests, albeit indirectly, that SHIP is unlikely to be a target for D-3 phosphoinositide dependent tyrosine kinases. This hypothesis could have been tested further by observing the effect of pre-treatment of DC.27 cells with pharmacological inhibitors of PI 3-K (including wortmannin and LY 294002) prior to CD28 stimulation and the subsequent effect on the tyrosine phosphorylation of SHIP. Unfortunately these experiments were not conducted in this study due to time constraints.

Figure 46: CD28 coupling to PI 3-kinase is not required for SHIP tyrosine phosphorylation in DC.27 murine hybridoma T cells.

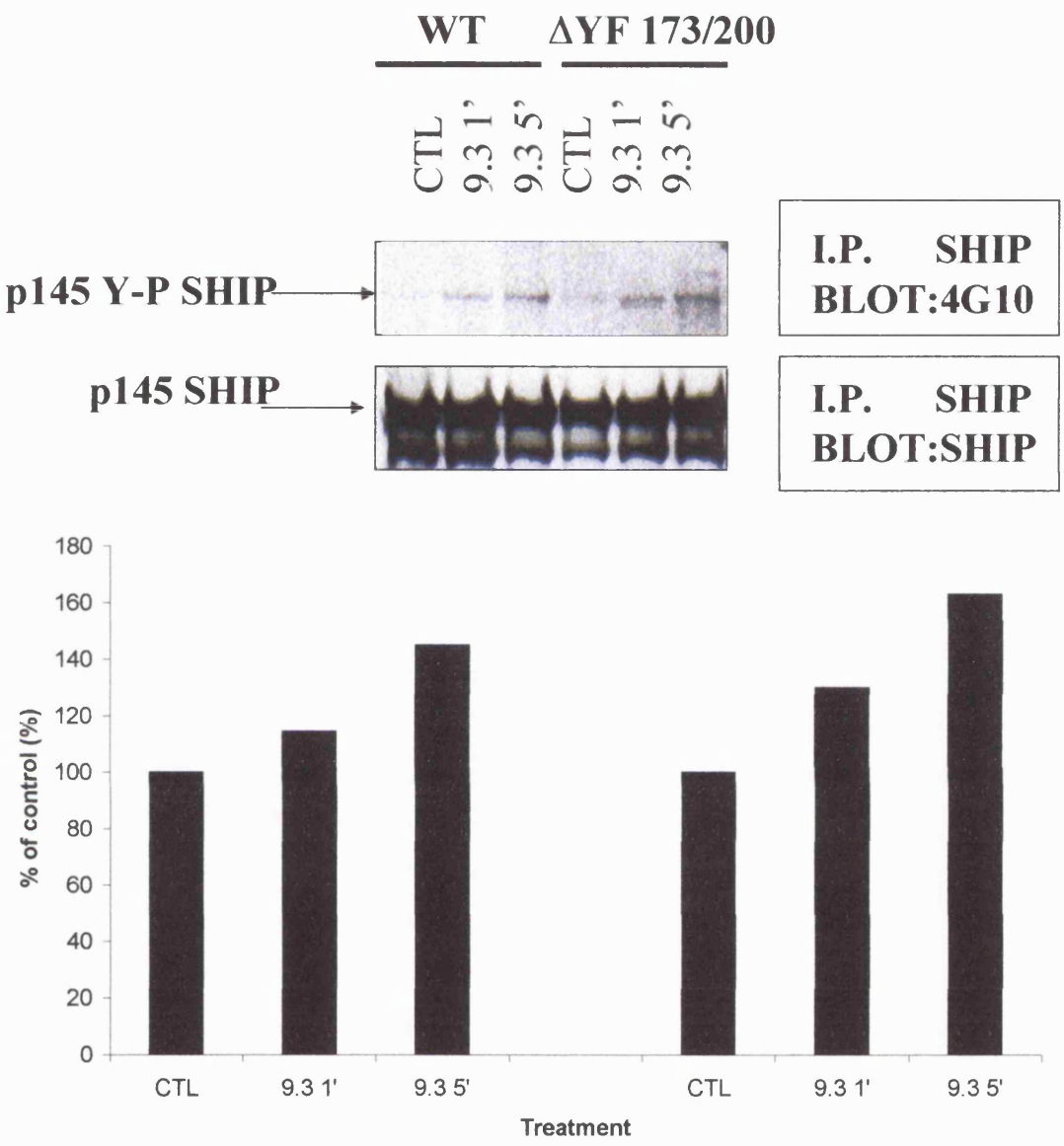

Figure 46: CD28 coupling to PI 3-kinase is not required for SHIP tyrosine phosphorylation. 10^7 DC.27 cells expressing wild type (WT) or ΔY/F 173/200 hCD28$^+$ were either left unstimulated as a control (CTL) or stimulated with anti-CD28 mAb 9.3 (1 μg/ml) for the times indicated. Cells were lysed and lysates immunoprecipitated with an anti-SHIP polyclonal Ab. Immunoprecipitates were resolved by SDS-PAGE and transferred to nitrocellulose and immunoblotted with an anti-phosphotyrosine antibody 4G10. Bands were quantified by densitometry and expressed as a % of control. Blots were stripped and immunoblotted with anti-SHIP polyclonal Ab to verify equal loading. Results are from a single experiment representative of 3 independent experiments.

SHIP is tyrosine phosphorylated in response to CD28, CD2, CD3 and IL-2 receptor stimulation in human T-lymphoblasts.

The evidence presented thus far suggests that SHIP is downstream target following CD28/CD3 stimulation in murine hybridoma T cells. It was deemed necessary to assess such signal transduction events of SHIP tyrosine phosphorylation in IL-2-treated human T-lymphoblasts. Human T cells, derived from peripheral blood of healthy volunteers, represent a more physiologically relevant cell model to monitor signal transduction and can potentially overcome some of the limitations of leukemic T cell lines (Astoul *et al* 2001).

Stimulation of T-lymphoblasts with anti-CD28 (9.3), anti-CD3 (UCHT-1), anti-CD2 (6F103 and 3C15- note two antibodies are required to stimulate the CD2 receptor-mediated signal transduction) mAbs and with recombinant human IL-2 resulted in tyrosine phosphorylation of SHIP as seen in figure 47 which is representative of two separate experiments. Approximate equal loading was verified by stripping and probing with anti-SHIP in this case. This data suggests that multiple receptors present on human T cells may potentially utilise SHIP as a biochemical target and therefore supports a role for SHIP in T-lymphocyte signalling. SHIP is also known to be tyrosine phosphorylated in response to a variety of cytokines and growth factors (Liu *et al* 1994) but this is the first evidence that SHIP is a downstream target for the CD2 and IL-2 receptors in human T lymphocytes. Closer analysis of figure 47 does reveal inconsistencies in the ability of receptors to tyrosine phosphorylate SHIP once stimulated. For example the CD28 receptor, once stimulated with Ab, in the top panel gives only modest phosphorylation of SHIP whilst a clear increase is seen in the bottom panel. These discrepancies, which are not readily explicable, represent experiments from different donors and a multitude of factors may responsible including experimental error, variation of receptor expression profiles between donors etc. As a result the data should be interpreted with a degree of caution.

Figure 47: SHIP is tyrosine phosphorylated in response to CD28, CD2, CD3 and IL-2 receptor stimulation in human T-lymphoblasts.

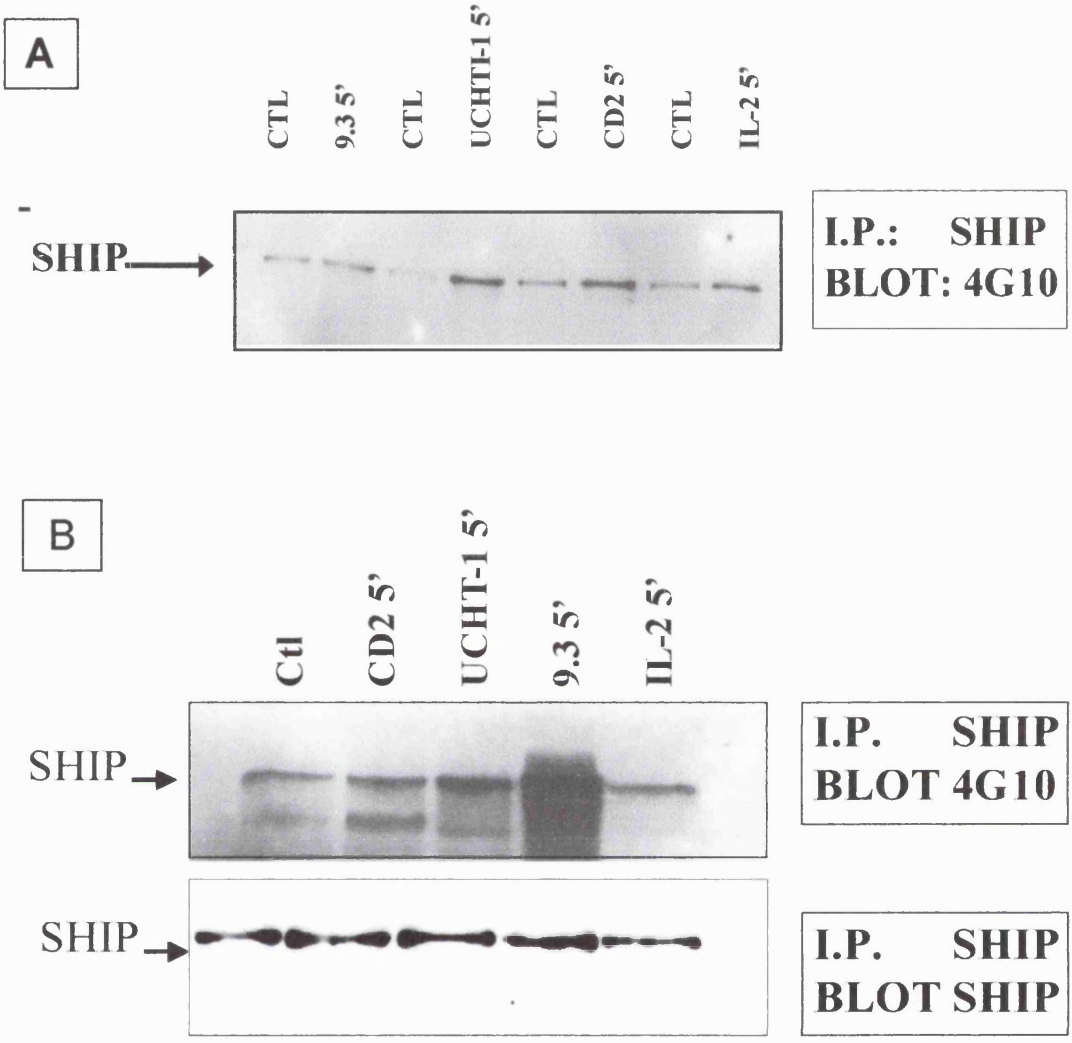

Figure 47: SHIP is a tyrosine phosphorylated in response to CD28, CD2, CD3 and IL-2 receptor stimulation in human T-lymphoblasts. 10^7 cells of human SEB-activated T-lymphoblasts were washed and aliquoted. Cells were left unstimulated as a negative control (CTL) or were stimulated at 10 μg/ml with anti-CD28 mAb (9.3), anti-CD3 mAb (UCHT-1), anti-CD2 mAbs (6F103 and 3C15) and human recombinant IL-2 at 20ng/ml. Cells were lysed and SHIP was immunoprecipitated using an anti-SHIP mAb. Immunoprecipitates were resolved by SDS-PAGE and transferred to nitrocellulose and immunoblotted with an anti-phosphotyrosine antibody 4G10. Note the strip and reprobe for SHIP did not work in top panel (figure A) but did in the second experiment (figure B). This data represents two independent experiments.

SHIP is tyrosine phosphorylated in the Leukemic cell lines MOLT-4 and CEM following CD28 and CD3 ligation.

As described in the earlier sections, SHIP is expressed at the protein level in the leukemic cell lines MOLT-4 and CEM but interestingly not in Jurkat cells. Experiments were performed to establish if SHIP was a biochemical target downstream from the CD28 and CD3 receptors in these leukemic cell lines. Figures 48a/b shows that SHIP is able to be immunoprecipitated from all of these cell lines (apart from Jurkat). In MOLT-4 and CEM cells SHIP is clearly tyrosine phosphorylated following CD28 stimulation but only modestly, if at all, when CD3 is stimulated. This data suggests that SHIP is a biochemical target in MOLT-4 and CEM cells and may partly explain the marked increase in PI(3,4)P_2, a SHIP metabolite of PI(3,4,5)P_3, observed following CD28 ligation in these cells (figures 32/34). The ability of these cells to generate signals to SHIP is ultimately determined by surface-expression of the receptor(s) in question. Therefore the weak cell surface expression of CD3/28 receptors on HUT 78 cells meant that these cells were not examined for SHIP tyrosine phosphorylation following stimulation with anti-CD3/CD28 Abs.

Figure 48a: SHIP is tyrosine phosphorylated in the Leukemic cell line CEM following cellular stimulation

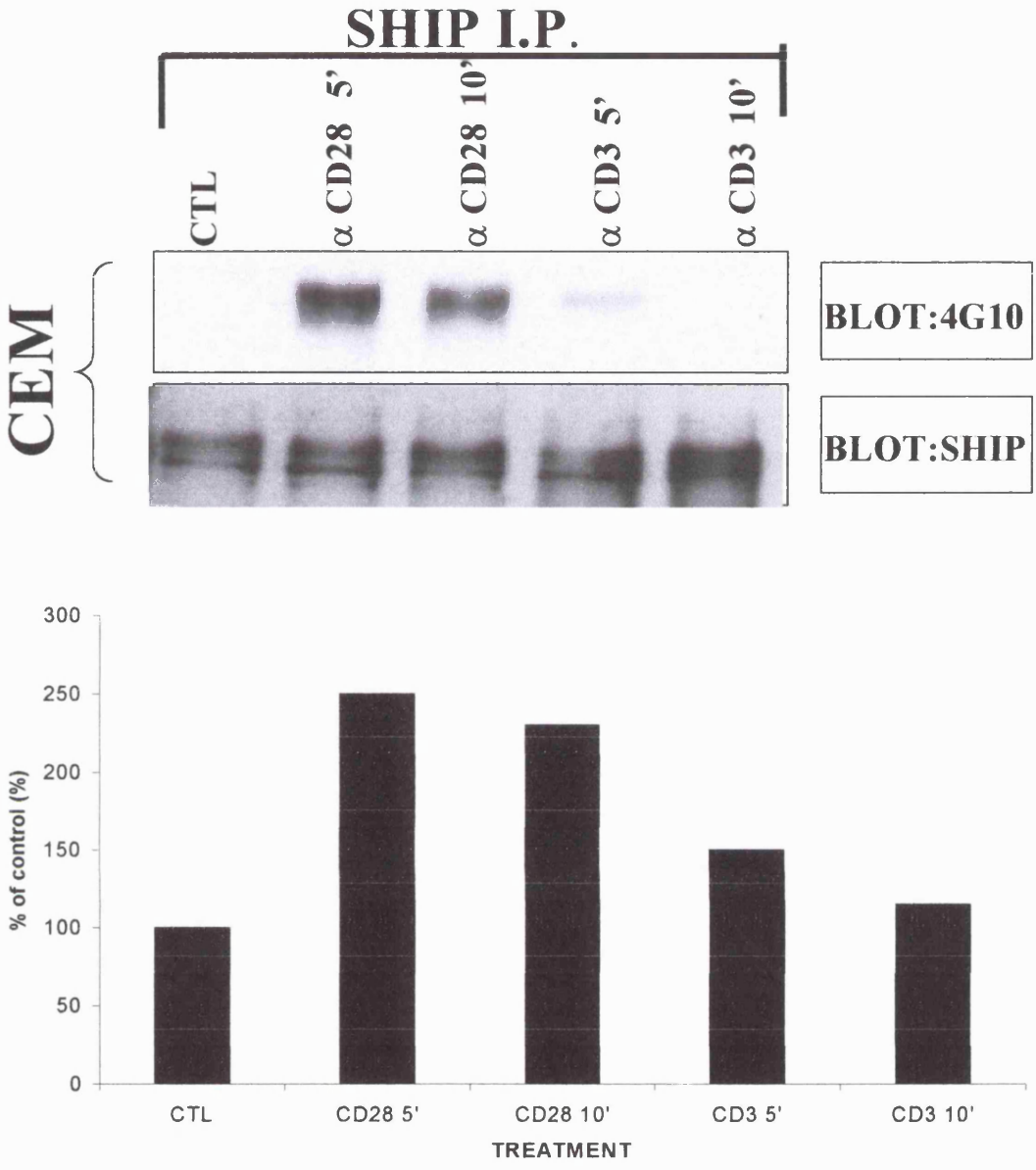

Figure 48a: SHIP is tyrosine phosphorylated in the cell line CEM following cell stimulation. 10^7 CEM cells were aliquoted and left either unstimulated as a control (CTL) or stimulated with 10 μg/ml of anti-CD28 mAb (9.3) or anti-CD3 mAb (UCHT-1). Cells were lysed and SHIP was immunoprecipitated using an anti-SHIP mAb. Immunoprecipitates were resolved by SDS-PAGE and transferred to nitrocellulose and immunoblotted with an anti-phosphotyrosine antibody 4G10. Blots were stripped and immunoblotted with anti-SHIP mAb to verify equal loading. Data was quantified by densitometry and expressed as a percentage of control (bottom panel). Results are from a single experiment representative of 2 others.

Figure 48b: SHIP is tyrosine phosphorylated in the Leukemic cell line MOLT-4 following cellular stimulation

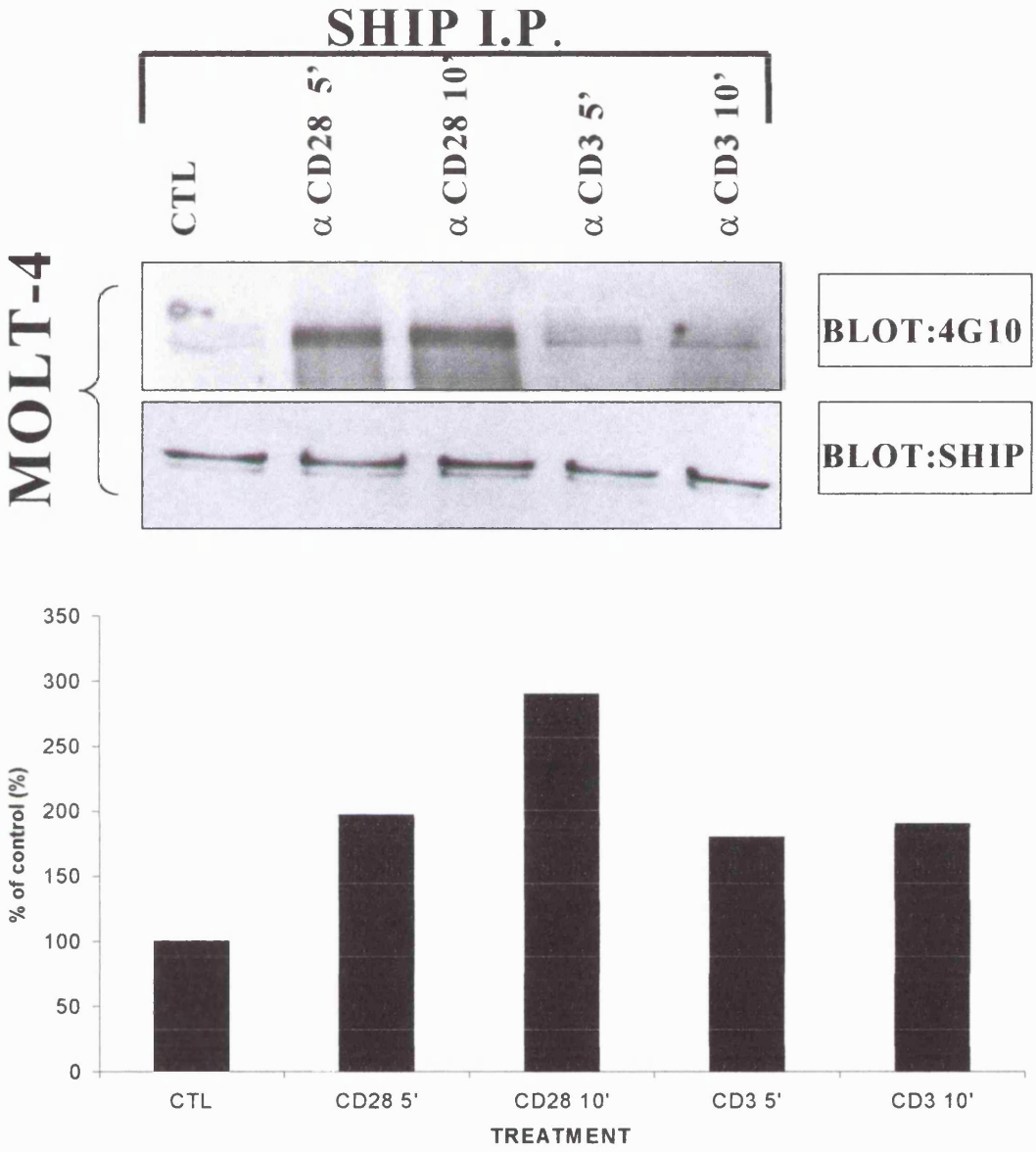

Figure 48b: SHIP is tyrosine phosphorylated in the cell line MOLT-4 following cell stimulation. 10^7 MOLT-4 cells were aliquoted and left either unstimulated as a control (CTL) or stimulated with 10 μg/ml of anti-CD28 mAb (9.3) or anti-CD3 mAb (UCHT-1). Cells were lysed and SHIP was immunoprecipitated using an anti-SHIP mAb. Immunoprecipitates were resolved by SDS-PAGE and transferred to nitrocellulose and immunoblotted with an anti-phosphotyrosine antibody 4G10. Blots were stripped and immunoblotted with anti-SHIP mAb to verify equal loading. Data was quantified by densitometry and expressed as a percentage of control (bottom panel). Results are from a single experiment representative of 2 others.

SHIP Immunoprecipitates derived from T Leukemic cells and T-lymphoblasts display *in vitro* phosphatase activity

It is generally regarded that SHIP has constitutive phosphatase activity in unstimulated cells and that SHIP function is controlled not by tyrosine phosphorylation but rather regulating its cellular localisation (Rohrschneider *et al* 2000). It is unknown if SHIP derived from CEM and MOLT-4 cell lysates is constitutively active and therefore SHIP immunoprecipitates from CD28-stimulated and non-stimulated cells were assayed for *in vitro* 5'-phosphatase activity against ^{3H}inositol-tetrakisphosphate (Ins(1,3,4,5)P_4-or IP4). For all the cell lines tested, SHIP immunoprecipitates were found to be constitutively active towards the IP4 substrate as measured by HPLC analysis of the substrates formed (table 14). It should be noted that data obtained is from a single attempt and therefore should be viewed as preliminary data. These experiments would need to be repeated to confirm the reported observations and we could also ascertain if there is a statistically significant difference between phosphatase activity derived from CD28-stimulated-SHIP I.Ps and basal-SHIP I.Ps, but unfortunately, due to time constraints, this was not determined. However, the data is consistent with the idea that SHIP is constitutively active and is probably regulated controlling access to its substrates (i.e. by membrane recruitment) (Carver *et al* 2000).

Cell Type	BASAL Ins(1,3,4)P3 (cpm)	CD28-STIMULATED Ins(1,3,4)P3 (cpm)
T-BLAST	3021	3483
CEM	3058	3324
MOLT-4	2944	2960

Table 14: *In vitro* phosphatase activity of SHIP immunoprecipitates. T-blasts, MOLT-4, and CEM were left unstimulated (CTL) or stimulated with anti-CD28 mAb 9.3 (1 μg/ml). Cells were lysed and subjected to immunoprecipitation with the an anti-SHIP mAb. The 5-phosphatase activity was determined by the *in vitro* hydrolysis of ^{3}H Ins(1,3,4,5)P_4 to ^{3}H Ins(1,3,4)P_3 as described in *Materials and Methods*. Data is from a single experiment.

SHIP co-associates with *in vitro* protein kinase activity following CD28 ligation

SHIP has been shown to be a target for CD28 activated PTK which may regulate its cellular localisation and association with other proteins. SHIP immunoprecipitates from DC.27 cells were assayed for *in vitro* protein kinase activity using ^{32}P γATP as a substrate. This will reveal whether there is kinase activity associated with SHIP I.Ps and if this is altered following CD28 stimulation. SHIP was found to rapidly (within 1 minute) co-precipitate with *in vitro* protein kinase activity following CD28 stimulation with CHO-B7.1^{+} (figure 49).

In vitro kinase activity appears to co-associate with SHIP under basal conditions and the level of kinase activity increased following CD28 ligation. Several phospho-proteins of varying densities, appear to co-associate with SHIP with apparent molecular weights of 145-150 kDa (presumably SHIP), 100 kDa, 70 kDa, 60 kDa, and approximately 40 kDa (figure 49). The identity of these proteins are currently unknown, as is whether the phospho-proteins are serine/threonine or tyrosine phosphorylated (the assay does not discriminate between PTK and serine/threonine protein kinases). To distinguish between these possibilities, future experiments would include appropriate inhibitors (e.g. PKC and MAPK-inhibitors) in order to determine the nature *in vitro* kinase activity associating with SHIP I.Ps. It would also be of importance to determine whether a similar spectrum of phosphoproteins co-precipitates with SHIP in MOLT-4/CEM/T-blast cells. It is likely that some of these SHIP co-associating proteins may potentially regulate the tyrosine phosphorylation, phosphatase activity and/or cellular redistribution of SHIP and SHIP-associating proteins following CD28 stimulation.

Figure 49: SHIP co-associates with *in vitro* protein kinase activity following CD28 ligation in DC.27 cells.

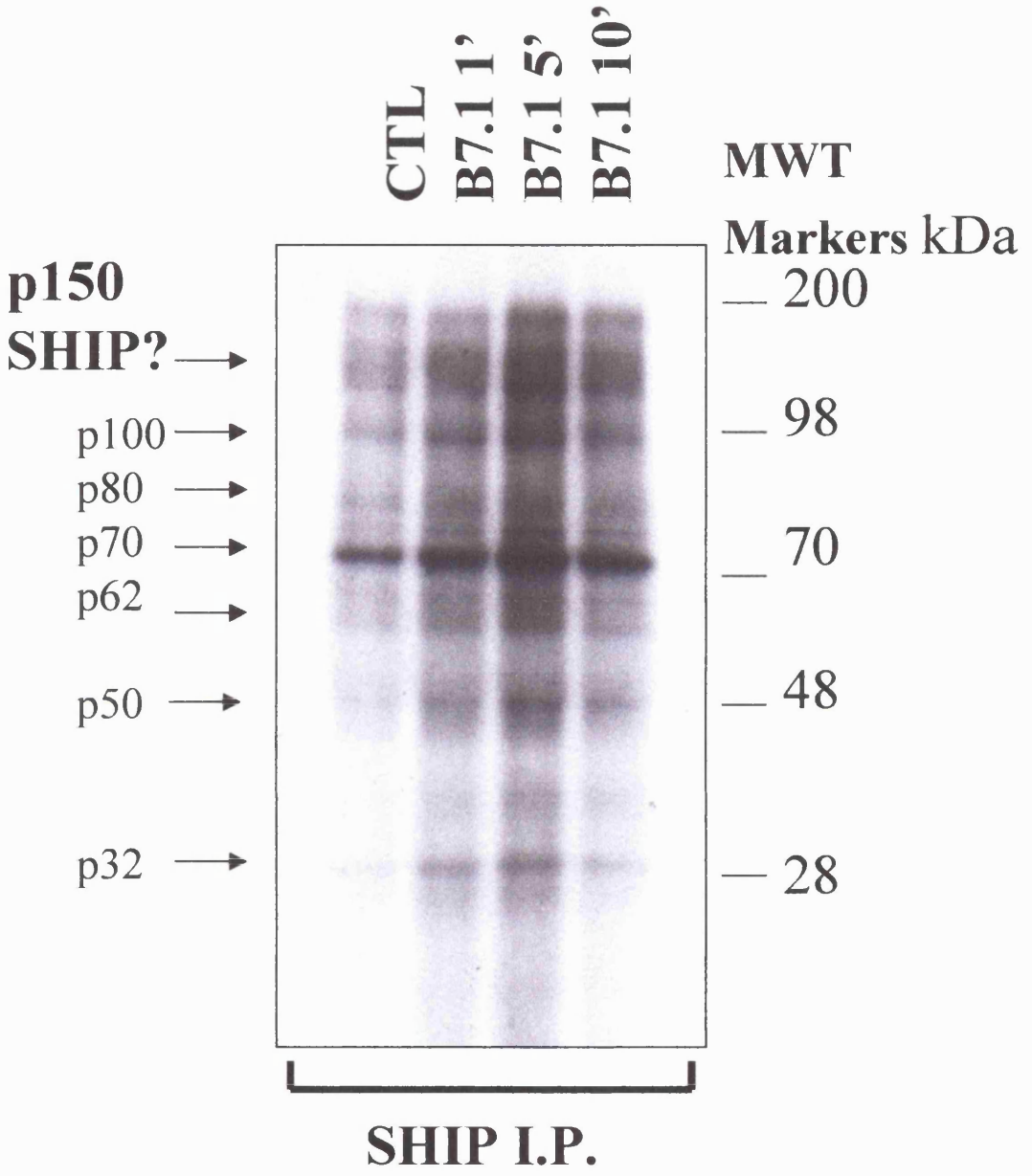

Figure 49: SHIP co-associates with *In Vitro* protein kinase activity. $2X10^7$ DC.27 murine hybridoma T cells expressing wild type $hCD28^+$ were stimulated with CHO-$B7.1^+$ cells at a ratio of 3 DC.27 T cells: 1 CHO-$B7.1^+$ cells as described in *Materials and Methods*. Cells were lysed and subjected to immunoprecipitation with anti-SHIP mAb. Immunoprecipitates were washed and reconstituted in kinase buffer with 1 μCurie of ^{32}P γATP for 20 minutes. Immunoprecipitated proteins were resolved on a 7%-15% gradient gel and incorporated ^{32}P was assessed by autoradiography. The arrows show distinct phospho-proteins, which co-immunoprecipitate with SHIP. Data are from a single experiment representative of three others.

CD28 ligation induces the association of the adapter protein p62^{dok} with SHIP

SHIP was originally identified as being able to bind a multitude of tyrosine phospho-proteins. In B cells, one of these has been identified recently as the PH-domain containing adapter protein p62^{dok} (Tamir *et al* 2001). This rasGAP associated protein is known to be tyrosine phosphorylated following CD28, but interestingly not CD3, receptor ligation (Nunes *et al* 1996). These data, coupled with the observation that a faint ^{32}P phosphoprotein, of approximately 60-65 kDa, co-associates with SHIP in the *in vitro* kinase assay, suggest p62^{dok} as a good candidate protein which may interact with SHIP downstream from CD28 signalling in T cells. Subsequent experiments revealed that SHIP does indeed inducibly immunoprecipitate with p62^{dok} following CD28 stimulation of DC.27 cells (figures 50/51).

Figure 51 shows p62^{dok} is associated with SHIP under basal conditions and which increases upon CD28 stimulation. SHIP may also associate, albeit at much lower levels, with p62^{dok} I.Ps (figure 52). Although the overall quality of the blot is poor, SHIP can be seen to recruit to p62^{dok} with maximal co-association between the two proteins occurring after 5 minutes post-stimulation and was observed to be transient in nature. Approximate equal loading was confirmed by stripping the blot and reprobing with the relevant antibodies.

It is accepted that immunoprecipitation of whole cell lysates does not prove that these associations occur *in vivo.* Other experiments would need to be performed to verify that this is indeed the case. These could include trying to extract p62^{dok} protein (from stimulated SHIP I.Ps) from SDS-PAGE gels and performing partial tryptic digests to attempt to get some protein sequence data to verify the existence of p62^{dok}. Alternatively an immunofluorescence approach, where SHIP and p62^{dok} are stained with different secondary conjugated antibodies, could provide evidence for co-localisation upon cellular stimulation in intact cells rather than cell lysates.

Ligation of CD28 and CD3 receptors induces the association of SHIP with the protein tyrosine phosphatase SHP-2 in DC.27 cells

SHIP has been widely documented to bind the protein tyrosine phosphatase SHP-2 following stimulation with cytokines and various growth factors (Sattler *et al* 1997). SHIP immunoprecipitates were shown to inducibly associate with SHP-2 following stimulation with anti-CD3/anti-CD28 mAb in DC.27 murine hybridoma T cells (figure 53). SHP-2 is detectable in basal/resting SHIP immunoprecipitates but levels are in general low. Upon CD28 stimulation a rapid association (≤ 1 minute) between SHIP and SHP-2 was seen which was sustained for 10 minutes. Equal loading was confirmed by stripping and reprobing the blots with an anti-SHIP polyclonal Ab that recognises C-terminal truncations of SHIP (i.e. p135/p145 SHIP). This data, albeit encouraging, was representative of a single experiment in a hybridoma T cell line and therefore should be viewed as preliminary and interpreted with caution. Results from similar experiments using T-lymphoblasts and DC.27 cells would be needed to confirm the possible association between SHIP and SHP-2.

Figure 51: SHIP co-associates with p62^{dok} following CD28 ligation in DC.27 cells.

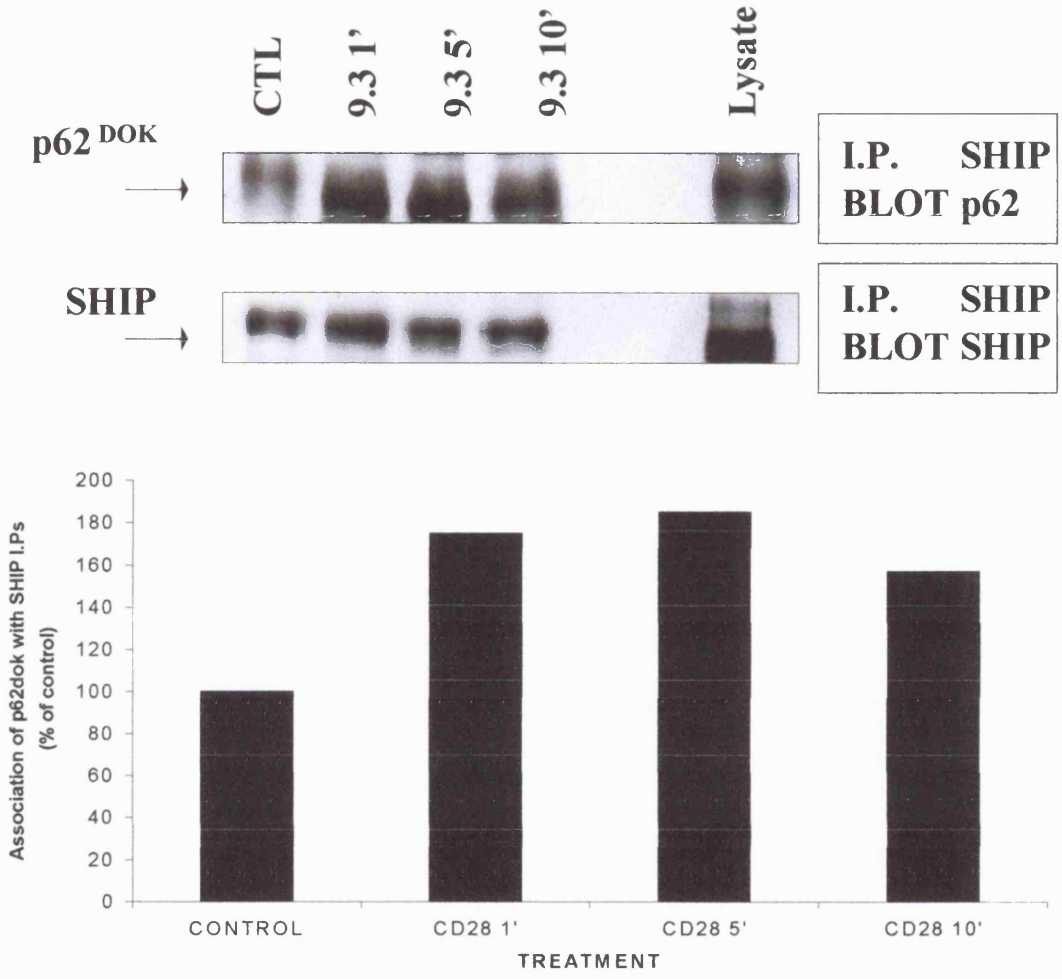

Figure 51: SHIP co-associates with p62^{dok} following CD28 ligation. 2X10^7 per point DC.27 T cells expressing wild type hCD28$^+$ were left unstimulated as a control (CTL) or stimulated with anti-CD28 mAb 9.3 at 1 μg/ml for the times indicated. Cells were lysed and pre-cleared lysates were subjected to immunoprecipitation with anti-SHIP mAb. Immunoprecipitates were resolved by SDS-PAGE and transferred to nitrocellulose and immunoblotted with anti-p62^{dok} mAb. A lysate was included on the gel to verify if western blotting was successful. Blots were stripped and reprobed with anti-SHIP mAb to verify equal loading. Data was quantified by densitometry and expressed as a percentage of control (bottom panel). Data is from a single experiment representative of 3 others.

Figure 52: SHIP co-associates with CD28-stimulated p62^{dok} Immunoprecipitates in DC.27 T cells

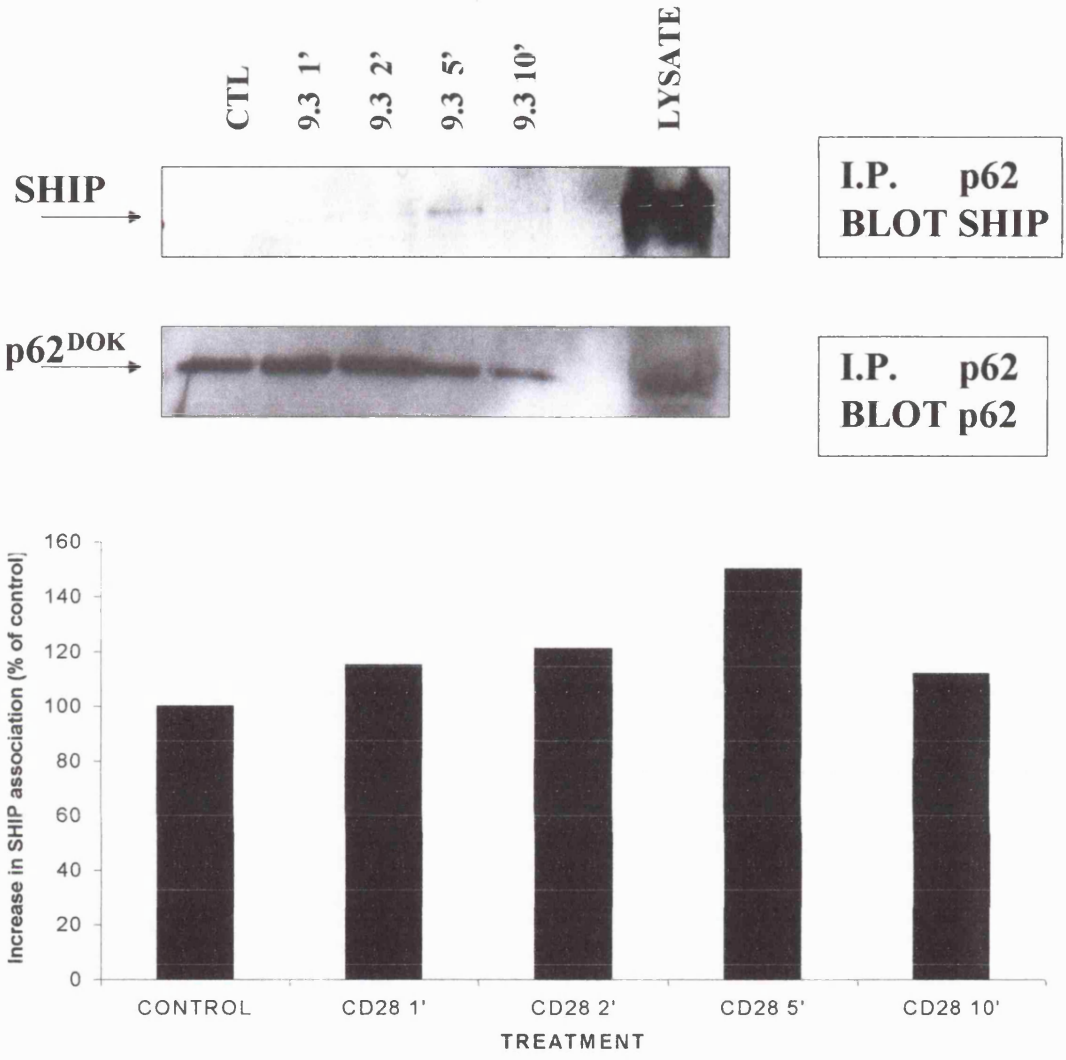

Figure 52: SHIP co-associates with CD28-stimulated p62^{dok} immunoprecipitates. 20^7 per point DC.27 T cells expressing wild type hCD28$^+$ were stimulated with anti-CD28 mAb (9.3) at 1 μg/ml for the times indicated. Cells were lysed and pre-cleared lysates were subjected to immunoprecipitation with anti-p62^{dok} mAb. Immunoprecipitates were resolved by SDS-PAGE and transferred to nitrocellulose and immunoblotted with anti-SHIP Ab. Blots were stripped and reprobed with anti-p62^{dok} mAb to verify approximate equal loading. Data was quantified by densitometry and expressed as a percentage of control (bottom panel). Data presented is from a single experiment representative of 2 others.

Figure 53: Ligation of CD28 and CD3 receptors induces the association of SHIP with the protein tyrosine phosphatase SHP-2 in DC.27 cells

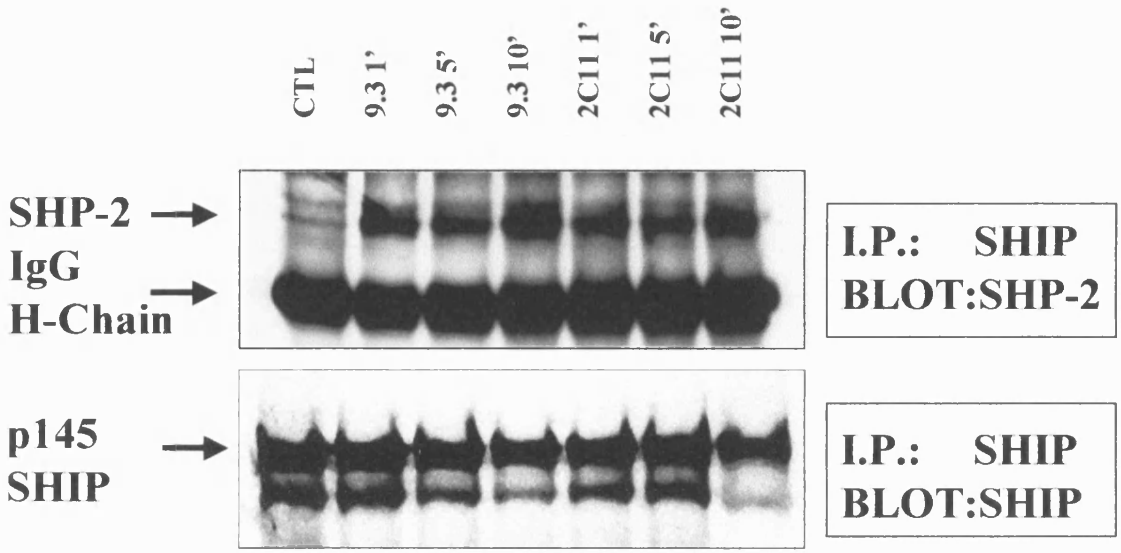

Figure 53: SHIP co-associates with the protein tyrosine phosphatase SHP-2 following CD28/CD3 stimulation in DC.27 murine hybridoma T cells. $2x10^7$ per point DC.27 T cells expressing wild type $hCD28^+$ were either left unstimulated (CTL) or stimulated with anti-CD28 mAb 9.3 at 1 μg/ml for the times indicated. Cells were lysed and pre-cleared lysates were subjected to immunoprecipitation with anti-SHIP mAb. Immunoprecipitates were resolved by SDS-PAGE and transferred to nitrocellulose and immunoblotted with anti-SHP-2 mAb. Blots were stripped and reprobed with anti-SHIP (which recognises c-terminal truncated isoforms of SHIP) polyclonal Ab to verify equal loading. Data is from a single representative experiment.

SHIP does not co-associate with the adapter protein Grb-2 following CD28 stimulation in murine DC.27 hybridoma T cells.

The Grb-2/Sos regulatory complex is reported to bind to both CD28 and CD3 T cell receptors (Schneider *et al* 1995). The possibility of SHIP binding to Grb-2 would provide a mechanism for coupling SHIP to CD28, thereby allowing it's tyrosine phosphorylation by CD3/CD28-activated-PTK. Western blot analysis of SHIP immunoprecipitates from DC.27 cells stimulated with CHO-B7.1^{+} could not identify any recruitment of Grb-2 over a 10 minute stimulation period (figure 54). Grb-2 is clearly visible in the CHO and DC.27 lysate controls and the subsequent strip and reprobe confirmed the presence of SHIP in the I.Ps derived from DC.27, but importantly not CHO, lysate.

Figure 54: SHIP does not detectably co-associate with the adapter protein Grb-2 following CD28 stimulation in murine DC.27 hybridoma T cells.

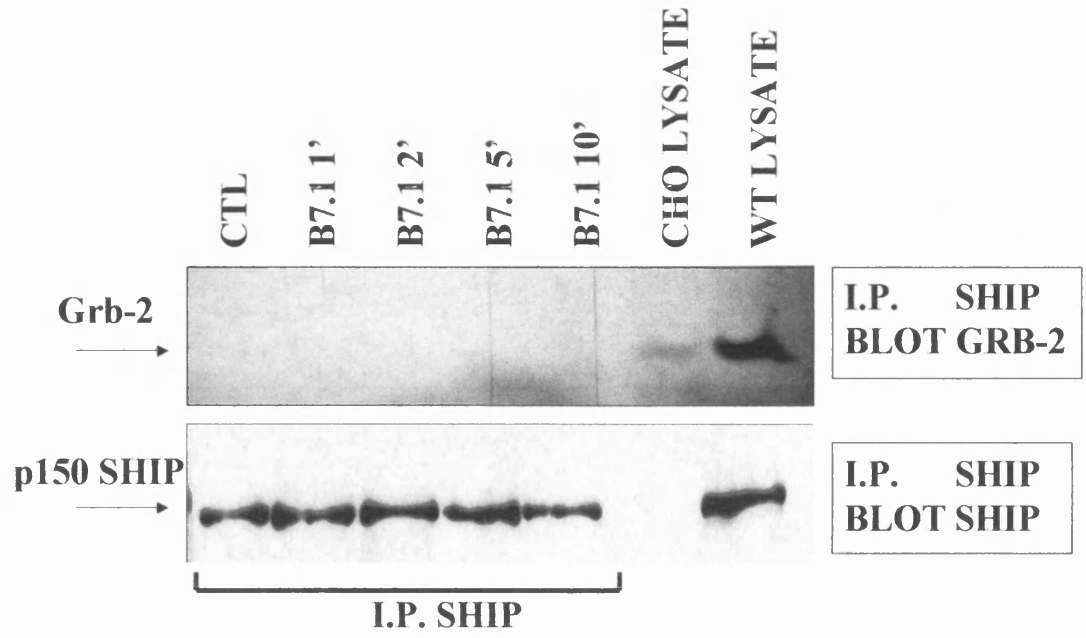

Figure 54: SHIP does not detectably co-associate with the adapter protein Grb-2 following CD28 stimulation. $2x10^7$ DC.27 cells stably expressing hCD28 were aliquoted and left unstimulated (CTL) as a control or stimulated with CHO-B7.1$^+$ cells at a ratio of 3 T cells: 1CHO-B7.1$^+$ cell. Cells were lysed and pre-cleared lysates were subjected to immunoprecipitation with anti-SHIP mAb. Immunoprecipitates were resolved by SDS-PAGE and transferred to nitrocellulose and immunoblotted with anti-Grb2 polyclonal Ab. A CHO lysate was added to verify no SHIP is expressed in these cells. Blots were stripped and reprobed with anti-SHIP mAb to verify equal loading. Data is from a single experiment representative of 2 others.

SHIP may co-associates with the adapter protein GRID following CD28 stimulation in DC.27 T cells

GRID is another adapter protein that is capable of binding to the tyrosine phosphorylated YXXM motif within the cytoplasmic tail of CD28 (Ellis *et al* 2000). GRID thus competes with PI 3-K for the same binding sites on CD28, and mutation of tyrosine residues 173/200 of CD28 abrogates these protein interactions (Ellis *et al* 2000). SHIP is known from *in vitro* kinase assays (figure 49) to potentially bind to phospho-proteins of approximately 44 kDa, the molecular weight of GRID. Therefore the capability of GRID to associate with SHIP following CD28 ligation was assessed.

Analysis of CD28-stimulated SHIP immunoprecipitates reveals that SHIP is able to recruit GRID in DC.27 expressing $hCD28^{+}$ cells (figure 55). These protein interactions are first detected at around 10 minutes and are maximal at 30 minutes post-CD28 ligation. It is interesting to note that SHIP association with $p62^{dok}$ is rapid and transient in nature whereas SHIP interaction with GRID occurs much later following stimulation. As reported previously (Ellis *et al* 2000), GRID, but not SHIP, was shown to associate with CD28 following receptor ligation at 5 minutes (figure 55). Equal loading was verified by stripping and reprobing with SHIP mAb.

This data alone, albeit encouraging, does not prove that an association between SHIP and GRID occurs *in vivo.* As discussed previously for the association between SHIP and $p62^{dok}$, this would require similar additional experiments, which unfortunately were not performed due to time constraints.

Figure 55: SHIP associates with the adapter protein GRID following CD28 stimulation.

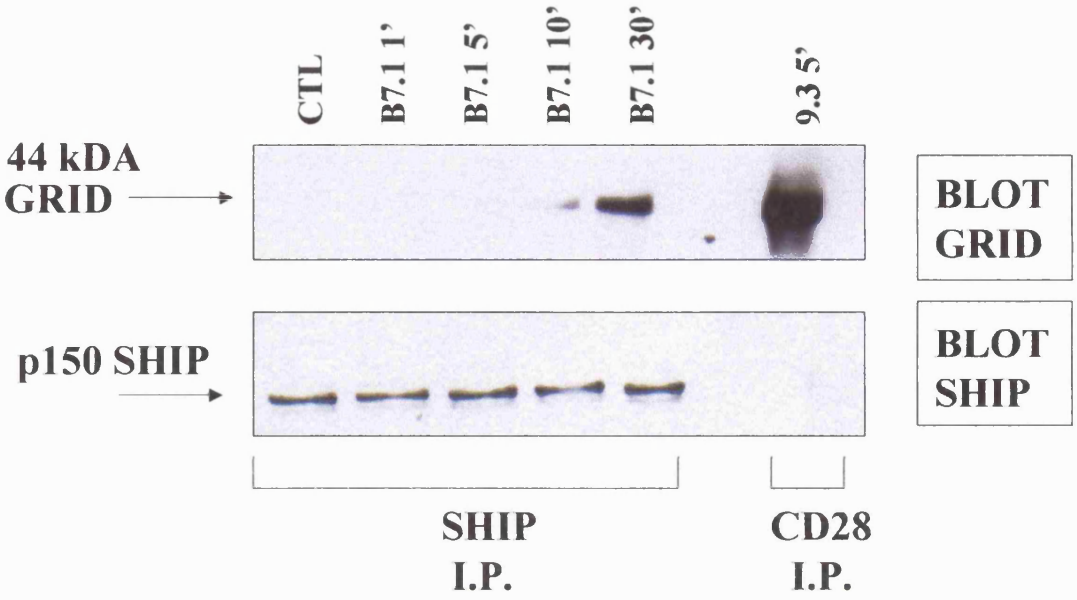

Figure 55: SHIP associates with the adapter protein GRID following CD28 stimulation. $2x10^7$ DC.27 cells stably expressing hCD28 were aliquoted and left unstimulated (CTL) as a control or stimulated with CHO-B7.1$^+$ cells at a ratio of 3 T cells: 1CHO-B7.1$^+$ cell. In addition a lysate was added to verify the efficiency of western blotting and also the recruitment of GRID to CD28 *i.ps* as previously reported (Ellis *et al* 2000). Cells were lysed and pre-cleared lysates were subjected to immunoprecipitation with anti-SHIP and anti-CD28 mAbs. Immunoprecipitates and lysates were resolved by SDS-PAGE and transferred to nitrocellulose and immunoblotted with anti-GRID polyclonal Ab. Blots were stripped and reprobed with anti-SHIP mAb to verify approximate equal loading. Data is from a single experiment representative of 2 others.

PTEN co-associates with *in vitro* protein kinase activity following CD28 ligation with B7.1 in DC.27 T cells

PTEN is a crucial regulator of D-3 phosphoinositides and directly antagonises PI 3-K signalling. The role of this phosphatase and its coupling to signalling complexes in T-lymphocytes is unclear. Unlike SHIP, PTEN does not become inducibly tyrosine phosphorylated and is thought to reside at the plasma membrane in resting unstimulated cells (Cantley *et al* 1999). Evidence described thus far in this study has revealed that PTEN is not expressed in Jurkat, CEM and MOLT-4 T cell lines, and that this lack of expression may have consequences for D-3 phosphoinositide turnover and for the regulation of key PI 3-K dependent signalling enzymes including PKB. It is as yet unclear if CD28 can signal to PTEN, inducing protein-protein associations and/or regulating its phosphatase activity. The C-terminus of PTEN contains a cluster of serine/threonine residues of which some can be phosphorylated. Mutations of these residues reduced the steady-state levels of PTEN and its half-life (Vazquez *et al* 2000) suggesting that phosphorylation of PTEN may mediate the regulation of PTEN. With the knowledge that SHIP can co-associate with *in vitro* kinase activity, PTEN immunoprecipitates from non-stimulated and CD28-stimulated DC.27 T cells was assayed for *in vitro* kinase activity.

PTEN immunoprecipitates, derived from DC.27 cells, were found to be associated with kinase activity stimulation with the B7.1 ligand (figure 56). In contrast, *in vitro* kinase activity was found to be virtually absent from PTEN i.ps from resting unstimulated DC.27 cells. Following CHO-B7.1^{+} stimulation, induced kinase activity could be detected at 1 minute post-stimulation. This activity was maximal at 5 minutes and sustained for 10 minutes. Prominent ^{32}P phosphoproteins at molecular weights of 150 kDa, 85 kDa, 72 kDa, 56 kDa and 40 kDa were revealed to co-associate with PTEN following CD28 ligation. The identity of these co-associating proteins is not known although [^{32}p]56 kDa could be PTEN itself. Interestingly, the labelled protein band at 150 kDa shares a similar molecular weight to SHIP (145 kDa). The possible identification of these potential unknown co-assocoating proteins may yield interesting clues to how CD28 signals to and/or possibly regulates PTEN. The p85 immunoprecipitate,

was used as a positive control for the assay, gave identifiable phosphoprotein bands of 85 and 110 kDa, representing the adapter and catalytic subunits of PI 3-K respectively as a result of autophosphorylation (figure 56).

Again it's unclear if the *in vitro* kinase activity observed in CD28-stimulated PTEN immunoprecipitates is through serine/threonine and/or tyrosine kinases due to the limitations of the assay. If these experiments were to be repeated inhibitors, e.g. those which block tyrosine kinase activity (herbimycin) or PKC inhibitors, could be included in the assay and may aid identification of the class of kinase possibly associating with PTEN. The data presented here is insufficient to prove that CD28 signals to PTEN and other experiments are required to prove this hypothesis. These might include assaying unstimulated/CD28-stimulated PTEN immunoprecipitates for *in vitro* lipid kinase activity towards a phosphatidylinositol substrate, and assessing the phosphatase activity of unstimulated/CD28-stimulated PTEN immunoprecipitates activity against Ins(1,3,4,5)P_4 (IP4). This would reveal whether or not PI 3-K is recruited to PTEN in a CD28-dependent manner and whether if ligation of CD28 can upregulate, or indeed downregulate, PTENs dephosphorylation of IP4 *in vitro.*

Figure 56: PTEN co-associates with *in vitro* protein kinase activity following CD28 ligation with B7.1 in DC.27 T cells.

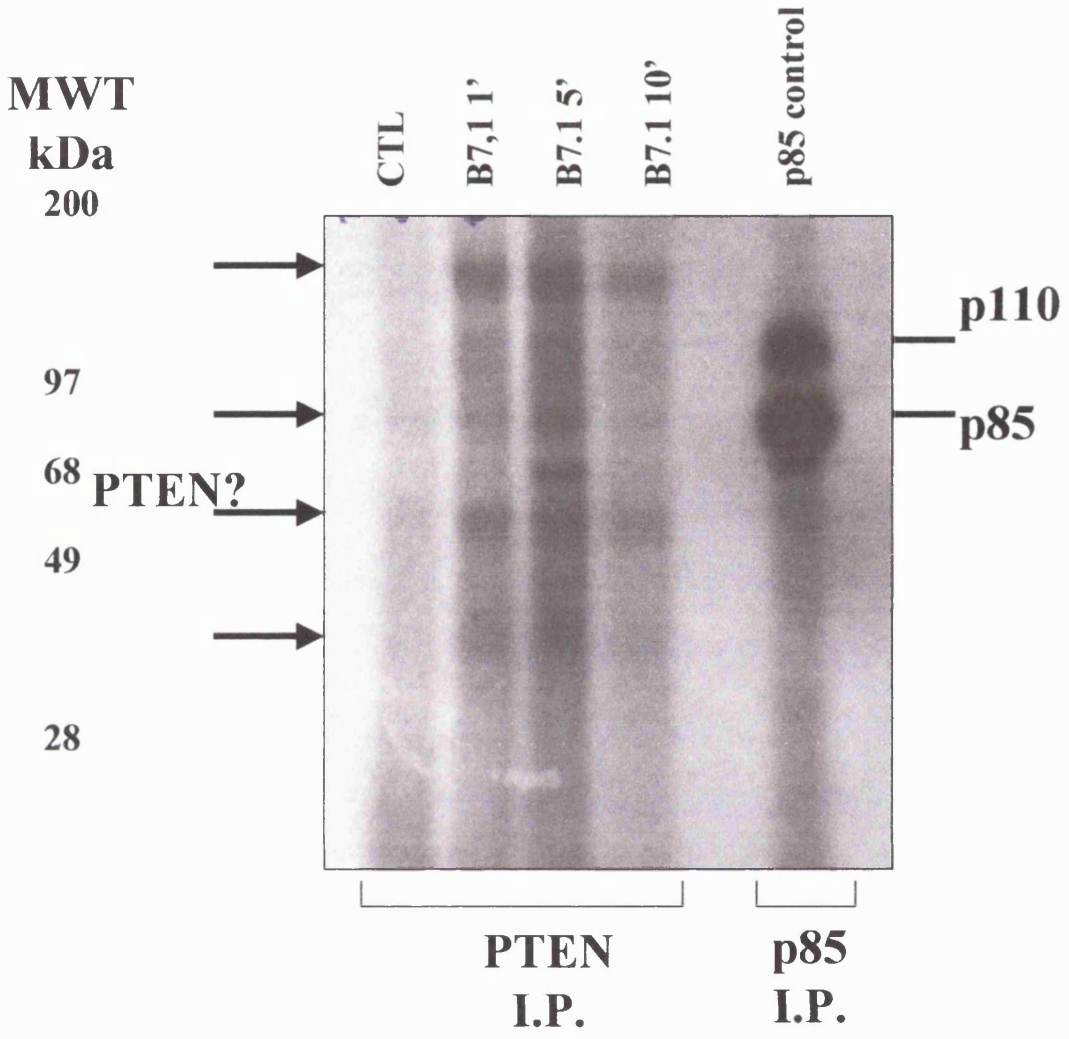

Figure 56: PTEN co-associates with *in vitro* protein kinase activity following CD28 ligation with B7.1 in DC.27 murine T cells. $2X10^7$ DC.27 cells stably expressing hCD28 were aliquoted and left unstimulated as a control or stimulated with CHO-$B7.1^+$ cells at a ratio of 3 T cells: 1CHO-$B7.1^+$ cell. Cells were lysed and pre-cleared lysates were subjected to immunoprecipitation with anti-PTEN mAb or p85 mAb (used as a positive control for the assay). Immunoprecipitates were washed and reconstituted in kinase buffer with 1 μCurie of ^{32}P γATP for 20 minutes as described in *materials and methods*. Immunoprecipitated proteins were resolved on a 7%-15% gradient gel and incorporated ^{32}P was assessed by autoradiography. Prominent unidentified 'hot' phospho-proteins, of varying molecular weight, co-immunoprecipitating with PTEN is shown in arrows. Data are from a single experiment representative of three others.

Summary of results

- SHIP is tyrosine phosphorylated following stimulation with anti-CD28 9.3 mAb and the natural ligands CHO-B7.1$^+$ and CHO-B7.2$^+$ in DC.27 hybridoma T cells.

- SHIP is tyrosine phosphorylated following stimulation of CD2 and CD3 and by human-recombinant Interlukin-2 in DC.27 T cells and T-lymphoblasts. Stimulation of CD28 and CD3 receptors with appropriate antibodies in combination enhanced tyrosine phosphorylation of SHIP when compared with either antibody alone.

- SHIP expressed in the leukemic cell lines MOLT-4 and CEM can also be tyrosine phosphorylated upon CD28 and CD3 stimulation.

- SHIP Immunoprecipitates derived from T Leukemic cells and T-lymphoblasts were shown to have constitutive *in vitro* phosphatase activity towards an Ins(1,3,4,5)*P*4 substrate. Phosphatase activity was not increased upon CD28 ligation.

- CD28 coupling to PI 3-K is not required for SHIP tyrosine phosphorylation as revealed by using CD28 mutants which are unable to bind PI 3-K.

- SHIP co-associates with *in vitro* protein kinase activity following CD28 ligation and reveals the presence of a variety of phosphoproteins, the identities of which are unknown.

- CD28 stimulation may induce the association of SHIP with the adapters p62^{dok} and GRID. The association between SHIP and p62^{dok} was rapid whereas that between SHIP and GRID was delayed. Further experiments will be needed to confirm the observed *in vitro* associations also occur *in vivo*. Grb-2, another adapter important for relaying mitogenic signals, was found not to associate with SHIP following CD28 ligation.

- PTEN, like SHIP, immunoprecipitates with *in vitro* kinase activity following CD28 stimulation. A variety of unknown phosphoproteins identified that appeared to co-associate with PTEN in a ligand dependent manner and whose function remains to be determined.

Discussion

Expression of the inositol phosphatases SHIP and PTEN in leukemic T cell lines and T-lymphoblasts.

Both SHIP and PTEN are proposed to play important regulatory roles in PI 3-K signalling in haemopoietic cells. The importance of these phosphatases is further highlighted in mice knockouts where $PTEN^{-/-}$ die *in utero* (Di Cristofano *et al* 1998) and $SHIP^{-/-}$ exhibit various lymphoproliferative disorders (Helgason *et al* 1998). Many leukemic cell lines are defective in key enzymes, including PTEN, which control cell cycle progression. The T-leukemic cell line Jurkat, a widely used cell model for T cell biology, lacks the phosphatase PTEN resulting in constitutive activation of PI 3-K mediated signal transduction pathways (Astoul *et al* 2001). This observation has raised questions as to the suitability of such cell lines as models for signal transduction research. This study described the expression of SHIP and PTEN at the mRNA and protein level in a variety of commonly used leukemic cell lines namely Jurkat, CEM, MOLT-4 and HUT 78 as well as from SEB-activated-T-lymphoblasts derived from healthy volunteers. An attempt was also made at establishing the effect of differential SHIP/PTEN expression on basal and stimulated D-3 phosphoinositide lipid profiles and the effect, if any, on PI 3-K-dependent downstream signalling cascades.

Using RT-PCR it was found that all the cell lines examined expressed SHIP and PTEN mRNA. However this data conflicted with that on protein expression of these same phosphatases obtained by western blotting. Jurkat cells lacked both SHIP and PTEN phosphatases, which is consistent with previous published work (Shan *et al* 2000 and Edmunds *et al* 1999). In Jurkat cells, several mutations causing premature stop codons have been described which result in truncated proteins that are highly unstable and hence rapidly degraded (Sakai *et al* 1998). The data presented here represents the first description of SHIP/PTEN phosphatase expression in other commonly used T-leukemic cell lines. MOLT-4 and CEM cells were shown to lack PTEN but express SHIP. It could still be argued that Jurkat, MOLT-4 and CEM cells still express the phosphatases in question, but below the limit of detection for Western blotting.

In contrast, HUT 78 cells and T-lymphoblasts expressed both SHIP and PTEN together. The expression of other relevant inositol phosphatases such as SHIP2 was not investigated in this study primarily due to the lack of suitable antibodies. The phosphatase SHIP 2 has been reported to be co-expressed with SHIP in T lymphocytes (Bruyns *et al* 1999), however it is presently undetermined if SHIP2 is expressed at detectable levels, if at all, in the leukemic cell lines used in this study. It is thus possible that the expression of SHIP 2 might be able to compensate to some extent for the loss of SHIP in Jurkat cells. However, the observed D-3 phosphoinositide profiles in Jurkat (discussed later) suggest that this is unlikely to be the case.

D-3 Phosphoinositde profiles in Leukemic T cell lines and T-lymphoblasts and consequences on downstream PI 3-K-driven signalling cascades .

Measurement of D-3 phosphoinositide levels as achieved by *in vivo* ^{32}P labelling revealed that radiolabelled-Jurkat cells had high basal levels of the PI 3-K product PI(3,4,5)P_3 when compared with the other cell lines used in this study; an observation consistent the findings of Ward *et al* (1995). Despite the fact that Jurkat PI(3,4,5)P_3 levels can increase 10-fold following CD28 stimulation, it is becoming increasingly accepted that Jurkat cells have constitutively active PI 3-K signalling (Astoul *et al* 2001). Unstimulated Jurkat cells revealed considerable levels of phospho-PKB that did not increase detectably upon stimulation. This observation was mirrored by phospho-GSK3 levels, a downstream effector of PKB, which were also high in unstimulated Jurkat cells. Interestingly, the high levels of PI(3,4,5)P_3 and phospho-PKB could be abolished by pre-treatment with the PI 3-K inhibitor, LY 294002, which supports the notion that phospho-PKB levels are intimately linked to PI(3,4,5)P_3 levels. However complete abrogation of basal phospho-PKB levels in Jurkat cells required pre-treatment with LY 294002 for up to 2 hours reflecting the high basal levels of phospho-PKB in these cells and the slow metabolism of phosphoinositides resulting from the lack of expression of SHIP and PTEN. Detectable levels of PI(3,4,)P_2, a bioactive second messenger in it's own right, were observed in Jurkat cells, but were very low when compared with those of PI(3,4,5)P_3. This is reflected in a ratio of the two lipids. Jurkat cells had an unstimulated PI(3,4,5)P_3: PI(3,4,)P_2 ratio of 27 which increased considerably to 152 upon CD28 stimulation.

The lack of expression of SHIP in Jurkat which generates PI(3,4,)P_2 via dephosphorylation of PI(3,4,5)P_3, may explain the relatively low levels of PI(3,4,)P_2 observed in both unstimulated and CD3/28-stimulated Jurkat cells.

The MOLT-4 and CEM leukemic cell lines ($SHIP^+/PTEN^-$) had a different phosphoinositide profile to Jurkats. Basal PI(3,4,5)P_3 levels were considerable in MOLT-4 and CEM cells, but they were not as high as that observed in Jurkat cells. Stimulation of the CD28 receptor by CHO-B7.1^+ resulted in the rapid and sustained accumulation of PI(3,4,5)P_3, indicating that the CD28 receptor functionally couples to PI 3-K in these cell lines, as observed in other cell models (Ward *et al* 1992). Although it is not valid to compare directly phosphoinositide levels between different cell lines, this approach does allow a comparison to be made of phosphoinositide profiles and relative PI(3,4,5)P_3: PI(3,4,)P_2 ratios obtained from the different cell types.

MOLT-4 and CEM cells exhibit substantial basal levels of PI(3,4)P_2, the metabolic product of SHIP, which increases markedly upon CD28 ligation with CHO-B7.1^+. The higher levels of PI(3,4,)P_2 in these cells are highlighted in substantially lower basal PI(3,4,5)P_3: PI(3,4,)P_2 ratios (CEM 1.3, MOLT-4 3.5) when compared with that of Jurkat. These observations are consistent with the lack of PTEN but presence of SHIP, which drives the unopposed catalytic shunt of PI(3,4,5)P_3 to PI(3,4)P_2. Considerable levels of basal phospho-PKB were observed in CEM and MOLT-4 cells that may, again reflect the considerable levels of basal D-3 phosphoinositides. As with Jurkat cells, LY 294002 could abolish basal phospho-PKB levels in MOLT-4 and CEM cells over time. In contrast to the apparent saturated nature of PI 3-K signalling observed in Jurkat cells, stimulation of CD28/CD3 in CEM and MOLT-4 cells did result in the increased phosphorylation status of PKB, albeit modestly, above basal levels.

There are several recently identified proteins which contain PH domains which bind specifically with high affinity towards PI(3,4)P_2 but not PI(3,4,5)P_3; the adapters DAPP and TAPP (Dowler *et al* 2001). The fact that MOLT-4 and CEM cells contain considerable basal levels of PI(3,4)P_2, which increases upon cellular stimulation, indicates that these cell lines are a more suitable surrogate

T cells model in which to assess the function of novel PI(3,4)P_2-dependent signalling cascades and also the unknown functional role of the novel PI(3,4)P_2–interacting adapter proteins, including the recently identified proteins TAPP/DAPP.

The T-helper like leukemic cell line HUT 78 and T-lymphoblasts were positive for SHIP and PTEN at both mRNA and protein level. Both cell lines had lower levels of basal PI(3,4,5)P_3/cell when compared with Jurkat cells. In particular the HUT78 cell line had very low levels of D-3 phosphoinositides, which only moderately increased upon anti-CD3 mAb and CHO-B7.1$^+$ stimulation. Subsequent FACS analysis, however, revealed that they expressed relatively low levels of CD28/CD3 (≤ 10% when compared with isotype matched controls). PI(3,4)P_2 levels in HUT 78 cells could hardly be detected upon *in vivo* lipid labelling. This may be attributed to the expression of both SHIP and PTEN, but could equally be explained by the cells having a naturally lower phosphoinositide pool compared to the other cell lines studied. As a result of the low phosphoinositides measured in the HUT 78 cell line, basal phospho-PKB/GSK3 levels were, predictably, absent indicating the importance of PI(3,4,5)P_3 in maintaining phospho-PKB levels.

T-lymphoblasts that also express SHIP and PTEN had D-3 phosphoinositide levels and basal/stimulated PI(3,4,5)P_3: PI(3,4,)P_2 ratios dissimilar to those observed in HUT 78 (T-blast 10, HUT 78 30). Basal levels of PI(3,4,5)P_3 in T lymphoblasts increased rapidly upon stimulation with anti-CD3 mAb, IL-2 (20 ng/ml) and with CHO-B7.1$^+$. Phospho-PKB could also be observed in unstimulated T-lymphoblasts and the amount seen increased upon CD28 stimulation. The possible roles of SHIP and PTEN in determining the D-3 phosphoinositide profile of the different cell types studied are summarised further in figure 57.

The Spearman's rank correlation test was applied to see if there was a positive association between basal levels of PI(3,4,5)P_3 and phospho-PKB levels (expressed as a ratio of total PKB) in the cell types studied. The observed correlation was statistically significant (p = 0.05) suggesting that higher basal levels of PI(3,4,5)P_3 contribute to higher relative levels of phospho-PKB: total

PKB ratios, at least in T lymphocytes. The result of the analysis therefore indirectly reveals the support of a crucial role for PTEN and SHIP in the metabolism of PI(3,4,5)P_3 metabolism and, thereby, in the regulation of the phosphorylation status, and hence, activity of PKB.

There is some controversy as to whether PI(3,4,5)P_3 or PI(3,4)P_2 is the critical second messenger that mediates the membrane recruitment of PKB and its associated kinases *in vivo.* Whilst the PH domain has been reported to have dual specificity, recent *in vitro* data suggests that PI(3,4,)P_2 binds PKB with a has a higher affinity than PI(3,4,5)P_3 (Franke *et al* 1997). More recently, studies using SHIP knockout mice have revealed that PI(3,4)P_2 is essential for the phosphorylation and activation of PKB Ser^{473} (Scheid *et al* 2002). In contrast, the data presented here suggest that PI(3,4,5)P_3 is a critical regulator of PKB activation (as seen with high basal PI(3,4,5)P_3 levels and saturated PKB signalling in Jurkat cells). However the possibility of PKB binding to the low levels of PI(3,4)P_2 cannot be ruled out.

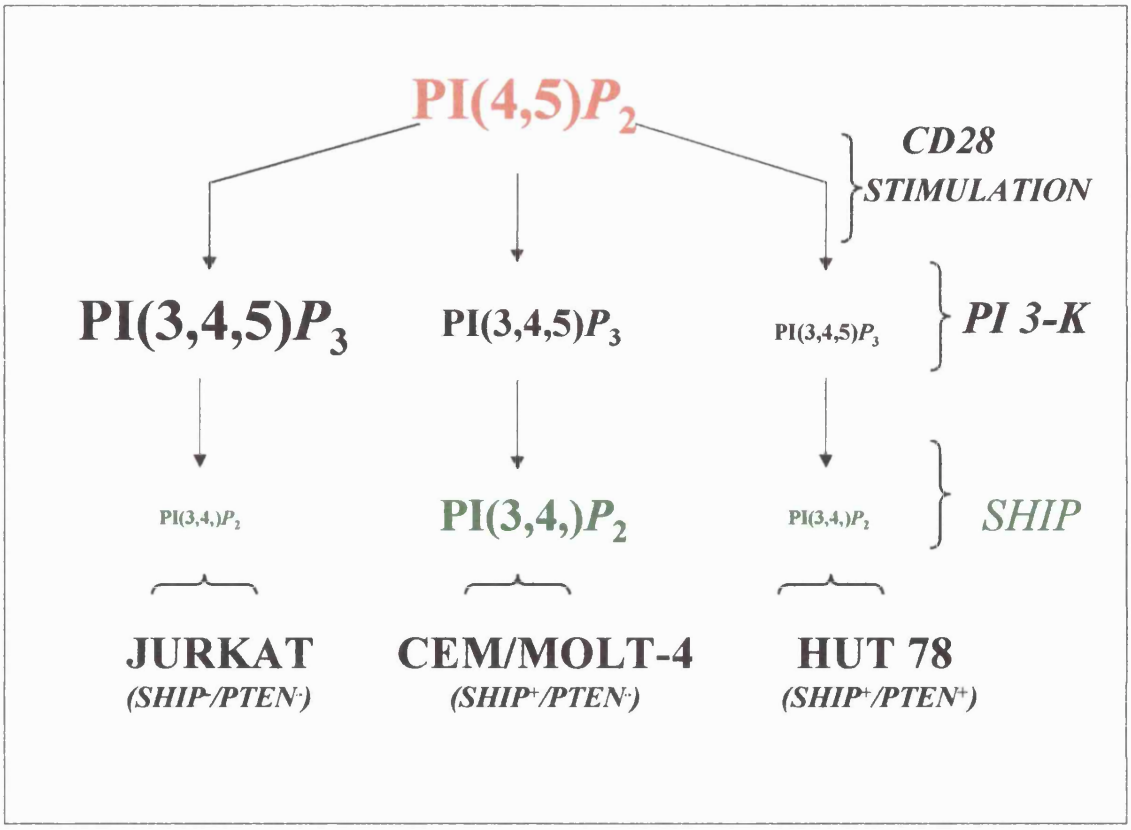

Figure 57: Effect of SHIP/PTEN expression on D-3 phosphoinositide levels in T-leukemic cell lines. Jurkat cells, which express neither SHIP or PTEN, exhibit high basal levels of PI(3,4,5)P_3 relative to PI(3,4)P_2 perhaps, in part, due to the lack of SHIP. Jurkats are thus inefficient in metabolising PI(3,4,5)P_3 and have high basal levels of phospho-PKB. CEM/MOLT-4 cell lines express SHIP but not PTEN and are therefore able to shunt PI(3,4,5)P_3 towards PI(3,4,)P_2 reflected in a low PI(3,4,5)P_3: PI(3,4)P_2 ratio. HUT 78 cells express both SHIP and PTEN and, according to this model, should be able to rapidly metabolise PI(3,4,5)P_3 more efficiently than the other leukemic cell lines, hence the lower observed level of basal D-3 phosphoinositides. The relative strength of the arrows estimates the relative production of D-3 phosphoinositide observed in each of the T leukemic cell lines.

Regulation of SHIP and PTEN by T cell surface receptors

The 5' phosphatase SHIP has previously been reported to be a downstream target for both CD3 (Liu *et al* 1997) and CD28 receptors (Edmunds *et al* 1999). Originally identified as 145 kDa tyrosine phosphoprotein in appropriately stimulated T cell lysates (Damen *et al* 1993). SHIP is now recognised as a constitutively active cytosolic phosphatase that moves to the plasma membrane following cellular stimulation (Rohrschneider *et al* 2001). In B cells and other cell types, SHIP is able to translocate to the plasma membrane via a direct interaction with cell surface receptors containing tyrosine phosphorylated ITIMs (e.g. the FcγRIIb receptor), thus placing it into proximity to its substrates (Bolland *et al* 1998). The precise molecular mechanisms responsible for the subcellular translocation of SHIP to the plasma membrane in T cells remain to be determined. SHIPs translocation from the cytoplasm to the plasma membrane in response to CD28 ligation has been observed in murine hybridoma T cells (Edmunds *et al* 1999). However, CD28 has no ITIMs or other recognisable motifs, that would allow its interaction with SHIP and the lack detectable association between SHIP and CD28 has been confirmed by western blotting of CD28 I.Ps (Edmunds *et al* 1999). The question therefore arises: how does CD28 signal to SHIP?

In this investigation it was shown that ligation of CD28 with mAb or B7 ligands and CD3 with mAb can lead to the tyrosine phosphorylation of SHIP in a variety of leukemic T cell lines (excluding Jurkat cells which do not express SHIP), murine hybridoma T cells and in human T-lymphoblasts. Co-ligation of CD28 and CD3 in murine hybridoma T cells resulted in increased tyrosine phosphorylation of SHIP compared to ligation of with either receptor alone. CD28-induced tyrosine phosphorylation of SHIP was independent of PI 3-K recruitment to the receptor. This suggests that a PI 3-K-dependent PTK is probably not responsible for the tyrosine phosphorylation of SHIP observed following CD28 stimulation and secondly, the that the formation of D-3 phosphoinositides are not essential for SHIP phosphorylation.

Also presented here is the first known evidence for the tyrosine phosphorylation of SHIP following CD2 and IL-2 receptor stimulation in T-lymphoblasts. The T cell receptors CD3, CD28 and CD2 are all known to cluster in the mature immunological synapse (IS) formed with antigen presenting cells. It is thus reasonable to hypothesise that co-engagement of these receptors by their physiological ligands present on APC would result in high local levels of tyrosine phosphorylated SHIP. This in turn would produce significant local levels of PI(3,4)P_2 within the vicinity of the IS. The potential increased accumulation of PI(3,4)P_2 in the IS may be sufficient to initiate PI(3,4)P_2-dependent signalling cascades, involving adapter proteins with PH domains specific for PI(3,4)P_2 such as DAPP-1 and TAPP (figures 58/59). Consistent with this possibility, additive tyrosine phosphorylation of SHIP using soluble anti-CD28 and CD3 signalling mAbs has been shown to occur in murine hybridoma T cells. SHIP therefore has the potential to increase the diversity of PI 3-K signalling via mediating the shunt from PI(3,4,5)P_3 to PI(3,4)P_2-driven signalling pathways (figure 54). SHIP, therefore has the potential to negatively regulate PI(3,4,5)P_3 signalling cascades but positively regulate PI(3,4)P_2 signalling.

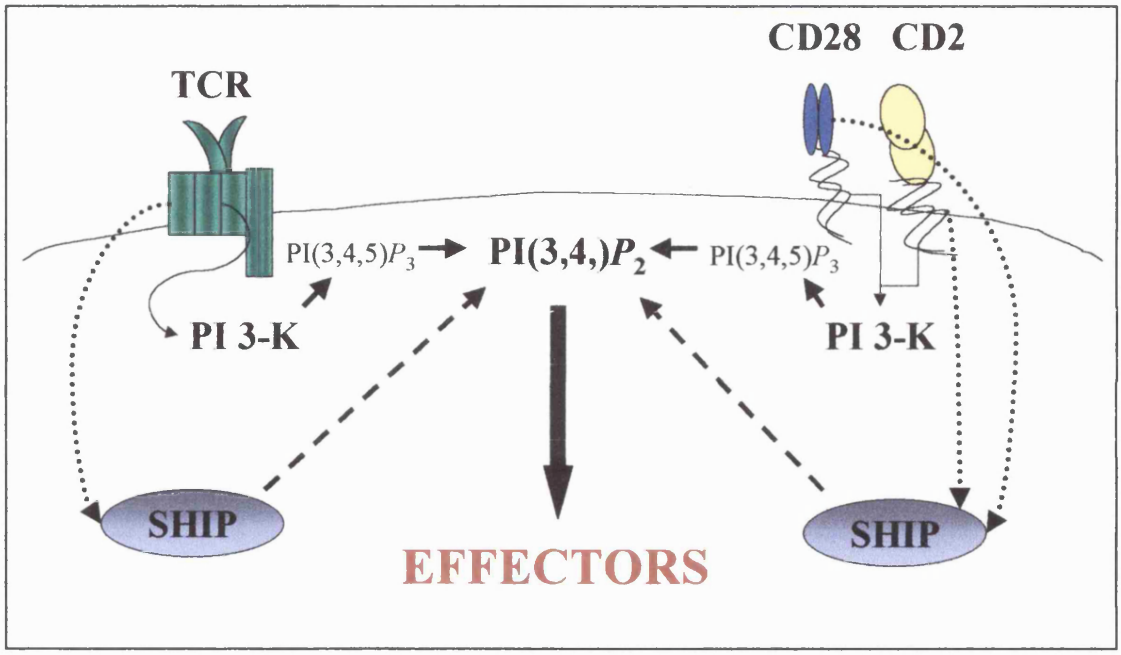

Figure 58: Proposed role for SHIP in the mature IS. Multiple engagement of clustered T cell molecules by their cognate ligands on the APC initiates cell signalling, including the tyrosine phosphorylation of SHIP and the local accumulation of PI(3,4)P_2. Specific PH-domain containing adapter proteins including the recently identified TAPP and DAPP and other as yet uncharacterised signalling proteins, have the potential to initiate poorly characterised PI(3,4)P_2-dependent signalling cascades.

SHIP co-associating proteins in T cells.

SHIP contains multiple domains capable of mediating a plethora of protein-protein interactions and was originally identified through its capacity to bind to Shc following cytokine stimulation (Damen *et al* 1996). SHIP, a target for CD28-activated PTKs, has been shown to co-immunoprecipitate with several tyrosine-phosphorylated proteins with predicted molecular masses of 62 and 100 kDa (Edmunds *et al* 1999). Data presented here suggests that the multi-functional adapter protein $p62^{dok}$ bind to SHIP immunoprecipitates in T cells following stimulation with anti-CD28 mAb. This particular adapter is known to be a downstream target for CD28-activated–PTK but not TCR-activated-PTK (Nunes *et al* 1996). SHIP was also found to associate in the reverse, p62 immunoprecipitates further supporting an association between these two

proteins. Similar associations have been reported to occur in B cells (Tamir *et al* 2000), and it has been postulated that $p62^{dok}$ and SHIP are key mediators of FcγRIIb signalling in B cells (Ott *et al* 2002). SHIP binding to $p62^{dok}$ may provide a mechanism for SHIP's translocation from the cytosol to the plasma membrane following CD28 stimulation, as $p62^{dok}$ contains a PH domain. However the fact that SHIP can still be tyrosine phosphorylated through stimulation of a CD28 mutant unable to recruit PI 3-K suggests that the formation of D-3 phosphoinositides and therefore the requirement for PH-domain containing adapter proteins, is not required for the translocation of SHIP. Another interesting observation regarding $p62^{dok}$ association with SHIP is that it is also known to associate with RasGAP proteins. These function to suppress active Ras GTP levels and therefore negatively regulate the mitogenic MAPK/Erk pathways (Tamir *et al* 2000). SHIP/$p62^{dok}$ regulation of Erk may contribute to CD28 signalling although further investigation is needed to confirm or refute this hypothesis. Other indirect evidence for SHIPs association with $p62^{dok}$ comes from the *in vitro* kinase assays. These showed that following CD28 stimulation, immunoprecipitation with anti-SHIP mAb revealed the presence of a 32-P labelled p62 phosphoprotein, which may be $p62^{dok}$.

SHIP has been shown to bind to the adapter protein Grb2 in B cells (Harmer *et al* 1999) and has been postulated to negatively regulate the MAPK/Erk cascade through its ability to sequester regulatory adapter proteins (Tridandapani *et al* 1997). In this study, no evidence was obtained to suggest an interaction of SHIP and Grb2 in T cells following CD28 stimulation. The recently identified 44 kDa adapter protein GRID was shown to associate with SHIP immunoprecipitates following CD28 stimulation. GRID, along with PI 3-K, is able to interact with CD28 at the ^{173}YXXM-consensus motif within the cytoplasmic tail and potentially regulate uncharacterised mitogenic signalling cascades (Ellis *et al* 2000). The data presented here is the first to provide evidence for an interaction between SHIP and GRID, although the mechanism and functional consequence remains to be determined. SHIP may act to sequester GRID away from the CD28 scaffold platform, thereby negatively regulating GRID signalling cascades. The mechanism(s) by which SHIP mediates these protein-protein interactions remains to be established. The observed associations may be direct or indirect, and perhaps mediated by an unidentified adapter protein. In a

single experiment, SHIP was shown to rapidly and inducibly associate with the protein tyrosine phosphatase SHP-2 following cellular stimulation with anti-CD28/CD3 mAbs. The observed association was rapid and sustained. Interestingly similar observations have been observed in other signalling systems, most notably after stimulation with BCR/ABL growth factors (Sattler *et al* 1997). SHIP and SHP-2 are also known to bind to ITIM motifs within the FcγRIIb receptor and mediate its inhibitory signalling (Sarmay *et al* 1999). Again the molecular nature of the protein interactions described is undefined, but SHP-2 may regulate the tyrosine phosphorylation of SHIP and other associated proteins, thereby regulating its activity. The protein-protein interactions SHIP exhibits following CD28 stimulation and their possible consequences are summarised in figure 59.

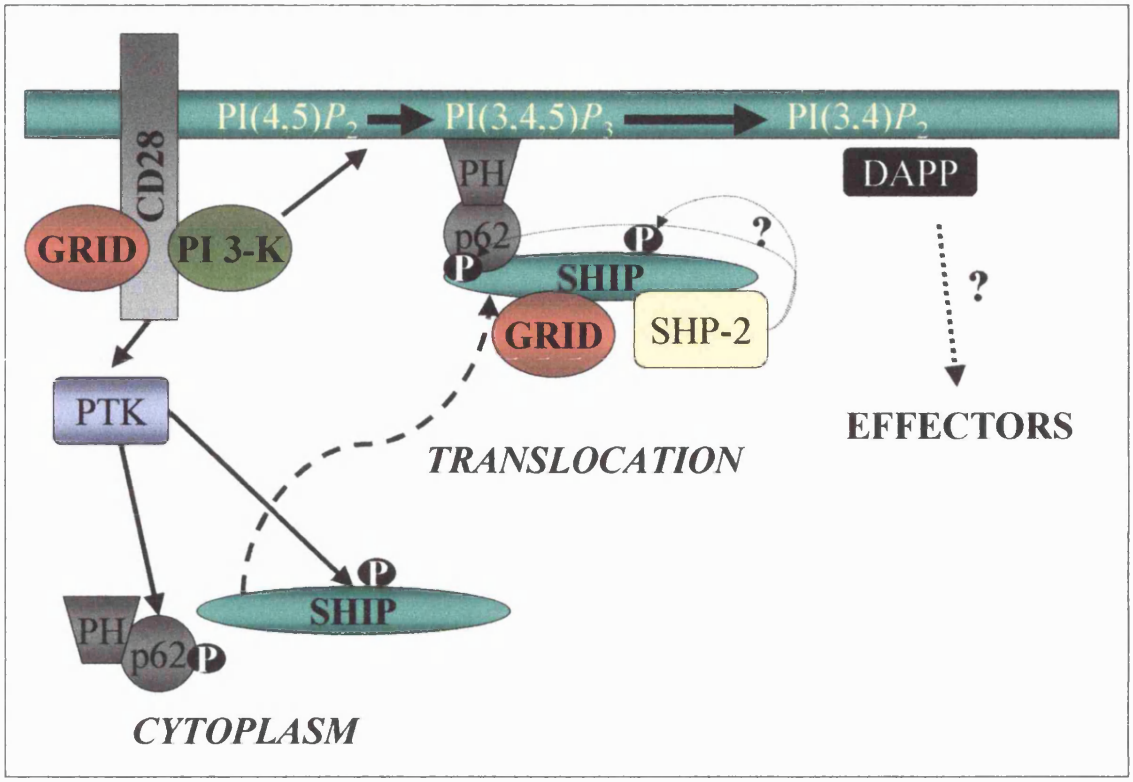

Figure 55: SHIP protein-protein interactions following CD28 stimulation in T cells. Ligation of CD28 results in the activation of PTK, phosphorylation of the CD28 cytoplasmic tail, recruitment of PI 3-K and the formation of D-3phosphoinositides including PI(3,4,5)P_3. CD28-activated-PTK also phosphorylates SHIP and the adapter $p62^{dok}$ perhaps inducing their association via the SH2 domain of SHIP (Tamir *et al* 2000). The PH domain of $p62^{dok}$ may serve to translocate cytoplasmic SHIP to the plasma membrane placing it in proximity to its substrates and resulting in the formation of PI(3,4)P_2 which may activate other signal transduction pathways. The functional significance of SHP-2 and GRID binding to SHIP is uncertain. SHIP may possibly negatively regulate GRID function by sequestering it away from the CD28 scaffold, whereas SHP-2 may regulate the tyrosine phosphorylation status of SHIP and its binding proteins. The molecular nature of the various protein interactions is unclear.

CD28 stimulated-SHIP immunoprecipitates were shown to contain *in vitro* protein kinase activity. This kinase activity was low in unstimulated cells, with a marked and sustained increase following CD28 stimulation. Unknown phosphoproteins of varying molecular masses, including 62 kDa ($p62^{dok}$?), 100 kDa and 145 kDa, presumably SHIP, being observed to co-precipitate with SHIP. The 100 kDa 32-P phosphoprotein found to immunoprecipitate with SHIP following CD28 stimulation may be Gab2 (Grb2 adapter binding protein 2), the molecular weight of which is 97 kDa. Gab2 has been shown to associate with

SHIP following IL-3 stimulation (Bone *et al* 2000). The *in vitro* kinase data presented here provides the first evidence that SHIP is able to inducibly associate with one or more proteins with kinase activity, although it is not known if this kinase(s) are tyrosine or a serine/threonine kinase. It is possible that the kinase(s) found to associate with SHIP might be responsible for its tyrosine phosphorylation following CD28 stimulation. A candidate tyrosine kinase is $p56^{lck}$, which has been shown to phosphorylate SHIP in T cells (Lamkin *et al* 1997). SHIP also exhibited *in vitro* 5' phosphatase activity towards Ins(1,3,4,5)P_4 resulting in the generation of the soluble metabolite Ins(1,3,4)P_3. Evidence is presented to suggest that this phosphatase is constitutively active and thus, in agreement with published data, it would seem that the translocation of SHIP to the membrane is the key factor regulating its access to substrates and hence biological activity (Rohrschneider *et al* 2000).

CD28 regulation of PTEN

In this investiagtion an attempt has been made to determine if PTEN is a downstream target for CD28 following stimulation. PTEN, unlike SHIP, is not a target for PTK and contains fewer recognised protein-protein interaction motifs. However, PTEN does contain PDZ domains that capable of mediating protein-protein interactions. The regulatory mechanisms governing PTEN function are poorly defined. Recent evidence, however, has shown that PTEN is under co-stimulatory control in $CD4^+$ primary T cells. Studies have shown that PTEN is upregulated at both mRNA and protein level following stimulation with CD28 and CD2 and that it controls T cell proliferation (Harris *et al* 2002). In contrast, PTEN expression was high in lymphoma cells but remained CD28 and CD2 unresponsive (Carsten *et al* 2002). Interestingly, this CD28 costimulatory upregulation of PTEN was not blocked by the PI 3-K inhibitor wortmannin, suggesting that upregulation is independent of PI 3-K signalling pathways (Carsten *et al* 2002). Data presented here show that PTEN immunoprecipitates contain *in vitro* protein kinase activity following CD28 stimulation. Furthermore, evidence was also obtained for recruitment and phosphorylation of several phosphoproteins (ranging in size from 150 - 40 kDa) induced upon CD28 stimulation, which may be involved in the regulation of PTEN activity. A PTEN multimeric protein complex has been described and observed to elute at >600

kDa in gel filtration columns (Vazquez *et al* 2001). Thus data described here are the first observations to reveal that CD28 can indeed signal to PTEN. The identities of the kinase and phosphoproteins immunoprecitating with PTEN following CD28 stimulation are unknown and warrant further investigation. Of added interest, one of the 32-P labelled phosphoproteins found to inducibly associate with PTEN following CD28 stimulation was of 145 kDa, the same molecular weight as SHIP. An association between these two phosphatases has never been described and unfortunately further analysis (western blotting) was not undertaken. It remains to be established whether stimulation of the TCR is also able to induce *in vitro* kinase activity and associating proteins in PTEN immunoprecipitates. PTEN has been reported to interact with focal adhesion kinase (Tamura *et al* 1999) and this may be a candidate kinase to co-precipitate with PTEN and is responsible for the observed *in vitro* kinase activity.

Unfortunately, *in vitro* phosphatase assays were not performed on PTEN immunoprecipitates for activity on the water soluble Ins(1,3,4,5)P_4. It would have been of interest to determine if PTEN immunoprecipitates from CD28 stimulated lysates had increased phosphatase activity towards IP4 when compared with unstimulated control PTEN immunoprecipitates. It is therefore unknown if CD28 and other T cell surface co-stimulatory receptors (such as CD3) can increase or decrease the D-3 phosphatase activity of PTEN under *in vitro* conditions. However the *in vitro* kinase data does suggest a regulatory role for CD28 in PTEN function.

Assessing the role of PPARγ agonist on T-lymphocyte proliferation.

Methods to measure T cell proliferation

Resting T lymphocytes require at least 2 signals to drive clonal expansion. The first signal is derived from a specific interaction between the TCR and antigen in complex with MHC proteins on the APC. Co-stimulatory receptors such as CD28 engaging with their respective B7 ligands provide signal 2. Activation and blast formation of T cells in an unphysiological setting can also be achieved by using pharmacological tools such as the phorbal ester, phorbal myristol acetate (PMA), and ionomycin in combination. A functional consequence of T lymphocyte activation is an increase in DNA synthesis, which can be measured, albeit indirectly, by assessing the T cells ability to incorporate ^{3}H-thymidine into DNA. In recent years therapeutic interest has focused the potential anti-inflammatory properties of PPARγ agonists (for review see Kersten *et al* 2000). This is due to their ability to inhibit the production by monocyte inflammatory cytokines (Jiang *et al* 1998) and also inhibiting the activation of T-lymphocytes by blocking production of the T cell cytokine IL-2 (Yang *et al* 2000). This section will describe the effect of various PPARγ agonists on the proliferation of resting primary T cells and T lymphoblasts.

Proliferation of primary T cells in response to CD3, CD28, CD3/CD28, PMA and PMA/CD28 signals.

Freshly purified primary T cells were assessed for their ability to proliferate in response stimulation with anti-CD28/CD3 mAb and phorbal ester (PMA) alone or in combination. As expected, ligation of the CD3 or CD28 receptors with anti-CD3/CD28 mAbs did not result in significant ^{3}H-thymidine incorporation (figure 60). Addition of both anti-CD3/CD28 antibodies together resulted in a 100-fold increase in ^{3}H-thymidine incorporation and in the blast-cell formation (assessed microscopically). PMA added alone did not induce significant ^{3}H-thymidine incorporation, but did so in the presence of a co-stimulatory signal (anti-CD28 mAb) resulted in a 95-fold increase in ^{3}H-thymidine incorporation that was increased to an extent comparable to that observed with combined anti-

CD3/CD28 mAb treatment. These findings are consistent with previously published work in that naïve primary T cells require at least 2 signals for proliferation with one emanating from the TCR-CD3 subunit and one from a co-stimulatory molecule such as CD28.

Figure 53: Proliferation of primary T cells in response to CD3, CD28, CD3/CD28, PMA and PMA/CD28 signals.

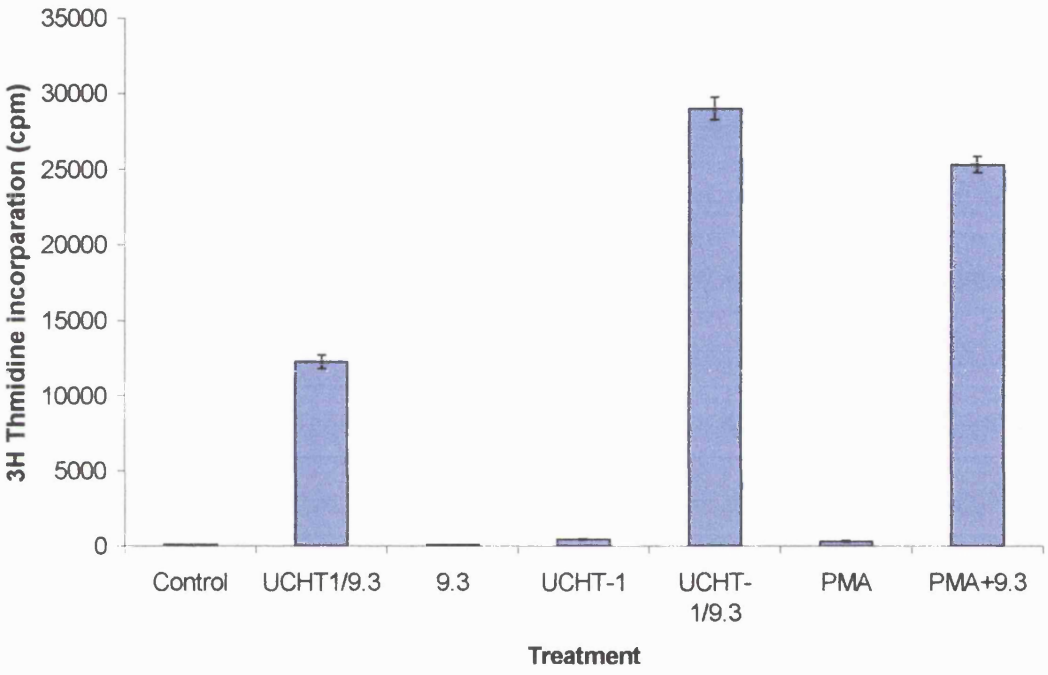

Figure 60: Proliferation of primary T cells in response to various mitogenic signals. 1×10^5 primary T cells/well were aliquoted and stimulated as indicated with anti-CD3 (UCHT-1) and anti-CD28 (9.3) mAbs in the combinations described. Alternatively, T cells were stimulated with 5 ng/ml PMA alone or in combination with anti-CD28 9.3 mAb. Data are the mean ± S.E.M of quintuplicate samples from a single experiment representative of at least 3 others.

T cell proliferation studies: Effect of Peroxisome Proliferator-Activated Receptor (PPAR) γ agonists.

The PPAR family of receptors (α,β and γ) are transcription factors and members of the nuclear receptor superfamily. The prostaglandin, 15-deoxy-$\Delta^{12,14}$ prostaglandin J_2 (PGJ_2), a derivative of PGE_2 and therefore downstream of cyclooxgenase-2 (COX2), is a natural ligand for PPARγ. PPARγ was initially implicated in the regulation of genes involved in lipid metabolism and adipocyte differentiation (Issemann *et al* 1990). The PPARγ ligand troglitazone, a thiazolidinedione compound formerly used to treat type II diabetes but was withdrawn due to toxic side effects. The studies of Yang *et al* looked at the ability of various PPARγ ligands to inhibit T lymphocytes stimulated with the pharmacological agents PMA and the mitogenic lectin phytoheamagglutinin (PHA). In this investigation I have sought to assess the role of PPARγ ligands in inhibiting CD3/CD28, IL-2 and PMA/Ionomycin-mediated proliferation of primary naïve T cells as well as SEB-activated T-lymphoblasts.

The PPARγ receptor is expressed at the protein level in SEB-activated T-lymphoblasts and T cell leukemic cell lines.

It has been published previously that mRNA for PPARγ is expressed in peripheral blood T-lymphocytes (Greene *et al* 1995). Cell-equivalent lysates were prepared from T-lymphoblasts and the T cell leukemic cell lines Jurkat, CEM, MOLT-4 and HUT 78 and immunoblotted for PPARγ using an anti-PPARγ mAb which reacts with exclusively to the PPARγ1 isoform (figure 61). PPARγ protein could be detected in the above cell lysates as revealed by Western blotting although expression was reduced in the MOLT-4 leukemic cell line. Rather than check protein expression levels of PPARγ using cell equivalents, an alternative approach would be to load equal amounts of protein from the different cell lines (via Bradford assay for determining protein concentration). This would help verify if the reduced levels of PPARγ observed in MOLT-4 cells compared to the other cell lines is real.

Figure 61: The PPARγ receptor is expressed at the protein level in SEB-activated T-lymphoblasts and T cell leukemic cell lines.

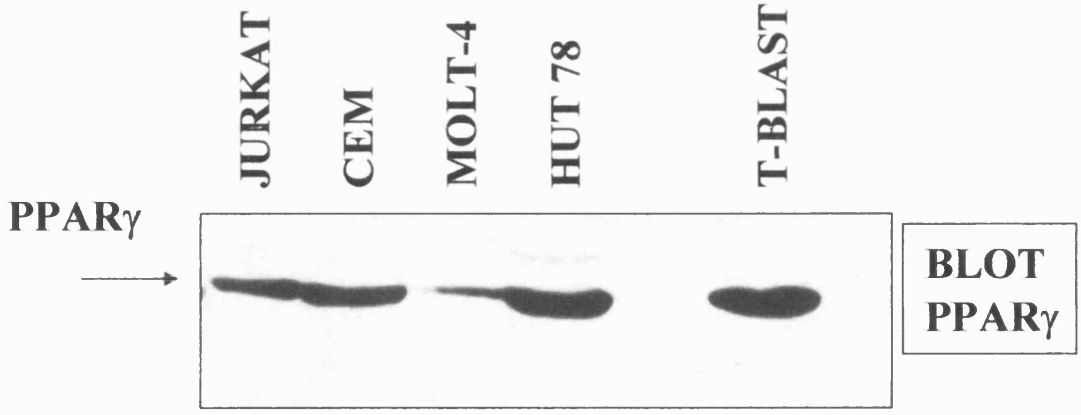

Figure 61: Expression of PPARγ in T cell lines. 10^7 of each cell line were washed, aliquoted and lysed in lysis buffer. The resultant cell lysates were acetone precipitated and the precipitated proteins boiled in lamelli sample buffer. Proteins were resolved by SDS-PAGE and transferred onto nitrocellulose and immunoblotted with an anti-PPARγ (which reacts with the PPARγ-1 isoform) mAb as described in *Materials and Methods*. Results are from a single experiment representative of two others.

The PPARγ ligands troglitazone and 15dPGJ$_2$ but not ciglitazone inhibit CD3/CD28 co-stimulation in primary T cells.

Transformation of purified, resting T lymphocytes could be achieved by the addition of anti-CD3/CD28 mAbs (1 μg/ml) covalently bound to M-450 dynabeads or by treatment with PMA/ionomycin (5 ng/ml and 1 μM respectively). Primary T cell proliferation could be potently inhibited by pre-treatment with the naturally occurring PPARγ ligand 15dPGJ$_2$ (figure 62). Inhibitors used were added before stimulating cells and were present for the remainder of the proliferation assay. The thiazolidinedione, troglitazone was able to inhibit CD3/28 co-stimulation at higher doses (30 μM) but interestingly had no effect on PMA/Ionomycin stimulation. In contrast, and consistent with previous findings (Yang *et al* 2000), ciglitazone, which is structurally related to troglitazone, had no inhibitory effects, on primary T cell proliferation stimulated with CD3/CD28 or PMA/Ionomycin (figure 62).

Of the PPARγ agonists examined, 15dPGJ2 appeared to be the most potent with an almost complete abrogation of ^{3}H-thymidine incorporation observed at 10 μM. The IC$_{50}$ for inhibition of CD3/CD28 co-stimulation by 15dPGJ$_2$ and troglitazone was 0.8 μM and 5 μM respectively (figure 63a). The estimated IC$_{50}$ for 15dPGJ$_2$-mediated inhibition of PMA/Ionomycin stimulation of primary T cell proliferation was 3 μM, slighter higher than its predicted IC$_{50}$ for CD3/CD28 inhibition (figure 63b).

Figure 62: Effect of PPARγ ligands on CD3/CD28 and PMA/Ionomycin induced primary T cell proliferation.

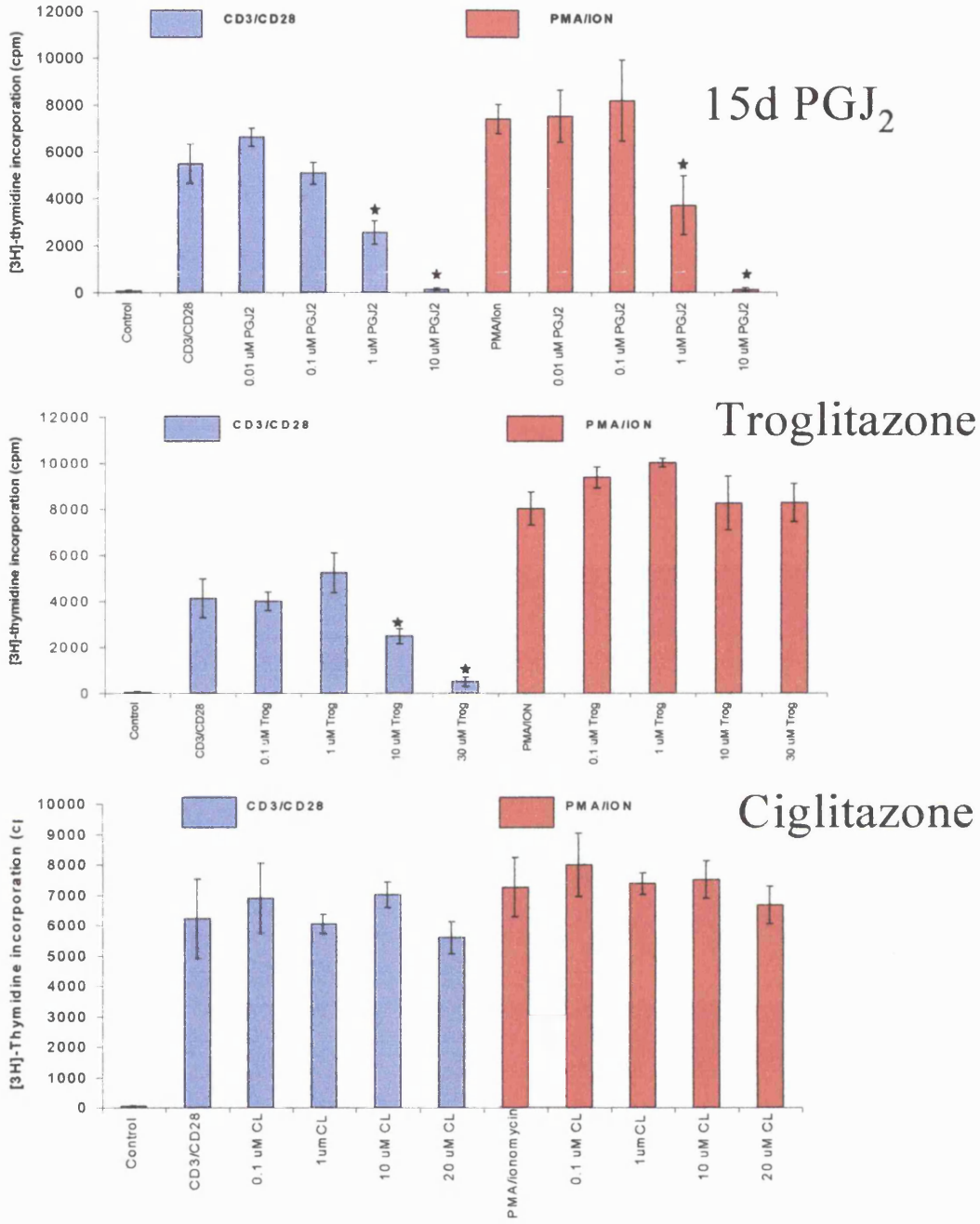

Figure 62: Effect of PPARγ ligands on CD3/CD28 and PMA/Ionomycin induced primary T cell proliferation. 10^5 primary T cells were aliquoted and pre-treated for 30 minutes with the PPARγ ligands as indicated (Inhibitors were present with cells for remainder of assay). Cells were stimulated with either 1 μg anti-CD3/CD28 bound to M-450 dynabeads at a ratio of 1 bead to 1 cell or with 5 ng/ml PMA and 1 μM Ionomycin as described in *Materials and Methods*. Cells were incubated for 48 hours at 37°C and then pulsed for a further 12 hours with 1 μ curie [3H]-thymidine. Cells were harvested onto filter plates, washed and thymidine incorporation was assessed using a scintillation counter. Data are the mean data ± S.E.M 3 independent experiments. ** = p value 0.010, * = p value of 0.005 and represent a significant difference compared to appropriate positive control.

Figure 63a: Percentage inhibition of CD3/CD28-mediated proliferation by PPARγ ligands in primary T cells.

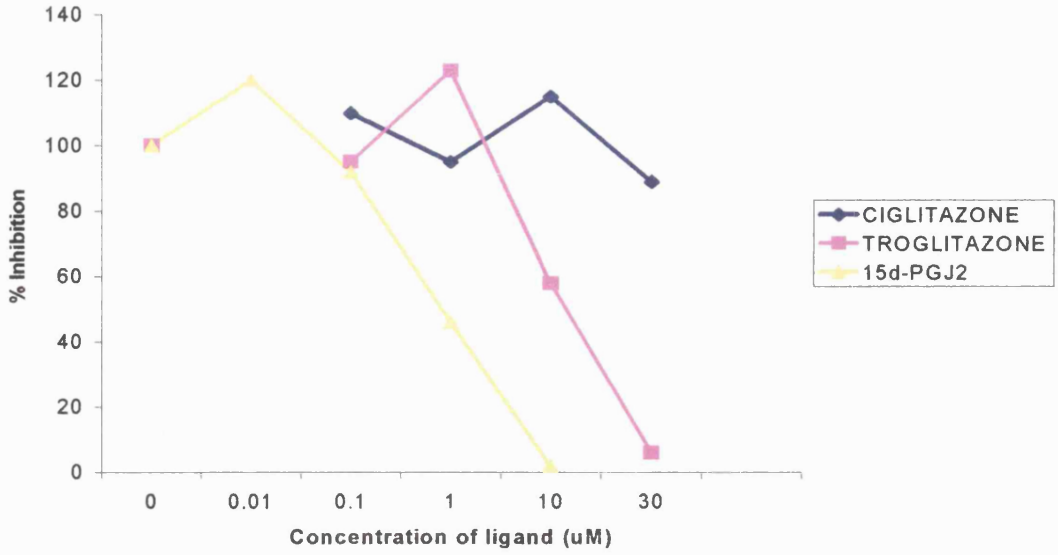

Figure 63b: Inhibition of PMA/Ionomycin stimulation of primary T cell by 15dPGJ$_2$.

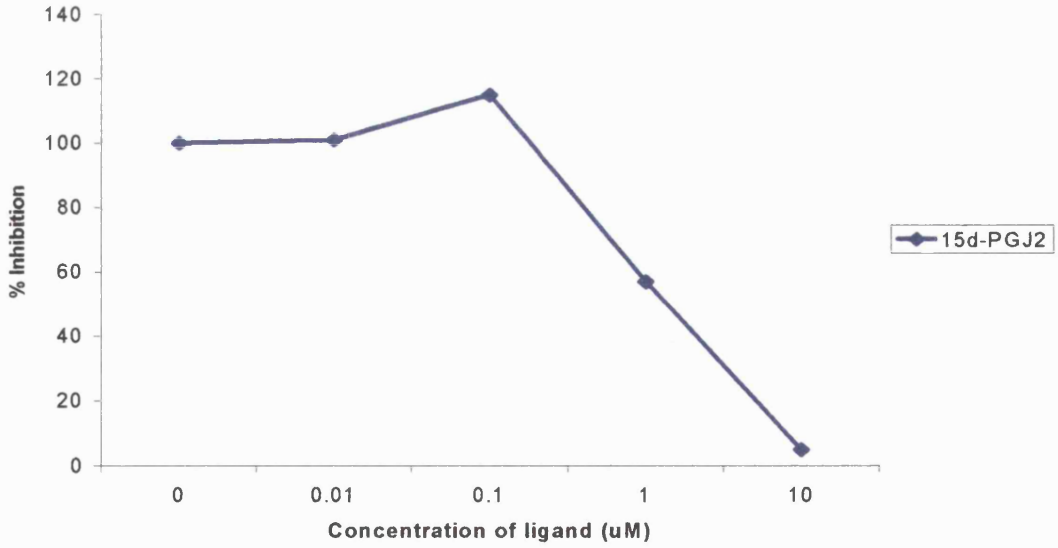

Figure 63a/b: Percentage inhibition of CD3/CD28 mediated proliferation by PPARγ ligands 15dPGJ$_2$ (yellow line), troglitazone (purple line) and ciglitazone (blue line) in primary T cells and also PMA/ionomycin-mediated proliferation by the PPARγ ligand 15dPGJ$_2$ (blue line bottom panel). Mean proliferation data generated from figure 63 were used to calculate inhibitory effects of PPARγ ligands as a percentage of stimulated cells without PPARγ ligand (positive control). Data are from mean pooled data from 3 independent experiments.

The PPARγ ligands troglitazone and 15dPGJ$_2$ but not ciglitazone inhibit CD3/CD28 co-stimulation in SEB-activated T-lymphoblasts.

Treatment of T lymphoblasts with the various PPARγ ligands tested gave similar results to those obtained using primary T cells. Both 15dPGJ$_2$ and troglitazone were able to inhibit CD3/CD28 induced [3H]-thymidine incorporation. Again, troglitazone was less potent when compared with 15d-PGJ$_2$, only effective at inhibiting CD3/CD28 T lymphoblast proliferation at concentrations of ≥10 μM with almost complete inhibition being observed at 100 μM (figure 64). However it cannot be ruled out that these high concentrations of troglitazone may been toxic and/or pro-apoptotic. The natural PPARγ ligand 15d-PGJ$_2$ seemed to be more effective at inhibiting proliferation at lower concentrations. Ciglitazone, as in the case of primary T cells, was ineffective in inhibiting CD3/CD28 costimualtion of T-lymphoblasts even at higher concentrations of upto 20 μM (figure 64).

The IC$_{50}$ of 15dPGJ$_2$ and troglitazone in inhibiting CD3/CD28-mediated T-lymphoblast proliferation from the data generated in figure 64 was 5 μM and 18 μM respectively (figure 65). It is apparent that the IC$_{50}$ for 15dPGJ$_2$ is similar (i.e. in low micromolar range) in both primary T cells and T-lymphoblasts. In contrast, the IC$_{50}$ for troglitazone is slightly higher in T-blasts when compared with that obtained for primary T cells. It would have been of great interest to see if the PPARγ ligands used in this study could inhibit PMA/Ionomycin-mediated proliferation of T-lymphoblasts but unfortunately this was not done due to time constraints.

Figure 64: The PPARγ ligands troglitazone and 15d-PGJ_2 but not ciglitazone inhibit CD3/CD28 co-stimulation in SEB-activated T-lymphoblasts.

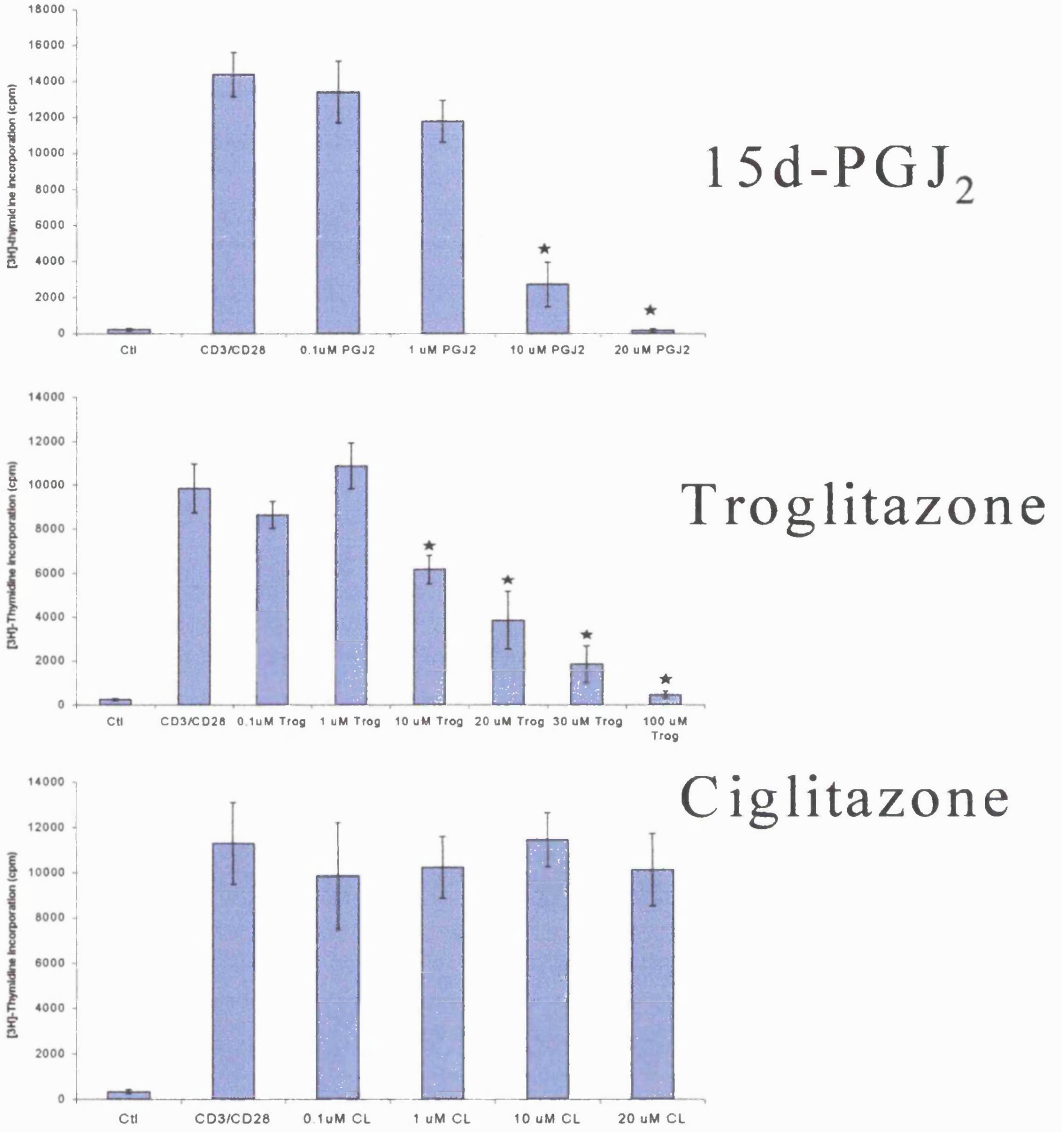

Figure 64: The PPARγ ligands troglitazone and 15dPGJ$_2$ but not ciglitazone inhibit CD3/CD28 co-stimulation in SEB-activated T-lymphoblasts. 10^5 T lymphoblasts were aliquoted and pre-treated for 30 minutes with the PPARγ ligands as indicated (Inhibitors were present with cells for remainder of assay). Cells were stimulated with 1 μg anti-CD3/CD28 bound to M-450 dynabeads as described in *Materials and Methods*. Cells were incubated for 48 hours at 37°C before being pulsed overnight with 1μ curie [3H]-thymidine. Cells were harvested onto filter plates, washed and thymidine incorporation was assessed using a β-scintillation counter. Data are the mean pooled data ± S.E.M of 3 experiments. .** = p value 0.010, * = p value of 0.005 and represent a significant difference compared to appropriate positive control.

Figure 65: Inhibition of CD3/CD28-mediated T-lymphoblast proliferation by PPARγ agonists.

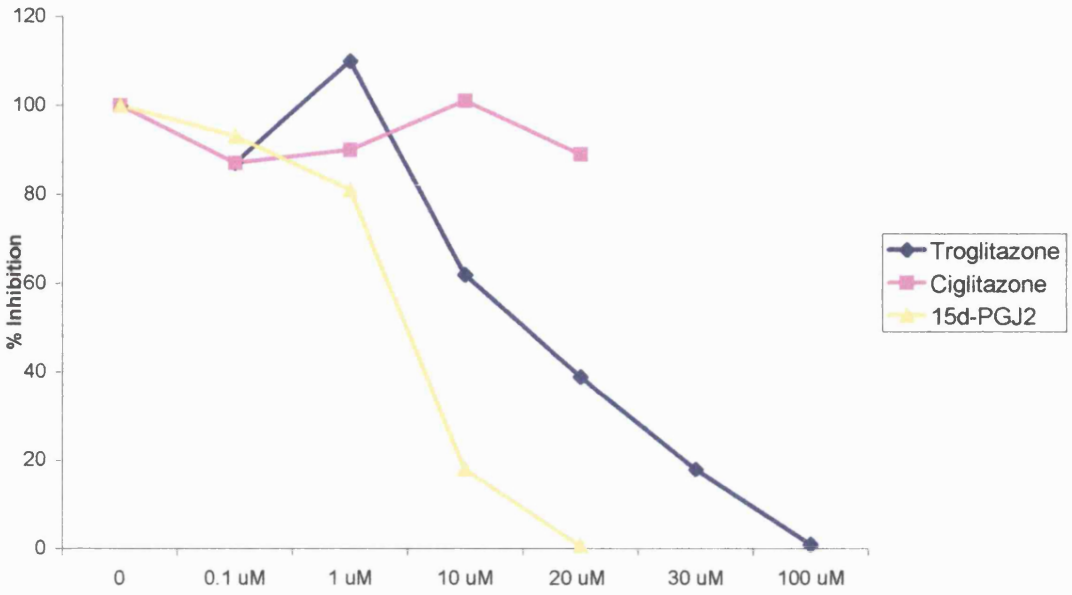

Figure 65: Inhibition of CD3/CD28-mediated proliferation by PPARγ ligands $15dPGJ_2$ (yellow line), troglitazone (blue line) and ciglitazone (purle line) in T-lymphoblasts. Mean proliferation data generated from figure 65 were used to calculate inhibitory effects of PPARγ ligands as a percentage of stimulated cells without PPARγ ligand (positive control). Data are from pooled data from 3 independent experiments.

Troglitazone and 15dPGJ$_2$ inhibit IL-2 driven proliferation in T-lymphoblasts

Transformation of peripheral primary T cells into T lymphoblasts by the superantigen SEB induces the surface expression of the IL-2 receptor. Engagement of the cytokine IL-2 with its receptor drives T cell proliferation (Smith K *et al* 1990). The ability of the PPARγ ligands troglitazone and 15dPGJ$_2$ to inhibit IL-2 driven T-blast proliferation was investigated in order to determine if IL-2 stimulated T cells were sensitive to PPARγ-mediated inhibition. Subsequent experiments revealed that both PPARγ ligands could inhibit IL-2 (20 ng/ml) mediated-[3H]-thymidine incorporation in SEB-activated T-lymphoblasts, with 15dPGJ$_2$, again, being slightly more potent than troglitazone (figure 66). Troglitazone significantly inhibited IL-2-mediated proliferation at concentrations ≥ 10 μM, with almost complete inhibition at 100 μM. The natural PPARγ ligand 15dPGJ$_2$, had significant inhibitory effects on T blast proliferation at concentrations as low as 1 μM. These experiments involving 15dPGJ$_2$ would have benefited with an extended lower range of concentrations of 15dPGJ$_2$ (i.e. low nanomolar range) to get a more accurate assessment of inhibition of IL-2 mediated T-lymphoblast proliferation by this PPARγ agonists.

The estimated IC$_{50}$ values for the inhibition for both 15dPGJ$_2$ and troglitazone generated from this data were 0.4 μM and 15 μM respectively (figure 67). The effect of ciglitazone on IL-2 dependent proliferation of T-lymphoblasts was unfortunately not tested. Estimated IC^{50} for PPARγ ligands on T cell proliferation are summarised and tabulated in table 15.

Figure 66: Troglitazone and 15dPGJ$_2$ inhibit IL-2 driven proliferation in T-lymphoblasts.

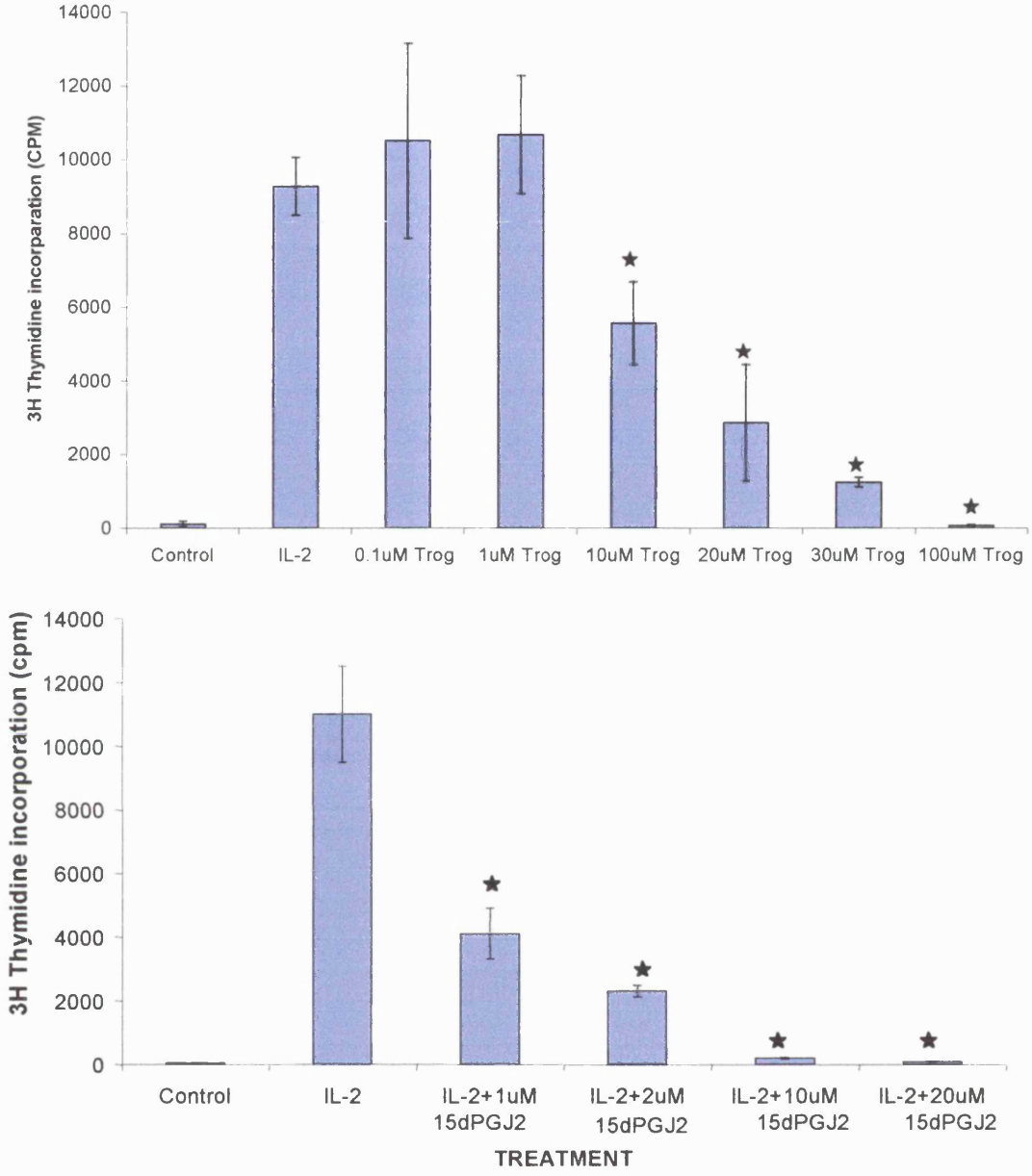

Figure 66: The PPARγ ligands troglitazone and 15dPGJ$_2$ inhibit IL-2-mediated proliferation in SEB-activated T-lymphoblasts. 10^5 T lymphoblasts were aliquoted and pre-treated for 30 minutes with the PPARγ ligands as indicated (Inhibitors were present with cells for remainder of assay). Cells were stimulated with IL-2 (20 ng/ml) described in *Materials and Methods*. Cells were incubated for 48 hours at 37°C before being pulsed overnight with 1μ curie [3H]-thymidine. Cells were harvested onto filter plates, washed and thymidine incorporation was assessed using a β-scintillation counter. Data are the mean pooled data ± S.E.M of 2 other independent experiments. ** = p value 0.010, * = p value of 0.005 and represent a significant difference compared to appropriate positive control.

Figure 67: Inhibition of IL-2-mediated proliferation by the PPAR γ ligands troglitazone and 15dPGJ$_2$ in T-lymphoblasts.

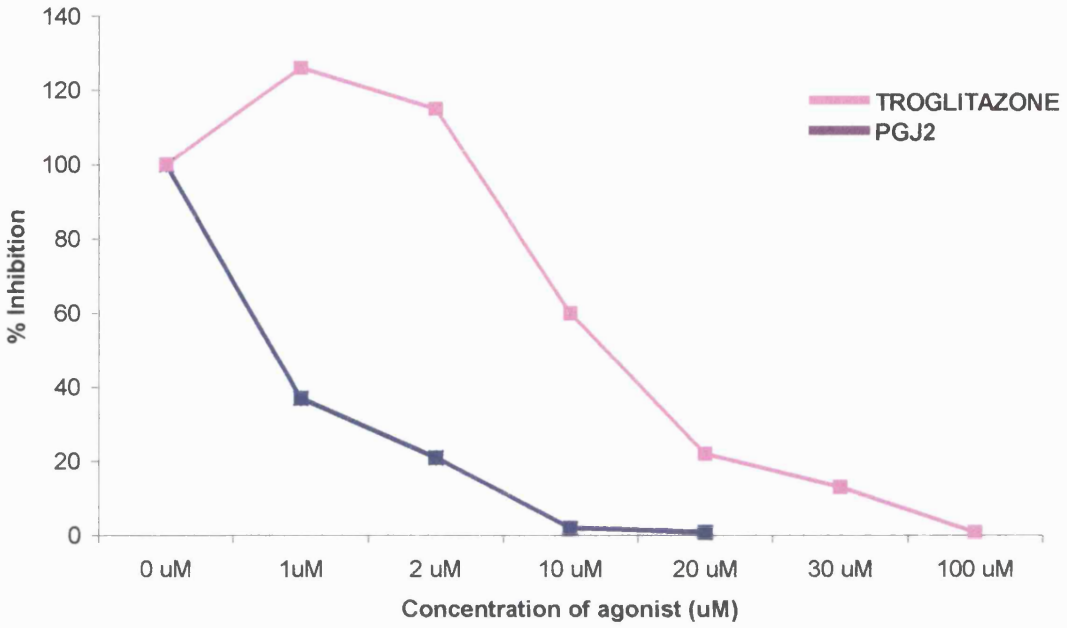

Figure 67: Inhibition of IL-2-mediated proliferation by the PPARγ ligands troglitazone (purple bar) and 15dPGJ$_2$ (blue bar) in T-lymphoblasts. Mean proliferation data generated from figures 66 were used to calculate inhibitory effects of PPARγ ligands as a percentage of stimulated cells without inhibitor (positive control). Data are the pooled mean data 2 separate experiments.

Table 15: IC^{50} values for inhibition of primary T cell/ T-lymphoblast proliferation upon pre-treatment with the PPARγ agonists

PRIMARY T CELLS			T-LYMPHOBLASTS		
IC^{50} (μM)	PMA/ION	CD3/ CD28	PMA/ION	CD3/ CD28	IL-2
$15dPGJ_2$	4	1	ND	1.5	0.1
TROGLITAZONE	NIO	5	ND	23	15
CIGLITAZONE	NIO	NIO	ND	NIO	ND

Table 14: Estimated IC^{50} values for inhibition of primary T cell/ T-lymphoblast proliferation upon pre-treatment with the PPARγ agonists 15dPGJ2, troglitazone and ciglitazone. Abbreviations used: NIO= no inhibition observed, ND = undetermined.

T-lymphoblast CD3/CD28 co-stimulatory proliferation can be inhibited by pre-treatment and post-treatment of the PPARγ ligands 15dPGJ$_2$ and troglitazone.

Cell signalling experiments, involving pharmacological inhibitors, are usually performed by pre-treating cells with the appropriate inhibitor for an appropriate time before a stimulus is added. In the proliferation studies described thus far, T cells have been pre-treated with PPARγ ligands for 30 minutes. PPARγ-treated T cells were then stimulated with CD3/CD28-coated M450-dynabeads, PMA/ionomycin or IL-2. The PPARγ agonists then remained with the cells for the duration of the assay. Additional experiments were designed to determine if untreated T-lymphoblasts, which had then been co-stimulated with CD3/CD28-coated dynabeads, and therefore actively proliferating, for set time periods were resistant to inhibition by 15dPGJ2 and troglitazone when added at later time points. It was found that the delayed addition of either PPARγ ligands (troglitazone or 15dPGJ$_2$) to CD3/CD28 stimulated samples was able to significantly inhibit the incorporation of [3H]-thymidine (figure 68).

Troglitazone (10 μM) was able to inhibit T-lymphoblast proliferation to control levels even after 48 hours post-CD3/CD28 co-stimulation. However it is acknowledged that a toxic effect of troglitazone used at these concentrations on T lymphoblasts cannot be ruled out. 15dPGJ2 (10 μM), was able to reduce proliferation when added up to 24 hours post-stimulation but was ineffective at the 48 hours time point (figure 68). This may be due to the instability of 15dPGJ$_2$ as once it was reconstituted it was then stored at 4°C for the remainder of the time course of the assay. These results may suggest that both troglitazone and 15dPGJ$_2$ are able to override and inhibit established proliferative co-stimulatory signals in T cells. However the data, albeit encouraging, was obtained in a single experiment and must therefore be interpreted with caution.

Figure 68: T-lymphoblast CD3/CD28 mediated-proliferation can be inhibited by pre-treatment or post-treatment of the PPARγ ligands 15dPGJ$_2$ (10 μM) and troglitazone (10 μM).

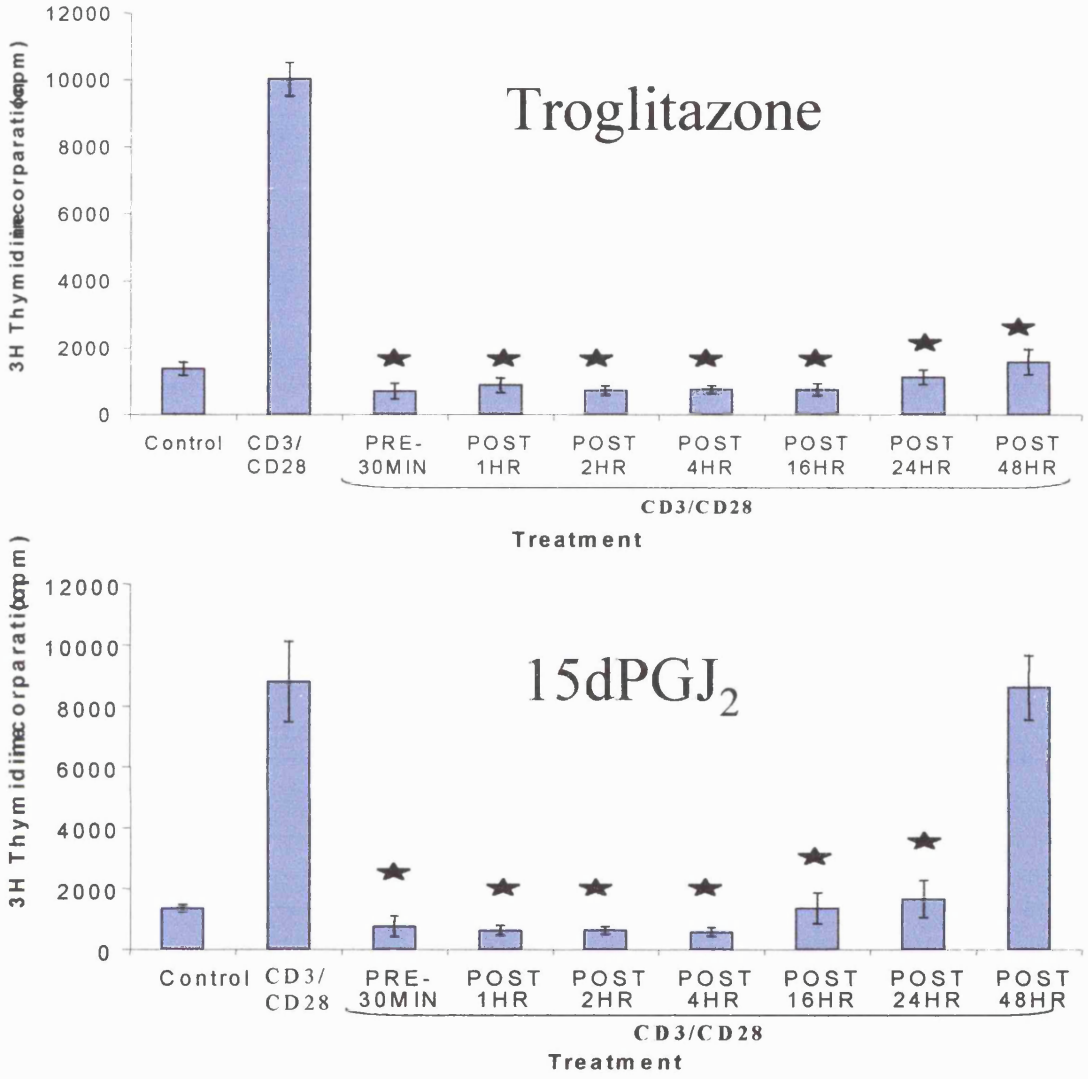

Figure 68: Co-stimulatory-mediated proliferation of T-blasts can be inhibited by pre- or post-treatment with the PPARγ ligands 15dPGJ$_2$ (10 μM) or troglitazone (10 μM). 10^5 T lymphoblasts were aliquoted and pre-treated or post-treated with the PPARγ ligands at the times indicated. Cells were stimulated with anti-CD3/CD28 bound to M-450 dynabeads at ratios described in *Materials and Methods*. Cells were incubated for 48 hours at 37°C before being pulsed overnight with 1μ curie [3H]-thymidine. Cells were harvested onto filter plates, washed and thymidine incorporation was assessed using a β-scintillation counter. This data is from a single experiment. ** = p value 0.010, * = p value of 0.005 and represent a significant difference compared to appropriate positive control.

The PPARγ ligand troglitazone doesn't inhibit proliferation in the leukemic cell lines Jurkat, CEM, MOLT-4 and HUT 78.

Western blot analysis of lysates from the above leukemic cell lines reveals the expression of PPARγ protein (figure 61). It was decided to investigate, therefore whether, the PPARγ ligand troglitazone (used at 10 μM) could inhibit the proliferation of these leukemic cell lines in a manner similar to that observed in CD3/28 stimulated primary T cells/T-lymphoblasts derived from normal volunteers (figures 62/64). Troglitazone had no significant effect on the proliferation of these leukemic T cell lines under basal conditions.

This data suggests that leukemic T cells are resistant to the growth-inhibitory effects of troglitazone. Further experimentation is confirm or refute this possibility. Unfortunately due to time constraints the PPARγ ligands $15dPGJ_2$ and ciglitazone were not tested for their potential inhibitory effect on leukemic T cell proliferation.

Figure 69: The PPARγ ligand troglitazone does not inhibit proliferation in the leukemic cell lines Jurkat, CEM, MOLT-4 and HUT 78.

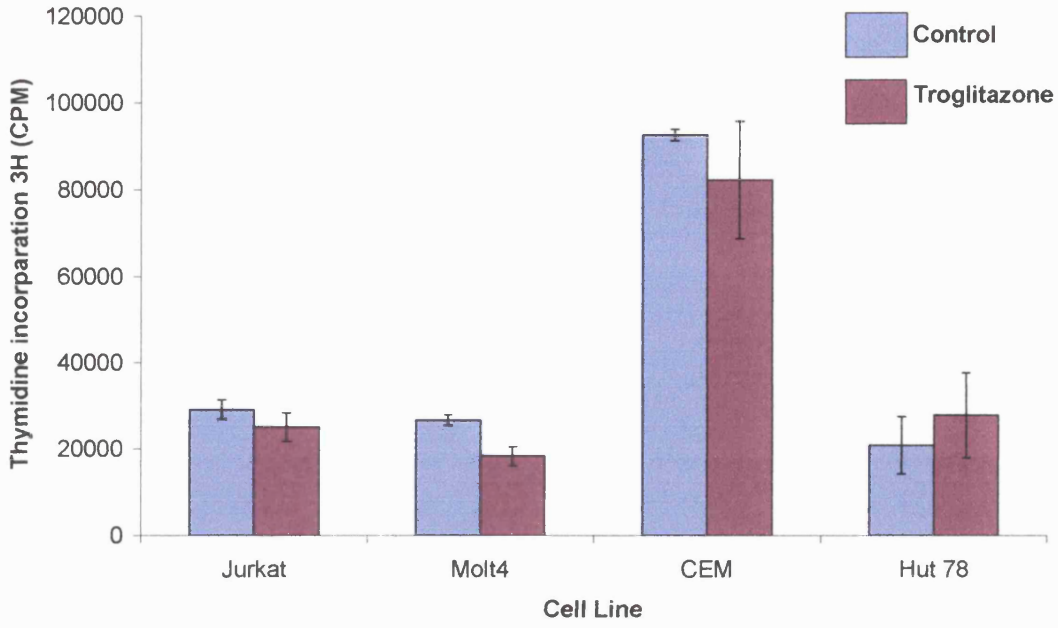

Figure 69: Troglitazone does not inhibit proliferation in the leukemic cell lines Jurkat, CEM, MOLT-4 and HUT 78. 10^5 leukemic cells from each cell line were washed and aliquoted. Cells were either left unstimulated (blue bar) or treated with troglitazone at 10 μM (red bar) and incubated for 48 hours before being pulsed with 1μ curie of [3H]-thymidine for 14 hours. Proliferation was assessed by β-scintillation counting as described in *Materials and Methods*. Data are the mean ± S.E.M of quintuplicate samples from a single experiment representative of 2 others. ** = p value 0.010, * = p value of 0.005 and represent a significant difference compared to appropriate positive control.

Summary

- Primary T cells proliferate in response to the simultaneous ligation of the CD3 and CD28 receptors but not in response to ligation of either receptor alone. T cells stimulated with 5 μg/ml PMA and 1μM ionomycin also proliferate. Both results are consistent with the literature.

- The PPARγ-1 isoform is expressed in T-lymphoblasts and the leukemic T cell lines Jurkat, CEM, MOLT-4 and HUT 78.

- The PPARγ agonists troglitazone and $15dPGJ_2$ inhibit CD3/CD28 proliferation in primary T cells and T-lymphoblasts with $15dPGJ_2$ being more potent on a molar basis than troglitazone. The structurally related PPARγ agonist ciglitazone had no observable effect on T cell proliferation.

- PMA/ionomycin stimulated primary T cells were resistant to the inhibitory effects of troglitazone but not the prostaglandin $15dPGJ_2$.

- Troglitazone and $15dPGJ_2$ are both able to inhibit IL-2 induced proliferation of T-lymphoblasts again with $15dPGJ_2$ showing greater potency (in molar terms) in inhibition.

- Preliminary findings suggest that the growth of CD3/28 stimulated T-lymphoblasts can be inhibited by addition of troglitazone/$15dPGJ_2$ at 10 μM post-stimulation.

- Troglitazone (10 μM), had no detectable significant effect on basal proliferation of the leukemic cell lines Jurkat, CEM, MOLT-4 and HUT-78 despite the apparent expression of PPARγ receptor at the protein level.

Control of T cell proliferation by PPARγ agonists

The PPAR proteins are members of the nuclear hormone receptor superfamily and all are believed to function as ligand dependent transcription factors. Studies have shown that PPARγ participates in diverse biological roles including differentiation, atherosclerosis and cancer and is therefore of significant clinical interest (Sporn *et al* 2001). Increasing research is being focussed on the role of PPARγ agonists in the regulation of immune cell function, particularly cells of the monocyte/macrophage series, and their clinical potential as anti-inflammatory agents. Studies have also revealed that specific PPARγ agonists such as troglitazone and $15dPGJ_2$ can inhibit activation of human T lymphocytes following stimulation with non-physiological ligands such as the mitogenic lectin phytoheamaglutin (PHA) and the phorbal ester PMA (Yang *et al* 2000) highliging the potential of PPARγ agonists as down-regulators of T cell-mediated inflammatory diseases. This study investigated the anti-proliferative effect of a variety of specific PPARγ agonists ($15dPGJ_2$, troglitazone and ciglitazone) in human primary T cells and T-lymphoblasts following a more physiological stimulus (anti-CD28/CD3 mAbs and IL-2) and compared the functional outcome (proliferation) with that obtained using PMA/Ionomycin.

In agreement with previous findings, western blotting with anti-PPARγ Ab revealed the high expression of PPARγ protein in human peripheral T lymphoblasts and leukemic T cell lines (Yang *et al* 2000 and Harris *et al* 2001). Visual inspection of blots from T cell lysates revealed lower expression of PPARγ receptor in MOLT-4 leukemic T cells than was observed in other cell lines. 30 minutes pre-treatment with the prostaglandin $15dPGJ_2$ prior to cellular stimulation, was shown to be a potent inhibitor of T cells and T-lymphoblasts proliferation in response to stimulation with the following anti-CD28/CD3 mAb (1 μg/ml), PMA/Ionomycin (used at 5 ng/ml and 1 μM respectively) and the T cell growth factor IL-2 (20 ng/ml). In agreement with previous reports $15dPGJ_2$, but not troglitazone, was also found to inhibit PMA/Ionomycin stimulated T cell proliferation (IC_{50} 100 nM) (Yang *et al* 2000). Data obtained using 15dPGJ2 has to be interpreted with increasing caution, as this is now known to interact and

modulate other PPARγ-independent pathways, including the NFκB pathway (Straus *et al* 2000). Indeed, a physiological specific and potent ligand of PPARγ has yet to be identified. The results of recent experiments suggest that $15dPGJ_2$ may elicit anti-inflammatory actions and even promote apoptosis of eosinophils via PPARγ-independent mechanisms (Ward *et al* 2002) but the effect of addition of $15dPGJ_2$ treatment on T cells was not reported. Other studies have shown $15dPGJ_2$ to physically interact with the transcription factor NF-AT and block activity of the IL-2 promoter (Yang *et al* 2000) and chemokine genes (Zhang *et al* 2001), in some cases inducing T cell apoptosis (Harris *et al* 2002).

The PPARγ pathway has been shown recently to impinge on inositol lipid metabolism in macrophages, primarily through its ability to upregulate expression of PTEN. This results in an inhibition of cell growth in macrophages mediated by the degradation of PI(3,4,5)P_3 and abrogation of PI 3-K signalling (Patel *et al* 2001). Interestingly, in the same study it was reported that the 5'-phosphatase SHIP-2 was not upregulated, and was therefore unlikely to contribute to the observed inhibition of proliferation. It would be of interest to determine if PPARγ ligands can upregulate SHIP (as opposed to SHIP-2) in haematopoietic cells, including T cells, and contribute to D3-phosphoinositide metabolism in a manner to that observed with PTEN. The same studie used the PPARγ-selective ligand rosglitazone that is structurally related to troglitazone (Patel *et al* 2001). It is not known whether $15dPGJ_2$ and other PPARγ -specific agonists (including troglitazone) can upregulate PTEN via a similar mechanism in T cells. Recent work has also identified a role for troglitazone and PPARα ligands in disrupting PI 3-K dependent endothelial cell migration by targeting and inhibiting the phosphorylation of PKB (Goetze *et al* 2002). It would be of considerable interest to know if PPARγ ligands could disrupt T cell chemotaxis via similar PI 3-K-dependent mechanisms.

The synthetic thiazolidinedione (TZD) compounds troglitazone and ciglitazone were also tested for inhibitory effects on T cell proliferation. Ciglitazone had no detectable effect on ^{3}H-thymidine incorporation into cultures of primary T cell or

T lymphoblasts, a result consistent with previous studies (Yang *et al* 2000). There is evidence, however, that ciglitazone, as well as $15dPGJ_2$, can inhibit experimental allergic encephalomyelitis, an experimental model of multiple sclerosis, by blocking IL-12 production and Th1 cell differentiation (Natarajan *et al* 2002). Collectively these data suggest that ciglitazone is potentially inactive in naïve, resting primary T cells but may have an inhibitory effect in differentiated (Th1) T cells.

Troglitazone did inhibit CD3/CD28, IL-2 induced T cell proliferation albeit at higher concentrations than $15dPGJ_2$ (IC_{50} approx. 15 μM), but interestingly had no effect on T cells stimulated with the non-physiological ligands PMA/Ionomycin. In contrast Yang *et al* observed an inhibitory effect of troglitazone on PHA/PMA induced proliferation, also a non-physiological stimulus (Yang *et al* 2000). Reasons for this conflicting evidence are not clear, but it may be that the use of Ionomycin as a second stimulus renders the T cells troglitazone-insensitive. Previous studies have shown a slight potentiation of T cell proliferation when using troglitazone at nanomolar concentrations (Yang *et al* 2000). A similar effect of using nano-molar concentrations of troglitazone was also seen in this investigation, but the magnitude of decrease was small and not statistically significant (figures 62, 64 and 66). Add-back experiments, where troglitazone (10 μM) and 15dPGJ2 (10 μM) were added back to actively proliferating T-lymphoblasts 24 hours post-CD3/CD28 stimulation revealed these PPARG ligands to be equi-potent with regards to anti-proliferative actions. Although this is preliminary data, and must therefore be interpreted with caution, this observation suggests that certain PPARγ ligands can override established mitogenic, proliferative cell signals and arrest cell growth or maybe induce toxic or apoptotic events. Further experiments need to be performed to eliminate the possibility if PPARγ agonists are indeed cytotoxic and not pro-apoptotic. These could include performing cell-based apoptotic assays including annexin V staining of PPARγ-treated T cells. It is worthy of note, however, that 15d-PGJ2, despite inducing apoptosis in transformed malignant T cells, has been shown recently to pre-dispose normal human T cells to apoptosis (Harris *et al* 2002).

A schematic model of anti-inhibitory action of PPARγ ligands on stimulated primary T cell/lymphoblasts derived from data generated in this study and other

published data (Yang *et al* 2000 and Patel *et al* 2001) is summarised in figure 70.

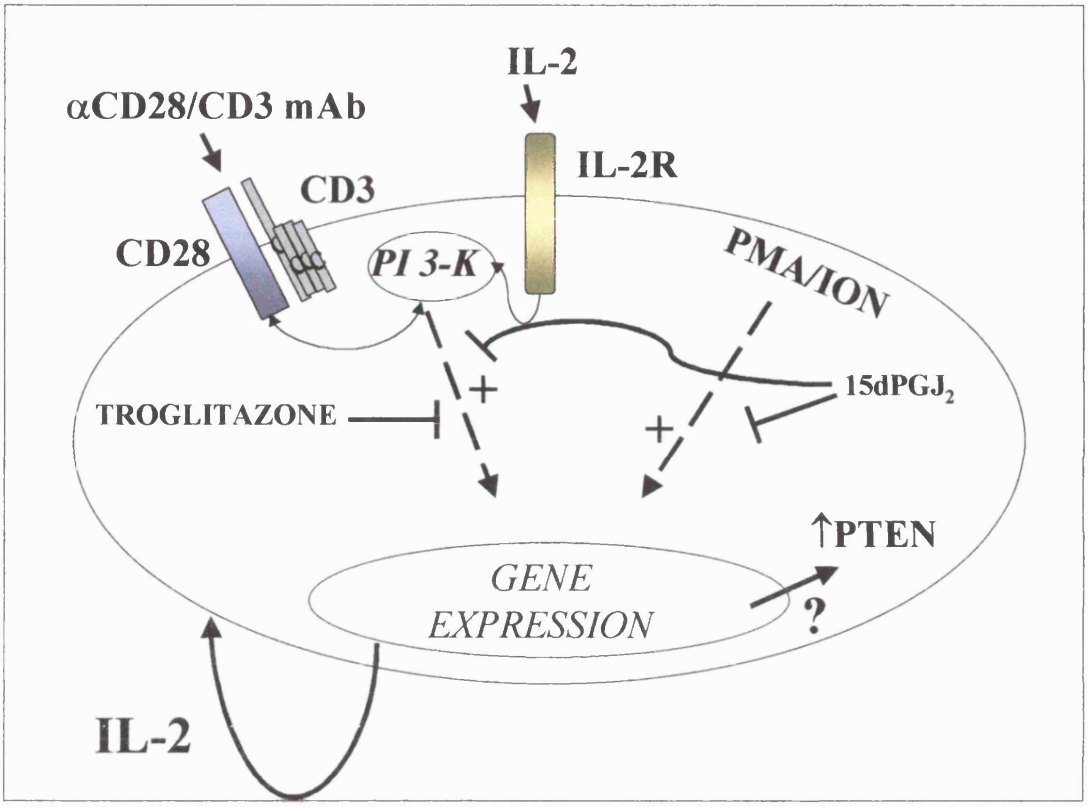

Figure 70: Potential role for the PPARγ ligands, troglitazone and $15dPGJ_2$ in inhibiting proliferation of T lymphocytes. In a physiological setting, stimulation of T cells via CD3/CD28 and IL-2 results in the activation of mitogenic intracellular signalling cascades, including the activation of PI 3-K. These signals regulate expression of genes, including the IL-2 gene that can drive clonal expansion of T cells. Troglitazone and $15dPGJ_2$ used at low micromolar levels can inhibit T cell proliferation following stimulation with IL-2 or with anti-CD3/CD28 mAb. In addition $15dPGJ_2$, but not troglitazone, is able to inhibit T cell proliferation following stimulation with the non-physiological ligands PMA/Ionomycin. The exact mechanisms of PPARγ ligand-mediated inhibition are still unclear. Some studies have showed that troglitazone is able to inhibit secretion/expression of IL-2 (Yang et al 2000), whereas others have described data showing upregulation of PTEN gene in monocytes that can antagonise PI 3-K signalling (Patel *et al 2001).*

The effect of troglitazone on proliferation (10 μM), was assessed in the leukemic cell lines Jurkat, CEM, MOLT-4 and HUT 78. Interestingly, troglitazone had no

effect on leukemic T cell proliferation suggesting that unstimulated leukemic cells are insensitive to the inhibitory actions of troglitazone, at least at 10 μM. It would have been of interest if troglitazone was able to inhibit proliferation in CD3/CD28-stimulated leukemic cells but due to time constraints ,this was unfortunately not determined. Analysis of the data revealed that leukemic T cells had different growth rates, with Jurkats showing greatest [3H]-thymidine incorporation compared to the other T cell lines. Of added importance was the fact that troglitazone was shown to be non-toxic to the leukemic T cells, at least when observed on the basis of their ability to exclude trypan blue. However, it cannot be ruled out that higher concentrations of troglitazone of above 10 μM may inhibit leukemic cell proliferation.

Unfortunately, time did not allow for the effect of the more potent $15dPGJ_2$ on leukemic T cell proliferation to be investigated. In a recent report, however, it was shown that $15dPGJ_2$ could inhibit proliferation and indeed induce apoptosis in the leukemic cell line Jurkat (Harris *et al* 2002), highlighting a potential therapeutic role for PPARγ ligands in T cell leukaemia. However these inhibitory events of $15dPGJ_2$ may be occurring through PPARγ-dependent as well as PPARγ-independent pathways. This study did not address the issue of apoptotic effects of the PPARγ ligands troglitazone and $15dPGJ_2$ on primary T cells and T-lymphoblasts and would have been of interest to know if treatment of PPARγ agonists, especially at higher doses, was responsible for the inhibition of proliferation observed.

Summary

Expression profiles, at both mRNA and protein level, of the key inositol phosphatases SHIP and PTEN in a variety of commonly used leukemic T cell lines are now better understood. The data presented in this study also provide direct evidence that SHIP contributes to PI(3,4,5)P_3 metabolism in T lymphocytes following CD28 stimulation, producing the metabolite PI(3,4)P_2. Jurkat cells, which expressed neither SHIP nor PTEN, exhibited high basal levels of PI(3,4,5)P_3, which were increased upon CD28 ligation, and comparatively low levels of PI(3,4)P_2, as reflected by a high PI(3,4,5)P_3 : PI(3,4)P_2 ratio. Basal phospho-PKB levels in Jurkat cells appeared to be maximal and did not increase further upon cell stimulation. MOLT-4 and CEM cells expressed SHIP but not PTEN and had moderate basal levels of both PI(3,4,5)P_3 and PI(3,4)P_2, which both increased significantly upon CD28 ligation. The PI(3,4,5)P_3 : PI(3,4)P_2 ratio was much lower in these cell lines compared to Jurkat reflecting higher relative levels of PI(3,4)P_2. HUT 78 cells expressed both SHIP and PTEN and had much lower levels of D-3 phosphoinositides which did not increase significantly upon CD28 ligation, perhaps due to either poor cell surface expression of CD28/CD3 or their rapid metabolism by PTEN and/or SHIP. T-lymphoblasts, which express both phosphatases, also had detectable levels of PI(3,4,5)P_3 which increased upon CD28 ligation but in a more regulated manner. PI(3,4)P_2 basal levels were low and did not significantly increase upon cellular stimulation. Accordingly, phospho-PKB levels were comparatively low in both HUT 78 cells and T-lymphoblasts.

SHIP was shown to be rapidly tyrosine phosphorylated by a multitude of T cell surface receptors including, CD28 (upon anti-CD28 mAb and natural CHO-B7.1/2$^+$ ligands), CD3, CD2 and IL-2. SHIP may also be able to mediate protein-protein interaction with the adapter proteins, p62^{dok} and the newly identified GRID. Also, SHIP was found to immunoprecipitate with *in vitro* kinase activity. The identity of the co-associating kinase(s) is unknown but was shown to inducibly associate with SHIP following CD28 stimulation, leading to the

phosphorylation of a number of uncharacterised proteins of different molecular weights.

Preliminary evidence was generated that CD28 may be able to signal to PTEN through *in vitro* kinase data. PTEN, like SHIP, was shown to inducibly associate with kinase activity following CD28 ligation, revealing several 'hot' co-associating proteins of different molecular weight. The identity of these co-associating proteins and kinase(s) remains to be discovered and may provide clues about the regulation of PTEN activity in T cells.

The effect of PPARγ ligands upon primary T cell proliferation, stimulated with anti-CD3/CD28, IL-2 or PMA/Ionomycin were also assessed in this study. Both troglitazone and $15dPGJ_2$ were shown to have inhibitory properties towards T cell proliferation with $15dPGJ_2$ being the more potent. The precise mechanism(s) of this inhibition were not evaluated. Ciglitazone, which is structurally related to troglitazone, was found to be ineffective in inhibiting T cell proliferation, which is in agreement with the published literature. In addition, troglitazone was shown to have no detectable effect on proliferation of leukemic T cell lines, the effect of 15dPGJ2 was unfortunately not determined. This data, viewed in the context of the published literature, suggests a potential therapeutic role for some PPARγ ligands in the treatment of certain T cell mediated diseases e.g. autoimmune diseases.

Future Work

Jurkat cells lack expression of both SHIP and PTEN and show signs of constitutively active PI 3-K signalling. It would be of interest to investigate what the effects, alone or in combination, would be of reintroduction of either SHIP and PTEN, perhaps using a Tet-regulated promoter to induce phosphatase expression, on D-3 phosphoinositide levels and downstream PI 3-K signalling cascades. The expression of PTEN and SHIP in Jurkats should, in theory, deplete phospho-PKB levels and may render the cell sensitive to apoptosis. Similar experiments could also be conducted in MOLT-4 and CEM cells i.e. reintroduction of PTEN. The observation that MOLT-4 and CEM cells exhibit high basal levels of the PI(3,4,5)P_3 metabolite, PI(3,4)P_2 means that closer analysis of PI(3,4)P_2 –dependent signalling cascades should be studied in these cell lines. PH-domains of TAPP, a specific PI(3,4)P_2 adapter, coupled to green-fluorescent protein (GFP) could allow us to observe the cellular translocation of this PH domain in various leukemic cells (i.e. Jurkat versus CEM) via confocal microscopy following stimulation of T cell surface receptors.

The exact mechanism of CD28 targeting SHIP and the nature of the protein-protein interactions between SHIP and co-associating proteins remains unclear. One approach to clarify this quandary would be to construct GST-fusion proteins of specific domains of SHIP i.e. SH2 domain of SHIP, and perform immunoprecipitation studies in CD28-stimulated T cell lysates. This would help decipher the molecular nature of such protein-protein interactions. In addition, it would be worth investigating PTENs inducible recruitment into a multimeric complex following CD28 ligation further. The other proteins observed associating with PTEN are likely to regulate PTEN activity/function and it would be of great interest to determine their identity of the co-associating proteins and that of the kinase(s) responsible for the *in vitro* phosphorylations.

The mechanisms of PPARγ anti-proliferative effects on primary T cells need to evaluated. Interestingly, recent literature has linked PPARγ with regulation of PI 3-K signalling through upregulation of PTEN in monocytes (Patel *et al* 2001). It

would be worth investigating if similar PTEN upregulation occurs in T cells following treatment with the PPARγ ligands troglitazone and 15dPGJ$_2$. Such an approach could also assess if SHIP is upregulated via similar mechanisms and what the potential biological consequence of such upregulation would be. In preliminary experiments, troglitazone (10 μM) was snot to have any anti-inhibitory effect on leukemic T cell lines. These studies need to be reproduced and extended to include the more potent, naturally occurring PPARγ ligand 15dPGJ$_2$, using both proliferative and apoptosis as the experimental end points.

Appendix 1

Materials and consumables

MATERIAL	SOURCE
Conical centrifuge tube (15ml)	Becton and Dickinson, USA
Conical centrifuge tube (50ml)	Becton and Dickinson, USA
Cryovials	NUNC, UK
Dialysis tubing	NUNC, UK
30ml Pipettes	NUNC, UK
10ml Pipettes	NUNC, UK
Eppendorf Centrifuge tubes (1.5ml)	NUNC, UK
3mm Filter paper	Whatmann, UK
Flasks 25cm2	NUNC, UK
Flasks 80cm2	NUNC, UK
Flasks 175cm2	NUNC, UK
Gel loading tips	Jinkins, USA
Gilson tips (all sizes)	Gilson, UK
HPLC column (SAX partishere)	Whatmann, UK
Immunosorbent 96-well plates	NUNC, UK
MACS CS column	Miltenyl Biotech, UK
Needles 19-gauge 'butterfly'	Terumo, Belgium
Nitrocellulose	BDH, Poole, UK
Pastettes (1ml/ 3ml)	NUNC, UK
PCR tubes (thin walled)	Promega, WI, USA
Petri dishes	NUNC, UK
Plastic tubes 7ml/30	Sterilin, UK
Plastic pots (60M/150M)	Sterilin, UK
Starstad screw-lid centrifuge tubes	Starstad, Germany
Stopcocks	BDH, Poole, UK
Syringes (all sizes)	NUNC, UK
Tissue culture 96-well plates	NUNC, UK
TLC Plates	Whatmann, Maidstone, Kent
TOP Seal™	Canberra Packard, UK

Unifilter™ GF/C™ 96 well filter plates	Canberra Packard, UK
Xomat film	Kodak, Harrow, UK

Media and Reagents

REAGENT	SOURCE
Acetone	Fisher scientific, UK
Acrylamide	Biorad
Agarose	Sigma, Poole, UK
Ammonium Phosphate $(NH_4)^2HPO_4$	Sigma, Poole, UK
Ammonium persulphate (APS)	Sigma, Poole, UK
Hapten-antibody cocktail	Miltenyl Biotech , UK
Anti-hapten microbeads	Miltenyl Biotech , UK
Aprotinin	Sigma, Poole, UK
ATP	Sigma, Poole, UK
Bovine serum albumin (BSA)	Sigma, Poole, UK
Bovine Foetal Calf Serum (FCS) (heat inactivated)	Gibco BRL, Paisley, UK
Bromophenol blue	Sigma, Poole, UK
β-glycerol phosphate	Sigma, Poole, UK
Chloroform	Fisons, Loughborough, UK
Ciglitazone	Alexis, Cambridge, UK
Coomoasie blue	Sigma, Poole, UK
Deoxynucloside triphosphates:dATP, dCTP, dGTP and dTTP	Boehringer Mannheim, Germany
DMEM (with L-glutamine)	Gibco BRL, Paisley, UK
DMEM (without L-glutamine)	Gibco BRL, Paisley, UK
DMEM (phosphate free)	Gibco BRL, Paisley, UK
Dimethyl sulphoxide (DMSO)	Sigma, Poole, UK
ECL	Amersham, UK
EDTA	Sigma, Poole, UK
Ethanol	Fisher Scientific, UK
Ethidium bromide	Sigma, Poole, UK

Ethyl Formate	Fisher Scientific, UK
Flo-scint IV liquid scintillant	Canberra Packard, UK
Folsh lipids	Sigma, Poole, UK
Fungizone	Gibco, BRL, UK
Glacial Acetic Acid	Fisher Scientific, UK
Gluteraldehyde	Sigma, Poole, UK
Glycerol	Sigma, Poole, UK
Glycine	Sigma, Poole, UK
HCl	BDH, Poole, UK
Heparin	Fisons, Loughborough, UK
HEPES	Sigma, Poole, UK
HPLC column (SAX partishere)	Whatmann, UK
Interlukin-2 (human recombinant)	Sigma, Poole, UK
Iodine	Sigma, Poole, UK
Iodoacetamide	Sigma, Poole, UK
Lauryl Sulphate (SDS)	Sigma, Poole, UK
Leupeptin	Sigma, Poole, UK
Lithium chloride	Sigma, Poole, UK
Lymphoprep™ (density 1.077)	Nycomed, Birmingham, UK
Magnesium Chloride	Anachem, Luton, UK
Manganese Chloride	BDH, Poole, UK
Marvel	Local stores
Methanol	Fisher Scientific, UK
Methylamine (25% w/v)	Fisher Scientific, UK
Microscint-OTM scintillant	Canberra Packard, UK
Molecular Weight Markers	Sigma, Poole, UK
M-450 dynabeads couple to CD28/CD3	C. June, Naval research institute, Bethedsa, USA
NaCl	Sigma, Poole, UK

NaF	Sigma, Poole, UK
Nitrocellulose	Invitrogen, UK
NP-40	Fisher Scientific, UK
Paraformaldehyde	Sigma, Poole, UK
Penicillin/Streptomycin	Gibco, BRL, UK
Petroleum ether (Bp 40-60°C)	BDH, Poole, UK
15d-PGJ_2	Cayman Chemicals, USA
Phenyl Methyl Sullenly Fluoride	Sigma, Poole, UK
PBS (without Ca^{2+} and Mg^{2+})	Gibco, BRL, UK
Phosphatidyl inositol	Sigma, Poole, UK
Phosphatidyl serine	Sigma, Poole, UK
Phosphoric acid	Fisher Scientific, UK
PMA	Calbiochem, Nottingham, UK
Potassium Oxalate	Sigma, Poole, UK
Propan-1-ol	Fisher Scientific, UK
Propan-2-ol	Fisher Scientific, UK
Propidium Iodide	Sigma, Poole, UK
Ponceau solution	Sigma, Poole, UK
Potassium acetate	Sigma, Poole, UK
Protein-A Sepharose	Pharamcia, UK
Protein-G Sepharose	Sigma, Poole, UK
RNAzol	Amos Biotechnology, Oxon, UK
RPMI-1640	Gibco, BRL, UK
SEB (superantigen)	Sigma, Poole, UK
Sodium Azide	Sigma, Poole, UK
Sodium orthovanadate	Sigma, Poole, UK
Small trypsin inhibitors	Sigma, Poole, UK
Sucrose	Fisher, UK
Tetra butyl ammoniumhydrogen	Sigma, Poole, UK

sulphate (TBAS)	
TEMED	Sigma, Poole, UK
Tris HCl	Sigma, Poole, UK
Triton X-100	Fisher, UK
Troglitazone	Alexis, Cambridge, UK
Trypsin/EDTA	Gibco, BRL, UK
Trypan Blue	Sigma, Poole, UK
Tween-20	Sigma, Poole, UK

Radiochemicals

Radiochemical	Source
[^{32}-P]-orthophosphoric acid (5 mCi/ml)	NEN, Stevenage, UK
[^{32}-P]γ ATP (5 μCi/ml)	NEN, Stevenage, UK
[3-H]-Thymidine (1 mCi/ml)	NEN, Stevenage, UK
[3H]-inositol[1,3,4,5]-tetrakisphosphate 0.5 μCi/ml	NEN, Stevenage, UK

Antibodies

ANTIBODY	SOURCE	WORKING DILUTION
Anti-CD28 (9.3)	Mouse/C. June, Naval Medical institue, Bethedsa, USA	Used at 10 μg/ml
Anti-murine CD3 (2C11)	Mouse/D. Olive, INSERM, Marseille	Used at 10 μg/ml
Anti-CD3 (UCHT-1)	Mouse/D. Cantrell, ICRF, UK	Used at 10 μg/ml
Anti-CD2	Mouse/ M. Glennie Southampton, UK	Used at 10 μg/ml
Anti-IgG_{2a}	Mouse/ Sigma, Poole, UK	Used at 10 μg/ml
Anti-mouse/rabbit-hrp	Dako, Denmark	Used at 1:1000 as appropriate
Anti-mouse/rabbit-FITC	Sigma, Poole, UK	Used at 1:1000-5000 as appropriate
Anti-SHIP (Monoclonal)	Mouse/Santa Cruz	1:2000 TBS/1% BSA

Anti-SHIP (Polyclonal)	Rabbit/ Kind gift from Mark Coggeshall	1:1000 TBS/1% Milk
Anti-SHP-2	Mouse/Santa Cruz	1:2000 TBS/1% BSA
Anti-PTEN	Mouse/Santa Cruz	1:2000 TBS/1% BSA
4G10 (ANTI-Y-P)	Mouse/Upstate, NJ, USA	1:10000 TBS/1%BSA
Anti-p62^{dok}	Mouse/Santa Cruz	1:2000 TBS/1% BSA
Anti-P-PKB	Rabbit/NEB, New England, USA	1:1000 TBS/ 1% BSA
Anti-P-GSK3	Rabbit/NEB, New England, USA	1:1000 TBS/ 1% BSA
Anti-PAN-PKB	Mouse/NEB, New England, USA	1:5000 TBS/ 1% BSA
Anti-PAN-GSK3	Mouse/NEB, New England, USA	1:5000 TBS/ 1% BSA
Anti-PPAR gamma	Rabbit/ Santa Cruz	1:1000/TBS 5% Milk
Anti-GRID	Rabbit/ J. Ellis GlaxoSmithkline, UK	1:1000/TBS 3% Milk
Anti-p85 (U5)	Mouse/ D. Cantrell ICRF	1:10000 TBS/ 1% BSA

Appendix 2: Buffer/solution recipes

Lysis buffer: 0.5% v/v NP-40, 65mM NaCl, 10 mM Tris pH 7.5, 1% β-glycerol phosphate, 5 mM NaF, 5 mM iodoacetamide, 1mM phenylmethyl-sulfonylflouride, 1 μg/ml leupeptin, 1 μg/ml pepstatin, 1 μg/ml small trypsin inhibitors, 1 μg/ml Na orthovanadate

Running buffer: 192 mM glycine, 25 mM Tris, 0.1% SDS

Semi-dry transfer buffer: 39 mM glycine, 48 mM Tris, 0.037% SDS

Stripping buffer: 200 mM Tris pH 6.8 with 60 μM β-2 Mercaptoethanol

***In Vitro* protein kinase assay buffer:** 100 mM NaCl, 25 mM HEPES pH 7.4, 10 mM $MgCl_2$, 5 mM $MnCl_2$, 100 μM sodium orthovanadate

***In Vitro* phosphatase assay buffer:** 10 mM TE pH 7.5, 10 mM $MgCl_2$

1X TBE: 10 mM Tris, 10 mM Boric acid, 2 mM EDTA, pH 8

Appendix 3

PTEN/SHIP primers

PRIMER	SEQUENCE	ACCESSION NUMBER
SHIP FORWARD (5'-3')	TGAACATTCTCCGGTTCCTG	XM 096169
SHIP REVERSE (5'-3')	TAAGACTGACACACCACGTG	As above
PTEN FORWARD (5'-3')	GTACTTTGAGTTCCCTCAGC	AF143312
PTEN REVERSE (5'-3')	GGAGAAAAGTATCCGTTGGC	As above

Appendix 4

Critical values for Spearman's rank correlation coefficient

n	***p* = 0.05**	***p* = 0.01**
5	1.000	
6	0.886	1.000
7	0.786	0.929
8	0.738	0.881
9	0.700	0.833
10	0.648	0.794
11	0.618	0.754
12	0.587	0.727

References

Abrams J. R, Lebwohl M. G, Guzzo C. A, Jegasothy B. V, Goldfarb M. T, Goffe B. S, Menter A, Lowe N. J, Krueger G, Brown M. J, Weiner R. S, Birkhofer M. J, Warner G. L, Berry K. K, Linsey P. S, Krueger J. G, Ochs H. D, Kelly S. L and Kang S. (1999) CTLA-4Ig-mediated blockade of T cell costimulation in patients with psoriasis vulgaris. *J. Clin. Invest.* **103,** 1243-1252.

Alberolla-Ila J, Forbush K. A, Seger R, Krebs E. G and Perlmutter R. M. (1995) Selective requirement for MAP kinase activation in thymocyte differentiation. *Nature* **373,** 620-623.

Alessi, D. R., James, S. R., Downes, C. P., Holmes, A. B., Gaffney, P. R., Reese, C. B. and Cohen, P. (1997) Characterisation of a 3'-phosphoinositide-dependent protein kinase which phosphorylates and activates protein kinase B α. *Curr. Biol.* **7,** 261-269.

Alessi D. R, Kozlowski M. T, Wing Q, Morrice N and Avruch J. (1997) Phosphoinositide-dependent protein kinase 1 (PDK1) phosphorylates and activates the p70 S6 kinase *in vivo* and *in vitro. Curr Biol* **8,** 69-81.

Algere M. L, Noel P. J, Eisfelder B. J, Chaung E, Clark M. R, Reiner S. L and Thompson C. B (1996) regulation of surface and intracellular expression of CTLA-4 on mouse T cells. *J. Immunol.* **157,** 4672-4670.

Astoul E, Edmunds C, Cantrell D. A and Ward S. G. (2001) PI 3-K and T-cell activation: limitations of T-leukemic cell lines as signalling models. *Trends Immunol* **22,** 490-496.

Aman J. M, Walk S. F, March M. E, Su H, Carver J and Ravichandran K. S. (2000) Essential role for the C-terminal non-catalytic region of SHIP in FcγRIIB1-mediated inhibitory signalling. *Mol. Cell. Biol.* **20,** 3576-3589.

Balendran A, Casamayor A and Deak M. (1999) PDK-1 aquires PDK2 activity in the presence of a synthetic peptide derived from the carboxyl terminus of Prk2. *Curr. Biol.* **9,** 393-404.

Bi, L, Okabe I, Bernard D. J, Wynshaw-Boris and Nussbaum R. L. (1999) Proliferative defect and embryonic lethality in mice homozygous for a deletion in the p110α subunit of phosphoinositide 3-kinase. *J. Biol. Chem.* **274,** 10963-10968.

Bollland S, Pearse R. N, Kurosaki T, and Ravetch J. V. (1998) SHIP modulates immune receptor response by regulating membrane association of Btk. *Immunity* **8,** 509-516.

Bruyns E, Marie-Cardine A, Kirchgessner H, Sagolla K, Schevchenko A, Mann M, Autschbach F, Bensussan A, Meuer S and Schraven B. (1998) T cell receptor (TCR) interacting molecule (TRIM), a novel disulphide linked dimer associated with the TCR-CD3-ζ complex, recruits intracellular signalling proteins to the plasma membrane. *J. Exp. Med.* **188,** 561-575.

Brunet, A., Bonni, A., Zigmond, M. J., Lin, M. Z., Juo, P., Hu, L. S., Anderson, M.J., Arden, K. C., Blenis, J. and Greenberg, M. E. (1999) Akt promotes cell survival by phosphorylating and inhibiting a forkhead transcription factor, *Cell* **96,** 857-868.

Brunner M. C, Chambers C. A Chan F. K, Hanke J, Winto A and Allison J. P. (1999) CTLA-4 –mediated inhibition of early events of T cell proliferation. J. Immunol. **151,** 3489-3499.

Cantley L. C, Neel B. G. (1999) New insights into tumor suppression: PTEN suppresses tumor formation by restraining the phosphoinositide 3-kinase/AKT pathway. *Proc. Natl. Acad. Sci. U S A.* **13,** 4240-5.

Cantrell DA, and Smith, KA. (1984) The Interlukin 2 T cell system: a new cell growth model. *Science* **224,** 1312-1315.

Carver D. J, Aman M. J, and Ravichandran K. S. (2000) SHIP inhibits Akt localisation in B cells through regulation of Akt membrane localisation. *Blood* **96,** 1449-1456.

Chan C. A, Irving B. A, Fraser J. D and Weiss A. (1991) The zeta chain is associated with a tyrosine kinase and upon T cell antigen receptor stimulation associates with ZAP-70, a 70 kDa tyrosine phosphoprotein. *Proc. Natl. Acad. Sci.* **20,** 9166-9170.

Chantry D, Vojtek A, Kashishian A, Holtzman D. A, Wood C, Gray P. W, Cooper J. A and Hoekstra M. F. (1997) p110δ, a novel phosphatidylinositol 3-kinase catalytic

subunit that associates with p85 and is expressed predominately in leukocytes. *J. Biol. Chem.* **272,** 19236-19246.

Chaung E, Fisher T. S, Morgan R. W Robbins M. D, Duerr J. M, Vander M. G, Gardner J. P, Hambor J. E, Neveu M. J and Thompson C. B (2000) The CD28 and CTLA-4 receptors associate with the serine threonine phosphatase PP2A. *Immunity* **13,** 313-322.

Chiang, Y. P, Kole H. K, Brown K, Naramura, M, Fuuhara S, Hu, R, Kyung I, Gutking S, Shevach E and Gu H. (2000) Cbl-b regulates the CD28 dependence of T-cell activation. *Nature* **403,** 216-220.

Chung S. W, Kang B. Y, Kim S. H, Kim Y. M, Cho D, Trinchieri G and Kim T. S. (2000) Oxidised low density lipoprotein Interlukin 12 production in lipopolysacharide-activated mouse macrophages via direct interaction between PPARγ and NFκB. *J. Biol. Chem.* **276,** 32681-32687.

Clement S, Krause U, Desmedt F, Tanti JF, Behrends J, Pesesse X, Sasaki T, Penninger J, Doherty M, Malaisse W,Dumont JE, Le Marchand-Brustel Y, Erneux C, Hue L, Schurmans S. (2001) The lipid phosphatase SHIP controls insulin sensitivity. *Nature* **4**, 92-97.

Condliffe A. J, Hawkins P. T (2000) Cell biology: Moving in mysterious ways. *Nature* **404,** 135-137.

Corvera S. (2001) Phosphatidylinositol 3-kinase and the control of endosome dynamics: New players defined by structural motifs. *Traffic* **2,** 859-866.

Cox D, Dale B. M, Kashiwada M, Helgason C. D and Greenberg S. (2001) A regulatory role for Src Homology 2 domain-containing inositol 5'-phosphatase (SHIP) in phagocytosis mediated by Fcγ receptors and complement receptor 3($\alpha_M\beta_2$; CD11b/CD18). *J. Exp. Med.* **193,** 61-71.

Craddock B and Welham M. J. (1997) Interlukin 3 induces the association of the protein tyrosine phosphatase SHP-2 and phosphatidylinositol 3-kinase with a 100 k Da tyrosine phosphorylated protein in haemopoetic cells. *J. Biol. Chem.* **272,** 29281-29289.

Croxford J. L, O'Neil J. K, Ali, R. R, Browne K, Byrnes A. P, Dallman M. J, Wood M. J, Feldman M, and Baker D. (1998) Local gene therapy with CTLA4-immunolglobulin fusion protein in experimental allergic encephalomyelitis. *Eur. J. Immunol.* **28,** 3904-3916.

Damen JE, Liu L, Rosten P, Humphries RK, Jefferson AB, Majerus PW, Krystal G. (1996) The 145-kDa protein induced to associate with Shc by multiple cytokines is an inositol tetraphosphate and phosphatidylinositol 3,4,5-triphosphate 5-phosphatase. *Proc Natl Acad Sci U S A.* **20,** 1689-93.

Damen JE, Liu L, Ware MD, Ermolaeva M, Majerus PW, Krystal G. (1998)
Multiple forms of the SH2-containing inositol phosphatase, SHIP, are generated by C-terminal truncation. *Blood.* **15,** 1199-205.

Damen JE, Ware MD, Kalensikoff J, Hughes M. R and Krystal G. (2001)
Ship's C-terminus is essential for its hydrolysis of PIP3 and inhibition of mast cell degranulation *Blood.* **97,**1343-1351.

Datta S. R, Dudek H, Tao X, Masters S, Fu H, Gotoh Y and Greenberg M. E. (1997) Akt phosphorylation of BAD coupled survival signals to the cell-intrinsic death machinery. *Cell* **91**, 231-241.

Debnah J, Chamorro M, Czar M. J, Schaeffer E. M, Leonardo M. J, Varmus H. E and Schwartzberg P. L. (1999) Rlk/Txk encodes two forms of a novel cysteine-string tyrosine kinase activated by src family kinases. *Mol. Cell. Biol.* **19,** 1498-1507.

Di Cristofano A, Kotsi P, Peng Y. F, Cordon-Cardo C, Elon K. B and Pandolfi P. P. (1999) Impaired fas response and autoimmunity in Pten+/- mice. *Science* **285**, 2122-2125.

Di Cristofano A, Pesce B, Cordon-Cardo C and Pandolfi P. P. (1998) Pten is essential for embryonic development and tumour suppression. *Nat. Genet.* **19,** 348-355.

Divecha M, Brooksbank C. E. L and Irvine R. F. (1992) Purification and characterisation of phosphatidylinositol phosphate 5-kinases. *Biochem. J.* **288,** 637-642.

Dong C, Juedes A. E, Temann U, Schresta S, Allison J. P, Ruddle N. H and Flavell R. A. (2001) ICOS co-stimulatory receptor is essential for T-cell activation and function. *Nature* **409,** 97-105.

Diehl J. A, Cheng M, Roussel M. F and Sherr C. J. (1998) Glycogen synthase kinase-3beta regulates cyclin D1 proteolysis and subcellular localization. *Genes Dev.* **12,** 3499-3511.

Dowler S, Currie R. A, Downes C. P and Alessi D. R. (1999) DAPP1; A dual adapter for phosphotyrosine and 3-phosphoinositides. *Biochem. J.* **342,** 7-12.

Dowler S, Currie R. A, Campbell D. G, Deak M, Kular G, Downes C. P and Alessi D. R. (2001) Identification of pleckstrin homology domain containing proteins with novel phosphoinositide binding specificities. *Biochem. J.* **351,** 19-31.

Dryer C, Keller H, Mahfoundi A, Laudet V, Krey G and Wahli W. (1993) Positive regulation of the peroxisomal β-oxidation pathway by fatty acids through activation of the peroxisome proliferator-activated receptor (PPAR). *Biol. Cell.***77**, 67-76.

Edmunds C, Parry R. V, Burgess S. J, Reaves B, and Ward S. G. (1999) CD28 stimulates tyrosine phosphorylation, cellular redistribution and catalytic activity of the inositol lipid 5-phosphatase SHIP. *Eur. J. Immunol.* **29,** 3507-3515.

Edmead C, Patel Y. I, Wilson A, Boulougouris G, Hall N. D, Ward S. G and Sansom D. M. (1996) Induction of AP-1 and NFκB by CD28 stimulation involves both PI 3-K and sphingomyelinase signals. *J. Immunol* **157,** 3290-3297.

Ellis J. H, Ashman C, Burden N, Kilpatrick K. E, Morse M. A and HamblinP. A. (2000) GRID: A novel Grb-2-related adapter protein that interacts with the activated T cell costimulatory receptor CD28. *J. Immunol* **164,** 5805-5814.

Flynn P, Wong M, Zavar M, Dean N. M and Stokoe D. (2000) Inhibition of PDK-1 activity causes a reduction in cell proliferation and survival. *Curr. Biol.* **10,** 1439-1442.

FoleybG.E (1965) Continuos culture of human lymphoblasts from peripheral blood of a child with acute leukaemia *Cancer* **18,** 522-529.

Franke T. F, Kaplan D. R, Cantley L. C and Toker A. (1997) Direct regulation of the Akt proto-oncogene by phosphatidylinositol 3,4-bisphosphate. *Science* **275,** 65-668.

Fruman, D. A., Snapper, S. B., Claudine, M., Davidson, L., Yu, J. Y., Frederick, W., Cantley, L. C. (1999) Impaired B cell development and proliferation in absence of phosphoinositide 3-kinase p85α. *Science* **283,** 393-399.

Germain R. N (2002) T-Cell development and the CD4-CD8 lineage decision. *Nature Immunol Reviews* **2,** 309-322.

Gootenberg J.E and Gazdar A.F (1981) Human cutaneous T cell lymphoma and leukemia cell lines produce and respond to T cell growth factor. *J. Exp. Med* **154,** 1403-1418.

Grakoui A, Bromley S. K, Sumen C, Davis M.M, Shaw A. S, Allen P. M and Dustin M. L. (1998). The immunological synapse; a molecular machine controlling T cell activation. *Science* **285,** 221-227.

Grossman S. L and Lessem J. (1997) Mechanisms and clinical effects thiazolidinediones. *Exp. Opin. Invest. Drugs.* **6,** 1025-1040.

Habib T, Hejna JA, Moses RE and Decker S. J. (1998) Growth factors and insulin stimulate tyrosine phosphorylation of the 51C/SHIP2 protein. *J Biol Chem. **273,*** 18605-9.

Harmer S. L and DeFranco A. L. (1999) The src homology domain 2-containing inositol phosphatase SHIP forms a ternary complex with Shc and Grb2 in antigen receptor-stimulated B lymphocytes. *J. Biol. Chem.* **274,** 12193-12191.

Harris S. G and Phipps R. P. (2001) The nuclear receptor PPARγ is expressed by mouse T lymphocytes and PPARγ agonists induce apoptosis. *Eur. J. Immunol.* **31,** 1098-1105.

Harris S. G and Phillips R. P. (2002) Prostaglandin D_2, its metabolite 15d-PGJ_2 and peroxisome proliferator receptor-γ agonists induce apoptosis in transformed, but not, normal, human T lineage cells. *Immunology* **105,** 23-24.

Helgason C. D, Damen J. E, Rosten R, Grewl R, Sorenson R, Chappel S. M, Borowski A Jirik F, Krysta G and Humphries R. K. (1998) Targeted disruption of SHIP leads to haemopoietic perturbations, lung pathology, and a shortened life span. *Genes Dev* **12,** 1610-1620.

Helgason C. D, Kalberer C. P, Damen J. E, Chappel S. M, Pineault N, Krystal G and Humphries R. K. (2000) A dual role for src homology 2 domain-containing inositol-5-phosphatase (SHIP) in immunity: Aberrant development and enhanced function of B lymphocytes in $SHIP^{-/-}$ mice. *J. Exp. Med.* **191,** 781-794.

Holdorf, A. D., Green, J. M., Levin, S. D., Denny, M. F., Straus, D. B., Link, V., Changelian, P. S., Allen, P. M and Shaw, A. S. (1999) Proline residues in CD28 and the Src Homolgy (SH3) domain of Lck are required for T cell costimulation. *J. Exp. Med.* **190,** 375-384.

Huber M, Helgason C. D, Damen J. E, Liu L, Humphries K, and Krystal G. (1998) The src homology 2-containing inositol phosphatase (SHIP) is the gatekeeper of mast cell degranulation. *Proc. Natl. Acad. Sci. USA* **95**, 11330-1135.

Hutloff A, Dittrich A. M, Beier K. C, Eljaschewitsch B, Kraft, R, Anagnostopoulos I and Kroczek R. A. (1999) ICOS is an inducible structurally and functionally related to CD28. *Nature* **397,** 263-266.

Ijpenberg A, Jeannin E, Wahili W and Desvergne B. (1997) Polarity and sequence specific requirements of PPAR:RXR heterodimer binding to DNA. *J. Biol. Chem.* **272,** 20108-20117.

Ishida Y, Agata Y, Shibahara T and Honjo T. (1992) Induced expression of PD-1, a novel member of the immunoglobulin gene superfamily, upon programmed cell death. *EMBO. J.* **11,** 3887-3895.

Issemann I and Green S. (1990) Activation of a member of the steroid hormone receptor superfamily by peroxisome proliferators. *Nature* **347,** 645-650.

Jackson S. P, Schoewaelder S. M, Matzaris M, Brown S and Mitchell C. A. (1995) *EMBO J* **14,** 4490-4500.

Jain J, Loh C and Roa A. (1995) Transcriptional regulation of the IL-2 gene. *Curr. Opin. Immunol.* **13,** 623-653.

Jefferson A. B and Majerus .P. W (1996) Sequence homology of 5-polyphosphate phosphatases *Biochemistry* **35,** 7890-7894.

Jiang, C, Ting, AT, and Seed, B. (1998) PPARγ agonists inhibit production of monocyte inflammatory cytokines *Nature* **391,** 82-86.

June C. H, Fletcher M. C, Ledbetter J. A and Samelson L. E. (1990). Increases in tyrosine phosphorylation are detectable before phospholipase C activation after T cell receptor stimulation. *J. Immunol.* **144,** 1591-1599.

June, C. H., Bluestone, J. A., Nadler, L. M and Thompson, C. B. (1994) The B7 and CD28 receptor families. *Immunol. Today* **15,** 321-331.

Kanai F, Liu H, Field S. J, Akbary H, Matsuo T, Brown G. E, Cantley L. C and Yaffe M. B. (2001) The PX domains of p47phox and p40phox bind to lipid products of PI(3)K. *Nature Cell Biol* **3,** 675-679.

Kane L. P,Shapiro V. S. S, Stokoe D and Weiss A. (1999) Induction of NFκB by the Akt/PKB kinase. *Curr. Biol.* **9,** 601-604.

Kane L. P, Andres P. G, Howland K. C, Abbas A. K and Weiss A. (2001) Akt provides the CD28 costimulatory signal for up-regulation of CD28 and IFNγ but not Th2 cytokines. *Nat. Immunol.* **2**, 37-44.

Kang H, Schneider H and Rudd C. E. (2002) Phosphatidylinositol 3-kinase p85 adapter function in T cells. *J. Biol. Chem.* **277,** 912-921.

Kersten S, Desvergne B and Wahli W. (2000) Roles of PPARs in health and disease *Nature* **405,** 421-428.

Kim J. S, Peng X, Pradip K, Geahlen R. L, and Durden D. L. (2002) PTEN controls immunoreceptor (immunoreceptor tyrosine based activation motif) signalling and the activation of Rac. *Blood* **99,** 694-697.

King. D, Sadra A, Teng J. M, Liu X. R, Han A, Selva-kumar A, August A and Dupont B. (1997) Analysis of CD28 cytoplasmic tail tyrosine residues as regulators and substrates for the protein tyrosine kinases EMT and Lck. *J. Immunol.* **158,** 580-590.

Klasen S, Pages F, Peyron J. F, Cantrell D. C and Olive D. (1998) two distinct regions of the CD28 intracytoplasmic tail mediate the tyrosine phosphorylation of Vav and GTPase activating protein associated p62 protein. *Intl Immunology* **10,** 481-489.

Kliewer , S. A, Lenhard J. M, Wilson T. M, Patel I, Morris D. C, and Lehman J. M. (1995) A prostaglandin J2 metabolite binds PPARγ and promotes adipocyte differentiation. *Cell* **83,** 803-812.

Kosugi A, Saitoh S, Noda S, Yasuda K, Hayshi F, Ogata M and Hamaoka T. (1999). Translocation of tyrosine-phosphorylated TCRζ chain to glycolipid-enriched membrane domains upon T cell activation. **11,** 1395-1401

Lamkin T. D, Walk S. F, Liu L, Damen J. E, Krystal G, and Ravichandran K. S. (1997) Shc interaction with Src homology 2 domain containing inositol phosphatase (SHIP) in vivo requires the Shc-phosphotyrosine binding domain and two specific phosphotyrosines on SHIP. *J. Biol. Chem.* **272**, 10386-10401.

Lee K-M, Chaung E, Griffin M, Khattri R, Hong D. K, Zhang W, Straus D, Samelson D. E, Thompson C. B and Bluestone J. A. (1998) Molecular basis of T cell inactivation by CTLA-4. *Science* **282,** 2263-2266.

Lee JO, Yang H, Georgescu MM, Di Cristofano A, Maehama T, Shi Y, Dixon JE, Pandolfi P, Pavletich NP. (1999) Crystal structure of the PTEN tumor suppressor: implications for its phosphoinositide phosphatase activity and membrane association. *Cell* **29,** 323-34.

LeGood J. A, Ziegler W. H, Parekh D. B, Alessi D. R, Cohen P and Parker P. J. (1998) Protein kinase C isotype controlled by phosphoinositide 3-kinase through the protein kinase PDK-1. *Science* **281,** 2042-2045.

Leferbvre Kroll T, Aiyer A, Kaufman DS, Oh W, Demetri G, Figg WD, Zhou XP, Eng C, Spiegelman BM and Kantoff t.(1998) Activation of PPARγ promotes the development of colon tumours in C57BL/6J-APC mice. *Nature Med* **4,** 1053-1057.

Lemmon, M. A., Ferguson, K. M and Schlessinger, J. (1996) PH domains: Diverse sequences with a common fold recruit signalling molecules to the cell surface. *Cell* **85,** 621-624.

Lenschow D.J, Zeng Y, Thistlehwaite J. R, Montag A, Brady W, Gibson M. G, Linsey P. S and Bluestone J. A. (1992) Long-term survival of xenogenic pancreatic islets grafts induced by CTLA-4Ig. *Science* **257,** 789-792.

Lin J, Weiss A, and Finco T. S. (1999) Localisation of LAT in glycolipid-enriched microdomains is required for T cell activation. *J Biol. Chem.* **274,** 28861-28864.

Linsay P. S, Greene J. L, Bradely W, Bajorth J, Ledbetter J. A and Peach R (1994) Human B7.1 (CD80) and B7.1 (CD86) bind with similar affinities but distinct kinetics to CD28 and CTLA-4 receptors. *Immunity* **1,** 793-801.

Liu L, Damen J. E, Cutler R. L and Krystal, G. (1994) Multiple cytokines stimulate the binding of a common 145-kilodalton protein to Shc at the Grb-2 recognition site of Shc. *Mol. Cell. Biol.* **14,** 6926-6935.

Liu, L., Damen, J. E., Ware, M., Hughes, M and Krystal, G. (1997) SHIP, a new player in cytokine-induced signalling. *Leukaemia* **11,** 181-184.

Liu L, Damen J. E, Hughes M. R, Babic I, Jirik F. R and Krystal G. (1997) The src homology 2 (SH2) domain of SH2-containing inositol phosphatase (SHIP) is essential for tyrosine phosphorylation of SHIP, its association with Shc and its induction of apoptosis. *J. Biol. Chem.* **272**, 8983-8988.

Liu L, Damen J. E, Ware M. D and Krystal G. (1997) Interlukin-3 induces the association of the inositol 5-phosphatase SHIP with SHP-2. *J. Biol. Chem.* **272,** 10998-11001.

Liu Q, Shalaby F, Jones J, Bouchard D, Dumont DJ. (1998) The SH2-containing inositol polyphosphate 5-phosphatase, ship, is expressed during hematopoiesis and spermatogenesis. *Blood.* **15,** 2753-9.

Liu Q, Sasaki T, Kozieradzki I, Wakeham A, Itie A, Dumont D. J and Penninger J. M. (1999) SHIP is a negative regulator of growth factor receptor-mediated PKB/Akt activation and myeloid cell survival. *Genes & Dev* **13,** 786-791.

Lu Y, Cuevas B, Gibson S, Khan H, LaPushin R, Imboden J and Mills G. B. (1998) Phosphatidylinositol 3-kinase is required for CD28 but not CD3 regulation of the Tec family tyrosine kinase EMT/ITK/TSK: Functional and physical interaction with Phosphatidylinositol 3-kinase. *J. Immunol* **161,** 5403-5412.

Lundgren R, Kristoffersson U, Heim S, Mandahl N and Mitelman F. (1988) Multiple structural chromosome rearrangements, including del(7q) and del(10q), in an adenocarcinoa of the prostate. *Cancer Genet, Cytogenet.* **35,** 103-108.

March M. E, Lucas D. M, Aman J, and Ravichandran S. (2000) p135 Src homology 2 domain-containing inositol 5'-phosphatase (SHIPβ) isoform can substitute for p145 SHIP in $F_c\gamma$RIIB1-mediated inhibitory signalling in B cells. *J. Biol. Chem.* **275,** 29960-29967.

Majerus P. W, Kisselva M. V and Norris F. A (1999) The role of inositol phosphatases in inositol signalling reactions. *J. Biol. Chem.* **274,** 1066910672.

Mcleod J. D, Walker. L.S Patel Y. I, Boulougouris G and Sansom D.M (1998) Activation of human T cells with superantigen (SEB) and CD28 confers resistance to apoptosis via CD95. *J. Immunol* **160,** 2072-2079.

Meier R, Alessi D. R, Cron P, Andejelkovic M and Hemmings B. A. (1997) Mitogenic activation, phosphorylation and nuclear translocation of protein kinase Bβ. *J. Biol. Chem.* **272,** 30491-30497.

Mikhalap S. V, Shlapatska L. M, Berdova A. G, Law C, Clark E. A and Sidroenko S. P. (1999) CDw150 associates with src homology 2-containing inositol phosphatase and modulates CD95-mediated apoptosis. *J. Immunol.* **162,** 5719-5727.

Minowada J. (1972) Rosette-forming human lymphoid cell lines. Establishment and evidence for origin of thymus-derived lymphocytes. *J. Natl. Cancer. Inst* **49,** 891-895.

Moniakis J, Funamoto S, Fukuzawa M, Meisenhelder J, Araki T, Abe T, Meili R, Hunter T, Williams J and Firtel R. A (2001) An SH2-domain-containing kinase negatively regulates the phosphatidylinositol-3 kinase pathway. *Gen & Dev* **15,** 687-698.

Monks C. R, Freiberg B. A, Kupfer H, Sciaky N and Kupfer A. (1998). Three-dimensional regulation of supramolecular activation clusters in t cells. *Nature* **395,** 82-86.

Montixi C, Langlet C, Bernard, A. M, Thimonier J, Dubois, C Wurbel M. A, Chauvin J. P, Pierres M and He H-T. (1998) Engagement of T cell receptor triggers its recruitment to low-density detergent-insoluble membrane domains. *EMBO J* **17,** 5334-5348.

Moore K. J Rosen E. D, Fitzgerald M. L, Randow F, Andersson L. P, Athshuler D, Milstone D. S, Mortensen R. D Speigelman D. M and Freeman M. W. (2001) The role of PPARγ in macrophage differentiation and cholesterol uptake. *Nature Med* **7,** 41-47.

Morgan S. J, Smith A. D and Parker P. J (1990) Purification and characterisation of bovine brain type 1 phosphatidylinositol kinase. *Eur. J. Biochem.* **267,** 627-636.

Mukherjee R, Jow L, Croston G. E and Paterniti J. R (1997) Identification, characterisation and tissue distribution of PPARγ2 versus PPARγ1 and activation with retoinoid X receptor agonists and antagonists. *J. Biol. Chem.* **272**, 8071-8076.

Muraille E, Bruhns P, Pesesse X, Daeron M, Erneux C. (2000) The SH2 domain containing inositol 5-phosphatase SHIP2 associates to the immunoreceptor tyrosine-based inhibition motif of Fc gammaRIIB in B cells under negative signalling. *Immunol Lett* **3,** 72-75.

Myers M. P, Stolarov C, Eng J, Li, S, Wang M. H, Wigler R, Parsons R, and Tonks N. K. (1997) P-TEN, the tumour suppressor from human chromosome 10q23, is a dual specificity phosphatase. *Proc. Natl. Acad. Sci. USA* **94,** 9052-9061.

Myers M. P, Pass, I, Batty H, Van der Kaay J. P, Stolarov B. A, Hemmings M. H, Wigler H, Downes C. P and Tonks N. K. (1998) The lipid phosphatase activity of PTEN is critical for its tumour suppressor function. *Proc. Natl. Acad. Sci. USA* **95,** 13513-13522.

Nolte R. T, Wisely B. G, Westin S, Cobb J. E, Lambert M. H, Kurokawa R, Rosenfeld M. G, Wilson T. M, Glass C. K and Milburn M. V. (1998) Ligand binding and co-activator assembly o the peroxisome proliferator-activated receptor-γ. *Nature* **395,** 137-143.

Nunès J. A, Collette Y, Truneh A, Olive D and Cantrell D. A. (1994) The role of p21 Ras in CD28 signal transduction: Triggering of CD28 with antibodies, but not the ligand B7 activates ras. *J. Exp. Med.* **180,** 1067-1076.

Nunès J. A, Alemseged T, Olive D and Cantrell D. A. (1996) Signal transduction by CD28 costimulatory receptor on T cells. B7.1 and B7.2 regulation of tyrosine kinase adapter molecules *J. Biol. Chem.* **271,** 1591-1598.

Ott VL, Tamir I, Niki M, Pandolfi PP, Cambier JC. (2002) Downstream of kinase, p62(dok), is a mediator of Fc gamma IIB inhibition of Fc epsilon RI signaling. *J Immunol.* **168,** 4430-9.

Pages, F, Ragueneua M, Rottapel R, Truneh A, Nunès J. A, Imbert J, and Olive D. (1994) Binding of PI 3-K to CD28 is required for T cell signalling. *Nature* **369,** 327-334.

Pages, F, Rageueneau, M, Klasen, S, Battifora, M, Couez, D, Sweet, R, Truneh, A, Ward, S. G, and Olive, D. (1996) Two distinct intra-cytoplasmic regions of the T cell adhesion molecule CD28 participate in PI 3-kinase association. *J. Biol. Chem.* **276,** 9403-9409.

Parry, R. V., Reif, K., Smith, G., Sansom, D. M. Hemmings, B. A and Ward, S. G. (1997) Ligation of the T cell co-stimulatory receptor CD28 activates the serine-threonine protein kinase protein kinase B. *Eur. J. Immunol.* **27,** 2495-2501.

Patel L, Pass I, Coxon P, Downes P. C, Smith S. A and Macphee C. H. (2001) Tumour suppressor and anti-inflammatory actions of PPARγ agonists are mediated via upregulation of PTEN. *Curr. Biol.* **11,** 764-768.

Pesesse X, Dewaste V, De Smedt F, Laffargue M, Giuriato S, Moreau C, Payrastre B and Erneux C. (2001) The Src homology 2 domain containing inositol 5-phosphatase SHIP2 is recruited to the epidermal growth factor (EGF) receptor and dephosphorylates phosphatidylinositol 3,4,5-trisphosphate in EGF-stimulated COS-7 cells. *J Biol Chem.* **276,** 28348-55.

Ramaswamy S, Nakamura N, Vazquez F, Batt D. B, Perera S, Roberts T. M and Sellers W. R. (1999) Regulation of G_1 progression by the *PTEN* tumour suppressor protein is linked of the phosphatidylinositol 3-kinase pathway. *Proc. Natl. Acad. USA* **96,** 2110-2115.

Rey-Ladino J. A, Huber M, Liu L, Damen J. E, Krystal G and Takei F. (1999) The SH2-containing inositol-5'-phosphatase enhances LFA-1-mediated cell adhesion and defines two signalling pathways for LFA-1 activation. *J. Immunol.* **162,** 5792-5799.

Rohrschneider LR, Fuller JF, Wolf I, Liu Y, Lucas DM. (2000) Structure, function, and biology of SHIP proteins. *Genes Dev.* **14,** 505-20.

Rogers W and Rose J. K. (1996) Exclusion of CD45 inhibits activity of $p56^{lck}$ associated with glycolipid-enriched membrane microdomains. *J Cell Biol.* **135,** 1515-1523.

Salojin K. V, Zhang J and Delovitch T. L. (1998) TCR and CD28 are couple via ZAP-70 to the activation of the Vav /Rac-1/PAK-1/p38 MAPK signalling pathway. *J. Immunol* **163,** 844-890.

Saraf E. (1998) Differentiation and reversal of malinant tumours in colon cancer through PPARγ. *Nature Med* **4,** 1046-1052.

Sarmay G, Koncz G, Pecht I, Gergely J. (1999) Cooperation between SHP-2, phosphatidyl inositol 3-kinase and phosphoinositol 5-phosphatase in the Fc gamma RIIb mediated B cell regulation. *Immunol Lett* **3**, 25-34.

Sattler M, Salgia R, Shirkhande G, Verma S, Choi J, Rohrschneider L. R and Griffin J. D. (1997) The phosphatidylinositol polyphosphate 5-phosphatase SHIP and the protein tyrosine phosphatase SHP-2 form a complex in haematopoietic cells which can be regulated by BCR/ABL and growth factors. *Oncogene* **15,** 2379-2384.

Scharenberg A. M, El-Hillal O, Fruman D. A, Beitz L. O, Li Z, Lin S, Gout I, Cantley L. C, Rawlings D. J and Kinet J. (1998) Phosphatidylinositol3,4,5-trisphosphate (PI(3,4,5)P3)/Tec kinase-dependent calcium signalling pathway: a target for SHIP-mediated inhibitory signals. *EMBO* **17,** 1961-1972.

Schmidt-Weber CB, Wohlfahrt JG, Akdis CA, Blaser K. (2002) The phosphatidylinositol phosphatase PTEN is under control of costimulation and regulates proliferation in human T cells. *Eur J Immunol* **32,**1196-204.

Schneider, H, Cai, Y. C, Prasad, K.V.S, Scholesen, S.E and Rudd, C. E. (1995) T cell antigen CD28 binds to the Grb-2/Sos complex, regulators of $p21^{ras}$. *Eur J. Immunol.* **25,** 1044-1050.

Schneider, H, Prasad, K.V.S, Scholesen, S.E and Rudd, C. E. (1995) CTLA-4 binding to lipid kinase phosphatidylinositol 3-kinase in T cells. *J. Exp. Med.* **181,** 351-355.

Schoa D, Rangwal S. M, Bailley S. T and (1998) Interdomain communication regulating ligand binding by PPARγ. *Nature* **396,** 377-380.

Servant G, Weiner O. D, Herzmark P, Balla T, Sedat J. W and Bourne H. R. (2000) Polarisation of chemoattractant receptor signalling during neutrophil chemotaxis. *Science* **287,** 1037-1040.

Shan X, Czar MJ, Bunnell SC, Liu P, Liu Y, Schwartzberg P. L, Wange R, L. (2000) Deficiency of PTEN in Jurkat T cells causes constitutive localisation of Itk to the plasma membrane and hyperresponsiveness to CD3 stimulation. *Mol. Cell. Biol.* **20,** 6945-6957.

Sharp LL, Schawz D. A, Bott CM, Marshall CJ, and Hedrick SM. (1997) The influence of the MAPK pathway on the T-cell lineage commitment. *Immunity* **7,** 609-618.

Simons K and Ikonen E. (1997). Functional rafts in cell membranes. *Nature* **387,** 659-572.

Simpson L and Parsons R (2001) PTEN: Life as a tumour suppressor. *Exp. Cell. Res.* **264,** 29-41.

Sotsios Y and Ward S.G (2000) Collection, separation and activation of human T lympocytes. *Methods in Molecular medicine* **56,** 205-215.

Sporn MB, Suh N, Mangelsdorf DJ. (2001) Prospects for prevention and treatment of cancer with selective PPARgamma modulators (SPARMs). *Trends Mol Med.* **7,** 395-400.

Su C. G, Wen X, Bailey S. T, Jiang W, Rangwala S. M, Keilbaugh S. A, Flanigan A, Murthy S, Lazar M. A and Wu G. D. (1999) A novel therapy for colitis utilising PPARγ ligands to inhibit the epithelial inflammatory response. *J. Clin. Invest.* **104,** 383-389.

Suzukhi A, Yamaguchi M. T, Ohetki T, Sasaki, T, Kaishio T, Kimura Y, Yoshida R, Wakeham A, Higuchi T, Fukumonto M, Tsubata T, Ohashi P. S, Nakano T and Mak T. W. (2001) T cell-specific loss of PTEN leads to defects in central and peripheral tolerance. *Immunity* **14,** 523-534.

Tafuri A, Shahinnian A, Bladt F, Yoshinga S. K, Jordana M, Wakeham A, Boucher L, Bouchard D, Chan V. S. F, Duncan G, Odermatt B, Ho A, Itie A, Horan T, Whoriskey J. S, Pawson T, Penninger J. M Ohashi P. S and Mak T. W. (2001) ICOS is essential for effective T-helper-cell responses. *Nature* **409,** 105-112.

Tamir I, Stolpa J. C, Helgason C. D, Nakamura K, Bruhns P, Daeron M and Cambier J. C. (2000) The RasGAP-binding protein p62dok is a mediator of inhibitory FcgammaRIIB signals in B cells. *Immunity* **12,** 347-358.

Tamura M, Gu J, Danen E. H. J, Takinov T, Miyamato S and Yamada K. M. (1999) PTEN interactions with focal adhesion kinase and suppression of the extracellular matrix dependent PI 3-K/Akt cell survival pathway. *J. Biol. Chem.* **274,** 20693-20703.

Tivol, E. A., Borroello, F., Schweitzer, N., Lynch, P., Bluestone, J. A. and Sharpe, A. H. (19915) Loss of CTLA-4 leads to massive lymphoproliferation and fatal multiorgan tissue destruction, revealing a critical negative regulatory role of CTAL-4. *Immunity* **3,** 541-548.

Tonotonoz P, Hu, E, and Spiegelman B. M. (1994) Stimulation of adipogenesis in fibroblasts by PPARγ2, a lipid activated transcription factor. *Cell* **79,** 1-20.

Torres J and Pulido R. (2001) The tumour suppressor PTEN is phosphorylated by the protein kinase CK2 at its C-terminus: Implications for PTEN stability to proteasome-mediated degradation. *J. Biol. Chem.* **276,** 993-998.

Turner H and Cantrell D. A. (1997) Distinct ras effector pathways are involved in FC epsilon regulation of the transcriptional activity of Elk-1 and NF-AT in mast cells. *J. Exp. Med.* **185,** 43-53.

Turner S.J, Domain J, Waterfield M. D. Ward S. J and Westwick J. (1998) The CC chemokine Monocyte attractant protein-1 activates both the class I p85/p110 phosphatidylinositol 3-kinase and the class II PI3K-C2α *J. Biol. Chem.* **273,** 25987-25995.

Truitt K. E, Nagel T, Suen L. F and Imboden J. B. (1996) Structural requirements for CD28 mediated Costimualtion of IL-2 production in Jurkat t cells. *J. Immunol.* **156,** 4539-4531.

Tu Z, Ninos J. M, Ma Z, Wang J, Lemos M. P, Desponts C, Ghansah T, Howson J. M and Kerr W. G. (2001) Embryonic and haematopoietic stem cells express a novel SH2-containing inositol 5'-phosphatase isoform that partners with the Grb2 adapter protein. *Blood* **98,** 2028-2038.

Vanhaesebroeck B, Leevers SJ, Panayatuo G and Waterfield M. D. (1997) Phosphoinositide 3-kinases: a conserved family of signal transducers. *Trends Biochem Sci* **22,** 267-272.

Vanhaesebroeck B, Higashi K, Raven C, Welham M, Anderson S, Brennan P, Ward S. G and Waterfield M. D. (1999) Autophosphorylation of p110 delta phosphoinositide 3-kinase: a new paradigm for the regulation of lipid kinases in vitro and in vivo. *EMBO J* **18,** 1292-1302.

Vanhaesebroeck B, Leevers SJ, Ahmadi K, Timms J, Katso R, Driscoll PC, Woscholski R, Parker PJ, Waterfield MD. (2001) Synthesis and function of 3-phosphorlyated inositol lipids. *Annu Rev Biochem.* **10,** 535-602.

Vazquez F, Ramaswamy S, Nakamura N, and Seller WR. (2000) Phosphorylation of PTEN tail regulates protein stability and function. *Mol. Cell. Biol.* **20,** 5010-5018.

Vinhinen M, Mattsson P. T and Smith E.C. (2000) Bruton tyrosine kinase (BTK) in X-linked agammaglobulinema (XLA) *Front Biosci* **5,** 917-928.

Viola A, Schrooeder S, Sakakibra Y and Lanzavecchia, A. (1999) T lymphocyte costimulation mediated by reorganisation of membrane microdomains. *Science* **283,** 680-682.

Virolle T, Adamson E. D, Baron V, Birle D, Mercola D, Mustelin T, and de Belle (2001) The Egr-1 transcription factor directly activates *PTEN* during irradiation-induced signalling. *Nature Cell. Biol.* **3,** 1124-1128.

Ueda Y, Levine BL, Huang ML, Freeman GJ, Nadler LM, June CH, Ward SG. (1995) Both CD28 ligands CD80 (B7-1) and CD86 (B7-2) activate phosphatidylinositol 3-kinase, and wortmannin reveals heterogeneity in the regulation of T cell IL-2 secretion. *Int Immunol.* **7,** 957-66.

Walker E. H, Perisic O, Reid C, Stephens L and Williams R. L (1999) Structural insights into phosphoinositide 3-kinase catalysis and signalling. *Nature* **402,** 313-320.

Walker D. M, Urbe S, Dove S. K, Tenza D, Raposo G and Clague M. J. (2001) Characterisation of MTMR3: an inositol lipid 3-phosphatase with novel substrate specificity. *Curr Biol.* **11,** 1600-1605.

Wang S, Zhu G, Chapoval A. I, Dong H, Tamada K, Ni J and Chen L. (2000) Costimulation of T cells by B7-H2, a B7-like molecule that binds ICOS. *Blood* **96,** 2808-2813.

Ward, S. G., Westwick, J., Hall, N. D and Samson, D. M. (1993) Ligation of CD28 receptor by B7 induces formation of D-3 phosphoinositides in T-lymphocytes independently of T cell receptor/CD3 activation. *Eur. J. Immunol.* **23,** 2572-2579.

Ward. S. G, Wilson A, Turner L, Westwick J and Sansom D. M (1995) Inhibition of CD28-mediated T cell co-stimulation by the phosphoinositide 3-kinase inhibitor wortmannin. *Eur. J. Immunol.* **25,** 526-532.

Ward, S. G., June, C. H and Olive, D. (1996) PI-3-kinase: a pivotal pathway in T-cell activation? *Immunol. Today* **17,** 187-197.

Ware, M. D., Rosten, P., Damen, J. E., Liu, L., Humphries, K and Krystal, G (1996) Cloning and characterisation of Human SHIP, the 145-kD inositol 5-phosphatase that associates with SHC after cytokine stimulation. *Blood* **88,** 2833-2840.

Weiss A and Imboden J. B. (1987) Cell surface molecules and early activation events involved in human T lymphocyte activation. *Adv. Immunol* **41,** 1-38.

Wu X, Hepner K, Castelino-Prabhu S, Do D, Kaye MB, Yuan XJ, Wood J, Ross C, Sawyers CL, and Whang YE. (2000). Evidence for the regulation of the PTEN tumor suppressor by a membrane-localised multi-PDZ containing scaffold protein MAGI2. *Proc. Natl. Acad. Sci. USA* **95,** 15587-15591.

Yang, XY, Wang, LH, Chen, T, Hodge DR, Resau, JH, DaSilva, L and Farrar, WL. (2000) Activation of T lymphocytes is inhibited by Peroxisome Proliferator-activated Receptor γ (PPARγ) agonists. *J. Biol. Chem.* **275,** 4541-4544.

Zhang W. J, Sloan-Lankester J, Kitchen J, Trible R. P, and Samelson J. E. (1998) Lat, the ZAP-70 tyrosine kinase substrate that links the T cell receptor to cellular activation. *Cell* **92**, 83-92.

Zhang W, Irvin B. J, Trible R. P, Abraham R. T and Samelson L. E. (1999). Functional analysis of LAT In TCR-mediated signalling pathways using a LAT-deficient Jurkat cell line. *Intl Immunol* **11,** 943-950.

Zhang X, Wang J. M, Gong W. H, Mukiaida N, and Young H. A. (2001) Differential regulation of chemokine gene expression by 15-deoxy-Δ12,14 prostaglandin J2. *J. Immunol.* **166,** 7104-7111.

Publications

Edmunds C, Parry RV, **Burgess SJ,** Reaves B, and Ward SG. (1999) CD28 stimulates tyrosine phosphorylation, cellular redistribution and catalytic activity of the inositol lipid 5-phosphatase SHIP. *Eur. J. Immunol.* 29, 3507-3515.

Freeburn RW, **Burgess SJ,** Astoul E, Cantrell DA and Ward SG (2002). Evidence that SH2 domain containing inositol poly phosphatase (SHIP) contributes to phosphatidylinositol (3,4,5) trisphosphate metabolism in T lymphocytes. *J. Immunol.*

Abstracts

Burgess SJ and Ward SG Characterisation of the expression of phosphatases SHIP and PTEN in T cell lines and T-lymphoblasts. Presented to the Biochemical society, Trinity College, Dublin 2001

Oral Presentation

Burgess SJ and Ward SG Role of Tec tyrosine kinase in SHIP activation. Presented to the British Society for Immunology, Harrogate 1999.

Thank fuck for that!